

**Historical biogeography and the evolution of environmental
niche and fruit type in Datureae (Solanaceae)**

by

Julia Guedes Rocha Dupin

B.Sc., Universidade Federal de Minas Gerais, 2009

A thesis submitted to the

Faculty of the Graduate School of the

University of Colorado in partial fulfillment

of the requirements for the degree of

Doctor of Philosophy

Department of Ecology and Evolutionary Biology

2017

This thesis entitled:
Historical biogeography and the evolution of environmental niche and fruit type in Datureae
(Solanaceae)
written by Julia Guedes Rocha Dupin
has been approved for the Department of Ecology and Evolutionary Biology

Dr. Stacey D. Smith

Dr. Erin Tripp

Dr. Christy McCain

Dr. Pamela Diggle

Dr. Daniel Doak

Date _____

The final copy of this thesis has been examined by the signatories, and we find that both the content and the form meet acceptable presentation standards of scholarly work in the above mentioned discipline.

Guedes Rocha Dupin, Julia (Ph.D., Ecology and Evolutionary Biology)

Historical biogeography and the evolution of environmental niche and fruit type in Datureae
(Solanaceae)

Thesis directed by Dr. Stacey D. Smith

My dissertation examines how the interplay between historical biogeographic events and environmental factors shaped species distributions and traits in the tomato family (Solanaceae). Historical biogeographic analyses were undertaken at a broad evolutionary scale level, considering the entire Solanaceae family (Chapter 1). To address environmental factors and plant traits, I then focused my work on a smaller group within Solanaceae, the tribe Datureae. Within this clade, I estimated the evolutionary relationships between its 18 extant species (Chapter 2), assessed environmental niche evolution of the different genera (Chapter 3) and evaluated changes in the plants morphology, specifically fruit morphology, related to dry and mesic environments (Chapter 4). My work demonstrated that South America is the ancestral area for Solanaceae, and dispersal was the principal driver of range evolution in the family. Most dispersals involved range expansions from South America into North and Central America, a trend that is likely due to the early build-up of species richness in South America, resulting in large pool of potential migrants. For Datureae, phylogenetic and biogeographic analyses point to an origin in the Andes of South America, with subsequent expansion to North America and other regions in South America. I also found that the ancestral environmental niche in the tribe is dry and that there has been a significant shift in one South American lineage towards a more mesic environment. Finally, my work showed an accumulation of morphological changes in the North American lineage of Datureae. In particular, this lineage (the genus *Datura*) evolved dehiscent capsular fruits from the ancestral state (berries) through a complex series of anatomical changes. Placing this work in a comparative developmental context, this work revealed the effect of ancestry on the trajectory of fruit evolution.

Dedication

Aos meus pais, Marcelo e Lúcia, à minha irmã, Caroll, e ao meu amor, Simon.

Acknowledgements

I express my whole-hearted gratitude to my advisor Dr. Stacey Smith. Stacey is a role model both as a teacher and as a researcher. She showed me how to conduct excellent research projects, and how to pass it on to younger generations, in the classroom and out. I will be forever grateful for her contributions to my PhD, to my professional development, and to my life.

I also want to thank my doctoral committee for dedicating their time to offering valuable feedback to my research. Their help, comments and suggestions were instrumental in getting this work the level of quality it has reached. My thanks also go out to the amazing collaborators and researchers I had the chance to work with. Thanks to Richard Olmstead, Lynn Bohs, J. Mark Potter, Susanne Renner, G.M. van der Weerden, the Huntington Botanical Gardens, and the International *Brugmansia* and *Datura* society for contributing with samples for this research. Many thanks to Manuel Lujan, Travis Columbus, Loraine Washburn, and other researchers at the Rancho Santa Ana Botanic Garden for their time and help with my samples. I am grateful for the hospitality at the Olson lab at UNAM, and to the great staff at the multiple herbaria I visited during this PhD (ARIZ, COLO, DES, GH, MEXU, QCA, QCNE, RSA).

I gratefully acknowledge the funding received from the Dept. of Ecology and Evolutionary Biology and Museum of Natural History at CU Boulder, the University of Nebraska Lincoln, American Society of Plant Taxonomists, Torrey Botanical Society, Society of Systematic Biologists, and National Science Foundation. Finally, I would not be here today without the support of family and friends; nor without the encouragements from my undergraduate advisor, Dr. Claudia Jacobi.

Muito obrigada!

Contents

Chapter

Introduction	1
1 Bayesian estimation of the global biogeographical history of the Solanaceae	6
1.1 Introduction	6
1.2 Materials and Methods	8
1.2.1 Solanaceae Phylogeny and Species Distribution	8
1.2.2 Ancestral Range Estimation	10
1.2.3 Estimation of number and type of biogeographical events	11
1.3 Result	12
1.3.1 Ancestral Range Estimation and Time-stratified Analyses	12
1.3.2 Estimation of number, type, and directionality of biogeographical events	13
1.4 Discussion	15
1.4.1 The ancestral range of Solanaceae	15
1.4.2 Patterns of speciation, vicariance and dispersal in Solanaceae history	17
1.4.3 Directionality of dispersal events	18
1.4.4 BSM as an approach to estimate biogeographical history of clades	19
1.5 Acknowledgments	20
1.6 Tables and figures	21

2	Phylogenetics of Datureae (Solanaceae), including Description of the New Genus <i>Trompettia</i> and Re-circumscription of the Tribe	28
2.1	Introduction	28
2.2	Materials and Methods	30
2.2.1	Taxon sampling	30
2.2.2	Data Collection	31
2.2.3	Phylogenetic inference	32
2.2.4	Character Evolution within Datureae	35
2.3	Results	36
2.3.1	Assessment of congruence among datasets	36
2.3.2	Phylogenetic relationships and divergence times in Datureae	36
2.3.3	Character evolution	37
2.4	Discussion	38
2.4.1	Phylogenetic Relationships	38
2.4.2	Dating the Diversification of Datureae	40
2.4.3	Character Evolution	41
2.4.4	Taxonomic Implications	42
2.5	Taxonomic Innovations	44
2.6	Taxonomic Treatment	46
2.7	Taxonomic Key of Worldwide Diversity in Datureae	47
2.8	Tables and figures	48
3	Integrating historical biogeography and environmental niche evolution to understand the geographical distribution of Datureae (Solanaceae)	60
3.1	Introduction	60
3.2	Methods	62
3.2.1	Historical biogeography of Datureae	62

3.2.2	Analyses of niche evolution	64
3.3	Results	67
3.3.1	Historical biogeography	67
3.3.2	Phylogenetic principal component analysis of environmental variables	68
3.3.3	Shifts in optima in environmental niche space	68
3.3.4	Niche overlap between genera	69
3.4	Discussion	69
3.4.1	Historical biogeography of Datureae – a clade of South American origin	70
3.4.2	Datureae’s environmental niche evolution	71
3.4.3	Contributions of historical events and niche dynamics over space and time to the distribution of Datureae species	73
3.4.4	Conclusions and future directions	74
3.5	Tables and figures	75
4	Evolution of fruit type in Datureae (Solanaceae)	82
4.1	Introduction	82
4.2	Methods	84
4.2.1	Anatomy and Morphology	84
4.2.2	Reconstruction of ancestral anatomical states	86
4.3	Results	87
4.3.1	Anatomical comparison between berries and capsules	87
4.3.2	Regular and irregular dehiscence mechanisms in <i>Datura</i>	88
4.3.3	Evolution of anatomical characters	89
4.4	Discussion	90
4.4.1	Transition from berry to capsule in Solanaceae	90
4.4.2	Capsules and berries in Datureae and other Solanaceae	91
4.4.3	Vascular system as the tissue of resistance in fruit wall of <i>Datura</i> capsules	92

4.4.4	Seed dispersal in Datureae	93
4.5	Conclusion and future directions	94
4.6	Tables and figures	95
Bibliography		108
 Appendix		
A	Supporting information to Chapter 1	126
A.1	Supplementary tables and algorithm validation	126
A.2	Maximum likelihood ancestral range estimates	153
A.3	Example of a BSM realization	153
B	Supporting information to Chapter 2	154
B.1	Voucher information	154
B.2	<i>lfy</i> primers designed for this study	160
B.3	starBEAST2 analysis of <i>Datura</i>	160
B.4	Divergence times with confidence intervals for Datureae and outgroups	160
C	Supporting information to Chapter 3	162
C.1	Biogeographical models tested in this study	162
C.2	List of environmental variables considered for this study	164

Tables

Table

1.1	Summary of biogeographical stochastic mapping counts for the Solanaceae	22
2.1	Taxon list	50
2.2	Properties of the nuclear regions used to estimate phylogenies for Datureae	51
2.3	Comparison of morphological characters between <i>Datura</i> , <i>Brugmansia</i> and <i>Trompettia</i>	52
3.1	Variable loadings for <i>pPC1</i> as a result of the <i>pPCA</i> analysis	77
3.2	Results of the ‘11ou’ simulation on the evolution of <i>pPC1</i>	77
4.1	Characters at late stage of fruit development in <i>Brugmansia</i> , <i>Datura</i> and <i>Trompettia</i>	98

Figures

Figure

1.1	Diagrams of different types of biogeographical events	23
1.2	Maximum likelihood ancestral range estimation in Solanaceae	24
1.3	Representation of timing of dispersal events in the Solanaceae chronogram	25
1.4	Number of dispersal events estimated in the history of Solanaceae with BSM	26
1.5	Summary of dispersal events estimated with BSM in the history of Solanaceae	27
2.1	Flowers of different species of Datureae	53
2.2	50% majority rule consensus trees from parsimony bootstrap analysis	54
2.3	Bayesian MCC phylogeny and divergence time estimation of Datureae and outgroups	55
2.4	Ancestral state reconstruction of characters using stochastic mapping	56
2.5	Short branches in <i>Trompettia cardenasiana</i>	57
2.6	Scientific illustration of <i>Trompettia cardenasiana</i>	58
2.7	Diagrams illustrating corolla constriction and seed margins	59
3.1	Historical biogeography of Datureae using MCC tree	78
3.2	Biplot of <i>pPC1</i> and <i>pPC2</i>	79
3.3	Niche regions and niche overlap of the genera in Datureae	80
3.4	Dynamics over space and time of Datureae's environmental niche	81
4.1	Fruit types in Datureae	99
4.2	Differences in fruit septa in the different genera in Datureae	100

4.3	Cell layer organization in Datureae fruits	101
4.4	Anatomical images of berries and capsules at their late stage of development	102
4.5	Anatomy and morphology of the dehiscence process in regularly dehisced capsules .	104
4.6	Results of the compression tests on regular and irregularly dehisced fruits	105
4.7	Stepwise reversal to regularly dehisced capsules in Datureae	106
4.8	Ancestral state reconstruction for anatomical characters	107

Introduction

Understanding the distribution of species is a major goal in ecology and evolutionary biology. Investigations of species distribution patterns trace as far back as the works of Buffon [20] in 1749, von Humboldt [228] in 1805, and De Candolle [40] in 1820. For example, Buffon [20] and von Humboldt [228] considered how climate and geographical distance influence species assembly, and De Candolle [40] factored in geological history and age to explain the distribution of different species. Darwin [36]) and Wallace [230] built on these ideas, acknowledging the importance of centers of origin and dispersal (including long distance), and recognizing that geographical distance was related to chronology, i.e., that species found close together likely share a more recent common ancestor. In the first half of the 20th century, new biogeographic theories emerged, including continental drift (Wegener [231]), mechanisms of allopatric speciation (Mayr [137]), multidimensional niche concept (Hutchinson [94]), and island biogeography (MacArthur and Wilson [241]). Theoretical and applied work in biogeography demonstrate that the distribution and ecological niche of a given clade are the product of the interplay of factors such as climate, geology and time (e.g. Lemmon [113]; Antonelli [2]; Niemiller [153]).

In this dissertation, these concepts and theories are used to form hypotheses and assess the relative contribution of factors influencing species distribution. Several factors can help us understand why species are found where they are today (Wiens [239]). For example, the initial level of isolation of a clade depends highly on where (geographically) it has originated. This geographical starting point will determine the environment where species originated and are adapted to, which may lead to a lag in moving and adapting to new areas. These areas can be accessible or not

depending on how close they are, or how contrasting their climate and species composition are. Moreover, the amount of time available for a given species to disperse to new areas should also be considered. Ultimately, these processes are influenced by clade-specific factors, including phylogenetic history and trait lability (Losos [123]; Mulroy [145]). One cannot talk about, for instance, ancestral environmental niche (or ancestral and derived states in general) if the relationships within a given clade are not well resolved.

Here, I consider the effects of these factors on species distributions by using methods to estimate historical biogeography and environmental niche evolution. Approaches for reconstructing historical biogeographic events have expanded from parsimony-based methods (Ronquist [194]) to the maximum likelihood (Ree [190]) and more recently, Bayesian-based ones (Landis [110]; Matzke [134]; Matzke [135]). Coincidentally, the available models have become more complex, and a wider range of processes and events (e.g. sympatric speciation, vicariance, range expansion, range contraction) are now included. With this suite of tools, it became a crucial step to clearly delimit the factors considered relevant and to use datasets that are powerful enough for the hypothesis being tested. For this work, I used model-based maximum likelihood and Bayesian approaches (Matzke [136]; Matzke [135]), and applied biogeographical stochastic mapping (BSM) to the first empirical dataset (Dupin [51]).

To complement the results on the frequency and asymmetric rates of dispersals, I added an analysis of niche evolution to assess the contributions of environmental variables. The rationale behind it is that the patterns seen at a historical biogeography level are the result of processes at an ecological scale. Hypothesis about the evolution of environmental niches have been addressed with the use of the continuous environmental variables (e.g. temperature, precipitation) as input for comparative methods that estimate ancestral states in a clade (Schluter [203]; Pagel [165]; Pagel [166]). These methods can be powerful to detect shifts in environmental preferences within a clade. The use of comparative methods complements other approaches that have shaped the study of environmental niches, namely species distribution modelling and the assessment of environmental suitability (reviewed in Peterson [177]).

Here, these methods for studying historical biogeography and environmental niche evolution were applied to determine the factors that influenced the distribution of two plant groups, the family Solanaceae and the tribe Datureae. These groups gave me a chance to work on two spatial scales, given that Solanaceae has a global distribution and Datureae is distributed exclusively in the Americas. Solanaceae, popularly known as the tomato or the nightshade family, occurs on most continents, with the exception of Antarctica. It has about 2,800 species, which makes it one of the largest plant families (Olmstead [161]; Särkinen [200]). This family is also known for its many economically important species, such as potatoes, tomatoes, and tobacco. Its age has been recently estimated as between 30 and 50 million years (My) and its diversification began in South America (Olmstead [160]; Särkinen [200]). The family's species richness, cosmopolitan distribution and well-resolved phylogeny makes Solanaceae a good candidate for understanding historical biogeographic patterns of South American plant clades. In contrast, Datureae is a small tribe of 18 species within Solanaceae, and these species are distributed in exclusively Andean areas, southeast Brazil, and Mexico and southwest USA (Lockwood [120]; Bye [23]). Some of the species are used as ornamentals (common names jimsonweeds and angel trumpets), but they are more famous for their hallucinogenic properties (Lockwood [120]; Schultes [205]). The disjunct aspects of Datureae's distribution, along with the variety of types of environments its species inhabit (cloud forests, tropical forests, deserts and dry forests), raises questions about historical biogeography but also about the influence of the evolution of environmental niche in the clades distribution.

With Solanaceae, I examined how biogeographical events (e.g., vicariance, founder events, and dispersals) in the context of time and space contributed to the widespread distribution of the family (Chapter 1). I found that South America is Solanaceae's current center of diversity and its ancestral range. The main type of biogeographical event that drives the evolution of geographical ranges in Solanaceae is dispersal events between areas, and these were most common in range expansions from South America into North and Central America. Dispersals from South America to other areas, in general, were more common than in the opposite direction. This directionality is likely due to the early build-up of species number in South America, resulting in large number of

potential dispersals from that area.

Now with Datureae, given the smaller size of the group, I combined a similar analysis of historical biogeography with the study of its environmental niche. In order to undertake both the biogeographical and niche analyses, the well-resolved phylogeny was required. While the tree for the Solanaceae family used here came from Sarkinen [200] work, a fully resolved phylogeny that includes all species in Datureae was not available. So, as part of the work on Datureae, I generated a phylogeny for the group (Chapter 2). This study presents the first phylogeny of the tribe that includes all accepted species to date. This phylogeny was estimated using nuclear markers, which have been useful in increasing the resolution of other clades within Solanaceae. As part of this study, I also reconstructed the history of morphological characters used to delimit genera in the tribe, such as flower position and size, and fruit type. The patterns of character evolution were largely consistent with the phylogeny, meaning that only minimal taxonomic changes were needed. Specifically, I reassigned a species that was currently placed in a different tribe within Solanaceae to Datureae and elevated it to its own genus.

In my studies of Datureae, I integrated historical and environmental factors to create a more detailed picture of how this clade colonized different parts of the Americas (Chapter 3). My results suggest that Datureae originated in Andean regions and subsequently expanded its range to North America and non-Andean regions. Moreover, I estimated that the ancestral environmental niche in the tribe is dry and that there has been a significant shift along the *Brugmansia* branch towards a more mesic type of environment. The long-distance dispersal to North America represented a range expansion into a familiar type of environment, a dry one. Even though range expansions ultimately resulted in a significant niche shift, our niche overlap estimates showed moderate overlap remains between *Datura* and *Brugmansia* niche regions. This is likely a result of as yet incomplete niche specialization within *Brugmansia* and two *Datura* species.

The long distance dispersal from the Andes to North America in Datureae was associated with changes in a large number of life history and morphological features, perhaps most notably the type of fruit. Fruits in Datureae are very diverse, and their traits are likely a product of adaptation

to distinct environments. In Chapter 4, I explored the anatomical differences between fleshy and dry fruits in the group, with special attention to the transition to the family's ancestral fruit state observed in one of the genera in the tribe (*Datura*). In addition to comparing the anatomical features of fleshy and dry fruits in the tribe, I explored the characters that could explain the different dehiscence mechanisms within species in *Datura*, including biomechanical tests of regular and irregularly dehisced fruits. Lastly, I placed these results into phylogenetic context to determine if the transition between berries and regularly dehisced capsules was a stepwise process, given the number of traits likely required for a dry fruit (e.g., creating dehiscence zones, opening to release seeds). I found that, while capsules and berries in Datureae are functionally different, there are overlapping anatomical characters between the two types of fruit. I also found that the vascular tissue is likely a major player in the dehiscence mechanism in *Datura*, in contrast to the mechanism seen in other genera with capsules in Solanaceae. These results demonstrated then the relevance of phylogenetic context when discussing the evolution of characters, and indicated that multiple mechanisms for the development of capsules exist within Solanaceae.

Chapter 1

Bayesian estimation of the global biogeographical history of the Solanaceae

[Published as: Dupin, J., Matzke, N. J., Särkinen, T., Knapp, S., Olmstead, R. G., Bohs, L., & Smith, S. D. 2017. Bayesian estimation of the global biogeographical history of the Solanaceae. *Journal of Biogeography* 44(4): 887-899.]

Additional Supporting Information may be found in the online version of this article and, when possible, in the appendix of this thesis

1.1 Introduction

The growing availability of large phylogenies together with developments in statistical methods provide researchers with new opportunities to explore the complex biogeographical history of large cosmopolitan clades (Matzke [134], Yu [245]). Worldwide distributions can be achieved either through dispersal events, vicariance, or a combination of the two (Yoder [244], Nauheimer [150]). For example, Gondwanan clades that arose and diversified before continental separation may become cosmopolitan largely through vicariance (Gamble [62], Rasmussen [188]). By contrast, groups that have evolved subsequent to continental separation can only achieve wide distributions through long-distance dispersal events (Givnish [71], Szovenyi [218]). The relative importance of these processes is expected to vary across groups of organisms given intrinsic differences in dispersal ability and level of ecological specialisation (Gillespie [67], Edwards [54]).

The interplay of vicariance and dispersal in shaping cosmopolitan distributions has been relatively well studied in plants. For many widely distributed plant families, dispersal appears to be

the principal driver of range evolution (Givnish [72], Christenhusz [28]), whether by water (Gallaher [61]), wind (Munoz [147]), or animals (Nogales [154]). By contrast, relatively few widespread families show strong signatures of vicariance in shaping their present day distributions (Barker [6], Mao [128]). This pattern may be attributable to the fact that long distance dispersal of seeds or other germplasm, while limited on ecological timescales (Cain [24]), appears to be relatively frequent on macroevolutionary timescales (Renner [191], Nathan [149]). Moreover, the establishment of distantly dispersed lineages may be favoured by the absence of their native competitors, pathogens and predators (Janzen [102], Howe [88]). One caveat, however, with respect to the apparent predominance of dispersal is that many of the studied lineages are relatively young (but see Beaulieu [10]). Also, vicariance becomes harder to identify in older clades as subsequent dispersal and population movement, along with local extinction, can obscure the original geographical signature (e.g., Clayton [30]).

Here we examine the biogeographical history of a relatively young plant family, the Solanaceae. This clade of about 2,800 species began to diversify roughly 50 to 65 million years ago (Ma) (Särkinen [200], Magallón [127]) and is presently distributed on all continents except Antarctica. The Solanaceae contains a large number of important crops such as potato (*Solanum tuberosum* L.), tomato (*Solanum lycopersicum* L.) and tobacco (*Nicotiana tabacum* L.), and has long been the focus of genetic, biochemical, and morphological studies (e.g., Pabón-Mora [164]; Sato [202], Itkin [97]). Solanaceae is one of the groups in the Asterids I (Lamiids) that is especially species rich in the Neotropics, along with the Verbenaceae and Bignoniaceae (Olmstead [160]), and the Acanthaceae (Tripp [223]). Its sister group is the large morning glory family, Convolvulaceae, which also has a worldwide distribution. Despite its economic importance, the biogeographical history of Solanaceae has received relatively little attention beyond taxonomic or floristic surveys (e.g., Gentry [65], Hepper [80]). In a recent review of Solanaceae biogeography in the context of its phylogenetic history, Olmstead [160] suggested that the family's cosmopolitan distribution is due to repeated dispersals from South America to both nearby and distant continents. However, identifying the timing, number, and direction of these events was limited by the level of taxon sampling (ca. 5%

of species of the family) and the lack of a time-calibrated phylogeny.

In this study, we combine a recent dated phylogeny that includes nearly 40% of the species in the family (Särkinen [200]) with newly developed biogeographical stochastic mapping (BSM; Matzke [135]) to estimate the biogeographical events that account for the global distribution of the Solanaceae. Stochastic mapping (Nielsen [152]; Huelsenbeck [90]) is a simulation approach that builds on likelihood models of trait evolution and, in addition to estimating ancestral states at nodes, provides possible histories of changes along branches. By summarizing across many of these possible histories, we can obtain estimates of the number and phylogenetic location of various types of events (e.g., vicariance, dispersal between areas) along with measures of uncertainty. This approach was originally developed for mapping mutations onto phylogenies (Nielsen [152]) and was later expanded to accommodate morphological characters (Huelsenbeck [90]). Just as the morphological stochastic mapping was built on Pagel's (1999) [165] likelihood models for trait evolution, the development of stochastic mapping for biogeographical patterns relies on existing likelihood models describing how geographical ranges evolve (Ree [190], [134]). In the context of Solanaceae biogeography, we apply likelihood methods and BSM to (1) infer the most likely ancestral range of the family and major groups within it, (2) assess the relative contribution of vicariance and dispersal events to the distribution of extant taxa, and (3) detect directionality in dispersal between areas. In addition to elucidating the biogeographical history of this economically and floristically important family, these results provide new insights into the relative importance of alternate dispersal routes in the spread of plant clades to new areas.

1.2 Materials and Methods

1.2.1 Solanaceae Phylogeny and Species Distribution

We used the time-calibrated maximum clade credibility (MCC) tree from Särkinen ([200]), which was estimated using two nuclear and six plastid loci from 1075 species. This taxon sampling includes all but three of the 98 Solanaceae genera [*Darcyanthus* Hunz., *Capsicophysalis* Averett &

M. Martnez and *Tubocapsicum* (Wettst.) Makino)] and nearly 40% of all species. For the present study, we pruned (1) taxa that are widely cultivated and whose native distributions have been obscured by extensive human transport, and (2) taxa that were duplicated in the phylogeny (Table S1.1 in Appendix A.1 in Supporting Information). The phylogeny was pruned using 'ape' package (Paradis [167]) in R (R Core Team [184]). We also updated species names according to the most recent literature (Table S1.1 in Appendix A.1). The final pruned phylogeny used for downstream analyses contained 1044 species.

The current distribution for each species in the phylogeny was determined using numerous literature sources (e.g., Bentez de Rojas [43], Garcia [63]; Dillon [45]), online databases (Solanaceae Source, <http://solanaceaesource.org/>, last accessed on Nov. 2015; TROPICOS, Missouri Botanical Garden, <http://www.tropicos.org>, last accessed on Nov. 2015; Global Biodiversity Information Facility, <http://www.gbif.org>, last accessed on Nov. 2015), and experts' input (Table S1.2 in Appendix A.1). Considering current distribution patterns within the family, we chose to recognize seven major areas: South America (SAm), Central America (CAm), Caribbean (Car), North America (NAm), Eurasia (EU), Africa (AF) and Australia (OZ; includes Australia, other islands of Oceania and the Hawaiian islands). The decision to focus on these seven areas reflects the need to balance model complexity (i.e., the number of dispersal rates, within-area extinction rates, etc.) with the ability to detect major biogeographical shifts within this widely-distributed family. The Caribbean and Central America were maintained as separate areas in order to examine the origins of the many solanaceous lineages endemic to those regions. We grouped the six species native to Hawaii (*Solanum incompletum* Dunal, *S. sandwicense* Hook. & Arn., *S. viridifolium* Dunal, *Nothoestrum latifolium* A. Gray, *N. longifolium* A. Gray, and *Lycium sandwicense* A. Gray) with the Australian taxa (Table S1.2 in Appendix A.1). While dispersal to Hawaii and remote Pacific islands represents a long distance dispersal from any potential source, three of them are nested within clades found in Australia and New Zealand (*S. incompletum*, *S. sandwicense* and *S. viridifolium*), whereas the others represent putative Eurasian or New World ancestry (Levin [117], Levin [118], Olmstead [161], Vorontsova [229]). Our divisions are similar to those used in other studies

of widespread clades (e.g., Buerki [19], Sessa [208]), and will allow us to detect intercontinental movements as well as shorter range dispersal events (e.g., South America to the Caribbean).

1.2.2 Ancestral Range Estimation

We used the R package “BioGeoBEARS” (Matzke [136]) to compare biogeographical models and estimate ancestral ranges in the Solanaceae. ‘BioGeoBEARS’ implements maximum likelihood (ML) methods that replicate the key assumptions of three most commonly used methods in historical biogeography, namely DEC (DispersalExtinctionCladogenesis; Ree [190]), DIVA (Dispersal-Vicariance Analysis; Ronquist [194]) and BayArea (Bayesian Inference of Historical Biogeography for Discrete Areas; Landis [110]). These three methods were originally developed in different frameworks (likelihood for DEC, parsimony for DIVA, and Bayesian for BayAREA), but are all represented as likelihood models in ‘BioGeoBEARS’ to allow for direct comparison. The latter two models are thus not identical to their original formulation, and are referred to as DIVALIKE and BAYAREALIKE within ‘BioGeoBEARS’ (Matzke [136]). Collectively, these models allow for a wide range of processes, including within-area speciation, vicariance, range expansion (dispersal to a new area), and range contraction (extinction in an area) (Fig. 1.1). We also tested models with and without founder-event speciation, which is incorporated with the j parameter. In such an event, range switching (e.g., South America to North America) occurs at a lineage-splitting event (a node in the phylogeny), leaving one daughter lineage in a new range and the other daughter lineage retaining the ancestral range. Such range switching events are restricted to nodes (instead of occurring along branches) as it is considered unlikely that an entire lineage would simultaneously disperse to a new area and go extinct in its ancestral area (Matzke [134]).

We also incorporated time-stratified dispersal multiplier matrices in the model-fitting to account for the changing distances between the regions over geological time. We divided the history of Solanaceae into three strata: 50 to 24 Ma, 24 to 10 Ma, and 10 Ma to present. We began the strata at 50 Ma given the estimated depth of the Solanaceae phylogeny (ca. 49 Ma for the stem group age; Särkinen [200]). The breaks at 24 Ma and 10 Ma reflect recent studies showing

significant shifts in plant dispersal between South and North America at these time points (Bacon [4]). Also, the 10 Ma threshold approximates a new estimated age of the closure of the Panama isthmus during the mid-Miocene (Montes [142]; Bacon [3], but see O’Dea [156]). The dispersal multiplier matrices for each of these strata give the relative probability of dispersal between areas and are roughly scaled to represent the relative distance between the areas during each time slice (Appendix A.1). We examined models using these multiplier matrices directly and also with the matrices modified by the w parameter, also estimated with ML (Appendix A.1).

In total, we tested a set of 18 models (Table S1.3 in Appendix A.1) that varied in the number and types of free parameters included and in the type of dispersal multiplier matrices used. The free parameters were w , d (the base rate of range expansion), j (the per-event weight of founder-event speciation at cladogenesis; Matzke [134]) and e (the rate of range contraction). For models without the dispersal multiplier matrices, the probabilities of all dispersal events are equal (set to 1). Because not all of the models are nested, we used the Akaike information criterion (AIC) (Burnham [22]) to select among the 18 models; the best fit model with the lowest AIC score was used to infer the relative probabilities of ancestral ranges within the phylogeny.

1.2.3 Estimation of number and type of biogeographical events

We estimated the number and type of biogeographical events using BSM implemented in ‘BioGeoBEARS’ (Matzke [135]). Previous implementations of stochastic mapping used transition rate models (Pagel [165]) to simulate the histories of mutations or trait changes (Huelsenbeck [90]). Whereas the transition rate models involve only trait gain and loss, the biogeographical models used in BSM will include a range of anagenetic and cladogenetic events (Fig. 1.1). After providing a biogeographical model with specified parameters, BSM generates simulated histories (‘realisations’), including the times and locations of all events along the branches in that simulation. These realisations of possible histories are constrained to produce the observed data given the phylogeny, and averaging over many realisations will result in the same ancestral state probabilities as those calculated analytically under the ML model (see Appendix A.1 for description and

BSM algorithm validation). Biogeographical events possible under the models include within-area speciation, vicariance, and dispersal events (range expansions and founder events; Fig. 1.1). For cases where a dispersal event occurs from a widespread ancestor occupying two or more areas, the exact source area was simulated using the dispersal probability multipliers matrix as modified by w . We conducted BSM on the Särkinen ([200]) MCC tree using a time-stratified four-parameter model (DEC+ j + w) that produced a significantly better fit to the data compared to other tested models (see Results). Event frequencies were estimated by taking the mean and standard deviation of event counts from 100 BSMs. All stochastic maps and derived statistical estimates are conditioned on not just the phylogeny, the observed range data, and the model, but the inferred model parameters and the implicit Yule process (no lineage extinction) assumption shared by DEC and all other biogeographical models considered here.

1.3 Result

1.3.1 Ancestral Range Estimation and Time-stratified Analyses

The AIC model selection strongly supported the DEC+ j + w model including the dispersal multiplier matrices as the best fit. This is among the more complex models fitted (with four free parameters), and it was 47 AIC units lower than the second best model (DEC+ j) (Table S1.3 in Appendix A.1). Across all the models, the inclusion of the j parameter (or the possibility of a founder event speciation where one of the lineages occupies an area not present in the ancestral range) consistently improved model fit, suggesting that range expansions alone are not sufficient to account for movements to new areas. Such an increase in the likelihood in models with j has been observed in other studies where, as in our case, the areas under consideration are continents or other large regions and thus, many lineages are single area endemics (Litsios [119], Voelker [227], Thacker [219]). It is also notable that the best model employed the user-specified dispersal matrices with the w modifier parameter. This result indicates that scaling the dispersal probabilities to the relative distance of the areas results in higher model likelihood. The w parameter, acting as an

exponent on the dispersal matrices, improves fit to our data (Table S1.3 in Appendix A.1, $+j$ models versus $+j + w$ models).

Ancestral range estimations under this best fitting model (DEC+ $j + w$) showed that the most probable ancestral area for extant species of Solanaceae is South America (probability = 0.8, with 0.14 for South America + Australia, and 0.06 for other state combinations) (Fig. 1.2 & Appendix A.2). Other deep nodes in the family also have South America as the estimated range, supporting the idea that this area is the centre of origin of the family and major clades within it (Fig. 1.2). The first two clades in the family confidently inferred as having an ancestral range outside of the New World are the Hyoscyameae (ca. 12 Ma), nested within Atropina, which has Eurasia as the most probable ancestral state (0.95) and the clade Anthocercidae (ca. 9 Ma), nested within Nicotianoideae, which has Australia as the most probable ancestral range (0.98) (Appendix A.2).

1.3.2 Estimation of number, type, and directionality of biogeographical events

A summary of our BSMs revealed that most biogeographical events comprise within-area speciation (76%) and dispersals (20%), with only a few vicariant events (3%) (Table 1; see Appendix A.3 for an example of a BSM). The high number of within-area speciation events was expected given the large size of our regions (e.g., North America, Eurasia). The number of these events within each area was closely related to species richness, where, for example, 60% of the within-area speciation events occurred within South America, which is home to about 64% of the taxa (Table S1.4 in Appendix A.1). Among the dispersal events, range expansions were much more common than founder events (mean of 218 versus 38; Table 1) and were clustered towards the present (Fig. 1.3). The relative rarity of vicariance (mean = 42 events; Table 1) may reflect the fact that the diversification of Solanaceae postdates the Gondwanan break-up (180 Ma, early Jurassic – 94 Ma, mid-Cretaceous; McLoughlin [138]). Most of the estimated vicariance events involved adjacent areas (e.g., South America and North America) (Table S1.5 in Appendix A.1) and occurred following a range expansion. For example, the ancestor of the genus *Jaltomata* was estimated to have expanded its range from South America to South and North America, and this

expansion was followed by a division into subclades most diverse in South and North America (Appendix A.2; see also Mione [141]).

Focusing on dispersal events, we found that movement patterns varied tremendously across areas. The highest number of dispersals involved movements from South America to Central America (ca. 49 of 256 total estimated events), closely followed by movements from South America to North America (ca. 42 of 256) (Fig. 1.4(a)). Overall, South America was the source for 47% of the estimated dispersal events. North America was the next most common source (20%), and most of these dispersals were toward Central America (Fig. 1.4(a), Fig. 1.5). In total, dispersals among the four New World areas accounted for 81% of the events, while dispersal among the three Old World regions or between the Old World and New World were less common (10% and 9%, respectively). Among the Old World areas, Australia and the nearby islands of Oceania were the least common source and sink for dispersal events, and three of the estimated 11 dispersals into the area comprise the Hawaiian taxa previously shown to have originated from Eurasia and the New World (Levin [117], Levin [118], Olmstead [161], Vorontsova [229]). The relative importance of different regions as sources and sinks for dispersal differed to some degree depending on the type of dispersal event (range expansions versus founder events). Since the vast majority of dispersal events were range expansions, the pattern of those movements (Fig. 1.4(b)) largely mirrors the overall pattern (Fig. 1.4(a)), where South America is the most common source and Central America is the most common sink. By contrast, the most frequent founder event type involved dispersal from South America to North America (Fig. 1.4(c)), with the other transitions (e.g., to Central America, to Africa) occurring with roughly equal frequency. Thus, whereas the range expansions commonly occur between adjacent areas, the founder events more often involve distantly related regions. Indeed, movements between the Old World and New World accounted for just 6% of estimated range expansions, but 24% of the estimated founder events.

Regardless of the type of dispersal event, we inferred strong asymmetry in the movements between areas. For example, dispersal events from Central America to the Caribbean were more than twice as common as those in the opposite direction (10.12 ± 1.41 versus 4.20 ± 1.14 ; Fig. 1.4(a)).

Such directionality was observed for nearly all pairs of areas (compare upper diagonals and lower diagonals in Fig. 1.4) and was most marked for events involving South America (see also Fig. 1.5). The most prominent exceptions to this overall trend are dispersals between Africa and Eurasia, which have occurred in approximately equal numbers in both directions (Figs. 1.4, 1.5). The general asymmetry of transitions was consistent across all of the individual BSM realisations (chi-square contingency analysis, $p < 10^{-45}$ for each of the 100 realisations).

1.4 Discussion

Our analyses of the historical biogeography of Solanaceae confirm that the early evolution of the family took place in South America. Moreover, major clades in the family, such as the large ‘ $x = 12$ ’ clade (genera with a base chromosome number of 12) and the Solaneae (*Solanum+Jaltomata*), are also estimated to have originated in South America (Fig. 1.2), despite the fact that these groups today are very diverse in the Old World. Our best model, which included time-stratified matrices representing the continental area distances over time, presented a significantly better fit than those that did not incorporate palaeogeographical information. This suggests that distance is an important factor when estimating dispersal events between areas in Solanaceae. Finally, Solanaceae presents a marked directionality of dispersals over its history, with range expansions and founder events being significantly more common from South America to other areas than in the opposite direction.

1.4.1 The ancestral range of Solanaceae

Our estimation of biogeographical history shows that, for Solanaceae, South America is not only the family’s distributional centre but also its ancestral range (Fig. 1.2). The radiation of the family appears to have continued in South America up to ca. 15 Ma, before the first lineages established on other continents (Fig. 1.2, Appendix A.2). Such a clustering of long distance dispersal events in the last 20 million years (Myr) was also observed in the Acanthaceae, a similarly species rich and largely Neotropical family (Tripp [223]). Across the history of the Solanaceae, we estimate

about 120 dispersals from South America to new areas, mostly to adjacent regions within the New World (Figs. 1.4, 1.5). This tendency for geographical movements to involve proximate areas is reflected in the fact that models that incorporated distance between areas through dispersal matrices were consistently a better fit for the data (Table S1.3 in Appendix A.1), as has been observed in studies of other taxa (e.g., Matos-Maravi [133]).

Although short range movements account for most of the spread of Solanaceae from South America, our results provide evidence of multiple long distance dispersals to Africa, Australia, and Eurasia. These dispersals to the Old World occur long after the separation of Gondwana (ca. 94 Ma), and therefore were likely to involve transoceanic movements. The Solanaceae have fruit types ranging from dry to fleshy and a variety of dispersal agents, including wind, water, and many animals such as birds, bats, small rodents, and ants (Knapp [106]). Thus, fruits could be blown in wind currents, float across the ocean, or be carried to new regions by migrating or rafting animals. Our results show that dry fruited and, more commonly, fleshy fruited lineages have experienced range expansions, including transoceanic movements (Table S1.7 in Appendix 1), consistent with previous studies in the family (Olmstead [160]). Transoceanic dispersal has been hypothesized to explain the spread of other New World families to the Old World (Perret [175], Tripp [223]). Still, we cannot exclude the possibility that these South American taxa reached the Old World through a series of shorter dispersal events (e.g., via a northern route through Beringia) followed by subsequent extinction in the intervening areas (Davis [39]).

Our estimate of the number of dispersal events from the New World to the Old World is strikingly similar to previous studies, despite the use of different methods. In surveying the biogeography of Solanaceae, Olmstead [160] suggested that a total of 15 to 17 long distance dispersal events from South America would be needed to account for the present distribution, assuming a most parsimonious reconstruction. Our model-based stochastic mapping estimates 20 ± 2.04 such events (summing all New World to Old World transitions, Fig. 1.3, Table S1.6 in Appendix A.1). Both of these totals are minimum estimates of the actual number of long distance dispersals in the history of extant Solanaceae because only ca. 40% of all species were sampled. For exam-

ple, the unsampled taxa include the monotypic genus *Tubocapsicum*, which is endemic to eastern temperate Asia and could represent an independent colonization from the New World. However, previous studies and overall morphology suggest that *Tubocapsicum* is closely related to the Hawaiian *Nothocestrum* and the African *Discopodium*, a placement that would favour an Old World origin as opposed to long distance dispersal from the New World (Olmstead [161]). By assigning Hawaiian native species to Australia in our analysis, we were able to include the one inferred dispersal to Hawaii from the New World (*Lycium*) in our estimates. We recognize that all dispersals to Hawaii, however, represent long-distance dispersals regardless of source area. Although a complete family-level phylogeny would be needed to arrive at a final estimate of the total number of New World to Old World dispersals, we expect the present study captures the vast majority of these events.

1.4.2 Patterns of speciation, vicariance and dispersal in Solanaceae history

Our simulations of biogeographical history using BSM identified within-area speciation as the most frequent type of event across the phylogeny (Table 1). This result is likely to reflect the scale of this analysis (global) and the size of the regions under consideration. The preponderance of within-area speciation events is consistent with the large clades of Solanaceae that are endemic to single areas as defined by our study. For example, the 31 species of Anthocercideae are restricted to Australia and New Caledonia and are inferred to have diversified entirely within Australia (Appendix A.2). Our study shows the importance of events at a global scale, but we acknowledge the need for future studies with a finer division of the regions, especially of South America, given its importance in the Solanaceae history. Such a division would likely reveal that many of these speciation events are actually associated with shifts in geographical range not revealed in our continental-scale analysis (see also Sanmartin [198]).

Among the remaining types of events, we found that dispersal was the principal driver of range evolution, occurring about six times more often than vicariance. While vicariant events appear to have been important for range evolution in many animal groups (e.g., Giribet [68]), dispersal seems to be the most common factor shaping the distribution of plant clades, even those whose origins

date to Pangaea or Gondwana (Sanmartin [198]). In the case of the Solanaceae, the crown age for the family is roughly 60 Myr after the separation of South America and Africa, making Gondwanan vicariance a less likely explanation for the family’s pantropical distribution. Indeed, we inferred multiple dispersal events between South America and the Old World (Fig. 1.4, 1.5), and these are confined to the last 15 Myr of the Solanaceae evolution (Fig. 1.3).

Dispersal events between both proximate and distant regions appear to have been frequent in the history of the Solanaceae and they may have been facilitated by colonization of similar niches. For example, the genus *Lycium*, distributed across all of the recognized regions except for Central America (Appendix A.2, Table S1.2 in Appendix A.1), is restricted to dry habitats (Levin [117]). Moreover, all of the species inferred to show recent range expansions along their terminal branch (Fig. 1.3) are found in a single type of terrestrial ecoregion (e.g., dry, tropical, or temperate), with the vast majority (80%) from wet tropical areas (Table S1.7 in Appendix A.1). This pattern of niche conservatism has been documented in many plant groups (e.g., Francisco-Ortega [59], Martinez-Meyer [129]), leading to the idea that, at least in some clades, it is easier to move than to evolve (Edwards [54]). In Solanaceae, additional studies will be needed to assess the extent of niche conservatism and to test the specific factors, biotic or abiotic, that affect colonization of new areas. Certainly, despite the tendency for clades of Solanaceae to be restricted to particular environments (Olmstead [160]), the family as a whole is found in a wide range of habitats, from the driest deserts to wet forests in both tropical and temperate zones, indicating that major niche shifts must have occurred during its history.

1.4.3 Directionality of dispersal events

One of the most striking patterns to emerge from our statistically robust estimation of biogeographical history was the strong asymmetry of dispersals. For every pair of areas considered, transitions were consistently higher in one of the two directions. The directionality was most notable for range expansion events, where for example, dispersals from South America to North America were over four times more common than dispersals in the opposite direction. Similar

patterns of dispersal asymmetry have been observed in other studies at deep as well as recent time scales (Sanmartin [197]; Sanmartin [199]). For example, Bacon [4] found the overall migration rates for animals and plants from South to North America during the last 6 to 7 million years was ca. 30% higher than in the reverse direction.

In the case of Solanaceae, the strong directionality in transitions from South America to other regions may be attributable to the age of the South American lineages and their species richness. As our ancestral range estimations show, the origin and early diversification of the family took place in South America, making this region the principal source for migrants for most of the past 50 Myr (Fig. 1.2, Appendix A.2). In our dataset, South American species comprise roughly half of the taxa (Table S1.4), and also account for roughly half of the dispersal events (Fig. 1.4(a)). We observed a similarly close relationship between the species richness of an area and the number of dispersals out of that area for the all of remaining regions, with the exception of Australia (home to 13% of taxa but only the source for 1% of dispersals, Table S1.4). Although more extensive analyses would be required to formally test the relationship between species richness and dispersal, this congruence suggests that extrinsic explanations, such as directional wind or water currents or migratory paths of dispersers (Renner [191], Sanmartin [199], Gillespie [67]), may not be needed to explain the apparent biases in inter-area movements.

1.4.4 BSM as an approach to estimate biogeographical history of clades

As demonstrated by this study, the application of stochastic mapping to the estimation of biogeographical history gives researchers new power to address questions about patterns of range evolution. Whereas parsimony and likelihood reconstruction provide estimates of ancestral ranges at nodes, stochastic mapping also gives possible histories along branches and at nodes, including any of the events incorporated in the model. By summarizing over many histories, we can extract distributions for the numbers of the events and determine the relative importance of each type of event (e.g., range expansions, vicariance) in shaping present day distributions. Inferring the numbers and types of biogeographical events can also be achieved in a parsimony framework (e.g.,

Sanmartin [198]); however, this approach requires user-defined costs for different events and an inferred area cladogram. Recently developed Bayesian MCMC approaches (Hohna [83], Hohna [84]) could also be used for estimating distributions of event counts and timing of events, and have the benefit of directly incorporating uncertainty in the rate parameters. While implemented models are currently limited to DEC, additional models and tools are likely to be added in the near future (Matzke, pers. comm.).

Although our study used BSM primarily to examine the frequency and directionality of events, this approach could be used to explore other questions, such as how the prevalence of different events (e.g., range expansions or vicariance) varies across clades. Moreover, subsequent studies targeting particular clades could employ a more fine-scale division of geographical areas, revealing dynamics that may not be apparent in this broad family-level analysis. We also envision that future work in biogeography will lead to the extension of the models with additional types of events, and as long as the models are developed in a probabilistic framework, the frequency of these events can be estimated with BSM. Applying these new methods to other plant families of New World origin would provide a powerful test of the generality of the patterns of speciation, dispersal and vicariance that we have inferred for the Solanaceae.

1.5 Acknowledgments

This work was supported by National Science Foundation grants to SDS (NSF DEB-1413855), SK and LB (NSF DEB-0316614), and RGO (NSF DEB-1020369). The authors wish to acknowledge the Research Computing high-performance facilities at University of Colorado Boulder for providing computational assistance. The Solanaceae phylogeny we used was done with support of NSF-DEB-0316614 to LB and SK. NJM and ‘BioGeoBEARS’ were supported by NSF DEB-0919124, the National Institute for Mathematical and Biological Synthesis sponsored by NSF Award EFJ-0832858, with additional support from The University of Tennessee, Knoxville. NJM was also funded by Discovery Early Career Researcher Award DE150101773, funded by the Australian Research Council, and by the Australian National University.

1.6 Tables and figures

Table 1.1. Summary of biogeographical stochastic mapping counts for the Solanaceae using the DEC+ $j+w$ model. Mean numbers of the different types of events estimated are shown here along with standard deviations. No range contractions were estimated because the relevant model parameter (e) was not required in the best fitting model (Table S1.3 in Appendix A.1).

Figure 1.1. Diagrams of different types of biogeographical events allowed in the models tested in this study (adapted from Matzke [135]). Cladogenetic events include within-area speciation, vicariance, and founder events. Anagenetic events include range expansion and range contraction.

Figure 1.2. Maximum likelihood ancestral range estimation in Solanaceae, using the best model DEC+ $j+w$ (model 16 in Table S1.3 in Appendix A.1). This tree is a simplified version of our 1044-tip tree (Fig 1.3, Appendix A.2 & Appendix A.3), and it includes 19 monophyletic groups within Solanaceae, representing either genera (italicized) or higher order taxa (not italicized). The pie diagrams at nodes show the relative probability of the possible states (areas or combinations of areas). The boxes on the right show the native ranges of taxa within these clades, including South America (SAm), Central America (CAm), the Caribbean (Car), North America (NAm), Africa (AF), Eurasia (EU), and Australia (OZ). The asterisk marks the ancestor for the $x=12$ clade, a group that shares the base number of 12 chromosomes and comprises roughly 85% of species in the family (Olmstead [159]). Outgroups are not shown.

Figure 1.3. Representation of timing of dispersal events in the Solanaceae chronogram. Range expansions = thick branches, founder-events = full circles. Transoceanic dispersals are represented in orange and non-transoceanic dispersals in black. Thicker branches and nodes with circles represented here were found in at least 95% of BSM realisations. Clade names follow Fig. 1.2.

Figure 1.4. Number of dispersal events estimated in the history of Solanaceae with biogeographical stochastic mapping. Counts of dispersal events were averaged across the 100 BSMs and are presented here with standard deviations in parentheses. Total event counts are given in (a)

and divided among the two types of dispersals in (b) and (c) (see Fig. 1.1 for depictions of range expansions and founder events). Colour temperature indicates the frequency of events; the warmer the colour, the more common the event. Note that given the standard deviations, values in green are often not different from zero. The ancestral states (where the lineage dispersed from) are given in the row, and the descendant states (where the lineage dispersed to) are given in the column. The sum and correspondent percentages of events involving each area, either as a source for dispersal (the rows) or as a sink (the columns) are given on the margins. Area names in rows and columns are: South America (SAm), Central America (CAm), the Caribbean (Car), North America (NAm), Africa (AF), Eurasia (EU), and Australia (OZ).

Figure1.5. Summary of dispersal events estimated with biogeographical stochastic mapping in the history of Solanaceae. Each of the seven areas in the analysis is shaded by its species richness (Table S1.4 in Appendix A.1), with darker areas being more species rich. Some species are native to more than one area thus contribute to species richness for more than one area. The arrows between areas represent direction and frequency of dispersal events. Only event counts that presented a mean of 0.95 or higher (Fig. 1.4 (a)) are depicted as arrows here; arrow line thickness corresponds to natural log of the events counts.

Table 1.1: Summary of biogeographical stochastic mapping counts for the Solanaceae using the DEC+j+w model. Mean numbers of the different types of events estimated are shown here along with standard deviations. No range contractions were estimated because the relevant model parameter (e) was not required in the best fitting model (Table S1.3 in Appendix A.1).

Mode	Type	Means (StDevs)	%
Within-area speciation	Speciation	883.38 (6.99)	70.11
	Speciation - Subset	79.28 (7.77)	6.29
Dispersal	Founder events	38.26 (4.25)	3.03
	Range expansions	217.55 (4.23)	17.26
	Range contractions	0	0
Vicariance	Vicariance	41.53 (4.18)	3.29
Total		1,260.00 (4.23)	100

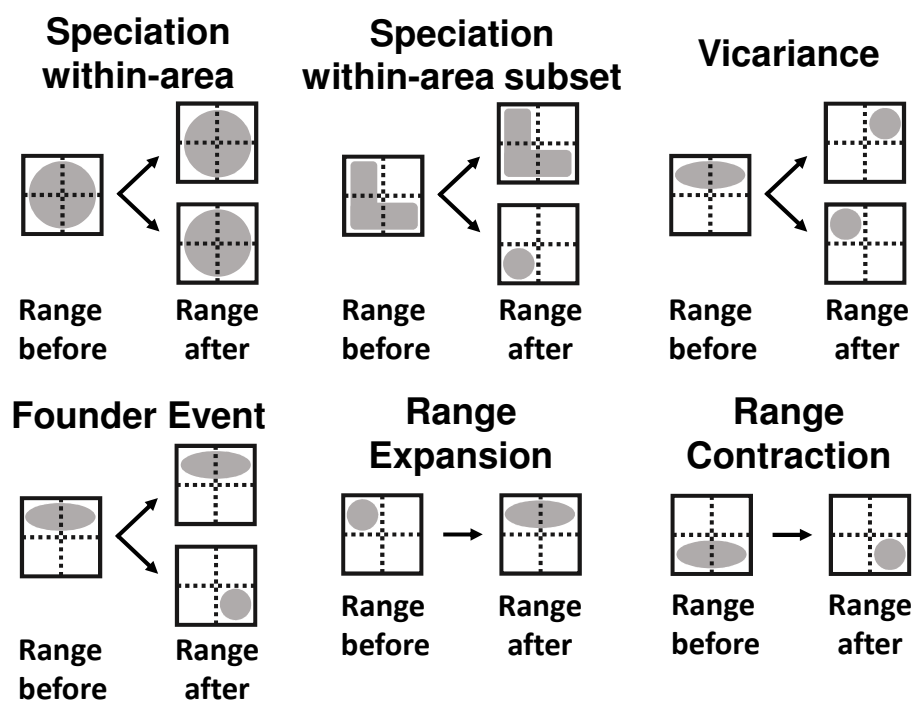


Figure 1.1: Diagrams of different types of biogeographical events allowed in the models tested in this study (adapted from Matzke [135]). Cladogenetic events include within-area speciation, vicariance, and founder events. Anagenetic events include range expansion and range contraction.

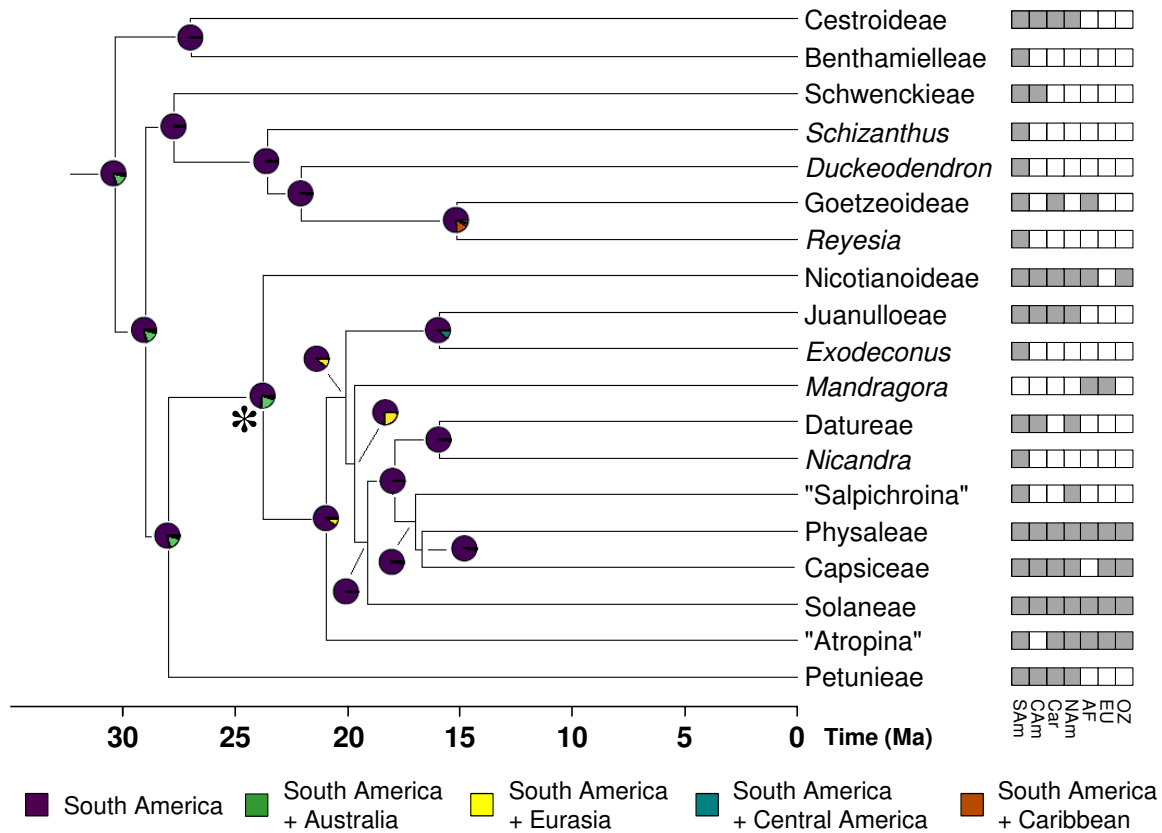


Figure 1.2: Maximum likelihood ancestral range estimation in Solanaceae, using the best model DEC+ j + w (model 16 in Table S1.3 in Appendix A.1). This tree is a simplified version of our 1044-tip tree (Fig 1.3, Appendix A.2 & Appendix A.3), and it includes 19 monophyletic groups within Solanaceae, representing either genera (italicized) or higher order taxa (not italicized). The pie diagrams at nodes show the relative probability of the possible states (areas or combinations of areas). The boxes on the right show the native ranges of taxa within these clades, including South America (SAM), Central America (CAM), the Caribbean (Car), North America (NAM), Africa (AF), Eurasia (EU), and Australia (OZ). The asterisk marks the ancestor for the $x=12$ clade, a group that shares the base number of 12 chromosomes and comprises roughly 85% of species in the family (Olmstead [159]). Outgroups are not shown.

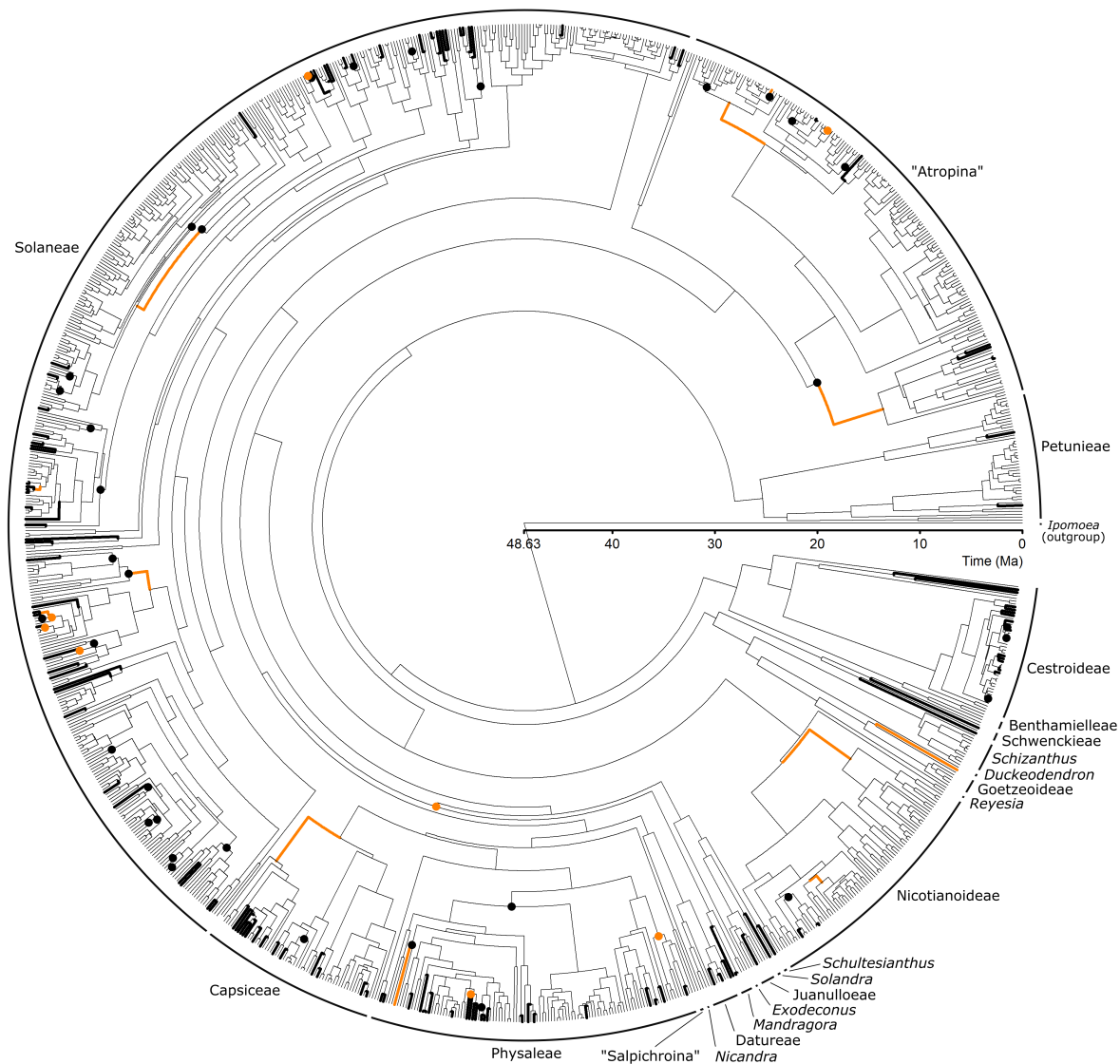


Figure 1.3: Representation of timing of dispersal events in the Solanaceae chronogram. Range expansions = thick branches, founder-events = full circles. Transoceanic dispersals are represented in orange and non-transoceanic dispersals in black. Thicker branches and nodes with circles represented here were found in at least 95% of BSM realisations. Clade names follow Fig. 1.2.

(a) Summary of dispersal events counts (and standard deviations)

	SAm	CAm	Car	NAm	AF	EU	OZ	
SAm	-	48.6 (2.63)	15.13 (1.62)	41.65 (2.83)	5.67 (0.89)	5.03 (1.14)	3.58 (0.77)	119.66 47%
CAm	11.35 (2.32)	-	10.12 (1.41)	23.26 (4.21)	0.22 (0.19)	0.35 (0.34)	0.32 (0.31)	45.62 18%
Car	1.21 (0.94)	4.20 (1.14)	-	3.09 (1.02)	0.22 (0.27)	0.11 (0.17)	0.14 (0.08)	8.97 4%
NAm	9.12 (1.51)	32.44 (4.01)	7.39 (1.20)	-	0.59 (0.29)	2.33 (0.78)	1.34 (0.52)	53.21 20%
AF	0.03 (0.21)	0.04 (0.22)	0.07 (0.33)	0.13 (0.31)	-	10.15 (1.39)	3.89 (0.83)	14.31 6%
EU	0.09 (0.22)	0.08 (0.32)	0.11 (0.21)	1.17 (0.32)	8.28 (1.32)	-	1.78 (0.37)	11.51 4%
OZ	0.06 (0.12)	0.04 (0.21)	0.04 (0.11)	0.12 (0.34)	1.39 (0.71)	0.88 (0.27)	-	2.53 1%
	21.86 9%	85.4 33%	32.86 13%	69.42 27%	16.37 6%	18.85 8%	11.05 4%	255.81 100%

(b) Range expansion event counts (and standard deviations)

	SAm	CAm	Car	NAm	AF	EU	OZ	
SAm	-	45.79 (3.51)	12.52 (1.9)	30.01 (3.24)	3.16 (1.42)	2.2 (1.29)	2.61 (1.03)	96.29 44%
CAm	10.7 (2.58)	-	9.11 (2.09)	22.23 (4.41)	0.17 (0.44)	0.28 (0.53)	0.3 (0.48)	42.79 20%
Car	1.15 (1.03)	3.78 (1.65)	-	2.94 (1.51)	0.22 (0.46)	0.09 (0.32)	0.14 (0.4)	8.32 4%
NAm	7.88 (2.01)	31.81 (4.25)	6.53 (1.7)	-	0.32 (0.55)	1.16 (0.91)	0.71 (0.77)	48.41 22%
AF	0.02 (0.14)	0.04 (0.2)	0.06 (0.24)	0.12 (0.33)	-	8.24 (1.88)	1.31 (1.13)	9.79 4%
EU	0.07 (0.26)	0.07 (0.26)	0.11 (0.31)	0.74 (0.71)	8.02 (1.52)	-	1.2 (0.88)	10.21 5%
OZ	0.05 (0.22)	0.04 (0.2)	0.04 (0.2)	0.12 (0.33)	0.93 (0.88)	0.56 (0.72)	-	1.74 1%
	19.87 9%	81.53 37%	28.37 13%	56.16 26%	12.82 6%	12.53 6%	6.27 3%	217.55 100%

(c) Founder event counts (and standard deviations)

	SAm	CAm	Car	NAm	AF	EU	OZ	
SAm	-	2.81 (1.71)	2.61 (1.26)	11.64 (2.51)	2.51 (1.25)	2.83 (1.12)	0.97 (0.74)	23.37 61%
CAm	0.65 (0.78)	-	1.01 (1.24)	1.03 (0.92)	0.05 (0.22)	0.07 (0.26)	0.02 (0.14)	2.83 7%
Car	0.06 (0.24)	0.42 (0.59)	-	0.15 (0.36)	0 (0)	0.02 (0.14)	0 (0)	0.65 2%
NAm	1.24 (1.07)	0.63 (0.84)	0.86 (0.51)	-	0.27 (0.47)	1.17 (0.79)	0.63 (0.54)	4.8 13%
AF	0.01 (0.12)	0 (0)	0.01 (0.13)	0.01 (0.11)	-	1.91 (0.89)	2.58 (0.91)	4.52 12%
EU	0.02 (0.14)	0.01 (0.12)	0 (0)	0.43 (0.54)	0.26 (0.65)	-	0.58 (0.54)	1.3 3%
OZ	0.01 (0.12)	0 (0)	0 (0)	0 (0)	0.46 (0.56)	0.32 (0.47)	-	0.79 2%
	1.99 5%	3.87 10%	4.49 12%	13.26 35%	3.55 9%	6.32 17%	4.78 12%	35.26 100%

Figure 1.4: Number of dispersal events estimated in the history of Solanaceae with biogeographical stochastic mapping. Counts of dispersal events were averaged across the 100 BSMs and are presented here with standard deviations in parentheses. Total event counts are given in (a) and divided among the two types of dispersals in (b) and (c) (see Fig. 1.1 for depictions of range expansions and founder events). Colour temperature indicates the frequency of events; the warmer the colour, the more common the event. Note that given the standard deviations, values in green are often not different from zero. The ancestral states (where the lineage dispersed from) are given in the row, and the descendant states (where the lineage dispersed to) are given in the column. The sum and correspondent percentages of events involving each area, either as a source for dispersal (the rows) or as a sink (the columns) are given on the margins. Area names in rows and columns are: South America (SAm), Central America (CAm), the Caribbean (Car), North America (NAm), Africa (AF), Eurasia (EU), and Australia (OZ).

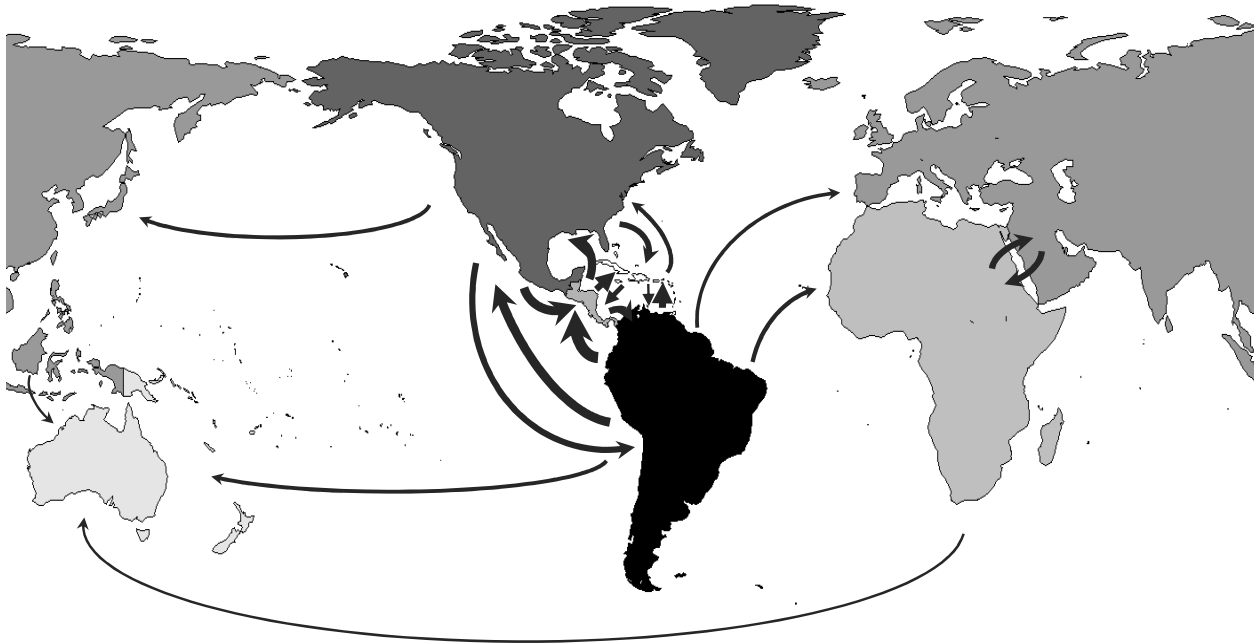


Figure 1.5: Summary of dispersal events estimated with biogeographical stochastic mapping in the history of Solanaceae. Each of the seven areas in the analysis is shaded by its species richness (Table S1.4 in Appendix A.1), with darker areas being more species rich. Some species are native to more than one area thus contribute to species richness for more than one area. The arrows between areas represent direction and frequency of dispersal events. Only event counts that presented a mean of 0.95 or higher (Fig. 1.4 (a)) are depicted as arrows here; arrow line thickness corresponds to natural log of the events counts.

Chapter 2

Phylogenetics of Datureae (Solanaceae), including Description of the New Genus *Trompettia* and Re-circumscription of the Tribe

[Manuscript to be submitted to the Taxon journal]

2.1 Introduction

Building on decades of molecular systematics research in Solanaceae, recent family-level phylogenies include over 40% of the roughly 2800 species and representatives of nearly all of the recognized genera (Olmstead [161]; Särkinen [200]; Ng [151]). Many of the major clades within the family, like the fleshy-fruited solanoids, have been supported as monophyletic since the earliest phylogenetic analyses (Olmstead [162]; Olmstead [159]) and are characterized by key differences in chromosome number, embryo shape, and fruit type. These diagnostic features had been previously used in family-level taxonomy (D'Arcy [35]; Hunziker [93]), facilitating revision of the traditional classification to create a new, phylogenetically structured classification (Olmstead [163], [161]). Given this well-supported phylogenetic classification, recent systematic studies have focused on tackling resolution of smaller clades through more comprehensive species sampling and increased numbers of loci (e.g., Peralta [174]; Levin [117]; Smith [211]).

The present study focuses on Datureae G. Don, a clade of 18 species sensu (Olmstead [162]). Species of Datureae, commonly known as jimsonweeds and angel trumpets, are easily recognizable due to their showy flowers, which are some of the largest in Solanaceae (Fig. 2.1). Their large flowers have made Datureae popular with horticulturists and gardeners, and indeed, humans have

been interested in this clade for hundreds of years (Schultes [205]). Some species are used by several Native American groups due to their hallucinogenic properties (Lockwood [120]; Schultes [205]), a phytochemical signature shared with many other species in the Solanaceae ([34]). Datureae is also known for its wide geographical distribution. Species comprising this clade range from the Mojave Desert in the southwestern USA to the Andes to southern portions of the Atlantic forest in Brazil. The tribe has two main centers of diversity: the northwestern Andes and Mexico. However, introductions by humans have expanded the native range of several species to other areas in North, Central, and South America, where several species are now commonly seen in disturbed areas.

In addition to being a well-supported clade in phylogenetic studies, Datureae and genera within the tribe can be easily distinguished through a suite of morphological features. Hunziker [93] delimited the tribe Datureae by its unusual contorted-conduplicate corolla aestivation, where the lobes are folded lengthwise and twisted to overlap in bud. Within the tribe, two genera - *Datura* and *Brugmansia* - are defined by fruit type (dry vs. fleshy), fruit shape (fusiform vs. spherical or ovoid), and seed shape (reniform vs. not reniform) (Lockwood [120]; Hunziker [93]). Additionally, characters such as seed margin and presence of elaiosomes help define subclades within *Datura* (Bye [23]). Recent phylogenetic studies (Smith [211]; Olmstead [161]) have concluded that Datureae also includes one species previously described in *Ioichroma*, but which possesses the contorted-conduplicate corolla aestivation diagnostic of Datureae. Here, we place this species in a new monotypic genus, *Trompsettia cardenasiana*, and revise the characters that delimit the tribe and its three included genera.

While the monophyly of Datureae is not contested, additional work is needed to clarify relationships within and among genera. For example, *Brugmansia* has not been the focus of prior phylogenetic analysis even though a taxonomic treatment is available for the genus (Lockwood [120]). Additionally, placement of *Trompsettia cardenasiana* within the tribe remains ambiguous: whereas some authors have placed it as sister to *Brugmansia* (Särkinen [200]), others have resolved it as sister to *Datura* + *Brugmansia* (Ng [151]). Finally, the sister group to Datureae remains unclear. Whereas some previous studies suggested that Datureae may be sister to the Solanoideae

clade containing Solaneae, Capsiceae, and Physaleae; Olmstead [161]; [151]) others have suggested Datureae is sister to the small South American genus *Nicandra* Adans. (Särkinen [200]).

In this study, we infer phylogeny and reconstruct evolution of morphological characters in Datureae (Solanaceae) in order to revise genus-level taxonomy and identify diagnostic characters. We use three nuclear markers to test the placement of *Trompettia cardenasiana* and incorporate fossil information to estimate divergence times in the tribe. We then reconstruct evolutionary history of characters used previously in taxonomic investigation of Datureae. Finally, we combine phylogeny and morphological reconstructions to identify characters diagnostic of clades and present a new classification for the tribe. This phylogenetic framework, which is based on complete sampling of species in Datureae, will facilitate future studies of biogeography, genetics, and biochemistry of this economically important group of plants.

2.2 Materials and Methods

2.2.1 Taxon sampling

In this study, we sampled a total of 26 species: 18 belong to the ingroup and seven representing outgroups (Table 2.1). The ingroup included all 18 species of Datureae: five *Brugmansia*, twelve *Datura*, and one *Trompettia*. Species sampling in *Datura* was based on Bye [23] (note that *D. ferox* was not included here because it was considered as a synonym of *D. quercifolia* as in Symon [217]), and in *Brugmansia* on Lockwood [120], who recognized five species. The outgroup sampling spanned species in six tribes within the subfamily Solanoideae (Capsiceae, Juanulloeae, Lycieae, Nicandreae, Physaleae, and Solaneae), which is the subfamily that includes Datureae, along with one species in the subfamily Nicotianoideae, the sister clade to Solanoideae. Of the total 26 species sampled, we included multiple accessions of 16 out of 18 ingroup species to assess reciprocal monophyly. Our total matrix consisted of 50 accessions (Appendix B.1).

2.2.2 Data Collection

We used several sources of leaf material: field collections, living collections from botanical gardens, specimens grown from donated seeds, and herbarium vouchers. We also obtained extracted DNA from collaborators and utilized Genbank sequences when available (Appendix B.1). For all leaf samples, we extracted total genomic DNA following a modified 2x CTAB protocol (Doyle [48]; Smith [211]).

For phylogenetic inference, we used three nuclear regions: the internal transcribed spacers 1 and 2 plus intervening *5.8S* (ITS; White [237]), the second to ninth exons, and introns, of the granule-bound starch synthase gene region (GBSSI or *waxy*; Peralta [174]), and the second and third exons, and second intron, of the LEAFY gene region (*lfy*; Schultz [206]). These regions have been useful for species level phylogenetics in other clades in the Solanaceae (e.g., Whitson [238]; Smith [211]; Tu [224]).

The ITS+*5.8S* region was amplified and sequenced using four different primers: ITS.leu1 (Andreasen [1]), ITS2 and ITS4 (White [237]), and ITS3B (Baum [8]). We used the following protocol for 25 μ L reactions: 2.5 μ L of 10x PCR Buffer (Qiagen, Valencia, California, USA), 2.5 μ L of 25 mM MgCl₂, 1.0 μ L of Bovine Serum Albumin (BSA), 1.0 μ L of 10mM dNTPs, 1.0 μ L of each primer (10 μ M dilutions), 0.125 μ L of Taq polymerase (5 units/ μ L), and between 10-100ng of template DNA. We used the following PCR program: 95.0°C for 4 min followed by 34 cycles of 95.0°C for 2 min of denaturation, 48.0°C for 1 min of annealing, and 72°C for 1 min of elongation, and finally a final extension of 72°C for 5 min.

The *waxy* region was amplified and sequenced using the primers *waxy5'*, *waxy3'* and *waxyB* developed by Peralta [174] and Spooner (2001), and *waxyF41*, *waxyF420* and *waxyR991* developed by Smith [211]. The protocol for *waxy* is similar to that of ITS+*5.8S* except we used only 2.0 μ L of 25 mM MgCl₂ and added 1.0 μ L of Q solution (Qiagen). We used the following PCR program: 95.0°C for 4 min, then 35 cycles of 95.0°C for 45s of denaturation, 52.0°C for 1 min of annealing, 72°C for 2 min of elongation, and finally a final extension of 72°C for 5 min.

The *lfy* region was amplified and sequenced using primers developed for this study (Appendix B.2). To accomplish this, we used transcriptome sequences for different *Datura* species as reference to design primers (transcriptome sequences available through the Medicinal Plants Transcriptome project, <http://apps.pharmacy.uic.edu/depts/pcrps/MedTranscriptomePlants>). The PCR protocol for *lfy* was the same as that for *waxy*, but we adjusted the annealing temperature depending on the primer pair used.

All PCR products were sequenced in both directions using ACGT Inc. sequencing services (Wheeling, Illinois, USA). The resulting sequences were manually edited in 4Peaks v1.7 and assembled into contigs using the MUSCLE online alignment tool (Edgar [53]) and secondarily edited in Mesquite v3.10 (Maddison [126]).

We used the $g1$ statistic (Hillis [82]) to assess phylogenetic signal in our datasets. This parsimony-based statistic measures the skew in the distribution of tree lengths for a set of random trees using the observed data; datasets with phylogenetic signal are expected to be left-skewed, with an excess of short (more-parsimonious) trees. For each of our datasets (ITS+*5.8S*, *lfy* and *waxy*), we estimated $g1$ using 10,000 randomly-drawn trees in PAUP* v4.0a150 (Swofford [216]) with significance levels based on Hillis ([82]).

2.2.3 Phylogenetic inference

We conducted three different phylogenetic analyses: analysis of the entire dataset using parsimony to yield initial phylogenetic hypotheses and to assess congruence between individual datasets conducted in PAUP* v4.0a150 (Swofford [216]); analysis of *Datura*-only sampling to assess gene tree-species tree conflict using starBEAST (Ogilvie [158]); and, Bayesian divergence time analyses on the combined dataset using two sets of fossils conducted in BEAST2 (Bouckaert [15]).

For the parsimony analysis, we built 50% majority rule consensus trees for each nuclear region separately using PAUP* v4.0a150 (Swofford [216]). Clade support was estimated through heuristic search with 1000 bootstrap replicates, each with 10 random sequence additions and tree-bisection-reconnection (TBR) branch swapping. For ITS+*5.8S* and *waxy*, the consensus tree included all

26 taxa. For *lfy*, it included 13 ingroup taxa. This latter reduction was due to a lack of complete *lfy* sequences for five species (*B. suaveolens*, *B. versicolor*, *D.lanosa*, *D. metel*, *D. reburra*) as well as difficulty aligning *lfy* sequences outside of Datureae given high variation in the intron. Next, we compared consensus trees for the three nuclear regions to identify cases of hard incongruence (conflicting clades with bootstrap support (BS) greater than or equal to 70%; Mason-Gamer[132]). This assessment was done in two steps: first, via a comparison between the consensus trees of ITS+5.8S and *waxy* that included all 26 taxa, and second via a comparison between all three region consensus trees but with a reduced dataset of 13 taxa to match all the species included in the *lfy* consensus tree.

Given minor instances of hard incongruence among gene trees for *Datura* (see results), we estimated the phylogeny of this genus only with the combined dataset of all three regions using methods that accommodate discordance. We implemented starBEAST2 (Ogilvie [158]), an extension of BEAST2 (Drummond [50]; Bouckaert [15]) that facilitates joint inference of a species tree topology and gene trees from multiple genes while allowing for potential conflicts in the estimated gene topologies. We included multiple samples for most species (with the exception of *D. arenicola* and *D. discolor* for which we had only one sample each) to assess reciprocal monophyly of species. Within starBEAST, we created 5 partitions: ITS+5.8S, *lfy*.exons, *lfy*.intron, *waxy*.exons and *waxy*.introns. For the *lfy* and *waxy* regions, we considered exons and introns as separate partitions to account for potential variation in rates and patterns of substitution among sites. The same was not done for ITS+5.8S given the small length of the 5.8S coding region (≈ 150 bp). Although introns and exons were input separately, we linked the molecular clocks and estimated linked trees for exons and introns belonging to the same region, as they are expected to share the same history. The substitution models for each partition were determined using Likelihood Ratio Tests (LRTs), where the following models were considered: JC, K81, HKY85, HKY85 + Γ , HKY85 + Γ + I, GTR, GTR + Γ , and GTR + Γ + I. The best fitting likelihood models for each partition are presented in Table 2.2. starBEAST2 also requires priors for the individual gene trees, along with a prior for the species tree. For the gene trees, under “multispecies coalescent models”, we chose the ‘Linear with

constant root populations' option that allows population size changes over time through the act of smooth (i.e., not abrupt) changes. We used an uncorrelated lognormal clock model to describe the branch-specific substitution rates for all partitions (Drummond [49]). Finally, for our species tree, we specified a Birth-Death prior.

After assessing congruence and addressing the conflicts within *Datura*, we estimated the phylogeny of Datureae and divergence times within the lineage using a Bayesian approach implemented in BEAST2 (Bouckaert [15]). We incorporated the starBEAST2 results (see below) into this divergence time analysis by constraining two *Datura* clades with high posterior probability (>95%) to be monophyletic (1: *D. arenicola*, *D. discolor*, *D. quercifolia* and *D. stramonium*, and 2: *D. inoxia*, *D. kymatocarpa*, *D. metel*, *D. lanosa*, *D. leichhardtii* ssp. *pruinosa*, *D. reburra* and *D. wrightii*). Given reciprocal monophyly of species in the starBEAST2 results, we used a single individual to represent each taxon for the divergence time analysis. We input the individual alignments in the same fashion as for starBEAST2, including the same substitution models and linkage of molecular clock and trees for exons and introns belonging to the same region. We used an uncorrelated, lognormal relaxed clock model to describe the branch-specific substitution rates (Drummond [49]) and a Birth-Death tree prior. We carried out three MCMC runs for 35 million generations each, sampling every 1000 generations. Convergence and stationarity of the parameters were assessed using Tracer v1.6 (Rambaut [187]) and LogCombiner (part of the BEAST2 package), targeting minimum effective sample sizes (ESS) for all variables of at least 200. Finally, we used TreeAnnotator (part of the BEAST2 package), discarding a burn-in of the first 25% of trees, to construct a maximum clade credibility (MCC) tree that included the median value for node ages, 95% highest posterior density (HPD) of divergence times, and posterior probabilities (pp) for all nodes.

For fossil calibrations, we incorporated fossil ages as node priors with log-normal distributions. The first fossil we used is a macrofossil (seed) identified as *Datura* cf. *stramonium* by Velichkevich [225]. Based on its reniform shape, its thick testa of dark coloration with numerous, irregular, shallow pits, a small incision, and lack of a convex margin triple-ridge, Velichkevich [225] assigned this fossil to the crown clade formed by *D. stramonium* and *D. quercifolia*. Since the mentioned

study was published, a new species of *Datura* has been described, *D. arenicola* (Bye [23]), whose seeds also resemble the macrofossil in all morphological aspects listed above except that it has a larger incision. Because *Datura arenicola* does not form a clade with *D. stramonium* and/or *D. quercifolia*, we chose to use the fossil age, between 3.6 and 2.6 million years ago (Ma), as a minimum age reference for the crown age of the entire *Datura* genus. The second fossil calibration was a set of macrofossils recently described as a *Physalis* species (Wilf [240]). The macrofossils (fruits) have an estimated minimum age of 52.2 Ma. Even though the fossils are assigned to *Physalis*, we here used it as a prior to constrain the Solanoideae node for two reasons. First, *Physalis* is paraphyletic (Olmstead [161]; Särkinen [200]) and overall the phylogeny of Physaleae, which includes many other taxa with similarly inflated calyces, is poorly resolved (Whitson [238]; Ng [151]). Second, the primary character used to identify the fossils as *Physalis* - the presence of an inflated calyx - may be plesiomorphic in Solanoideae. Indeed, this character occurs in multiple Solanoid lineages, including Hyoscyameae, Juanulloae, Nicandreae, Solaneae and Withaninae (He [77]; Hu [89]).

2.2.4 Character Evolution within Datureae

We estimated the history of character changes for seven traits: flower orientation (pendant vs. erect), flower pigmentation (presence of anthocyanins vs. absence), fruit type (fleshy vs. dry) and fruit shape (fusiform vs. round/ovoid), seed elaiosomes (presence vs. absence), seed margin type (single ridge vs. triple ridge margin, see diagram in Taxonomic key below), and life history (perennial vs. annual/bi-annual). We defined this set of characters based on significance to Solanaceae (Hunziker [93]) and Datureae (Lockwood [120]; Bye [23]) taxonomy. We scored character states based on species descriptions and observations of living and herbarium collections.

For ancestral state reconstructions, we used a pruned version of the MCC tree estimated here. This pruned tree included all Datureae species and the inferred sister group, *Nicandra*. We carried out these analyses using the R (R Core Team [184]) packages 'ape' v4.1 (Paradis[167]) and 'phytools' v0.5-64 (Revell [193]). For each character separately, we first compared models that assumed equal rates of transition between character states or different rates (using the function

ace in 'ape'). The likelihood of each model was estimated and compared using a likelihood ratio test. Once we identified the best model, we estimated the history of each character using the function `make.simmap` in 'phytools'. This function uses stochastic character mapping (Nielsen [152]; Huelsenbeck [90]) to sample states at ancestral nodes and build possible histories for a given character. For each of our characters, we simulated 100 histories and summarized the results at each node to give the relative posterior probability at each state.

2.3 Results

2.3.1 Assessment of congruence among datasets

Our results suggest little incongruence among the three nuclear regions. The individual consensus trees showed no conflict among the datasets regarding the position of *Trompettia cardenasiana*, the monophyly of the two genera, or the sister group to Datureae. Nonetheless, there was variation in resolution and phylogenetic signal that the individual datasets provided (see Fig. 2.2 for individual consensus trees and Table 2.2 for summary statistics). The only instance of hard incongruence (BS > 70%) was between ITS+5.8S and *waxy*, which yielded conflicting information regarding the position of two clades: (1) *Datura stramonium* and *D. quercifolia* and (2) *D. kymatocarpa* and *D. leichhardtii* ssp. *pruinosa*. In ITS+5.8S these four taxa form a clade while in *waxy* they do not (Fig. 2.2). Our combined starBEAST2 analysis, which estimated the species tree topology while allowing for gene tree conflict, supported the *waxy* topology where *D. stramonium*, *D. quercifolia*, *D. kymatocarpa* and *D. leichhardtii* ssp. *pruinosa* do not form a clade (Appendix B.3).

2.3.2 Phylogenetic relationships and divergence times in Datureae

Our Bayesian analysis of the combined dataset yielded a MCC tree in which *Datura* and *Brugmansia* were resolved as monophyletic with strong support (posterior probability [pp] of 1.0), with *Trompettia cardenasiana* as sister to the two (Fig. 2.3). The combined dataset analysis is

mostly driven by the patterns seen in the *waxy* dataset. The sister group to the tribe was well supported as *Nicandra physalodes* (0.97 pp). Our analyses resolved two major clades within *Datura* (Fig. 2.3). The first clade comprised *D. wrightii*, *D. lanosa*, *D. metel*, *D. reburra*, *D. kymatocarpa*, *D. inoxia*, and *D. leichhardtii* ssp. *pruinosa* while the second clade was formed by *D. stramonium*, *D. quercifolia*, *D. discolor*, and *D. arenicola*. *Datura ceratocaula* was well supported as sister to all other *Datura* species. These relationships differ from those of Bye [23] except in the position of *D. ceratocaula* as sister to the rest. Only two nodes within *Datura* were marked by low pp values (0.5 and 0.52; Fig. 2.3). We attribute these to the lack of variation in ITS+*5.8S* and *waxy* sequences for many species in *Datura* along with the missing *lfy* sequences for three species in *Datura* (*D. lanosa*, *D. metel*, and *D. reburra*). Within *Brugmansia*, our analyses resolved two clades with strong support, the first comprising *B. arborea* and *B. sanguinea* and the other containing *B. suaveolens* and *B. versicolor* as sister species, with *B. aurea* sister to the pair (Fig. 2.3).

The divergence time estimates placed the origin of subfamily Solanoideae in the Eocene (ca. 54 Ma) and early stages of diversification of Datureae in the late Eocene to early Oligocene (Fig. 2.3; see Appendix B.4 for divergence dates with confidence intervals). The median age of the crown Datureae, and *Trompettia*, was estimated as 34.7 Ma (95% HPD interval: 23.8-46.8 Ma). The split between *Datura* and *Brugmansia* was estimated as 28.5 Ma (95% HPD interval: 18.7-39.2 Ma), during the middle Oligocene (Fig. 2.3). Major splits within these two genera were inferred to occur during the Miocene (between 10 and 18 Ma; Fig. 2.3).

2.3.3 Character evolution

Many of the characters analyzed in this study were diagnostic for clades or subclades of Datureae and thus may be useful for classification (Fig. 2.4). Flower orientation, fruit type and life history characters distinguish *Datura* from *Brugmansia* and *Trompettia*. These three traits show the same pattern where one transition between states is estimated along the *Datura* stem lineage (Fig. 2.4). The remaining four characters vary within the genera, and most are associated with particular subclades. For example, fusiform fruit shape is diagnostic for the *B. versicolor*

and *B. suaveolens* lineage, with one change inferred along their stem branch. Within *Datura*, seed margins with a triple ridge are present only in the clade containing *D. metel*, *D. wrightii*, *D. lanosa*, *D. reburra*, *D. kymatocarpa*, and *D. inoxia*, although this state has apparently been lost in *D. kymatocarpa*. In addition, the clade comprising *D. wrightii* and *D. lanosa* (Fig. 2.4) is the only lineage of *Datura* that lacks elaisosomes. Compared to these characters, flower pigmentation (presence of anthocyanins vs. absence) was highly homoplastic across the phylogeny, and thus is not likely to be of taxonomic utility (Fig. 2.4).

2.4 Discussion

Our molecular results show that Datureae is formed by three genera: *Datura* and *Brugmansia*, which are sister taxa, and the monotypic genus *Trompettia*, which is sister to both other genera. The placement of *Trompettia* is furthermore supported by our comparison of morphological features among the genera. Diversification analysis here demonstrate that Datureae started diversifying around 35 Ma, likely in dry areas in the central and southern Andes. Finally, our results show that evolution of numerous morphological characters (e.g., transition from fleshy to dry fruits and from pendant to erect flowers) within the tribe happened along the branch giving rise to *Datura*.

2.4.1 Phylogenetic Relationships

Our study supports the placement of Datureae within subfamily Solanoideae and recovered most of the major relationships among Solanoids identified in previous studies. As in Olmstead ([161]) and Särkinen ([200]), the lineage containing *Lycium* is sister to all other species in Solanoideae, and *Physalis* plus *Capsicum* form a monophyletic group (Fig. 2.3). The position of some of the outgroup taxa (*Mandragora*, *Juanulloa*) differ from previous studies, but it does not conflict prior results. Thus, our analyses do not present any instances of hard conflict in terms of the outgroup taxa compared with other recent phylogenies (Olmstead [161] and Särkinen [200]).

We also recovered *Nicandra* as the sister clade to the monophyletic Datureae, as in Särkinen ([200]). Like *Trompettia* and some species of *Brugmansia*, *Nicandra* has an Andean distribution,

with its three described species occurring from Peru to northern Argentina (Hunziker [93]; Leiva Gonzalez [111]; Leiva Gonzalez [112]). The genus has many unique features (a 3 to 5-carpellate gynoeceium, auriculate calyx segments, imbricate-plicate corolla aestivation) and has thus been placed in its own tribe, Nicandreae (Wettstein [235]). Beyond these characters, *Nicandra* shares many features in common with Datureae. Additional studies may seek to identify morphological synapomorphies that unite *Nicandra* with Datureae.

Within Datureae, our analysis confirms the monophyly of each genus and places *Trompettia* as sister to the remaining two. The monophyly of the genera in Datureae, once disputed based on morphological characters (Persoon [176]; Bernhardt [12]; Safford [196]; Barclay [5]), has been supported in multiple studies (Bye [23]; Särkinen [200]; Ng [151]) and is corroborated here with comprehensive species sampling. By contrast, the position of *Trompettia* has varied across analyses, sometimes appearing as sister to *Brugmansia* (Särkinen [200]). Our molecular phylogenetic analysis confidently places *Trompettia* within the tribe as sister to both *Datura* and *Brugmansia*, as demonstrated in Ng [151]. While the MCC combined analysis result is likely driven by the *waxy* dataset, the integration of the molecular analysis with the analysis of the several shared morphological features prompts our establishment of a new genus to accommodate this monotypic lineage (see Taxonomic Innovations).

While many of the clades that we inferred mirror those in prior studies, relationships within *Datura* differ markedly from those presented in previous analyses. Bye [23] also sampled all species of *Datura* and defined two major sections within *Datura*: *Dutra* and *Datura*. Our study failed to recover monophyly of species representing these two sections (Fig. 2.3). These different outcomes likely relate to the markers used (plastid DNA in Bye [23]; nuclear in the present study) and may reflect introgression or incomplete lineage sorting (Soltis [212]; Wendel [234]). Nonetheless, both our study and that of Bye [23] recovered *D. ceratocaula* as sister to all other species in the genus, suggesting concordance along some branches. Future phylogenetic work within the genus would benefit from the inclusion of more accessions of each species, a greater number of markers, and the application of methods that allow for a mix of both reticulate and divergent processes (e.g. Eaton

[52]).

Although this study represents the first comprehensive molecular phylogenetic analysis of *Brugmansia*, relationships within the genus recovered here were similar to those proposed by Lockwood [120] in his monographic treatment. Based on morphology, geographical distribution, and crossing experiments, Lockwood [120] divided the genus into two informal groups: *B. suaveolens* and *B. versicolor* from the Amazonian and Ecuadorian lowlands, and *B. arborea*, *B. sanguinea*, and *B. aurea* from high elevations in the northern and central Andes. The concordance of our phylogeny with the distribution of the taxa suggests that geographic isolation may have played a key role in the divergence of these lineages.

2.4.2 Dating the Diversification of Datureae

Divergence time estimates within Solanaceae have been challenging because of the scarcity of fossils that can be confidently assigned to the family or clades within it. Here, we incorporate recently described fruit macrofossils (Wild [240]) into divergence time analyses and recover dates that are older than those estimated in previous studies (Särkinen [200]; De-Silva [44]). Although we conservatively assigned these fruit fossils to the Solanoideae stem lineage, they are roughly twice as old as any of the fossils previously used to calibrate this node (52.2 Ma vs. 28 Ma, Särkinen [200]). With our two calibration points (the *Datura* seed fossil of 3.6 Ma and the fruit macrofossils of 52.2 Ma), we estimate a crown age for Datureae of 34.7 Ma (95% HPD interval: 23.8-46.8 Ma; Fig. 2.3). This compares to 8.5 Ma (95% HPD interval: 5.5-11.7 Ma) in Särkinen ([200]) and 11.5 Ma (95% HPD interval: 6.8-17.4 Ma) Ma in De-Silva [44] who used secondary calibrations from an angiosperm wide analysis (Magallón [127]).

Although divergence times in Solanaceae are likely to remain contentious until more fossils are described, the older dates we estimate for cladogenetic events in Datureae are well aligned with major changes in the global climate and geological events in the Americas. The Andean uplift began roughly 40 Ma (Sebrier [207]; Ege [55]; Graham [73]), with the diversification of Datureae starting soon thereafter, around 35 Ma. The rise of the Andes created new habitats and new

ecological opportunities that fostered speciation (Pennington [173]; Särkinen [200]). Moreover, around the same time, which corresponds to the late Eocene/early Oligocene boundary, there was a major shift from a global “greenhouse” climate to an “ice-house” climate (Prothero [183]). This decrease in mean temperatures and increase in seasonality (Zachos [246]; Zachos [247]) was already a trend in the global climate and the proportion of global areas with arid, cooler, open-habitat environments was closer to what we observe today (Prothero [183]; Stromberg [214]). The distribution of *Trompettia cardenasiana* in the dry, central Andes as well as *Nicandra physalodes* in similar dry areas in the central and southern Andes suggests that the ancestor of Datureae was adapted to dry environments. The expansion of seasonal areas that occurred during the Oligocene could have contributed to the expansion of ancestral populations into other areas of South America and North America, where the *Datura* species are most species-rich today.

2.4.3 Character Evolution

The evolution of Datureae is marked by major transitions in morphology and life history, which may be driven by differences in geographical distribution and habitat. The woody, perennial taxa (*Brugmansia* spp. and *Trompettia*) are native to tropical regions of the Americas, while the herbaceous, annual taxa (*Datura* spp.) are distributed in dry, seasonal areas of Mexico and the southwestern United States. Correlated shifts in life history and habitat seasonality have been observed in many other plants groups, such as Onagraceae and Asteraceae (Evans [58]; Cruz-Mazo [33]). Annual habit likely evolves as an adaptive response to seasonal or unpredictable environments, where the shift represents a defense against conditions that would adversely affect adult perennial plants (Friedman [60]).

In *Datura*, the transition to seasonal dry areas has also been accompanied by changes in reproductive traits. All species in the genus produce capsules, unlike the rest of Datureae, and many release seeds with elaiosomes. Within Solanaceae, the production of elaiosomes is exclusive to *Datura* and is associated with dispersal by ants (O’Dowd [157]; Marussich [130]). Elaiosomes have evolved at least 100 times in angiosperms, often in seasonal, northern hemisphere taxa like *Datura*

and several genera in the Asteraceae, Fabaceae and Malvaceae families, to cite a few examples (Lengyel [114]; Lengyel [115]). *Datura* also shows a shift toward erect flowers, with one exception, *D. ceratocaula*, whose flowers are oriented at roughly 90 degrees from the branch. Erect or semi-erect flowers in short shrubs are advantageous for pollination by moths, which are common floral visitors in open, dry areas, and indeed the principal pollinators of *Datura* are hawkmoths (Raguso [186]; Bronstein [18]). Although less is known about pollination of *Brugmansia* and *Trompsettia*, the pendant flowers, which are fragrant in some species, are likely visited by moths, bats, and/or hummingbirds (Lockwood [120]; Knudsen [107]; Weiss [233]).

2.4.4 Taxonomic Implications

The separation of *Datura* and *Brugmansia* has long been a topic of debate in the taxonomic literature. *Datura* was described in 1753 by Linnaeus based on the type species, *D. stramonium*. Subsequently, Persoon [176] transferred *D. arborea* to a new genus, *Brugmansia*, based on its persistent calyx with a lateral split, and non-spiny, bilocular fruits. This separation was subsequently rejected by many others (e.g., Bernhardt [12]; Safford [196]; Barclay [5]) because some of the diagnostic characters could also be found in one *Datura* species, *D. ceratocaula*. Specifically, *D. ceratocaula* produces fruits with smooth surfaces that do not completely dry before dehiscing and a fugacious calyx once fruit development initiates. This combination of characters is intermediate between species of *Datura*, which have dry, spiny, dehiscent fruits without persistent calyces and species of *Brugmansia*, which for the most part have fleshy, smooth, indehiscent fruits with persistent calyces. Hence, *D. ceratocaula* was seen by Bernhardt [12], Safford [196], and Barclay [5] as an irrevocable link between *Datura* and *Brugmansia*, justifying the argument to maintain all the species as belonging to a single genus. Only with the work of Lockwood [120] did the recognition of the generic rank of *Brugmansia* become more popular. In addition to their many differences in habit, longevity, habitat, fruit type, flower position, and seed morphology (Table 2.3), species in the two genera have proved extremely difficult to cross artificially (Carson [25]; Joshi [103]). The position of *D. ceratocaula* as sister to all other *Datura* species (see Fig. 2.3; see also Bye [23])

reaffirms that this species should be treated in *Datura*. Its unique combination of characters may represent changes specific to its lineage and/or retention of ancestral or intermediate states (e.g., smooth fruits, incomplete dehiscence).

Given the distinctiveness of *Trompettia* we recognize it was a third lineage in Datureae, as a new genus. When first described (Hunziker [92]), *T. cardenasiana* was placed in *Iochroma* due to morphological similarities with other species in the Iochrominae such as size of the flower, its infundibuliform (trumpet-shaped) corolla, and its geographical distribution. However, the lack of flower buds, fruits, and seeds on the type specimen prevented comprehensive comparison of this species to other species in *Iochroma* and other genera. Even though *T. cardenasiana* has fruits that are small, round berries, which are common in Iochrominae and several other clades in Solanoideae, the seeds are tetrahedral and have a thin corky seed coat, very similar to those of *Brugmansia*. Also, the small trumpet-shaped flowers of *T. cardenasiana* have distinctly flared corolla lobes that are arranged in a contorted-conduplicate fashion in the bud, a character diagnostic of Datureae. These features support a close relationship of *Trompettia* to remaining Datureae, as further emphasized by our molecular data. *Trompettia* can, however, easily be distinguished from *Datura* and *Brugmansia* by several features, in particular the size of flowers and fruit and the distinct form of the fruiting calyx (Table 2.3). Additionally, *T. cardenasiana* has a very restricted distribution in the southern parts of Bolivia, which does not overlap with the native ranges of species of *Datura* or *Brugmansia* in the north and central Andes, Central America, and southern parts of North America.

Below, we describe *Trompettia* and make the new combination. We then formally re-circumscribe Datureae to include all through genera and their species. Finally, we provide a taxonomic key to identify species of Datureae worldwide.

2.5 Taxonomic Innovations

Trompettia J. Dupin, **gen. nov. ined.** (ICN Article 30.8, McNeill [139])

TYPE: *Trompettia cardenasiana* (basionym: *Iochroma cardenasiana* Hunz.)

Perennial shrubs with simple and alternate leaves. Flowers solitary in leaf axils, pedicellate, and pendant. Corollas infundibuliform. Stamens five, filaments adnate to basal portion of corolla tube, included entirely within the corolla. Anthers basifixed, dehiscence latrorse. Ovaries superior, bilocular, surrounded by a nectary at the base, the styles included within corollas. Fruits baccate. Seeds tetrahedral, embryos coiled.

Etymology: The generic name *Trompettia* from the French trompette, diminutive of trompe (horn), alludes to the type species' flowers that are shaped like small trumpets.

Trompettia cardenasiana (Hunz.) J. Dupin, **comb. nov. ined.** (ICN Article 30.8, McNeill [139]) \equiv *Iochroma cardenasiana* Hunz., Kurtziana 10: 21. 1977. TYPE: Bolivia, Dpto. Potosí: Cotagaita, 3000m alt., XII 1932, M. Cardenas 323, (holotype, US-00385907!). EPITYPE in support of the holotype, **designated here**: Bolivia, Dpto. Potosí: Nor Chichas, 3113m, Carretera Potosí-Orkhola-Tumusla, 5 km N of Orkhola, dry west-facing slope with cacti and Acacia, II 2004, S.D. Smith, S. Leiva & S.J. Hall 384 (epitype, MO-1393217!).

Woody shrubs to 2m tall. Stems erect but arching towards apices, many of these becoming spiny, older portions glabrous, becoming pubescent towards younger portions of stem, the internodes 4-35mm long. Leaves borne in clusters on very short shoots (these < 1 mm long), subtended by dense protrusions of trichomes (Fig. 2.5), on short petioles to 5mm long, these pubescent with short eglandular trichomes or glabrous, the blades simple, alternate, narrowly obelliptic to narrowly elliptic, 20-50 x 3-10mm, (2-)4.7 to 7.5 times longer than wide, the bases attenuate, the apices broadly acute to obtuse, the margins entire, both surfaces covered by glandular trichomes (these appearing as black spots on pressed specimens) with occasional sparse simple trichomes along midrib of abaxial surface. Flowers solitary in leaf axils, on pedicels to 6mm long, pubescent with eglandular trichomes, pendant. Calyces 9 to 12mm long at anthesis, the tubes 5-6 x 4-5mm, light green, the

lobes subulate, 5-6mm long, pubescent adaxially, slightly accrescent during fruit maturation and eventually splitting along longitudinal axis to expose mature fruit. Corollas infundibuliform (these more tubular just before anthesis), 30-35mm long including lobes and 12-17mm wide at the mouth, yellow (paler at base, becoming more vibrant towards apex), the lobes 2-4 x 7-10mm, primary lobe veins extending into acuminate tip, external surfaces pubescent with uniformly distributed short, eglandular trichomes. Stamens 5, the filaments 22-25mm, adnate to the basal 5-8mm of the corolla tube, free portions 17-19mm, included within corolla, pubescent only along the adnate portion. Anthers 3-4 x 2-2.5mm, basifixed, dehiscence latrorse, glabrous. Ovary superior, bilocular, surrounded by dark red nectary at base, glabrous, the styles 27-29mm, included within the corolla. Fruits baccate, round, 5-10mm wide, immature fruits green turning dark brown in pressed specimens. Seeds tetrahedral, 3-4mm, brown to dark brown, ca. 10-20 per fruit, embryo coiled. Scientific illustration of *Trompettia cardenasiana* in Fig. 2.6.

Notes: Above, we designate an epitype in support of the holotype given that the former contains reproductive structures not present in the holotype and has a greater abundance of vegetative tissue (ICN Article 9.8, McNeill [139]). To reflect a more complete understanding of this species in light of additional material collected since the holotype, we have provided a fuller, revised species description that expands upon the original description presented by Hunziker [92].

At present, there exist only five collections of this *Trompettia cardenasiana*, all deriving from a small region in southern Bolivia in the department of Potosí. This record suggests that the species is rare (albeit still extant) in its native environment. However, we caution that Bolivia remains underexplored botanically such that future fieldwork in the area and surrounding countries may yield discovery of new, additional populations.

2.6 Taxonomic Treatment

Datureae G. Don. 1838. Gen. Hist.: 4, 472.

Brugmansia

Datura

Trompettia

Brugmansia Pers.

Brugmansia arborea (L.) Lagerh.

Brugmansia aurea Lagerh.

Brugmansia sanguinea (Ruiz & Pav.) D. Don

Brugmansia suaveolens (Humb. & Bonpl. ex Willd.) Sweet

Brugmansia versicolor Lagerh.

Datura L.

Datura arenicola Gentry ex Bye & Luna-Cavazos

Datura ceratocaula Ortega

Datura discolor Bernh.

Datura inoxia Mill.

Datura kymatocarpa A.S. Barclay

Datura lanosa Barclay ex Bye

Datura leichhardtii ssp. *pruinosa* (Greenm.) A.S. Barclay ex K. Hammer

Datura metel L.

Datura quercifolia Kunth

Datura reburra A.S. Barclay

Datura stramonium L.

Datura wrightii Regel

Trompettia J. Dupin

Trompettia cardenasiana (Hunz.) J. Dupin

2.7 Taxonomic Key of Worldwide Diversity in Datureae

1. Flower pendant, fruit baccate 2
- 1'. Flower never pendant, fruit a capsule 7
2. Flower 2.5 to 3.5cm long, corolla always yellow *T. cardenasiana*
- 2'. Flower > 3.5cm, corolla never yellow 3
3. Flowering calyx tubular, with apex 2-5 toothed 4
- 3'. Flowering calyx spathe-like, clearly splitting along one side and tapering to a long point 5
4. Flower more than 25cm long, corolla tube constricted beyond calyx, fruit oblong *B. versicolor*
- 4'. Flower 15 to 20cm, corolla tube not constricted beyond calyx, fruit ovoid *B. arborea*
5. Corolla tubular, base yellow and apex red *B. sanguinea*
- 5'. Corolla not tubular, base not yellow 6
6. Flowering calyx glabrous, corolla tube constricted beyond calyx apex (Fig. 2.7), anthers connivent to free *B. suaveolens*
- 6'. Flowering calyx slightly pubescent, corolla tube not constricted beyond calyx apex, anthers free
B. aurea
7. Fruit surface spiny 8
- 7'. Fruit surface not spiny, surface smooth *D. ceratocaula*
8. Fruit erect, seed without elaiosome 9
- 8'. Fruit never erect, seed with elaiosome 10
9. Fruit spines numerous, of similar length, evenly distributed *D. stramonium*
- 9'. Fruit spines of unequal length, with long apex spines, distribution uneven *D. quercifolia*
10. Seed convex margin of triple-ridge (Fig. 2.7) 11
- 10'. Seed convex margin without triple ridge 15
11. Seed testa dark brown with smooth, shiny depressed central area *D. reburra*
- 11'. Seed testa black, rey, or light brown without distinctive central area as above 12
12. Leaf glabrous, fruit spines short, blunt, sometimes reduced to bumps, corolla commonly with two verticils and purple outer surface *D. metel*
- 12'. Left pubescent, fruit spines not reduced, sharp to the touch, corolla with single vertical and not purple on the outside 13
13. Corolla outer surface glabrous *D. inoxia*
- 13'. Corolla outer surface pubescent 14
14. Leaf surface densely covered with short trichomes giving it a gray aspect; leaf has peanut butter smell when rubbed *D. wrightii*
- 14'. Leaf surface covered with fine, long trichomes giving it a white and lanate aspect; leaf has no peanut butter smell *D. lanosa*
15. Seed coat verrucose (Fig. 2.3) *D. kymatocarpa*
- 15'. Seed coat not verrucose 16
16. Circumscissile fruiting calyx deflexed *D. leichhardtii* ssp. *pruinosa*
- 16'. Circumscissile fruiting calyx reflexed 17
17. Corolla longer than 8cm, with purple throat *D. discolor*
- 17'. Corolla no longer than 4cm, without purple throat *D. arenicola*

2.8 Tables and figures

Table 2.1. Taxon list. All species in the ingroup are within Solanoideae. Subfamily and tribe are specified for each outgroup species.

Table 2.2. Properties of the nuclear regions used to estimate phylogenies for Datureae.

* indicates the following: for our analysis of the combined dataset, we used partial sequences of *lfy* exons 2 and 3 for six outgroup species: *J. speciosa*, *N. physalodes*, *N. tabacum*, *P. peruviana*, *S. demissum*.

(a) denotes significant phylogenetic signal ($P < 0.001$) according to the *g1* statistic critical values (see Hillis [82])

Table 2.3. Comparison of morphological characters between *Datura*, *Brugmansia* and *Trompettia cardenasiana* (see Lockwood [120]).

Figure 2.1. Flowers of different species of Datureae. On the left, *Datura stramonium* (top), *D. wrightii* (middle) and *Trompettia cardenasiana* (bottom; formerly *Iochroma cardenasiana*). On the right, *Brugmansia sanguinea* (top), *B. suaveolens* (middle) and *B. aurea* (bottom). *Datura* flowers vary in length from 5 to 18cm, *Brugmansia* flowers vary between 20 and 35cm, and *Trompettia cardenasiana* flowers vary between 2.5 and 3.5cm. Photos by J. Dupin.

Figure 2.2. 50% majority rule consensus trees from parsimony bootstrap analysis on individual regions. Numbers on nodes indicate bootstrap support values. Outgroup species names were abbreviated to genus only (see Table 2.1 for full names).

Figure 2.3. Bayesian Maximum Clade Credibility phylogeny and divergence time estimation of Datureae and outgroups, as result from combined dataset analysis. Numbers on nodes represent posterior probabilities (*pp*); nodes with an asterisk have a *pp* of 1.0. Blue node bars represent the 95% highest posterior density (HPD) of divergence times. Most recent common ancestor of Solanoideae pointed with arrow. Outgroup species names were abbreviated to genus only (see Table 2.1 for full names). Timescale represent main periods and epochs.

Figure 2.4. Ancestral state reconstruction of the following characters using stochastic map-

ping: flower orientation, fruit type, life history, seed margin, elaiosomes, fruit shape, and flower color. Below each reconstruction we indicate the mean number of transitions (changes) between the states given the indicated transition directionality.

Figure 2.5. Short branches in *Trompettia cardenasiana*

Figure 2.6. Scientific illustration of *Trompettia cardenasiana*. a, *Trompettia* branch showing leaves, flower, fruit and flower bud. b, longitudinal section of flower. c, seed longitudinal section. d, gynoecium. e, fruit with fruiting calyx. f, fruit cross section. g, anther. Illustration by J. Dupin.

Figure 2.7. Diagrams illustrating corolla constriction and seed margins. a, corolla tube constricted beyond calyx. b, seed margin of triple-ridge. c, seed coat verrucose. Illustration by J. Dupin.

Table 2.1: Taxon list. All species in the ingroup are within Solanoideae. Subfamily and tribe are specified for each outgroup species.

	<i>Trompettia cardenasiana</i> (Hunz.) J. Dupin
	<i>Brugmansia arborea</i> (L.) Lagerh.
	<i>Brugmansia aurea</i> Lagerh.
	<i>Brugmansia sanguinea</i> (Ruiz & Pav.) D. Don
	<i>Brugmansia suaveolens</i> (Humb. & Bonpl. ex Willd.) Sweet
	<i>Brugmansia versicolor</i> Lagerh.
	<i>Datura arenicola</i> Gentry ex Bye & Luna-Cavazos
	<i>Datura ceratocaula</i> Ortega
	<i>Datura discolor</i> Bernh.
Ingroup	<i>Datura inoxia</i> Mill.
	<i>Datura kymatocarpa</i> A.S. Barclay
	<i>Datura lanosa</i> Barclay ex Bye
	<i>Datura leichhardtii</i> ssp. <i>pruinosa</i> (Greenm.) A.S. Barclay ex K. Hammer
	<i>Datura metel</i> L.
	<i>Datura quercifolia</i> Kunth
	<i>Datura reburra</i> A.S. Barclay
	<i>Datura stramonium</i> L.
	<i>Datura wrightii</i> Regel
	Solanoideae, Capsiceae - <i>Capsicum lycianthoides</i> Bitter
	Solanoideae, Juanulloae - <i>Juanulloa speciosa</i> Dunal
	Solanoideae, <i>Mandragora chinghaiensis</i> Kuang & A.M. Lu
	Solanoideae, Lycieae - <i>Lycium tenue</i> Willd.
Outgroups	Solanoideae, Nicandreae - <i>Nicandra phyalodes</i> (L.) Gaertn.
	Solanoideae, Physaleae - <i>Physalis peruviana</i> L.
	Solanoideae, Solaneae - <i>Solanum demissum</i> Lindl.
	Nicotianoideae - <i>Nicotiana tabacum</i> L.

Table 2.2: Properties of the nuclear regions used to estimate phylogenies for Datureae

* indicates the following: for our analysis of the combined dataset, we used partial sequences of *lfy* exons 2 and 3 for six outgroup species: *J. speciosa*, *N. physalodes*, *N. tabacum*, *P. peruviana*, *S. demissum*.

(a) denotes significant phylogenetic signal ($P < 0.001$) according to the *g1* statistic critical values (see Hillis [82])

Region	Coverage (No. taxa sequenced)		No. characters	No. variable characters	No. parsimony informative characters	g1 statistic	Best fitting likelihood model
	Ingroup	Outgroup					
ITS	18	9	813	273	141	-0.48 (a)	GTR+ Γ
<i>lfy</i>	13	*	1669	277	113	-1.26 (a)	exons: JC69 intron: GTR+ Γ
<i>waxy</i>	18	9	1451	477	161	-0.49 (a)	exons: HKY85 intron: HKY85

Table 2.3: Comparison of morphological characters between *Datura*, *Brugmansia* and *Trompettia*

<i>Datura</i>	<i>Brugmansia</i>	<i>Trompettia</i>
Habit and Life history		
Shrubs with large leaves	Woody, arborescent shrubs or small trees with large leaves	Shrub with very small leaves and old branches becoming spines
Annual (or bi-annual)	Perennial	Perennial
Flower		
Flower 5 to 18cm	Flower 20 to 35cm	Flower 2.5 to 3.5 cm
Position erect or semi erect	Position pendant	Position pendant
Anthesis one or two days	Anthesis several days	Anthesis several days
Flowering calyx not spathe-like (except in <i>D. ceratocaula</i>), calyx teeth usually separating more or less equally	Flowering calyx frequently spathe-like or split along more than one side, calyx teeth not separating or splitting into two groups	Flowering calyx campanulate, with teeth separating equally
Fruiting calyx circumscissile near the base and falls away with the corolla (except in <i>D. ceratocaula</i> where it falls away completely), the persistent base forming a disk, cup or reflexed frill subtending the mature fruit.	Fruiting calyx not circumscissile, either falling away entirely or forming a persistent husk-like structure around the mature fruit	Fruiting calyx not circumscissile, slightly accrescent during fruit maturation and eventually splitting along a longitudinal axis to expose mature fruit
Fruit		
Fruit a capsule, round to ovoid, borne on short pedicels in an erect, sub-erect or nodding position.	Fruit a large, ovoid to elongated, pendant berry borne on much elongated pedicel	Fruit a small, round, pendant berry
Bicarpellate and tetralocular due to presence of false septa.	Bicarpellate and bilocular	Bicarpellate and bilocular
Fruit regularly or irregularly dehiscent	Fruit indehiscent	Fruit indehiscent
Pericarp usually spinose (except in <i>D. ceratocaula</i> where it is smooth)	Pericarp smooth and unarmed	Pericarp smooth and unarmed
Seeds		
Seeds relatively small, discoid, lacking a corky seed coat	Seeds large, slightly tetrahedral, with a thick, corky seed coat	Seeds relatively small, tetrahedral, with a thin, corky seed coat
Elaiosomes present in most species	Elaiosomes not present	Elaiosomes not present



Figure 2.1: Flowers of different species of Datureae. On the left, *Datura stramonium* (top), *D. wrightii* (middle) and *Trompettia cardenasiana* (bottom; formerly *Iochroma cardenasiana*). On the right, *Brugmansia sanguinea* (top), *B. suaveolens* (middle) and *B. aurea* (bottom). *Datura* flowers vary in length from 5 to 18cm, *Brugmansia* flowers vary between 20 and 35cm, and *Trompettia cardenasiana* flowers vary between 2.5 and 3.5cm. Photos by J. Dupin.

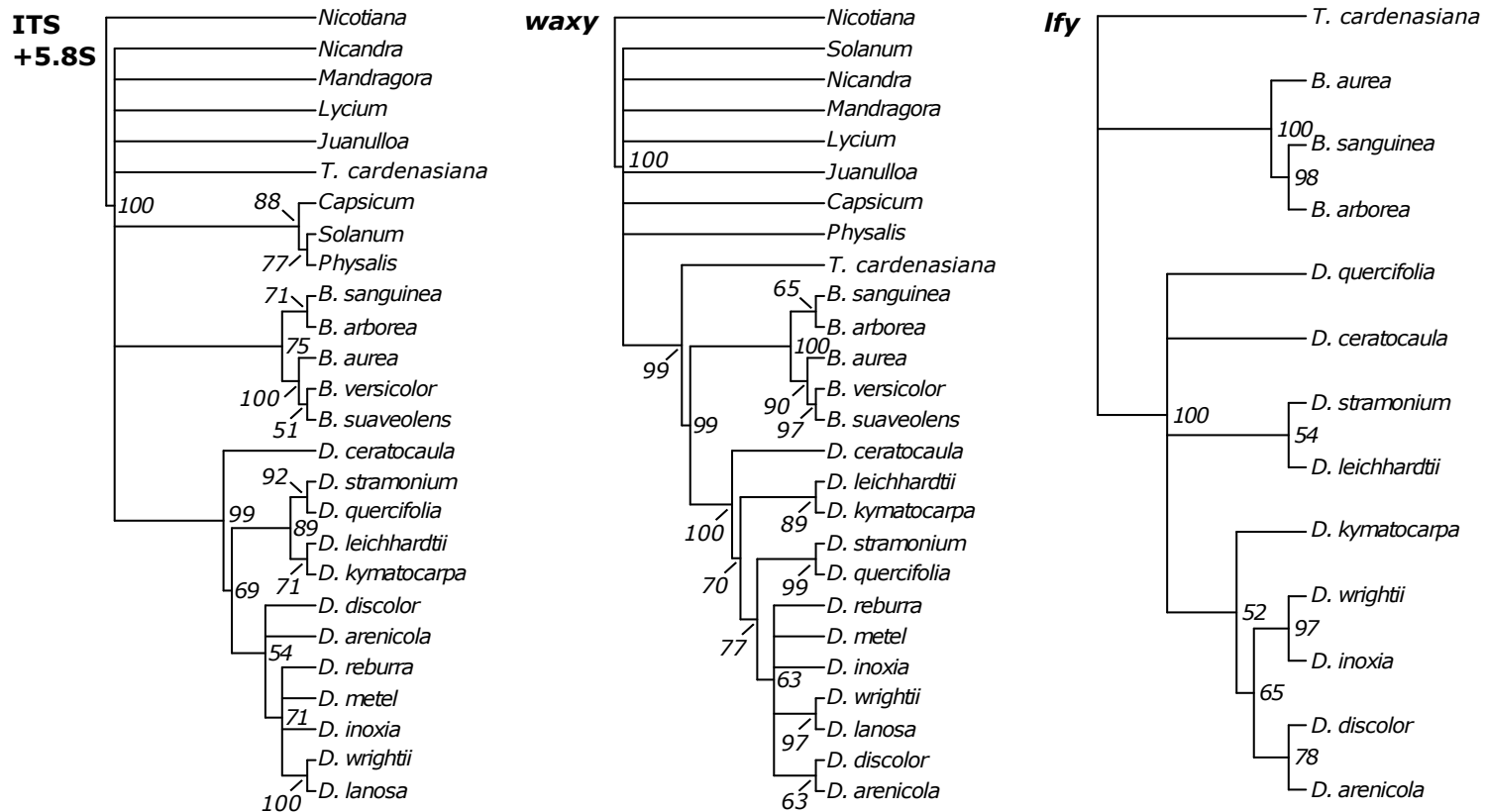


Figure 2.2: 50% majority rule consensus trees from parsimony bootstrap analysis on individual regions. Numbers on nodes indicate bootstrap support values. Outgroup species names were abbreviated to genus only (see Table 2.1 for full names).

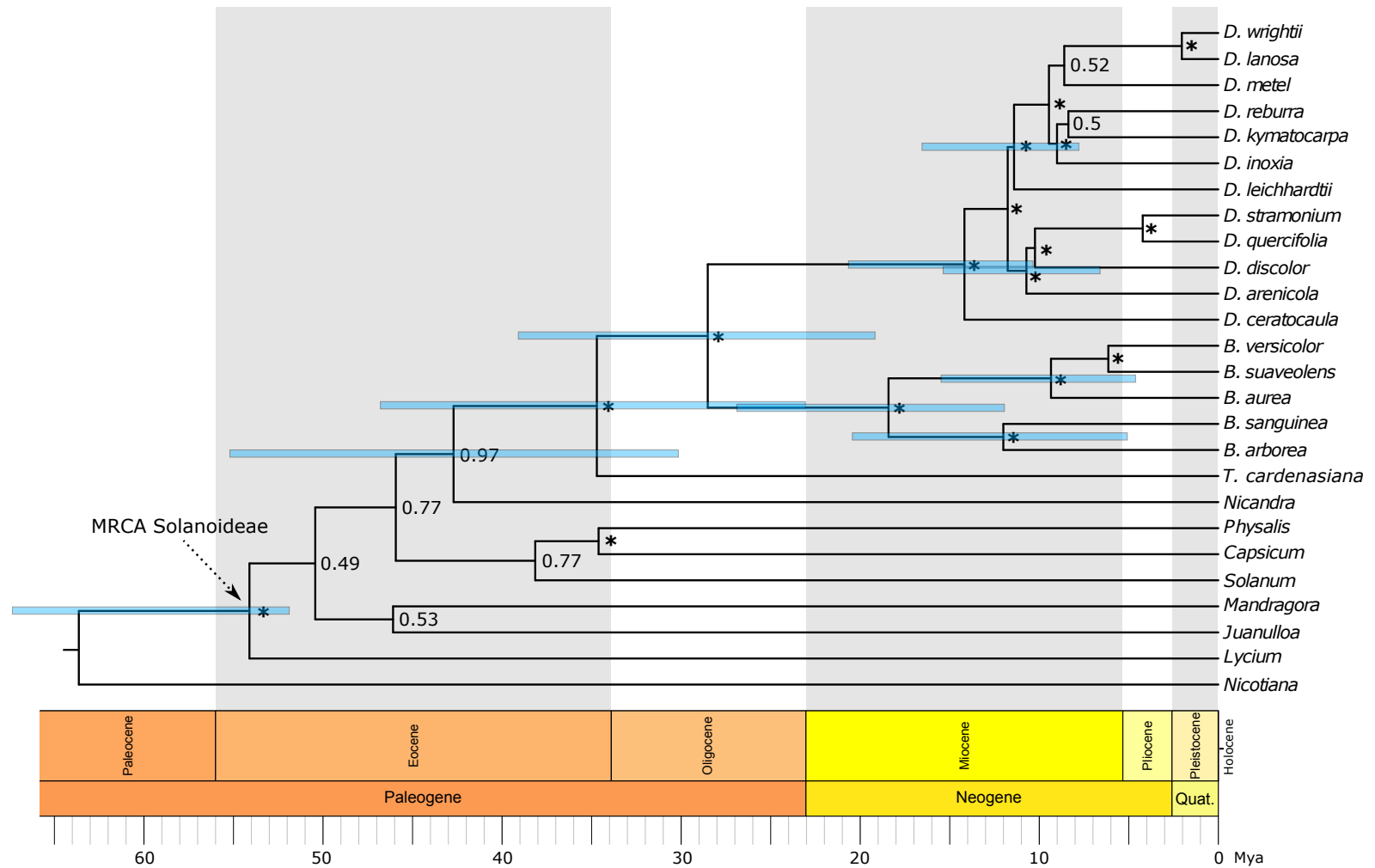


Figure 2.3: Bayesian Maximum Clade Credibility phylogeny and divergence time estimation of Datureae and outgroups, as result from combined dataset analysis. Numbers on nodes represent posterior probabilities (pp); nodes with an asterisk have a pp of 1.0. Blue node bars represent the 95% highest posterior density (HPD) of divergence times. Most recent common ancestor of Solanoideae pointed with arrow. Outgroup species names were abbreviated to genus only (see Table 2.1 for full names). Timescale represent main periods and epochs.

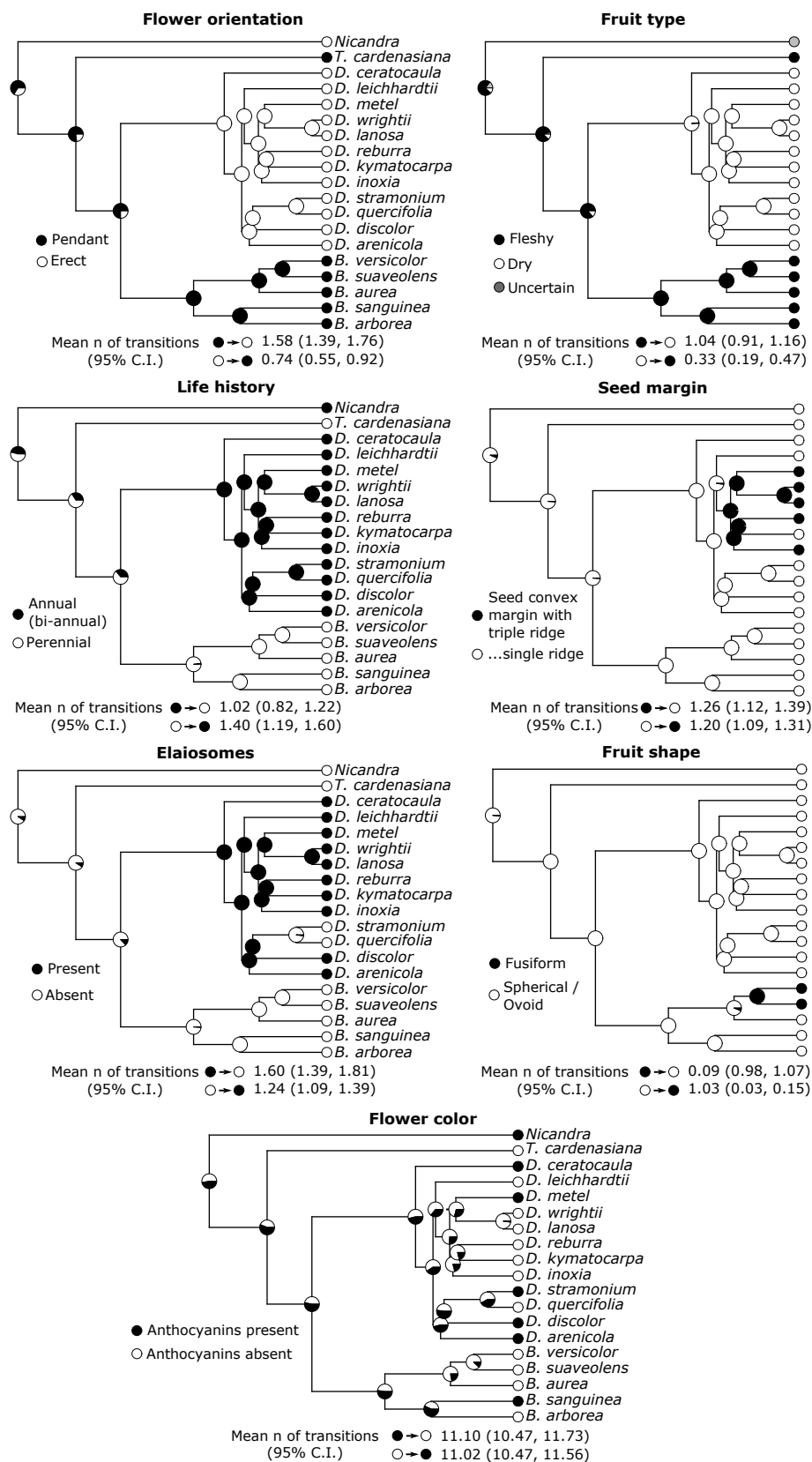


Figure 2.4: Ancestral state reconstruction of the following characters using stochastic mapping: flower orientation, fruit type, life history, seed margin, elaiosomes, fruit shape, and flower color. Below each reconstruction we indicate the mean number of transitions (changes) between the states given the indicated transition directionality.



Figure 2.5: Short branches in *Trompettia cardenasiana*

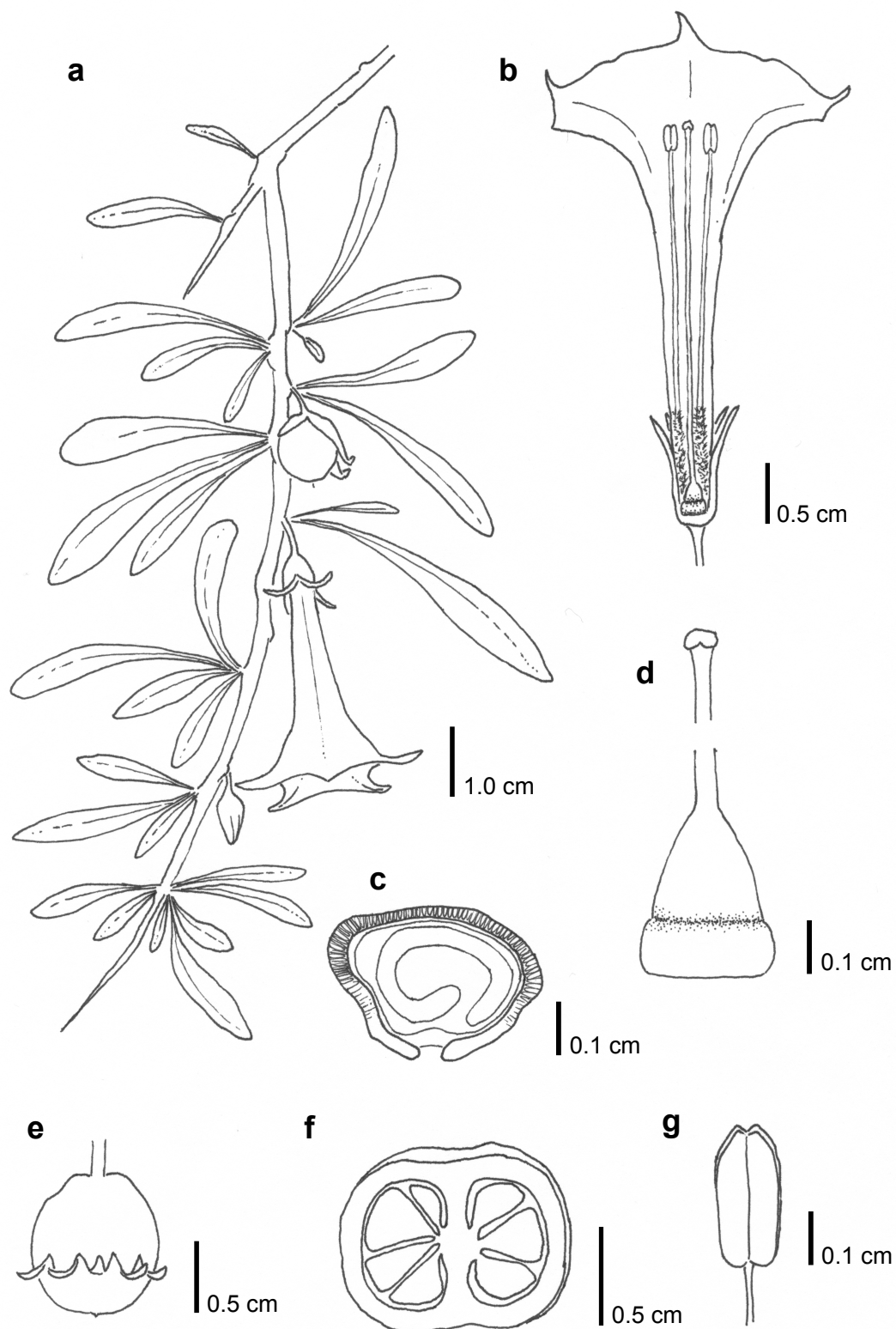


Figure 2.6: Scientific illustration of *Trompettia cardenasiana*. a, *Trompettia* branch showing leaves, flower, fruit and flower bud. b, longitudinal section of flower. c, seed longitudinal section. d, gynoecium. e, fruit with fruiting calyx. f, fruit cross section. g, anther. Illustration by J. Dupin.

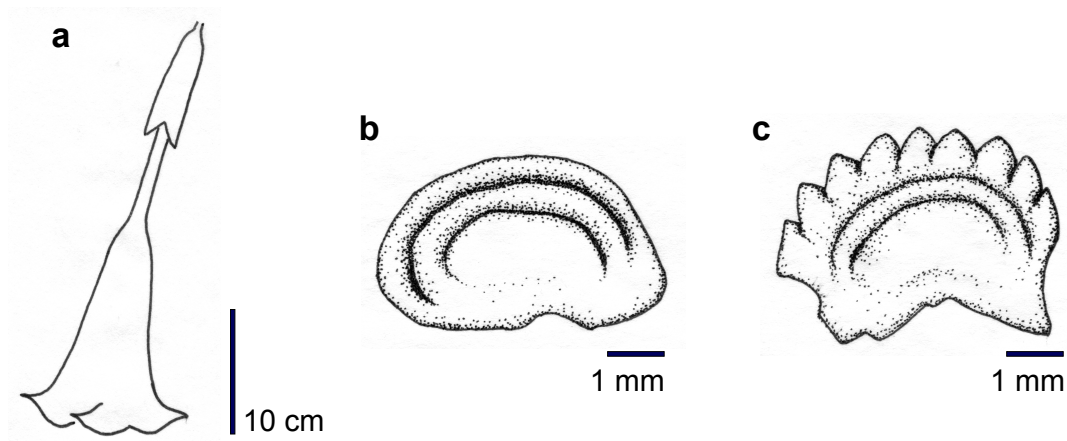


Figure 2.7: Diagrams illustrating corolla constriction and seed margins. a, corolla tube constricted beyond calyx. b, seed margin of triple-ridge. c, seed coat verrucose. Illustration by J. Dupin.

Chapter 3

Integrating historical biogeography and environmental niche evolution to understand the geographical distribution of Datureae (Solanaceae)

[Manuscript to be submitted to the American Journal of Botany]

3.1 Introduction

A main goal in biogeography is to understand patterns of clade distribution, that is, why different lineages have dispersed and established populations in some areas and not in others. Distribution patterns are shaped by abiotic factors such as climate and edaphic aspects, biotic factors such as competition or mutualism, and historical aspects such as dispersal limitation. For example, abiotic variables like temperature and precipitation are key in predicting the success of range expansion in invasive plants (e.g. Beerling [11]; Petitpierre [178]), while the addition of biotic factors, such as positive interactions between species, help explain the distribution of sympatric species in marine systems (e.g. Pigot [180]; Crotty [32]). Further, the geographical starting point of a clade along with limitations to its dispersal imposed by geographical barriers over time can be a major player in shaping the distribution of clades, as observed in birds and marsupials (e.g. White [236]; Giarla [66]).

These diverse abiotic, biotic and historical factors shaping distributions may act at different scales. For instance, while the climatic variables such as annual temperature and precipitation seasonality on a species' niche influence species distributions at continental scales, biotic interactions are more predictive of local and regional patterns of occurrence at a regional, local scale (Elith [56]).

Historical factors can act at multiple scales (Wiens [239]) as the amount of time available for a clade to expand its range can determine if there was opportunity for dispersal. As an example, a clade's center of origin determines its ancestral environment and, indirectly, contributes to defining a clade's dispersal limitations, such as physical barriers and type of surrounding environment.

In the present study, we estimate historical events and aspects of the environmental niche evolution in Datureae to explain the current geographical distribution of this clade. Here we use niche to refer to a clade's environmental space, which includes climate and soil factors. Datureae is a tribe in the Solanaceae family, with an estimated age of ca. 35 million years (My; Chapter 2 of this dissertation) and it is composed of 18 species divided into three genera, *Brugmansia* Pers., *Datura* L. and *Trompettia* J. Dupin. These species are distributed in contrasting types of environments. *Brugmansia* species occupy areas in North and Central Andes at varying elevations, and one of its five species is native to southern portions of the Brazilian Atlantic forest. Most *Datura* species are native to tropical dry forests in Mexico and arid lands in northern Mexico and southwest USA (Luna-Cavazos [124]). *Trompettia*, a monotypic genus, is only found in dry high elevation areas in southern portions of the Bolivian Andes.

This investigation of the historical biogeography of Datureae presents an opportunity to assess how movements between areas separated since the Oligocene influenced the niche evolution in this clade of South American origin. Under a niche evolution scenario, the dispersal events during Datureae's history may have directly contributed to shifts in environmental niche. Studies have shown that range expansions are associated with environmental niche shifts in many widely distributed clades such as *Microseris* (Asteraceae) (Vijverberg [226]), *Clarkia* (Onagraceae) (Raven [189]) and *Gilia* (Polemoniaceae) (Morrell [144]). Niche evolution may be likely in the case of Datureae given that long distance dispersal events have the potential to introduce species to areas that are environmentally distinct from the ancestral area. Alternately, range evolution in Datureae may follow a pattern of niche conservatism, where species disperse between similar habitats (Donoghue [47]; Edwards [54]). In order to test these contrasting hypotheses, we estimated the historical biogeography of Datureae to determine where the group originated and the directionality of its range

expansions over time. We then characterized the realized niche of the genera of Datoreae (portion of the fundamental niche that the species occupy as a result of limiting factors; Hutchinson [94]) and tested shifts in environmental niche across the phylogeny. Lastly, we quantified niche breadth for each genus and estimate the degree of overlap between them. Combining these results we consider how range evolution in Datoreae has influenced niche diversity and breadth. More broadly, our results will contribute to a better understanding the relative importance of movements between South and North America and niche shifts in shaping the distribution of clades and the formation of floras in both portions of the American continent.

3.2 Methods

3.2.1 Historical biogeography of Datoreae

3.2.1.1 Datoreae phylogeny

For our historical biogeography analysis and the study of environmental niche evolution in Datoreae, we used the time-calibrated maximum clade credibility (MCC) tree from Chapter 2 of this dissertation. This phylogeny was estimated using three nuclear loci, ITS+*5.8S* (White [237]), *waxy* (Peralta [174]) and *lfy* (Schultz [206]). The original tree included all 18 recognized species in Datoreae and seven outgroups. For our purposes, we pruned the tree using the ‘ape’ package v4.1 (Paradis[167]) in R (R Core Team [184]) to retain all species in Datoreae and a representative of its sister clade, the small Andean genus *Nicandra* Adans. (Fig. 3.1).

Geographic ranges of Datoreae - To determine species distribution ranges, we compiled a database with location points for all 18 species in Datoreae species based on voucher information from several herbaria (ARIZ, BHCB, COLO, DES, GH, MEXU, QCA, QCNE, RSA) along with online databases (TROPICOS, Missouri Botanical Garden, <http://www.tropicos.org>, last accessed on Nov. 2016; Global Biodiversity Information Facility (GBIF), <http://www.gbif.org>, last accessed on Nov. 2016). To determine species native ranges, we cross-checked collection points with numerous literature sources, including taxonomic research papers, species descriptions and

floras (e.g., [120]; [124]; [23]).

3.2.1.2 Historical biogeography estimation

We used the R package ‘BioGeoBEARS’ v0.2.1 (Matzke [136]) to compare biogeographical models and estimate ancestral ranges and events in Datureae. ‘BioGeoBEARS’ implements maximum likelihood (ML) methods that replicate the key assumptions of two of the most used types of models in historical biogeography, DEC (Dispersal-Extinction-Cladogenesis; Ree [190]) and DIVA (Dispersal-Vicariance Analysis; Ronquist [194]). Both DEC and DIVA allow for a wide range of processes, including within-area speciation, vicariance, range expansion (dispersal to a new area), range contraction (extinction in an area) and founder-event speciation. A founder-event is characterized by range switching (e.g., Andes to North America) that occurs at a lineage-splitting event (a node in the phylogeny), leaving one daughter lineage in a new range and the other daughter lineage retaining the ancestral range (Matzke [134]).

For this set of analyses, we classified native species distributions into three main areas, Andean (AA), Non-Andean regions of South America (AN) and North America (NO), and combinations of the three. We limited the number of single areas to these three given the small number of species in Datureae and the current distribution patterns within the tribe. Moreover, we chose not to code Central America as a separate area in the analysis given that this area forms the southern part of the native range for only two otherwise North American species (*Datura metel* L. and *Datura innoxia* Mill.), which are nested within the North American clade. Thus, dispersal into Central America would be estimated as independent range expansion events with no significant influence on node state estimations.

We also incorporated time-stratified dispersal multiplier matrices in the model-fitting to account for the changing distances between the regions over geological time. The continental distribution of Datureae in areas of North and South America required that we incorporate the potential influence of the closure of the Panama isthmus in our analysis. Therefore, to accommodate the recent discussion about the closure of the isthmus *sensu stricto*, we set up three sets of analyses:

one that include the date suggested by O’Dea ([156]) of ca. 3.5 million years ago (Ma), a second one to address the estimates made by Montes ([142]) of a closure between 16 and 7 Ma, and a third set of models with matrices with a date of ca. 20 Ma as the results from Bacon ([4]) indicated. The dispersal multiplier matrices for each of these strata give the relative probability of dispersal between areas and are roughly scaled to represent the relative distance between the areas during each time slice. All models included the matrices modified by the w parameter (matrix exponent), also estimated with ML.

In total, we tested 12 models (Appendix C.1) that varied in the number of free parameters included and in the time periods used for the dispersal multiplier matrices. The free parameters were w (matrix exponent), d (the base rate of range expansion), j (the per-event weight of founder-event speciation at cladogenesis; Matzke [134]) and e (the rate of range contraction). Because not all models are nested, we used the Akaike information criterion (AIC, Burnham [22]) to select among the 12 models; the best fit model with the lowest AIC score was used to infer the relative probabilities of ancestral ranges within the phylogeny.

3.2.2 Analyses of niche evolution

3.2.2.1 Environmental data

We retrieved environmental data for all species using the locations database described under “Geographical data” and summarized it as mean values. We initially considered 34 environmental layers at 30 arc-seconds resolution (listed in Appendix C.2): 19 bioclimatic layers of temperature and precipitation (Hijmans [81]) and 15 soil layers (Hengl [79]; Hengl [78]). The bioclimatic variables represented annual trends (e.g., mean annual temperature, annual precipitation), seasonality (e.g., annual range in temperature and precipitation) and extreme factors (e.g., temperature of the coldest and warmest month). These variables are the translation of monthly temperature and rainfall values into variables that are meaningful from a biological point of view because they represent annual trends (Hijmans [81]). The soil layers included variables that characterize physical soil properties,

such as percentage of sand, silt and clay fractions, soil bulk density (kg/m^3) and percentage of coarse fragments. All of these factors influence the water-storage capacity of the soil, which in turn, influences the levels of soil moisture available for plant growth. Soil texture, then, becomes important in highly seasonal areas, such as dry areas in Mexico, especially when compared to mesic, tropical areas (Prentice [181]).

We reduced the complexity of these environmental data in two steps before carrying on the niche analysis. First, we performed a collinearity test on these layers using the function `removeCollinearity` from the R package ‘`virtuallspecies`’ v1.4-1 (Leroy [116]). This function uses the Pearson’s correlation coefficient to analyze correlation among variables with a given cut-off value. We chose the default value of 0.7, meaning variables that presented a correlation index above 0.7 would be grouped together. The results of this test reduced the number of environmental layers from 34 to 12 (these 12 are highlighted in Appendix C.2). Second, we used a phylogenetic PCA (pPCA) approach to estimate principal components while correcting for phylogenetic relatedness. We input the mean value for each of the 12 environmental variables for each species in the function `phyl.pca` from the R package ‘`phytools`’ v0.5-64 (Revell [193]) to estimate the principal components along with their loadings and scores. To determine which principal components significantly contribute to the variation seen in our dataset, we used the broken-stick test (Jackson [101]) through the function `sreeplot` in the R package ‘`vegan`’ v2.4-2 (Oksanen [98]).

3.2.2.2 Shifts in optima in environmental niche

We tested for shifts in environmental niche in *Datureae* using the R package ‘`lloou`’ v1.41 (Khabbazian [104]). We used the pPCA scores for phylogenetic principal component 1 (*pPC1*) to represent *Datureae* environmental niche as a continuous variable, given that pPC1 explained 94% of the variance in the data. Even though the scores for pPC1 were generated under a method that corrects for phylogenetic relatedness, it is recommended to use those results in subsequent analyses that also take the phylogeny into consideration (Revell [192]). The ‘`lloou`’ algorithm identifies changes in the expected mean trait values by using the OrnsteinUhlenbeck (OU) process and

assesses the likelihood of the data under different models of character evolution. Moreover, `l1ou` does not require that the regimes of tips and internal branches are identified a priori. The algorithm uses a phylogenetic Bayesian information criterion (pBIC) that accounts for the phylogenetic correlation between species. This criterion does not suffer model overfitting as it can occur to other information criteria (Khabbazian [104]). Finally, the 'l1ou' package also allows for evaluation of the uncertainty in the detected shifts by incorporating a bootstrap option. Here we estimated the supported for the identified shifts by running 500 bootstrap replicates.

3.2.2.3 Estimating niche region and testing for niche overlap between genera

We used the R package 'nicheROVER' v1.0 (Lysy [125]) to estimate the niche region for each genus in Datureae and quantify the pairwise niche overlap between the genera. Niche region here is equivalent to niche size or niche breadth. In this approach, the niche is constructed following Hutchinson's [94] definition of a niche as an n -dimensional hypervolume embedded in the n -dimensional space generated by the n environmental layers (with here $n = 2$, $pPC1$ and $pPC2$). The input data here was different from the one described for the test of optima shifts with surface. Instead of using pPC scores that resulted from a $pPCA$ of mean values for each species, we considered each collection location as an independent data point within each genera and obtained pPC scores for each individual point. For instance, *Brugmansia*, which has only five species, was represented here by more than 300 data points (collection localities). This approach makes the test more conservative with respect to the hypothesis of niche divergence. It increases the number of data points and so better represents the niche regions, making it possible to identify overlap that could go undetected when using a dataset reduced to species means. To construct the environmental niche of each genus, we then extracted the scores for $pPC1$ and $pPC2$ for all individuals of the genus and built a 2-dimensional niche ellipse in the $pPC1$ - $pPC2$ space that represented a 95% probability region in multivariate space (Swanson [215]).

Once the niche region was estimated, we quantified the pairwise niche overlap between the genera. Overlap values range from 0 (no overlap) to 1 (complete overlap) with a cutoff of 0.05.

Overlap is calculated as the probability that an individual from a genus is found in the niche region of another. This pairwise comparison accounts for asymmetry, meaning the probability that an individual from this latter genus is found in the niche region of the former will be distinct. Finally this metric of niche overlap also incorporates uncertainty by adopting a Bayesian inference framework (Jackson [100]). Specifically, it assigns a prior distribution to the model parameters so these are sampled and used to estimate niche region ellipses and niche overlap values, and it assesses the variability in each of these measures (Swanson [215]).

3.3 Results

3.3.1 Historical biogeography

The ancestral state for Datureae is Andean (probability = 0.74) in accordance with previous work with a smaller sampling of taxa (Dupin [51] (Chapter 1 of this dissertation)) (Fig. 3.1). The colonization of North America is inferred to have occurred via a jump dispersal from Andean regions between 28 and 15 Ma. The range expansion into non-Andean areas of South America occurred ca. 6 Ma on the stem branch of the clade formed by *B. versicolor* and *B. suaveolens*.

Our model selection supported the use of models that included the founder-event parameter (range switching at a lineage-splitting event, j). These results also showed that the most likely biogeographical history for Datureae is independent of the dating of the closure of the Panama isthmus (Appendix C.1) because the estimates for the splits between the three genera in Datureae all pre-date even the oldest date for the closure of the Panama isthmus. Moreover, there was no significant difference between the histories estimated using DEC+ j and DIVALIKE+ j models, as all models recover the same highest probability state at every node. The inclusion of j , allowing for one of the daughter lineages to inhabit a new area not part of the ancestral range, was crucial to allow for events such as the one between the Andes and North America, as a priori an estimation of a widespread ancestor seemed as likely as a jump dispersal between North and South America. The alternative to a jump dispersal would be range expansion resulting in a widespread ancestor

(spanning North, Central and South America) followed by extinction in the latter two areas. This scenario would not have been possible as the split between the North and South American lineages occurred before the rise of the isthmus and the Central American connection. We present the results for the historical biogeography estimation of Datureae under DEC+ j in Figure 3.1.

3.3.2 Phylogenetic principal component analysis of environmental variables

Our results show that $pPC1$ (out of 12 estimated $pPCs$) explains 94% of the variance in our dataset. Under $pPC1$, the variables are organized in two sets with distinct response profiles (Fig. 3.2). Four variables load strongly in the $pPC1$ axis, with Annual Precipitation and Precipitation of the Driest Quarter being positively correlated (loading values of 0.99 and 0.92) and Mean Diurnal Range and Soil being negatively correlated (loading values of -0.93 and -0.88) (see Table 3.1 for the full list of loading values). The estimated scores for the species in Datureae place them in different areas of the pPC biplot. *Brugmansia* species occupy the space where precipitation amounts are higher. *Datura* species and *Trompsettia* cluster in regions of the plot where seasonality aspects are more significant (e.g. mean diurnal range and precipitation seasonality) and soil bulk and clay content are higher.

3.3.3 Shifts in optima in environmental niche space

Species in Datureae were inferred to track two significantly different environmental optima. We estimated that Datureae started diversifying under a dry environmental niche and this environmental state was retained by species in *Datura* and *Trompsettia*. *Brugmansia*, on the other hand, presents a shift from the tribe's ancestral environmental niche. Its species tracked a significantly different optimum, under a more mesic environment. These results were reinforced by our bootstrap analysis, where the detected shift along the *Brugmansia* stem branch was recovered in 80% of the replicates, and other branches or tips, where no shifts were reported in our results, had bootstrap support of less than 0.8%. We incorporated the results of this optima analysis in Figure 3.1, where the branch width in the tree identifies the species under a same optimum (with the exception of

the tribe's sister group, *Nicandra*, which was not included in this set of analyses because of uncertainty about its native environmental niche). We report the estimated values, under I1ou, for the log-likelihood of the data, shift value, pBIC score, adaptation rate α , variance σ^2 , stationary variance σ^2_{∞} , and pBIC score in Table 3.2.

3.3.4 Niche overlap between genera

Our estimates of generic niche overlap revealed that between *Datura* and *Brugmansia* there is moderate to low overlap in their environmental niche regions (Fig. 3.3(a)). The probability of finding a *Brugmansia* individual in the niche region of *Datura* is 49.3 (95% CI: 36.5 - 57.6, Fig. 3.3(b)). Conversely, the probability of finding a *Datura* individual in the niche region of *Brugmansia* is 9.6 (95% CI: 6.8 - 12.2, Fig. 3.3(b)).

We report the results involving *Trompettia* with caution given the low number of samples and the small niche region estimated for this species. The results show that the probability of finding a *Trompettia* individual in *Brugmansia* or *Datura* niche regions is very small (0.46 and 3.73, respectively). The reverse situation gave us probabilities of 1, when estimating the chances of finding a *Brugmansia* or *Datura* individual in the niche region of *Trompettia*. We show the estimated niche regions and the niche overlap results in Figure 3.3.

3.4 Discussion

Our analyses show that Datureae originated in Andean regions and subsequently expanded its range to North America and non-Andean regions. Moreover, we estimated that the ancestral environmental niche in the tribe is dry and that there has been a significant shift along the *Brugmansia* branch towards a more mesic type of environment. The long-distance dispersal to North America represented a range expansion into a familiar type of environment, a dry one. Over time, *Datura* and *Brugmansia* continued to expand their realized niche towards different areas of the niche space creating a niche shift, with *Brugmansia* occupying a significantly different niche region from the ancestor (Fig. 3.4). While such expansion generated the detected shift, it did not erase

the overlap in environmental preferences between the genera in Datureae.

3.4.1 Historical biogeography of Datureae – a clade of South American origin

An Andean orogenesis that starts ca. 40 Ma (Sebrier [207]; Ege [55]; Graham [73]) makes Datureae, stem age estimated as 35 Ma, as one of the clades whose diversification was possible due to the new habitats created by the uplift. Within the Andes, the ancestral range was likely centered in the mid-elevation areas (1,000-3,000 m) in the Central Andes where both *Trompettia* and *Nicandra* (the sister clade of Datureae) are distributed. Under this scenario, the more northern Andean distribution of *Brugmansia* would reflect a northward range expansion within South America as those sections of the Andes formed in the Oligocene, ca. 30 Ma (Parra [168]). Our results also revealed that Datureae further expanded north leading to the clade currently recognized as *Datura* (Fig. 3.1).

Considering the wide disjunction between *Datura* and the other members of Datureae, there are two possible explanations for its present-day distribution of *Datura*. One possibility is a series of shorter dispersal events followed by extinction in the intervening areas. The ancestors of *Datura* could have first colonized Central America before the closure of the isthmus via dispersal from South America. From Central America, the clade could have then expanded its range northward into drier portions of North America. The present-day disjunction could then be explained by subsequent extinction of the Central American populations. Alternately, the disjunction could have arisen from successful longer distance dispersal between Andes and North America, without the intermediate step of colonization of Central America. In the absence of an extensive fossil record, it is not possible to confidently reject one of the two explanations. However, it is notable that the latter scenario, involving dispersal from dry areas in South America to similarly dry areas in North America, fits the patterns reported by Donoghue ([47]) and Crisp ([31]) that transoceanic colonizations are often accompanied by niche conservatism.

In general, the directional expansion of Andean clades towards the north is an emerging theme in biogeographical analyses. For example, Gentry ([64]) described 61 families of plants centered in

the Andes but which subsequently dispersed to Central and North America, and other continents. Bacon ([3]) also report that migration rates between South and North America were asymmetric, with northward bound events around 30% higher than in southward ones. This pattern is found across Solanaceae at the family level, where Dupin ([51]) estimated that the number of dispersal events from South America to Central and North Americas is at least four times larger than in the opposite direction. Dupin ([51]) suggested this directionality was due to the early diversification of the family in South America, providing a large pool of migrants for dispersal. Similar analyses in other clades of inferred South American origin would be needed to test the generality of this explanation.

3.4.2 Datureae’s environmental niche evolution

Datureae’s likely center of origin in Central Andes places the clade’s initial diversification in a dry environment, an inference that is supported by our analysis of optima in which the tribe’s root is placed under the drier optimum (Figs. 3.1, 3.4). *Datura* species and *Trompettia* have retained the dry optimum while the second optimum, mesic, is occupied only by *Brugmansia* species. Lockwood’s monograph [120] defines the Andes of southern Colombia and Ecuador (Northern Andes) as the native range for three of the five species of *Brugmansia*, *B. aurea*, *B. arborea*, and *B. sanguinea*, while *B. suaveolens* and *B. versicolor* are found in the low tropics of the southern Atlantic Brazil and the Guayaquil Basin of Ecuador, respectively; putting the evolution of all *Brugmansia* species under mesic areas in South America. Within the mesic regime, *Brugmansia* has expanded from high elevation Andean areas to lowland tropical forest. Additionally, the estimated crown age of the *B. suaveolens* and *B. versicolor* clade (ca. 6 My) is compatible with the availability of the Guayaquil Basin for colonization by *B. versicolor*, given that this basin formed around the middle Miocene (ca. 12 Ma).

These results contradict the hypothesis that dispersal events in Datureae’s history corresponded to shifts in environmental niche and instead support a pattern of niche conservatism during dispersal. The two main dispersal events estimated, from Andean areas to North America and

to non-Andean areas do not correspond to environmental niche shifts. Instead, the detected shift happened within clades of Andean distribution. We estimated that the ancestral niche environment in Datureae was dry and that *Brugmansia* represented a significant shift from that ancestral state to a mesic one. Datureae started diversifying during the Eocene-Oligocene boundary, when major climatic changes were underway. The Eocene-Oligocene boundary marks the change from a dominance of tropical biomes to more arid, cooler, open-habitat environments worldwide (Prothero [183]; Stromberg [214]). This change is a consequence of a decrease of mean temperatures and increase in seasonality (Zachos [246]; Zachos [247]). These changes accentuated the differences between the drier Central and Southern Andes, and the more mesic Northern Andes.

The environmental shift we estimated in *Brugmansia* aligns with results from studies on other clades that originated in seasonally dry areas and present directional transitions into mesic environments. For example, Ireland ([96]) estimated that transitions from seasonally dry to ever wet vegetation in the genus *Ateleia* DC. (Fabaceae) were more frequent than in the opposite direction. Similarly, *Bursera* Jacq. ex L. (Burseraceae), which originated in dry areas in North America, has experience multiple shifts away from seasonally dry environments, including one to the tropical rain forest (De-Nova [42]). One explanation for this pattern is that fewer special adaptations are required to survive a wetter climate, favoring transitions from dry to wet instead of the reverse.

Successful dispersal events of ancestral populations from dry areas into mesic ones should be seen as likely given the patterns of invasiveness seen in *Datura* today. A quick analysis of floras of South American countries along with the distribution of collection points available in the GBIF database shows that *Datura* species have been introduced and have escaped garden's successfully in much of South America. This indicates that, without dispersal limitation, these could expand their ranges into more mesic areas, as the ancestral populations likely did. The opposite does not hold true however. While *Brugmansia* species have been brought into North America for horticultural uses, they are not seen thriving on roadsides or dry areas after having escaped from cultivation. This difference is also present in our results for the pairwise niche overlap between genera: the probability of finding a *Datura* species in the *Brugmansia* niche region is roughly 5 times greater

than the reverse situation (Fig. 3.2).

3.4.3 Contributions of historical events and niche dynamics over space and time to the distribution of *Datureae* species

Our results suggest that the current geographical distribution of *Datureae* results from three elements: an initial diversification in Central Andes under a dry environmental niche, a subsequent long distance dispersal to North American areas of similar environment and a crucial, and constant, exposure to mesic environments of the northern Andes and non-Andean areas of South America (Fig. 3.3). While there were certainly limitations to dispersal between these areas, the amount of time elapsed since the beginning of the tribe's diversification, at least 17 Ma, likely allowed for enough successful dispersal events and the evolution of the niche in *Datureae* to happen. The colonization of areas in North America represented a range expansion into a known type of environment, a dry one. On the other hand, the colonization of non-Andean areas of South America was likely a consequence of an initial range expansion that allowed for a continuous specialization into the mesic environment (Fig. 3.3). Even though range expansions into these two types of environments ultimately resulted in a significant niche shift, our niche overlap estimates showed that moderate overlap remains between *Datura* and *Brugmansia* niche regions. This is likely a result of as yet incomplete niche specialization within *Brugmansia* and two *Datura* species, *D. metel* and *D. inoxia*, that have native ranges that include areas in Central America representing then the expansion of the niche towards the wetter side of the spectrum.

These changes in geography and niche may be the main drivers of the morphological and life history differences among the genera. *Datura* is composed entirely of species with annual and bi-annual cycles, a life history that accords with the strong seasonality of these dry areas (Evans [58]; Cruz-Mazo [33]; Friedman [60]). Moreover, the large erect flowers of these short herbs (< 1m) are principally pollinated by hawkmoths, common floral visitors in open, dry areas (Raguso [186]; Bronstein [18]). By contrast, *Brugmansia* species are large perennial shrubs (two to three meters tall), with pendant flowers often pollinated by hummingbirds, moths and bats (Lockwood

[120]; Knudsen [107]; Weiss [233]). *Trompettia* is also a perennial species but of smaller size than *Brugmansia*. The smaller flowers and fruits of *Trompettia* may reflect of the cost of being a perennial shrub in a dry area. Nothing is known with respect to the pollination biology of this monotypic genus, but the lack of detectable scent and floral phenology suggests diurnal pollinators, like insects and hummingbirds.

3.4.4 Conclusions and future directions

The results seen here for Datureae of an initial diversification in dry habitats in South America align with patterns of the appearance and spread of seasonal areas in the continent. The transition between the Eocene and the Oligocene eras (ca. 40-35 Ma) is marked by a decrease of global temperatures, triggering the transition from areas heavily forested to a mix of open areas and forests (Stromberg [214]). Studies on the flora of Patagonia show that, with the change in global mean temperatures, at first, dry areas, here specifically grasslands, became a minor components in overall forested habitats (Barreda [7]; Stromberg [214]). The continuity of such low temperatures for the next several million years up to middle Miocene (ca. 12 Ma) led to a significant expansion of such grasslands in southern South America. It is possible that a similar pattern followed in central portions of South America, meaning that small pockets of arid areas appeared ca. 35 Ma and their abundance slowly increased towards the present. This pattern of isolation can, for instance, help us understand the level of endemism found in small, dry areas along the Andes (see Särkinen ([201], for an example in Fabaceae genera). Such an interpretation could explain why *Trompettia* is isolated in a small portion of southern Bolivia in dry intermountain valleys.

This study on the range and niche evolution of Datureae provides the foundation for future studies of distribution dynamics at regional and local scales. Such fine scale studies would benefit from incorporating biotic factors, which have been shown to be relevant when explaining distributions at smaller scales (e.g. Meier [140]; Boulangeat [16]; Wisz [242]). For example, *Datura* species' ranges may be shaped by the distributions of ants, which are thought to be their primary disperser (O'Dowd [157]; Marussich [130]). By coupling the results on abiotic preferences shown here (e.g.

drier environments for species in *Datura*) with regional biotic factors (e.g. specific dispersers and pollinators native to regions of North America) we can test the potential role of adaptation to distinct environments and ecological interactions in morphological divergence and speciation. Such an integration of factors can help us explain the differences in species richness among the genera in Datureae and between regions of South and North America.

3.5 Tables and figures

Table 3.1. Variable loadings for $pPC1$ as a result of the $pPCA$ analysis. Precipitation variables (Annual Precipitation, Precipitation Driest Quarter and Precipitation Warmest Quarter) along with soil bulk density and mean diurnal range are the variables that contribute more for the variation within $pPC1$. (1) Soil bulk refers to soil bulk density in kg/m^3 , an indicator of soil compaction. (3) Soil fragment refers to the percentage of soil coarse fragments (mean estimates). (2), (4), (5) refer to the percentage of clay, sand and silt fractions, respectively (mean estimates).

Table 3.2. Results of the ‘surface’ simulation on the evolution of $pPC1$. An OU model with two optima best explains the environmental data in Datureae.

Figure 3.1. Historical biogeography of Datureae using MCC tree from Dupin ([51]). Node states and biogeographical events represented here were estimated using the DEC+ j model (although there was no significant difference between the estimated history under any of DEC+ j or DIVA+ j models). The most likely ancestral state in Datureae is Andean. Branches represented by plain lines identify the two optima for the environmental niche in Datureae - dry (thin branches) and mesic (bold branches). The outgroup, *Nicandra*, was not included in the shift analysis, hence its dashed branch.

Figure 3.2. Biplot of $pPC1$ and $pPC2$. The first element of this plot is the set of vectors. Vectors represent how much each variable contributes to the pPC . The longer the vector the higher its contribution. The angle between vectors represents the amount of correlation between variables. The second element is the distribution of pPC scores in the $pPC1$ - $pPC2$ space for all the data points, in our case, the species in Datureae. Here we only present variables with loading

values above 0.6 or below -0.6. Variable names have been abbreviated, see Table 3.1 for full names. (Plot made with most recent version of the `biplot.phyl.pca` function (March 15th 2017))

Figure 3.3. Niche regions and niche overlap of the genera in Datureae. (a) Niche regions of *Brugmansia* (dark grey circles), *Datura* (light grey triangles) and *Trompsettia* (black squares), given $pPC1$ and $pPC2$. Individual collection points for each genus were included to represent the distribution and placement of each niche region in trait space. (b) Pairwise niche overlap between genera, the first column on the left represents the probability that an individual of *Brugmansia* would be found living in the niche region (NR) of *Datura* (top graph) and NR of *Trompsettia* (bottom graph). The same organization follows on the other two columns. The scale of the graphs aligned in columns is equivalent, but a zoomed in region is presented for the instances where the results are tightly clustered. Plain vertical black line marks the mean probability value; dashed vertical lines delimit the 95% region of the estimated overlap probabilities.

Figure 3.4. Dynamics over space and time of Datureae's environmental niche. This diagram (adapted from figure 1 in Pearman [170]) represents the evolution of Datureae's environmental niche. Curves with full colors represent realized niche regions while curves with equivalent but transparent colors represent the fundamental niche as a reference to the niche space that is not occupied by the species due to competition and other factors not measured in this study. The abscissa on the left represent the a scale for type of environment, where the extremes are a dry environment and a wet one.

Table 3.1: Variable loadings for $pPC1$ as a result of the $pPCA$ analysis. Precipitation variables (Annual Precipitation, Precipitation Driest Quarter and Precipitation Warmest Quarter) along with soil bulk density and mean diurnal range are the variables that contribute more for the variation within $pPC1$. (1) Soil bulk refers to soil bulk density in kg/m^3 , an indicator of soil compaction. (3) Soil fragment refers to the percentage of soil coarse fragments (mean estimates). (2), (4), (5) refer to the percentage of clay, sand and silt fractions, respectively (mean estimates).

Variable	pPC1 Loading
Annual Mean Temperature	-0.234
Mean Temperature Warmest Quarter	-0.532
Annual Precipitation	0.997
Precipitation Seasonality	-0.669
Precipitation Driest Quarter	0.917
Precipitation Warmest Quarter	0.879
Mean Diurnal Range	-0.926
Soil bulk 0.3m (1)	-0.879
Soil clay 0.3m (2)	-0.591
Soil fragment 0.3m (3)	-0.334
Soil sand 0.3m (4)	0.49
Soil silt 0.3m (5)	0.63

Table 3.2: Results of the ‘llou’ simulation on the evolution of $pPC1$

Log-Likelihood	-28.59
Number of shifts	1
Shift value	-5.44
pBIC score	77.47
Adaptation rate α	11.79
Variance σ^2	33.19
Stationary variance γ	1.41

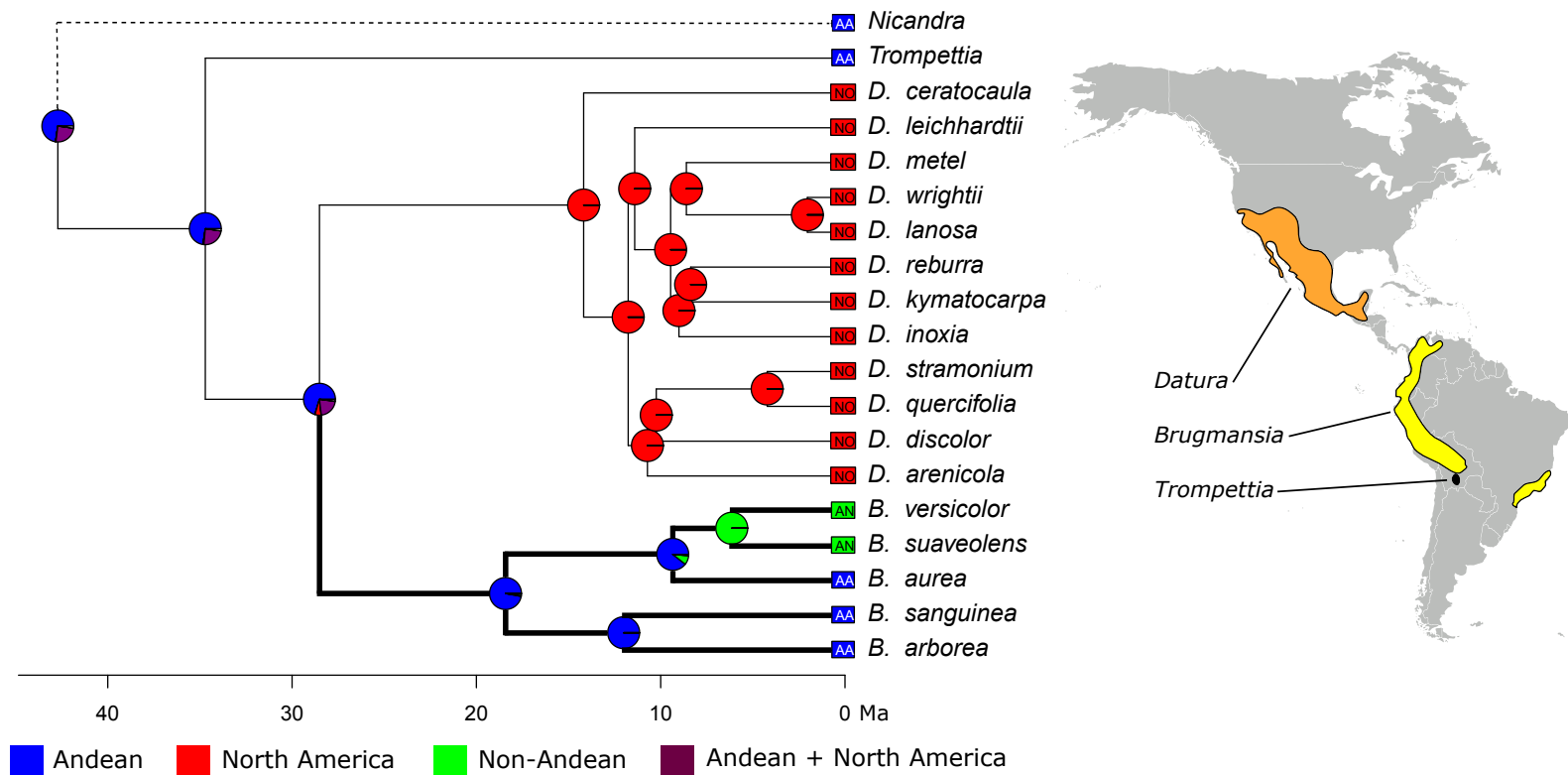


Figure 3.1: Historical biogeography of Datureae using MCC tree from Dupin ([51]). Node states and biogeographical events represented here were estimated using the DEC+ j model (although there was no significant difference between the estimated history under any of DEC+ j or DIVA+ j models). The most likely ancestral state in Datureae is Andean. Branches represented by plain lines identify the two optima for the environmental niche in Datureae - dry (thin branches) and mesic (bold branches). The outgroup, *Nicandra*, was not included in the shift analysis, hence its dashed branch.

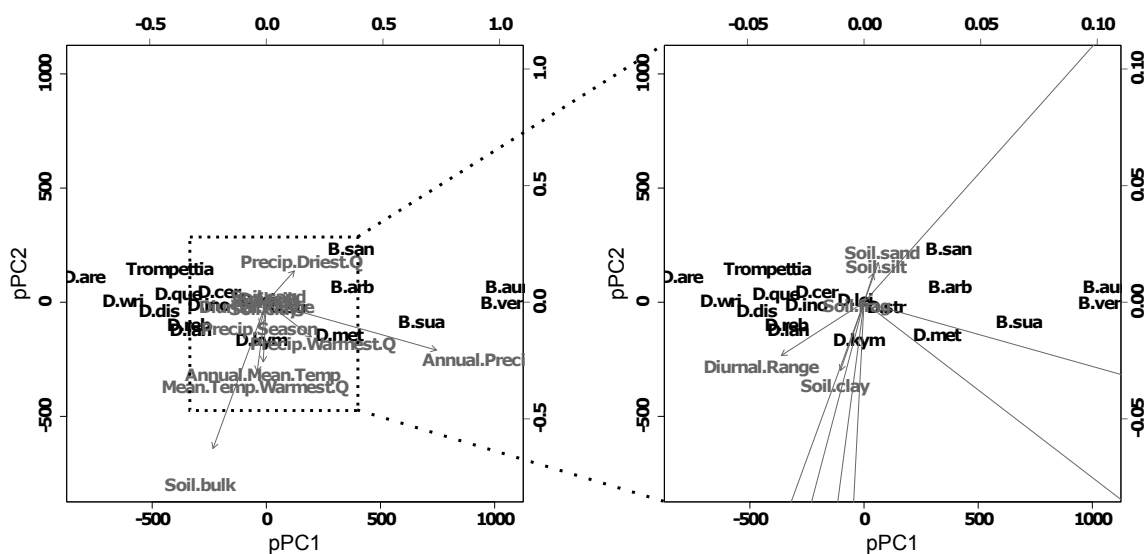


Figure 3.2: Biplot of $pPC1$ and $pPC2$. The first element of this plot is the set of vectors. Vectors represent how much each variable contributes to the pPC . The longer the vector the higher its contribution. The angle between vectors represents the amount of correlation between variables. The second element is the distribution of pPC scores in the $pPC1$ - $pPC2$ space for all the data points, in our case, the species in Datureae. Here we only present variables with loading values above 0.6 or below -0.6. Variable names have been abbreviated, see Table 3.1 for full names. (Plot made with most recent version of the `biplot.phyl.pca` function (March 15th 2017))

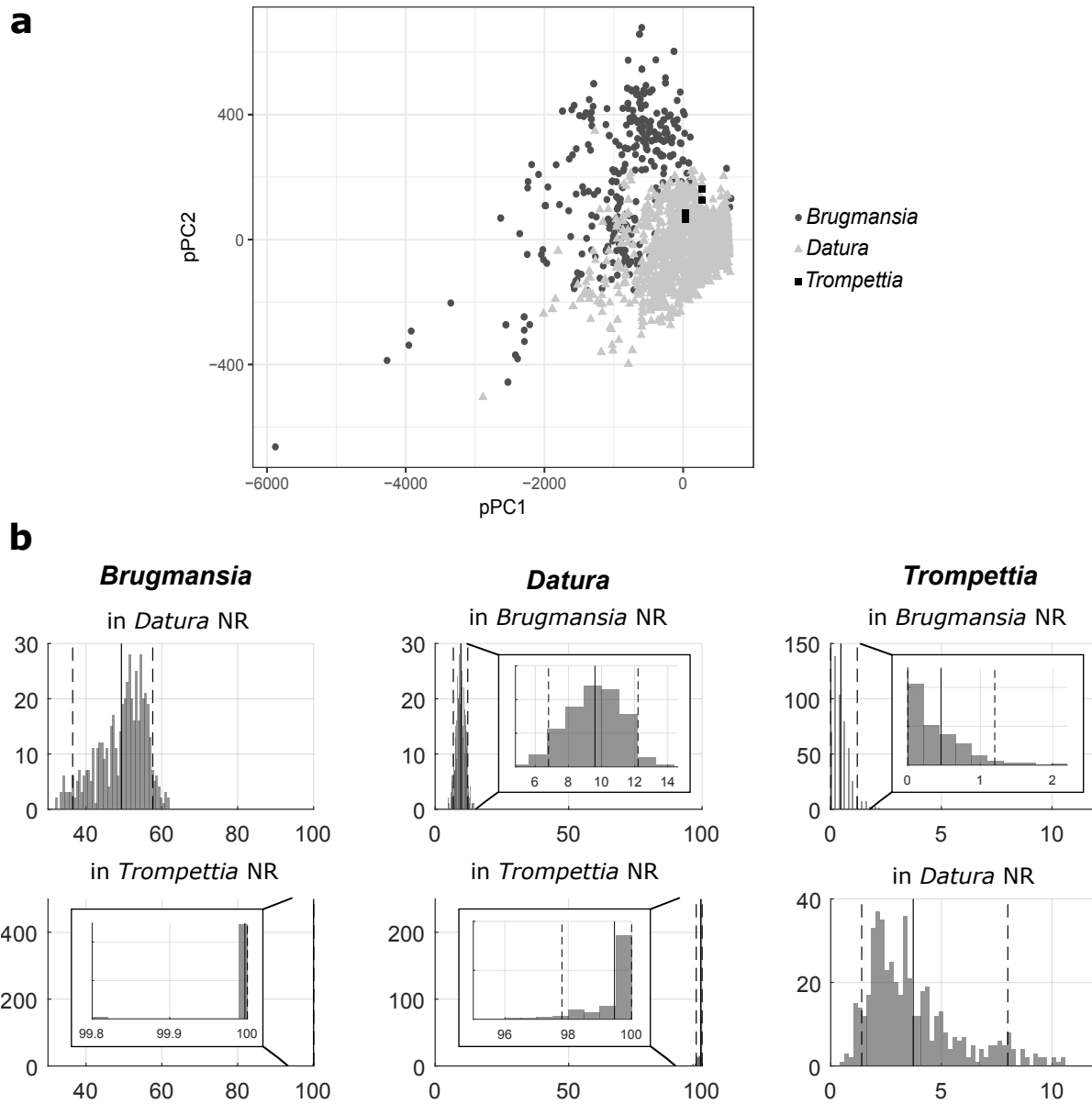


Figure 3.3: Niche regions and niche overlap of the genera in Datureae. (a) Niche regions of *Brugmansia* (dark grey circles), *Datura* (light grey triangles) and *Trompettia* (black squares), given $pPC1$ and $pPC2$. Individual collection points for each genus were included to represent the distribution and placement of each niche region in trait space. (b) Pairwise niche overlap between genera, the first column on the left represents the probability that an individual of *Brugmansia* would be found living in the niche region (NR) of *Datura* (top graph) and NR of *Trompettia* (bottom graph). The same organization follows on the other two columns. The scale of the graphs aligned in columns is equivalent, but a zoomed in region is presented for the instances where the results are tightly clustered. Plain vertical black line marks the mean probability value; dashed vertical lines delimit the 95% region of the estimated overlap probabilities.

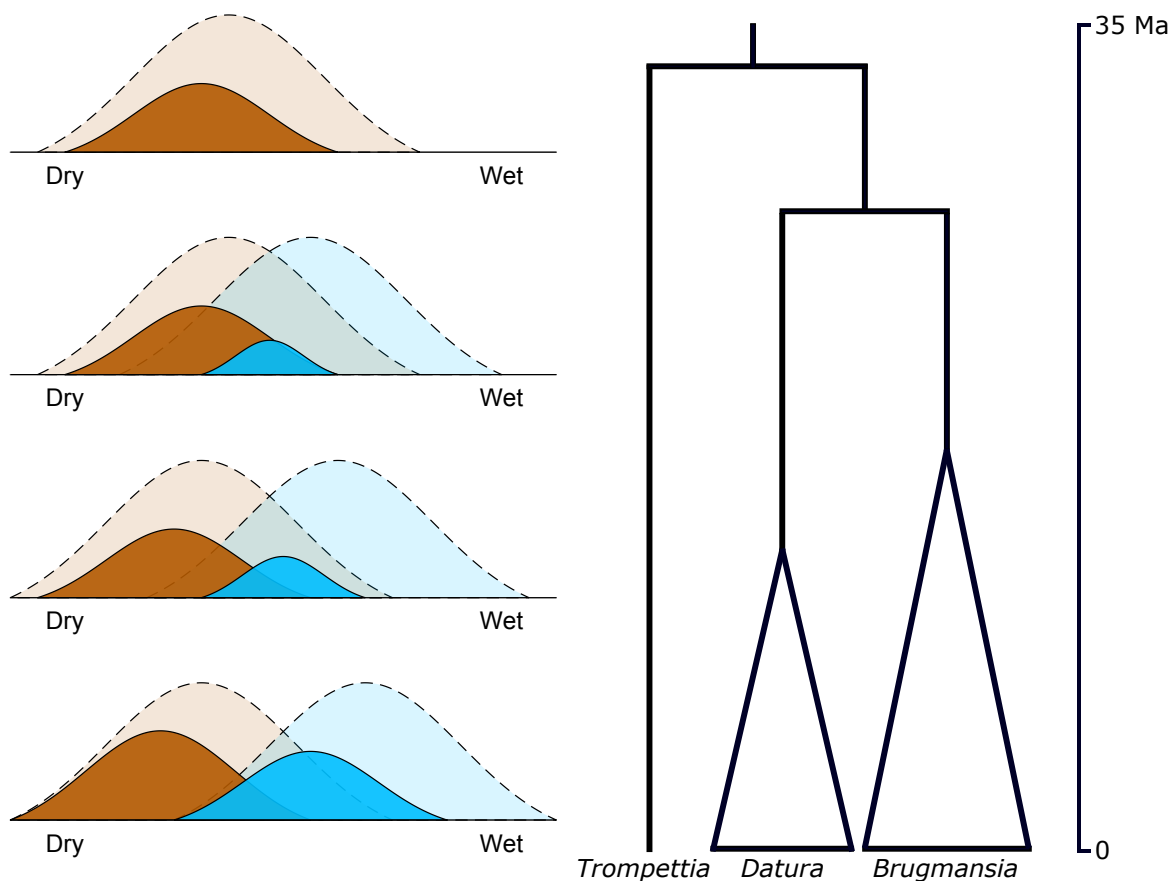


Figure 3.4: Dynamics over space and time of Datureae's environmental niche. This diagram (adapted from figure 1 in Pearman [170]) represents the evolution of Datureae's environmental niche. Curves with full colors represent realized niche regions while curves with equivalent but transparent colors represent the fundamental niche as a reference to the niche space that is not occupied by the species due to competition and other factors not measured in this study. The abscissa on the left represent the a scale for type of environment, were the extremes are a dry environment and a wet one.

Chapter 4

Evolution of fruit type in Datureae (Solanaceae)

[Manuscript to be submitted to the International Journal of Plant Sciences]

4.1 Introduction

Angiosperms produce a wide diversity of fruit forms, ranging from berries to drupes to capsules. In addition, transitions among these forms are frequent on evolutionary timescales. For example, the high number of transitions between fleshy and dry fruits in families such as Melastomataceae (Clausing [29]) and Solanaceae (Knapp [106]) likely helped generate the diversity in fruit morphology that is seen today in both groups. Such diversity in fruits can be a product of factors as adaptations to new habitats, for example in monocots (Givnish [70]), or adaptations to dispersers, as seen in Rubiaceae (Bremer [17]). Variations in fruit type are then ultimately tied to plant dispersal success, and consequently to plant fitness (e.g. Smith [210]; Price [182]; Biffin [13]).

Phylogenetic studies show that transitions between dry and fleshy fruits can occur in both directions, but the degree of bias in these transitions varies across clades. For instance, studies on subclades in the Campanulaceae have showed that while there is a tendency toward transitions from fleshy to dry fruits, transitions on the opposite direction are also present, meaning it is not a unidirectional process (Givnish [69]; Lagomarsino [109]). In contrast, a study on the Campanulid clade of ca. 35,000 species estimated no reversals to the clade's capsular ancestral state following multiple transitions to berries and achenes, suggesting strong constraint on fruit evolution (Beaulieu [9]). Several factors that can give rise to directional trends in evolutionary transitions such as time,

trait lability, and fitness consequences. A longer period of time provides more opportunities for trait transitions, and these transitions depend on the lability of the underlying characters. Additionally, a specific fruit type can increase the fitness of species, which leads to transitions favoring that type of fruit (e.g. Beaulieu [9]).

The Solanaceae is a useful model system for studying the evolution of fruit morphology because it presents a high diversity of fruit forms and has a robust phylogeny. The types of fruits for all the genera and major clades within the family have been previously classified (Hunziker [93]) and they encompass berries and drupes (both fleshy fruits), as well as capsules, mericarps and non-capsular dehiscent fruit (all forms of dry fruit) (Knapp [106]). Even though the family is best known for its fleshy fruits, Knapp ([106]) inferred that ancestral state for Solanaceae fruit is dry (capsule). She also estimated a similar number of transitions between fleshy and dry fruits. Using the phylogenetic framework presented by Knapp ([106]), Pabon-Mora ([164]) compared the development of several dry and fleshy fruited members of the family and suggested that fleshy and dry fruits can be differentiated anatomically, although variations within each fruit type were also observed. Nonetheless, many of the focal taxa were distantly related, making it difficult to identify the specific changes required to transition from fleshy to dry fruits and vice versa. Studies at finer phylogenetic scales comparing sister taxa that differ in fruit type may offer a greater potential to determine the developmental steps required for fruit type transitions (e.g. Hall [76]; Chiarini [27]; Mummenhoff [146]).

In this study, we explore the transitions between fruit types in Datureae, a tribe in the Solanaceae that displays a range of fruit types and presents a rare case of reversal from fleshy berries to dry capsules. Datureae is a clade of 18 species that belongs in the otherwise fleshy-fruited subfamily Solanoideae. Among the species in its three genera, *Brugmansia* Pers., *Datura* L. and *Trompettia* J. Dupin, we observe both fleshy and dry fruits (berries and capsules, respectively, Fig. 4.1). Within each fruit type there is variation in morphology. For example, the large berries of *Brugmansia* differ in size, shape and fruit wall thickness from the small round berries of *Trompettia*. The capsules of *Datura* species also vary in shape and size, and particularly in the mechanism of

dehiscence. Two species, *D. stramonium* and *D. quercifolia*, produce regularly dehisced fruits, where the fruit opens along four valves that coincide with the septa. The remaining species produce irregularly dehisced capsules, where the fruit wall ruptures irregularly. Another peculiarity of *Datura* fruits is that they produce false septa that give the bottom half of the fruits four chambers instead of the regular two seen in other Solanaceae fruits (Fig. 4.2).

Here we sample all principal fruit types in the Datureae tribe to trace the anatomical and developmental changes associated with the transition from a fleshy berry to a dry capsule. By focusing on Datureae, we can build on the previous work by Pabon-Mora ([164]), which included the irregularly dehisced capsules of *Datura innoxia*. In addition to comparing the anatomical features of fleshy and dry fruits in the tribe, we explore the characters that could explain the different dehiscence mechanisms within species in *Datura*. Specifically, we test the hypothesis that regularly dehisced fruits are anatomically more organized, that is, that dehiscence zones are clearly marked, and pericarp cell organization is more uniform. Lastly, we place these results into phylogenetic context to determine if the transition between berries and regularly dehisced capsules was a stepwise process, given the number of traits likely required for a dry fruit (e.g., creating dehiscence zones, opening to release seeds).

4.2 Methods

4.2.1 Anatomy and Morphology

Our species sampling included examples from all the fruit types in Datureae. We collected fruits at different developmental stages from the following species: *Brugmansia versicolor* (berry) and *B. sanguinea* (berry), *Trompettia cardenasiana* (berry), *Datura ceratocaula* (non-spiny, irregular dehisced capsule), *D. discolor* (irregularly dehisced capsule), *D. lanosa* (irregular dehisced capsule), *D. wrightii* (irregular dehisced capsule), and *D. quercifolia* (regularly dehisced capsule) and *D. stramonium* (regularly dehisced capsule). Samples of fruits of *B. versicolor* and *B. sanguinea* came from specimens growing at living collections in botanic gardens (Huntington Botanical Gar-

dens, CA, and Mildred E. Mathias Botanical Garden, UCLA, respectively), making the observations for these taxa more limited, and harder to control for specific stages. Individuals of *Trompettia* and *Datura* were sampled from living greenhouse collections at the University of Colorado-Boulder. In order to compare similar stages (which were limited for *Brugmansia*), we focused on the late stage of fruit development (fruit fully developed, largest developmental size) to identify the main differences between fruit types (Table 4.1).

Fruit materials were either sampled fresh or fixed in a formalin acetic acid alcohol (FAA) solution for at least 24 hours. We sampled three fruits per individual, in at least two individuals per species. Fixed material was dehydrated through an alcohol-xylene series and embedded in Paraplast X-tra (Fisher Healthcare, Houston). We sectioned the samples at 10 μ m with an AO Spencer 820 rotary microtome (GMI, Ramsey, MN), and stained them following a Sharman Stain Series (Sharman [209]) that uses 2% tannic acid and 1% iron alum solutions with safranin and orange G stains. These sections were digitally photographed using a compound microscope equipped with a Leica EC4 digital camera. We conducted most of the anatomy work at the facilities of Rancho Santa Ana Botanic Garden, California. Fresh samples were hand sectioned and stained with toluidine blue O. Images for these samples were taken using a dissecting scope.

To identify the anatomical differences between berries and capsules in Datureae, we first considered the characters described by Pabon-Mora ([164]). We followed their definition of the layers in the pericarp of Solanaceae fruits: endocarp is defined as the innermost layer of cells and all layers internal to the vascular tissue, mesocarp is the tissue found between the endocarp and the outer epidermis, and exocarp is the outer epidermis (outermost layer of cells) ((Fig. 4.3)). In their study, Pabon-Mora ([164]) listed the following features as characteristic of capsules: formation of a sclerified endocarp, dehiscence zones delineated by discontinuities of the sclerified endocarp, dehiscence upon drying of the fruit, and extensive intercellular spaces form in the pericarp and the placenta (these can be also common in berries, but not as numerous as in capsules) . For berries, the main characters were the presence of collenchyma in the mesocarp, expansion of the endocarp into the locules, forming fleshy protrusions, and expansion of the placenta into the locules, forming

fleshy outgrowths. For this study, we considered the presence and location of both collenchyma and sclerenchyma tissues in the fruits, along with the presence of any intercellular spaces (lacunae), and the presence and type of dehiscence. We also recorded the type and location of vascular bundles. In *Datura stramonium*, the vascular bundles have been reported to constitute the tissue of resistance, crucial for building the tension along the fruit wall that results in the fruit opening (Roth [195]).

Finally, to test the effects of dehiscence zones delimitation and the amount of tension required to open the capsule we complemented the study of differences in dehiscence types in *Datura* with a compression test. Fruits of *D. discolor* and *D. wrightii* (both irregularly dehisced), and *D. quercifolia* and *D. stramonium* (regular dehiscence) at late stages of development, but before starting to visibly dry out, were placed in an Instron 3345 Single Column System, where they were compressed with controlled pressure increments (in kilonewtons, kN, units) until a crack in the fruit wall occurred. We recorded the final compressive load before the crack and the compressive strain (how much, in mm, the fruit deformed), and compared the means of maximum load and strain under both types of dehiscence with a Student's t test. With this test we identified if there was a significant difference on the load required for each fruit type to crack open (e.g. if regularly dehisce fruits required less force to crack), and where that crack happened (e.g. if regularly dehisced fruits tend to open along the septa).

4.2.2 Reconstruction of ancestral anatomical states

For our analysis of fruit type evolution in Datureae, we used the time-calibrated maximum clade credibility (MCC) tree from Dupin (see Chapter 2). The original tree included all 18 recognized species in Datureae and seven outgroups. For our purposes, we pruned the tree using the ape package (Paradis [167]) in R (R Core Team [184]) to retain only the representative species analyzed here: *Brugmansia versicolor*, *B. sanguinea*, *Trompettia cardenasiana*, *Datura ceratocaula*, *D. discolor*, *D. lanosa*, *D. quercifolia*, *D. stramonium*, and *D. wrightii*. We reconstructed the ancestral state of six characters: fruit type (berry, capsule), endocarp collenchyma (present, absent), intercellular spaces in the pericarp (present, absent), dehiscence type (none, regular, irregular), mesocarp

sclerenchyma (present, absent), and placement concentric vascular bundles (pericarp, septa, both). We conducted these reconstructions using the R packages 'ape' (Paradis [167]) and 'phytools' (Revell [193]). For each character separately, we first compared models that assumed equal rates of transition between character states or different rates (using the function `ace` in 'ape'). The likelihood of each model was estimated and compared using a likelihood ratio test. Once we identified the best model, we estimated the history of each character using the function `make.simmap` in 'phytools'. For each of our characters, we simulated 100 histories and summarized the results at each node to give the relative posterior probability at each state. The final reconstructions were analyzed to address our hypothesis of a stepwise transition between the two fruit types.

4.3 Results

4.3.1 Anatomical comparison between berries and capsules

Capsules and berries in *Datureae* present some of the expected characters of each fruit type, but we also see overlap in traits not previously reported. Intracellular spaces are common in both capsules and berries in *Datureae*, but capsules tended to have more of these, especially at a late developmental stage (qualitative observation only; intercellular spaces marked with blue circles in Fig. 4.4). In *Trompettia* berries, which do not have false septa, these spaces are restricted to the septa tissue, likely as a result of having very few pericarp cell layers. In all other fruits, they are found in the pericarp, the septa and the false septa. *Datura* fruits do not possess an endocarp, as is the case with other capsules in *Solanaceae* (Pabon-Mora [164]). *Datura* capsules do present a mesocarp with fibers, where the sclerenchyma fibers are associated with the formation of the spines (Fig. 4.4 f). These fibers are not seen in *D. ceratocaula* as it lacks spines. Berries present collenchyma tissues in both the meso and endocarp tissues (collenchyma layers showed with blue arrows in Fig. 4.4), as expected, but they lack any signs of expansion of the endocarp into the locules and the expansion of the placenta into the locules. Notably, the capsules studied here present collenchyma in the mesocarp, and the capsules in *D. discolor* show expansion of the endocarp into

the locules (Fig. 4.4 l), both characters described as common in berries of Solanaceae (Pabon-Mora [164]). Finally, berries in both *Brugmansia* and *Trompettia* present a distinct innermost layer of cells in the pericarp that is characterized by cells with thicker, secondary walls, a trait not seen in any of the capsules (marked with black triangles in Fig. 4.4 a, d, e).

Our results also show that the presence, placement, and elaboration of concentric vascular bundles varies between and within fruit types when comparing mature fruits. The berries of *Brugmansia versicolor* and *B. sanguinea*, and the capsules of *Datura quercifolia* and *D. stramonium* present thick, well developed concentric vascular bundles in the pericarp, and in the septa and false septa tissues (Fig. 4.4 a, c, g, i). These are classified as amphicribal bundles given that the xylem is internal to the phloem. *Trompettia* berries, as many other berries in Solanaceae, present only underdeveloped amphicribal bundles (Fig. 4.4 d, e), meaning the bundles are not fully circular and there are fewer layers of low lignified xylem and phloem cells. For the remaining samples, *D. discolor*, *D. lanosa*, *D. wrightii* and *D. ceratocaula*, there are fully developed amphicribal bundles in the septa and false septa tissue (Fig. 4.4 p) but only underdeveloped ones in the pericarp (Fig. 4.4 m, q).

4.3.2 Regular and irregular dehiscence mechanisms in *Datura*

Fruit opening in regularly dehisced capsules is always basipetal (Fig. 4.5 a, b), while in irregular dehisced capsules, the direction is variable but typically basipetal. We identify the well-developed amphicribal vascular bundles in the pericarp as one of the major determinants of the type of dehiscence in *Datura*. Regularly dehisced capsules have these bundles in their pericarp, and their distribution and function as the tissue of resistance when the fruit is drying out delimits the four valves in the fruit and the dehiscence zones (Fig. 4.5 c). These vascular bundles are not found in the pericarp of irregularly dehisced fruits so, once the drying process starts, the lack of an orientation defined by the large vascular bundles along the pericarp allows the fruit to rupture at any region or orientation.

Examining the anatomical changes in the dehiscence zones, we can identify the steps leading

to regular dehiscence. First (Fig. 4.5 a), the septa detach from the apex of the fruit creating a discontinuity on the innermost layer of cells. This detachment happens not only along the connection point of the septa and the fruit wall but also coincides with the position of the false septa, even though the latter does not touch the full extension of the fruit wall, only the bottom half. This detachment creates four weak lines that are translated towards the base of the fruit. This translation is maintained and promoted by the drying process that happens on the pericarp. With the loss of water, the cells shrink and increase the tension within the fruit wall. The dehiscence process starts on the innermost layer of cells and proceeds outward towards the exocarp (Fig. 4.5 b).

As predicted, the compression tests showed that regularly dehisced fruits require less compression load to crack open than the irregularly dehisced fruits (Fig. 4.6). Regularly dehisced fruits of *Datura quercifolia* and *D. stramonium* deformed less (mean of compressive strain = 3.5 mm) and took a lighter compressive load (mean = 0.05 kN) to open. In contrast, the mean number for both compressive strain and compressive load were significantly higher in the irregularly dehisced fruits of *D. discolor* and *D. wrightii*, 18.8 mm and 0.21 kN respectively. Additionally, regularly dehisced fruits always opened along the septa and false septa regions, while the irregular ones presented a variation in the position of the crack.

4.3.3 Evolution of anatomical characters

The history of the characters we reconstructed with a stochastic mapping approach points to a stepwise anatomical evolution in Datureae towards regularly dehisced capsules (Figs 4.7, 4.8). Our results show that the loss of endocarp collenchyma is likely coordinated with the gain of mesocarp sclerenchyma, and this step precedes the development of amphicribal bundles in the pericarp of regularly dehisced capsules (Fig. 4.7). Moreover, the results show that the evolution of fruit type, endocarp collenchyma, and intercellular spaces is consistent with the phylogenetic relationships in the tree, meaning the number of changes observed is the minimum possible to explain the data. Fruit type and endocarp collenchyma present a single change along the *Datura* stem branch, and

the placement of intercellular in the pericarp shows one change along the *Trompettia* branch. The remaining characters present multiple changes between states. In dehiscence type, with three possible states, we found a mean of 4.13 changes along the phylogeny; in mesocarp sclerenchyma, with two states, a mean of 3.5; and in amphicribal (concentric) vascular bundles, given its three states, a mean of 5.7 (Fig. 4.8).

4.4 Discussion

Our anatomical comparison of capsules and berries in Datureae and the analyses of character evolution show that the reversal seen in *Datura* fruits (from berry to capsule) results from a complex series of steps. The transition to a regularly dehisced capsule involves first the loss of endocarp collenchyma and gain of mesocarp sclerenchyma, followed by a change to having fully developed amphicribal bundles in the pericarp. The presence and distribution of amphicribal vascular bundles is homoplasious in Datureae, but even so, we conclude that the organization of bundles is an important factor in dehiscence mechanism in capsules of *Datura*, and in differentiating regular and irregular dehiscence. While capsules and berries in Datureae are functionally different, we found overlapping anatomical characters between the two types of fruit, such as the presence of collenchyma in the mesocarp.

4.4.1 Transition from berry to capsule in Solanaceae

The reversal in fruit type observed in Datureae is rare in Solanaceae. In fact, *Datura* is the only genus in a family of estimated size of 2800 species described as producing capsules that evolved from berries. There are several possible explanations for the rarity of reversals. On the one hand, transitions towards berries might prevent the re-evolution of capsules. A similar pattern of strong directionality was documented in the Campanulids, where capsules could not be re-evolved once any of the component characters (being dehiscent, dry, or containing multiple seeds) were lost (Beaulieu [10]), and in Rubiaceae, where transitions from capsules to berries are unlikely because of the evolutionary costs of de-specializing the highly sclerified endocarp tissue (Bremer [17]). On the

other hand, there is the possibility of non-equilibrium when it comes to fruit types in Solanaceae, if the overall transition rates between states is slow. In this case the rarity seen in Datureae could mean that there has not been enough time to observe multiple transitions, given low rates of capsule evolution. This implies that at equilibrium we might expect additional cases of reversal across the family.

The limited transitions between capsules and berries observed in Solanaceae and the Campanulids is not necessarily the rule. Clausing ([29]) showed that, in Melastomataceae, shifts between those fruit types are common in both directions, a pattern which may be attributed to their fruit anatomy between Melastomataceae. In Melastomataceae, fruits can be originated from the development of the hypanthium (expanded flower receptacle), the ovary or a combination of both, which allows for multiple opportunities for tissue differentiation resulting in a great diversity in fruit morphology (Clausing [29]). This lability is not observed at the anatomical level in Solanaceae, given that its fruits are a product of the development of the ovary wall only.

4.4.2 Capsules and berries in Datureae and other Solanaceae

Capsules and berries in Datureae do not present the entire suite of characters that distinguish the two types in other species in Solanaceae. Pabon-Mora ([164]) studied the fruit development of six representative taxa in Solanaceae, the capsules of *Nicotiana sylvestris*, *Petunia hybrida* and *Datura innoxia*, and the berries of *Solanum lycopersicum*, *Iochroma fuchsoides*, and *Cestrum diurnum*. Both *N. sylvestris* and *P. x hybrida* belong to lineages which have retained the pleisiomorphic state of capsules, and they present the following character states: constant number of cell layers in the ovary wall and pericarp throughout development, sclerified endocarp, elongation of the epidermal cells of the placenta, dehiscence zones delineated by discontinuities of the sclerified endocarp, and fruit dehiscence. The major difference between these and the capsules of *Datura*, as pointed out by Pabon-Mora ([164]), is the lack of a sclerified endocarp in the latter. This may relate to the fact that *Datura* capsules have recently transitioned from berries, fruits that do not develop such a specialized endocarp. Pabon-Mora ([164]) concluded that the capsules of *D. innoxia* were the excep-

tion when it comes to capsule anatomy in Solanaceae (see also Dave [38]). The berries produced by *S. lycopersicum*, *I. fuchsoides*, and *C. diurnum* show an increase in the number of layers of the pericarp following fertilization, fruit growth due to cell expansion, collenchyma in the mesocarp, expansion of the endocarp into the locules, and plasticity in mature fruit size (Pabon-Mora [164]). By comparison, *Brugmansia* and *Trompsettia* berries lack the expansion of the endocarp tissue. Furthermore, the capsules of *Datura* have at least two of the characters listed as characteristic of berries, collenchyma in the mesocarp (Fig. 4.4, blue arrows), expansion of the endocarp into the locules (Fig. 4.4 l); and berries of *Brugmansia* and *Trompsettia* present what looks like a sclerified endocarp (innermost layer of cells, Fig. 4.4 a, d, e).

Said overlap in anatomical characters of *Datura* capsules and berries in Solanaceae could be an indication of the different ways to make and open a capsule. While *Datura* capsules are not as sclerified as those of *Nicotiana* and *Petunia* (Dave [38]; Pabon-Mora [164]), the fruits in *Datura* still present effective dehiscence mechanisms, regular and irregular, as described here. Indeed, *D. ceratocaula* fruits have few fiber bundles on the mesocarp (due to the lack of spines on its fruit wall), a demonstration that capsules in Datureae that do not rely solely on the hardening of the fruit wall to open. *Datura ceratocaula* fruits could make use of the continued growth of the mesocarp without accompanying growth in the endocarp, which ultimately creates suture regions in the endocarp (as suggested by Dave [38]).

4.4.3 Vascular system as the tissue of resistance in fruit wall of *Datura* capsules

Datura fruits dehisce differently than those of *Petunia* and *Nicotiana*. The fruit dehiscence mechanism in *Petunia* and *Nicotiana* relies heavily on the extensive lignification of the inner cell layers of the fruit, and on the delimitation of dehiscence zones at the junction of the septum and pericarp. These zones constitute a gap in the lignified tissue, making those the weak points in the fruit wall (Pabon-Mora [164]). *Datura* fruits, on the other hand, appear to open using a different mechanism. The lack of lignification in the endocarp, or the lack of cell layers with thinner cell walls to define dehiscence zones, differentiates the dehiscence mechanism of *Datura* from *Petunia*

and *Nicotiana*. Here we propose that the vascular tissue is one of the main components of the dehiscence mechanism in *Datura*. Along with the structure provided by the observed sub-epidermal collenchyma (Fig. 4.4 g, h, j, k, n, o), the vascular tissue creates a tissue of resistance that may increase the tension within the fruit wall while it dries out. Variations in the organization of the vascular tissue of the fruit wall and the different levels of vascular bundle differentiation (well-developed amphicribal bundles vs. underdeveloped) are tied to the two types of dehiscence, regular and irregular. Thicker vascular bundles, with a large number of lignified xylem cell layers results in a tissue that resists to the deformation as the pericarp cells lose water, resulting in regular dehiscence.

The development of amphicribal vascular bundles in fruits of *Datura* is not an innovation, however. The carpels of multiple genera in Solanaceae present amphicribal vascular bundles (Murray [148]). These bundles seem to be common in the flower gynoecium, where bicollateral vascular bundles transition to amphicribal bundles that can be found in the placenta (more commonly) and later in parts of the pericarp (Roth [195]). These bundles have also been described in the berries of *Capsicum annuum* (although their structural function, if any, is not discussed) (Roth [195]), and an underdeveloped version seems to be common in berries in Solanaceae (Pabon-Mora [164]). Nevertheless, this co-option (and further development) of the vascular tissue as a key feature in capsule dehiscence in *Datura* appears to be unique in Solanaceae, and rare in other families (but see Kriebel [108]).

4.4.4 Seed dispersal in Datureae

Fruit type transitions in Datureae are likely associated with differences in modes of seed dispersal. All species in *Datura*, except for *D. quercifolia* and *D. stramonium*, produce seeds with elaiosomes. These fleshy seed structures take on the role of attracting animal dispersers, usually ants. Seed dispersal in *Datura* is primarily done by ants, and water serves as a secondary disperser (O'Dowd [157]; Marussich [130]). The seeds have a thin but present corky outer layer that makes them float, and *Datura* specimens have been observed growing along or near riverbeds (J. Dupin

pers. obs.). In contrast, the dispersal mechanisms in *Brugmansia* and *Trompettia* are unknown. There are no reports of animal dispersal in any of these genera, but both produce corky seeds, making water a potential disperser. In addition, *Brugmansia* fruits tend to rot on the plant, and the pericarp is completely removed, leaving behind the net of vascular tissue holding the seeds (J. Dupin, pers. obs.). Notably, while *Brugmansia* fruits have always been classified as fleshy and indehiscent, a rare instance of a *Brugmansia* fruit showing signs of desiccation and dehiscence has been observed (Pabon-Mora pers. comm.). This could be an example where the usual thick, fleshy pericarp was not developed well enough to resist the tension caused by the net of amphicribal bundles. The large size of *Brugmansia* fruits (elongated fruits of length between 10 and 25 cm) and the lack of records about dispersers could indicate that the main animal disperser of these fruits has gone extinct. In the case of *Trompettia*, the lack of records is likely a product of the rarity of this species. *Trompettia* is restricted to dry intermountain regions along the Andes of southern Bolivia, making the study of the biology of this species challenging.

4.5 Conclusion and future directions

Our results demonstrate the relevance of phylogenetic context when reconstructing the evolution of complex traits. We found that the re-evolution of capsules in *Datura* fruits is due to different character changes when compared to other genera that produce capsules in Solanaceae. *Petunia* and *Nicotiana*, not only retained the ancestral state in the family but they also have about a 70-million-year headstart on *Datura* (Särkinen [200]) when it comes to producing capsules, once we consider that the ancestor of Solanaceae and Convolvulaceae (its sister group; Magallón [127]) likely produced capsules too. The overlap of characters between the capsules of *Datura* and berries may represent the signature of common ancestry, given that the ancestral state in Datureae is a berry. Our study of the reversal in fruit type in *Datura* also shows that the making of capsules in Solanaceae is variable. Consider the dehiscence patterns of *D. ceratocaula*, we conclude that high levels of sclerification of the endocarp are not required for dehiscent capsules, as the tension within the fruit wall can be a product of the resistance in other tissues, such as the vascular and

the collenchyma tissues. As a matter of fact, the dehiscence in *D. ceratocaula* capsules merits an independent study given that the fruits rupture while the pericarp is still fleshy.

The results presented here provide a foundation for future studies of the drivers of transitions among fruit types in Solanaceae, and other plant families. For example, different fruit types have often been associated with different habitat types (e.g. Givnish [70]; Chen [26]) and Datureae fits this pattern in being distributed among both mesic and arid areas. Indeed, the transition to capsules coincides with long distance dispersal from South America to North America in *Datura* (see Chapter 3). Transitions in fruits have also been reported as being associated with type of dispersers, where fleshy fruits (or fruits with fleshy appendices) tend to be dispersed by animals (Bremer [17]; Lorts [121]), and dry fruits by abiotic factors such as wind (reviewed in Howe [87]). The results of such correlated analysis can be put in context and compared with causes of transitions in other plant families to tests for broad patterns of association between specific fruit types and a given environment or disperser. As we consider how habitat transitions, changes in dispersal mode, and other selective factors that might influence fruit evolution, we have to incorporate the phylogenetic framework. For studies to determine ancestral and derived states and directionality of transitions, it is crucial to determine how closely related species are, and the overall amount of time available for transitions in a given clade.

4.6 Tables and figures

Table 4.1. Characters at late stage of fruit development of species of *Brugmansia*, *Datura* and *Trompettia*.

Figure 4.1. Fruit types in Datureae. Fleshy fruits (berries) of: a, *Brugmansia versicolor*; and b, *Trompettia cardenasiana*; dry fruits (capsules) of c, *Datura quercifolia*; d, *D. discolor*; e, *D. ceratocaula*. Capsules are shown with a picture of their dehisced state. Images are representative of the relative sizes of fruits.

Figure 4.2. Differences in fruit septa in the different genera in Datureae. *Brugmansia* and *Trompettia* berries have two locules along the whole extension of the fruit, while *Datura* fruits,

up to the middle, have a fake septa (arrows) that comes from the placenta and that creates four locules in the fruits bottom half. Horizontal lines represent position of cross section. Dark, full circles mark the dorsal veins of the two fused carpels that form the fruit. Fruits and sections not to scale.

Figure 4.3. Cell layer organization in Datureae fruits. From top to bottom, the exocarp corresponds to the outer most layer of cells; mesocarp all layers between the exocarp and the vascular bundles (these included), and the endocarp corresponds to the remaining layers below the mesocarp.

Figure 4.4. Anatomical images of berries and capsules in Datureae at their late stage of development. All images are arranged in the same fashion, with the exocarp on the top and the endocarp towards the bottom. Reference scale indicates 200 μm in all images. Arrows indicate the layers of collenchyma tissue, circles highlight some of the intercellular spaces. Red coloration indicate lignified cell walls. a-c *Brugmansia versicolor*, in c a close-up of vascular bundle; d-e, *Trompsettia cardenasiana*; f-i, *Datura quercifolia*, in f one of the fruits spines with the fibers that help form it; j-m, *D. discolor*, in l expansion of the endocarp cells into the locule, in m a close-up of vascular bundle; n-q, *D. ceratocaula*, in p one of the amphicribal vascular bundles found in the septa, in q a close-up of vascular bundle.

Figure 4.5. Anatomy and morphology of the dehiscence process in the regularly dehisced fruits of *Datura quercifolia*. The order of the images begins with the earliest stage at top left, moving counterclockwise towards maturity. a, detail of *D. quercifolia* fruit seen from the top (left), section of the fruit apex (middle) showing the separation of the septa (in the center) from the fruit wall, and the horizontal lines of cells (marked with asterisks) from the fruit tip that mark two out of the four dehiscence zones, half way the fruit wall (cross section seen on the right picture) showing the continuity of the dehiscence zones (lines). b, anatomical detail of the dehiscence zones focusing on the middle portion of the fruit and the connection points between the septa and the false septa with the fruit wall (diagram on the left), in the middle images we see the moment right before the dehiscence zones start rupturing, and on the right advanced stages of dehiscence where the

innermost layer of cell is discontinuous which triggers the degradation of cells in those regions. *c*, *D. quercifolia* fruits completely dry, arrows point to the massive vascular bundles (same ones showed in b) that delimit the four valves that are formed once the fruits dehiscence is complete.

Figure 4.6. Results of the compression tests on regularly dehisced fruits of *Datura quercifolia* and *D. stramonium*, and irregularly dehisced fruits of *D. discolor* and *D. wrightii*. The distribution of the points in space is concordant with dehiscence type. Regularly dehisced fruits require less load, and deform less, before a crack happens on the fruit wall, when compared to irregularly dehisced fruits. Pictures show how the compression test was set up on the Instron machine, on the left a fruit of *D. quercifolia*, on the right, one of *D. wrightii*.

Figure 4.7. Stepwise reversal to regularly dehisced capsules in Datureae. 1. loss of endocarp collenchyma and gain of mesocarp fibers; 2. production of large concentric vascular bundles in the pericarp.

Figure 4.8. Ancestral state reconstruction for six characters: fruit type, dehiscence type, presence of intercellular spaces, presence of sclerenchyma in mesocarp, and placement concentric vascular bundles.

Table 4.1: Characters at late stage of fruit development of species of *Brugmansia*, *Datura* and *Trompettia*.

Species	Fruit type	Dehiscence type	Intercellular spaces in pericarp	Mesocarp col-lenchyma	Endocarp col-lenchyma	Mesocarp sclerenchyma	Endocarp sclerenchyma	Placement concentric vascular bundles
<i>B. versicolor</i>	Berry	None	+	+	+	-	-	Pericarp, septa
<i>B. sanguinea</i>	Berry	None	+	+	+	-	-	Pericarp, septa
<i>Trompettia</i>	Berry	None	-	+	+	-	-	None
<i>D. quercifolia</i>	Capsule	Regular	+	+	-	+	-	Pericarp, septa
<i>D. stramonium</i>	Capsule	Regular	+	+	-	+	-	Pericarp, septa
<i>D. discolor</i>	Capsule	Irregular	+	+	-	+	-	Septa
<i>D. lanosa</i>	Capsule	Irregular	+	+	-	+	-	Septa
<i>D. wrightii</i>	Capsule	Irregular	+	+	-	+	-	Septa
<i>D. ceratocaula</i>	Capsule	Irregular	+	+	-	-	-	Septa

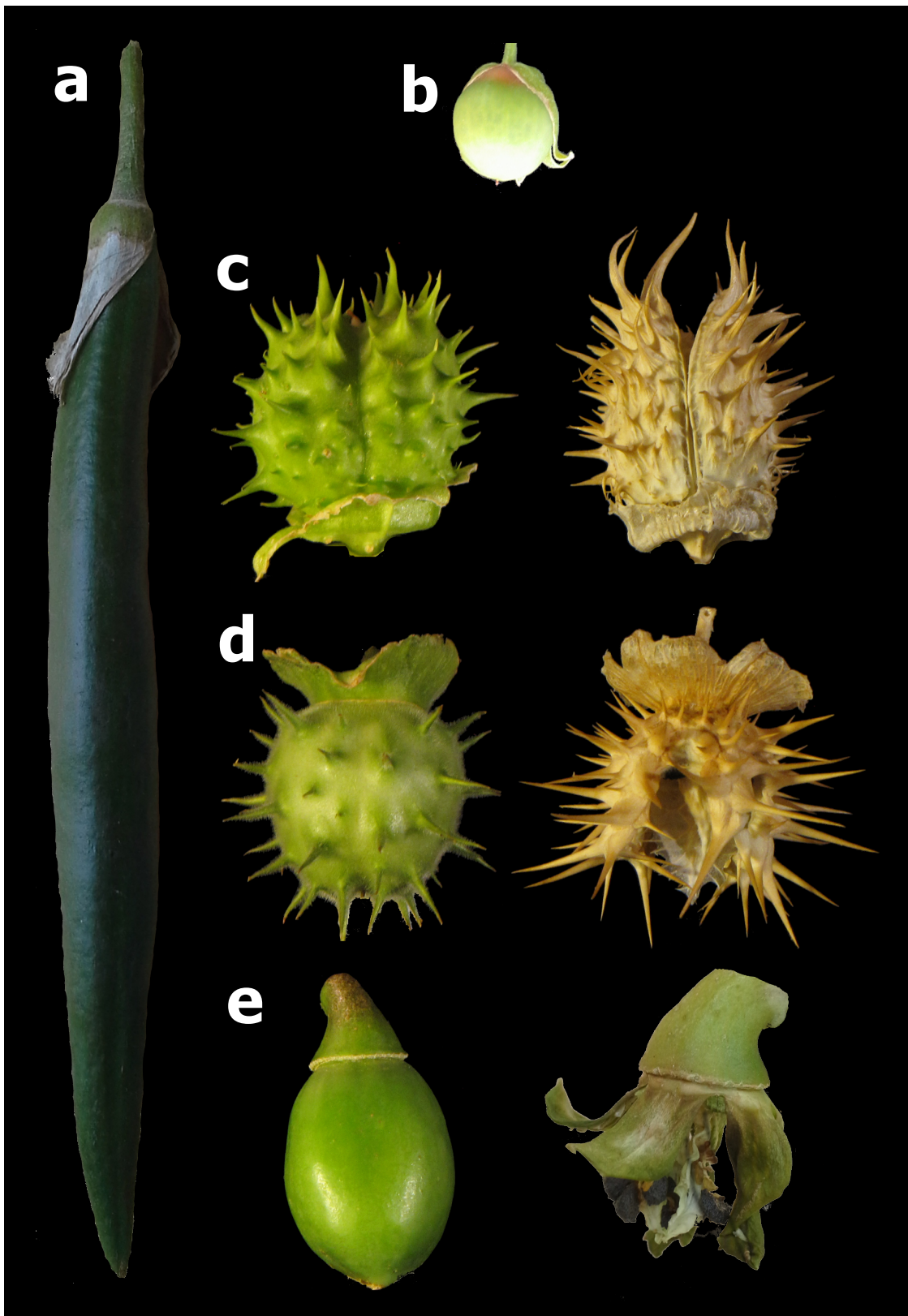


Figure 4.1: Fruit types in Datureae. Fleshy fruits (berries) of: a, *Brugmansia versicolor*; and b, *Trompettia cardenasiana*; dry fruits (capsules) of c, *Datura quercifolia*; d, *D. discolor*; e, *D. ceratocaula*. Capsules are shown with a picture of their dehiscent state. Images are representative of the relative sizes of fruits.

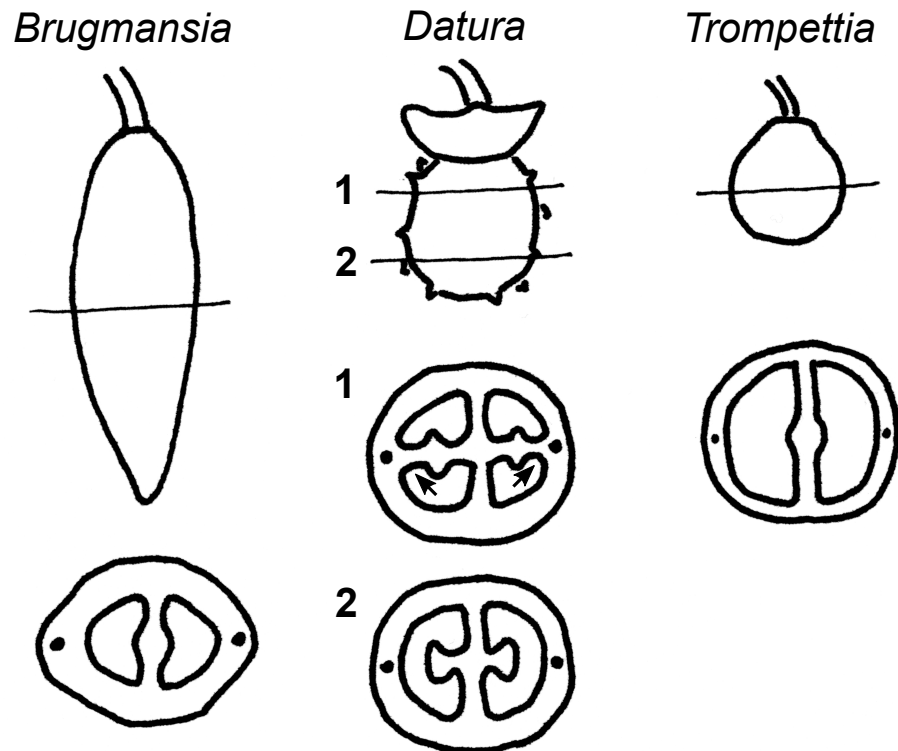


Figure 4.2: Differences in fruit septa in the different genera in Datureae. *Brugmansia* and *Trompettia* berries have two locules along the whole extension of the fruit, while *Datura* fruits, up to the middle, have a fake septa (arrows) that comes from the placenta and that creates four locules in the fruits bottom half. Horizontal lines represent position of cross section. Dark, full circles mark the dorsal veins of the two fused carpels that form the fruit. Fruits and sections not to scale.

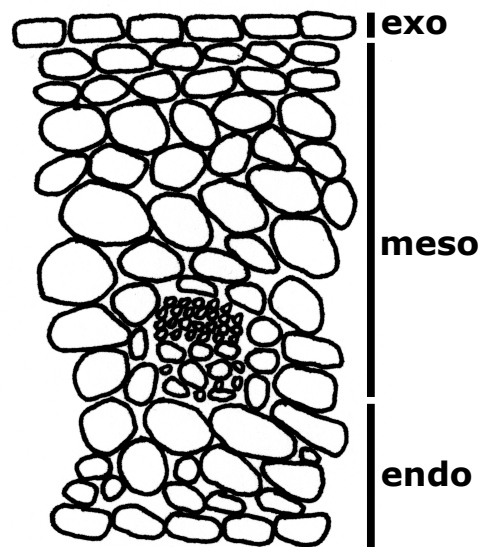


Figure 4.3: Cell layer organization in Datureae fruits. From top to bottom, the exocarp corresponds to the outer most layer of cells; mesocarp all layers between the exocarp and the vascular bundles (these included), and the endocarp corresponds to the remaining layers below the mesocarp.

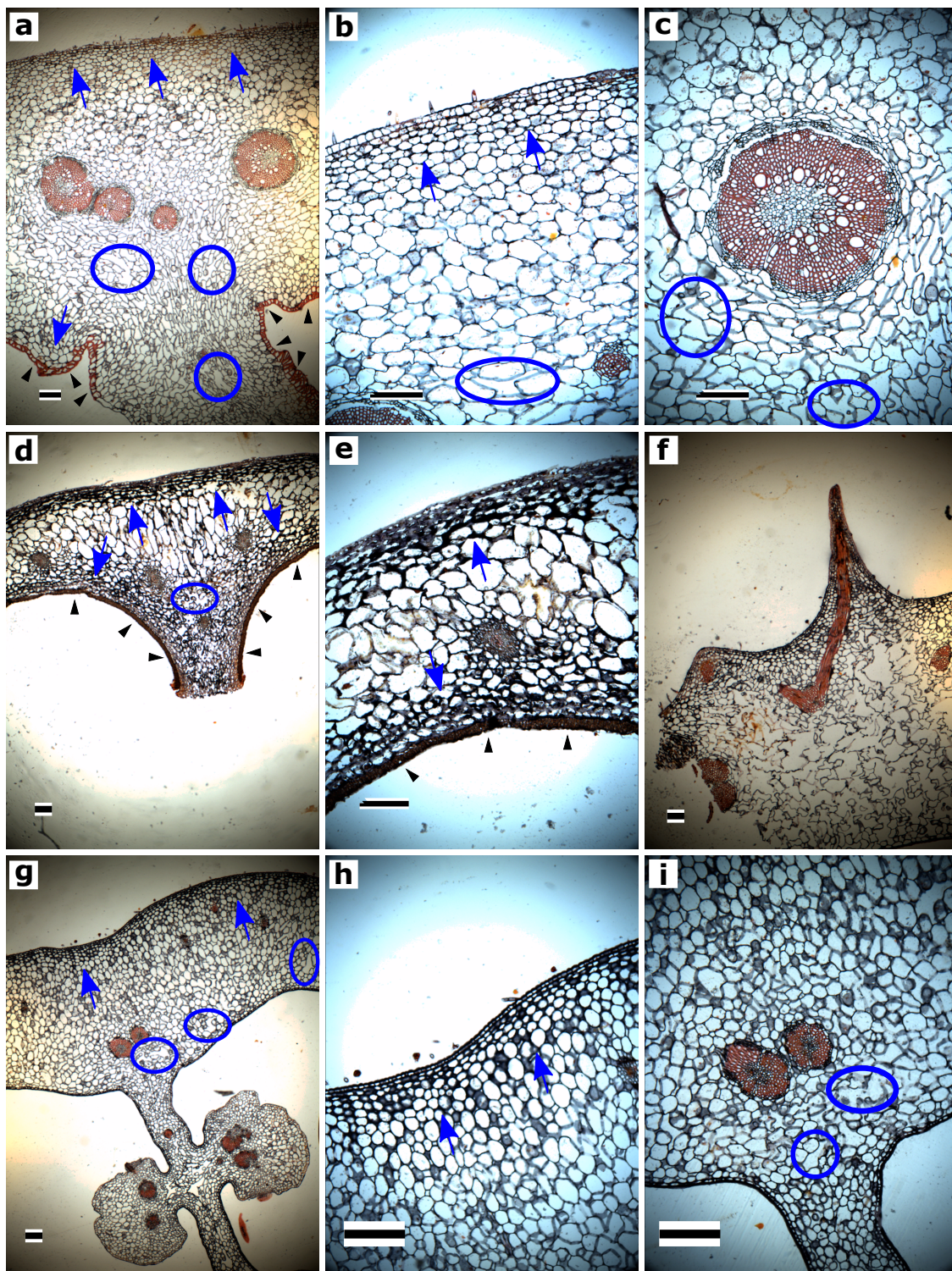
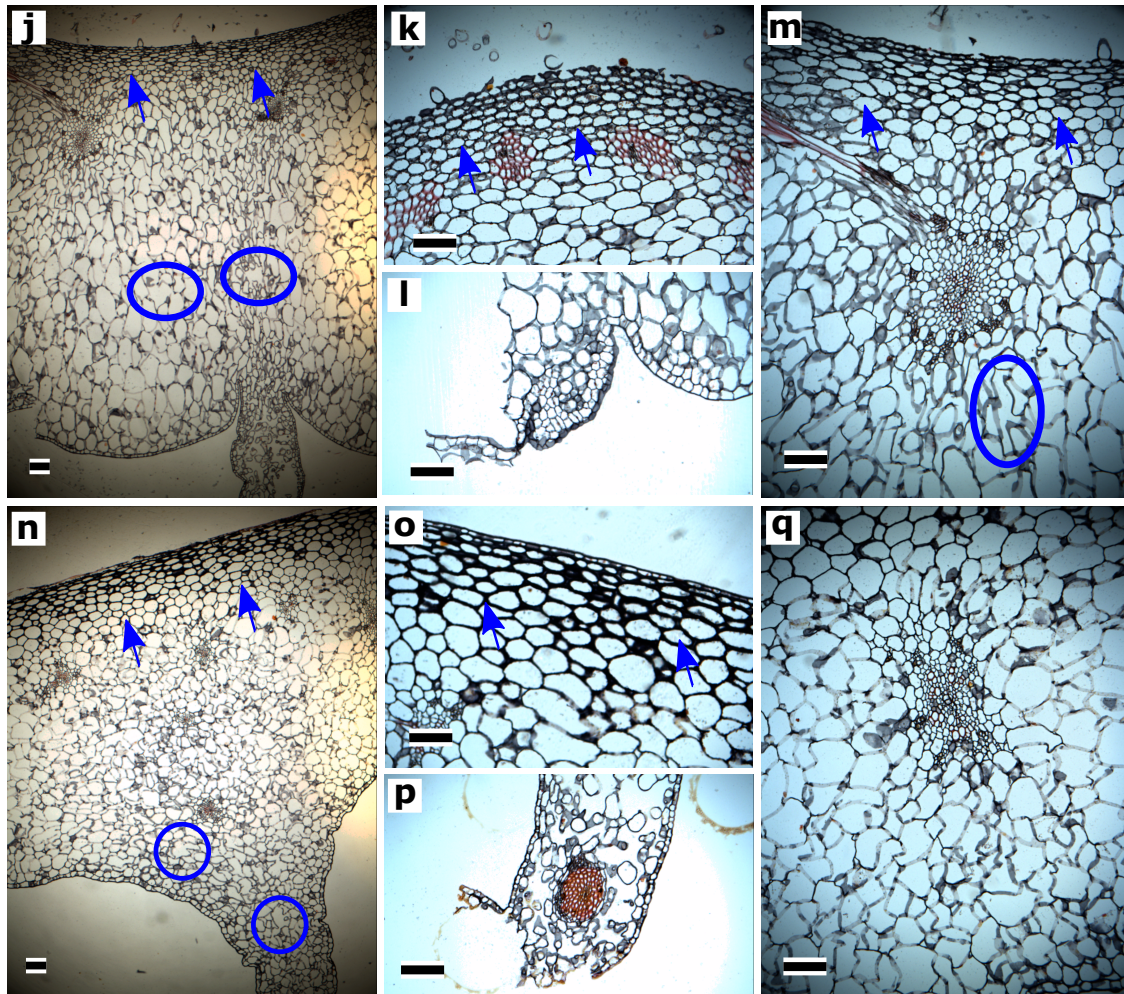


Figure 4.4: Anatomical images of berries and capsules in Datureae at their late stage of development. All images are arranged in the same fashion, with the exocarp on the top and the endocarp towards the bottom. Reference scale indicates $200 \mu\text{m}$ in all images. Arrows indicate the layers of collenchyma tissue, circles highlight some of the intercellular spaces. Red coloration indicate lignified cell walls. a-c *Brugmansia versicolor*, in c a close-up of vascular bundle; d-e, *Trompettia cardenasiana*; f-i, *Datura quercifolia*, in f one of the fruits spines with the fibers that help form it. (continues on next page)



(continued) j-m, *D. discolor*, in l expansion of the endocarp cells into the locule, in m a close-up of vascular bundle; n-q, *D. ceratocaula*, in p one of the amphicribal vascular bundles found in the septa, in q a close-up of vascular bundle.

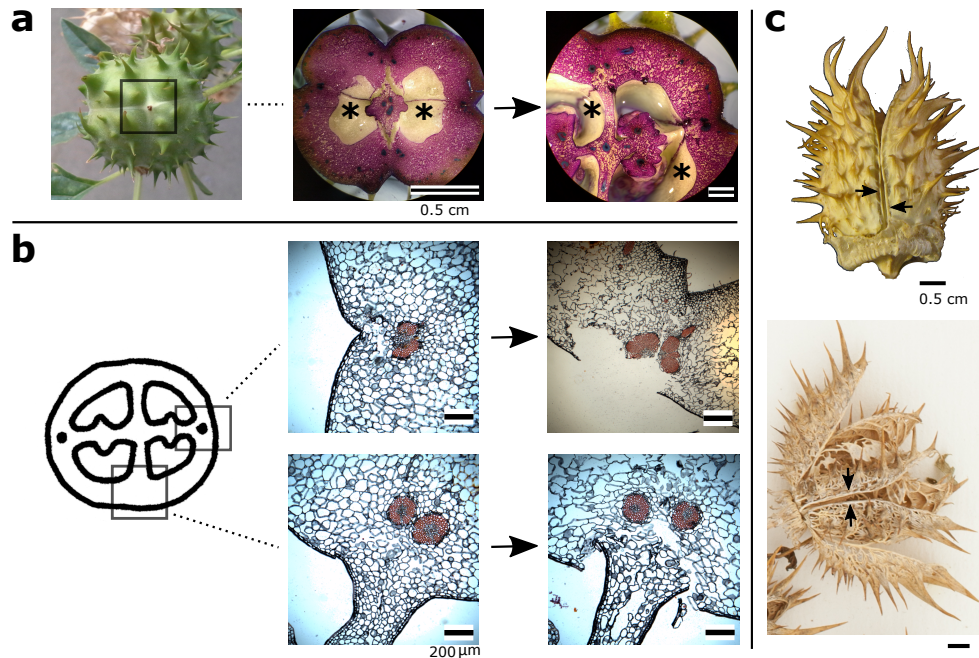


Figure 4.5: Anatomy and morphology of the dehiscence process in the regularly dehiscent fruits of *Datura quercifolia*. The order of the images begins with the earliest stage at top left, moving counterclockwise towards maturity. a, detail of *D. quercifolia* fruit seen from the top (left), section of the fruit apex (middle) showing the separation of the septa (in the center) from the fruit wall, and the horizontal lines of cells (marked with asterisks) from the fruit tip that mark two out of the four dehiscence zones, half way the fruit wall (cross section seen on the right picture) showing the continuity of the dehiscence zones (lines). b, anatomical detail of the dehiscence zones focusing on the middle portion of the fruit and the connection points between the septa and the false septa with the fruit wall (diagram on the left), in the middle images we see the moment right before the dehiscence zones start rupturing, and on the right advanced stages of dehiscence where the innermost layer of cell is discontinuous which triggers the degradation of cells in those regions. c, *D. quercifolia* fruits completely dry, arrows point to the massive vascular bundles (same ones showed in b) that delimit the four valves that are formed once the fruits dehiscence is complete.

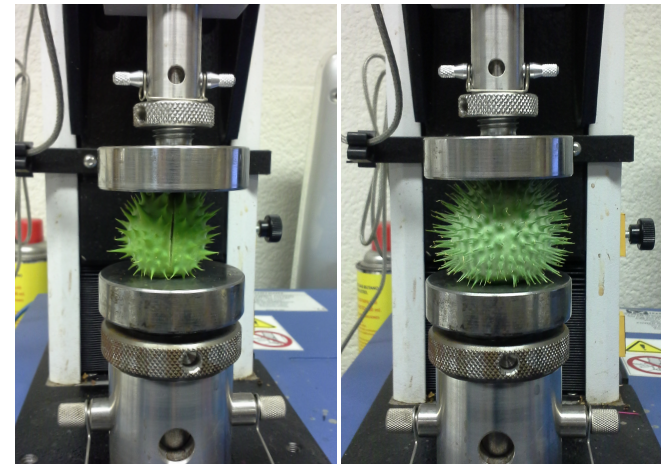
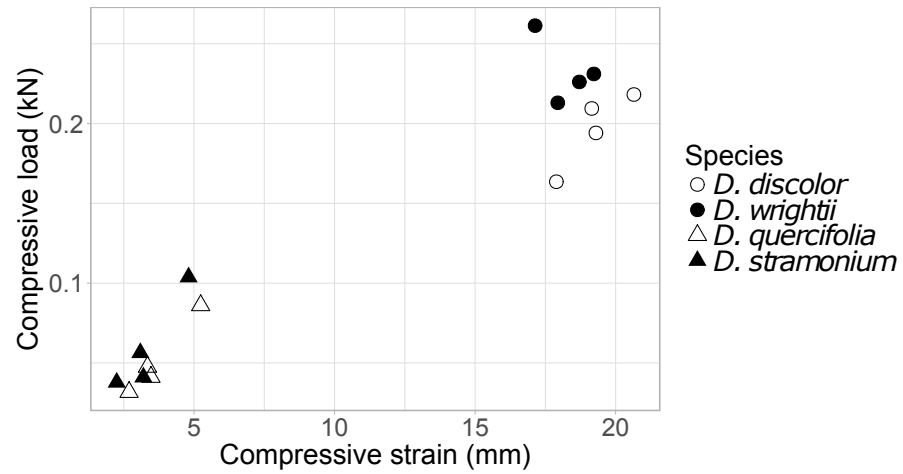


Figure 4.6: Results of the compression tests on regularly dehiscent fruits of *Datura quercifolia* and *D. stramonium*, and irregularly dehiscent fruits of *D. discolor* and *D. wrightii*. The distribution of the points in space is concordant with dehiscence type. Regularly dehiscent fruits require less load, and deform less, before a crack happens on the fruit wall, when compared to irregularly dehiscent fruits. Pictures show how the compression test was set up on the Instron machine, on the left a fruit of *D. quercifolia*, on the right, one of *D. wrightii*.

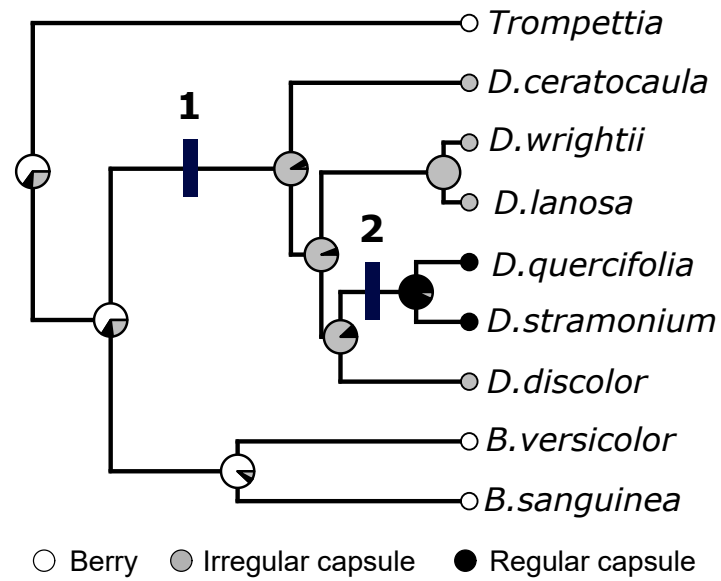


Figure 4.7: Stepwise reversal to regularly dehiscent capsules in Datureae. 1. loss of endocarp collenchyma and gain of mesocarp fibers; 2. production of large concentric vascular bundles in the pericarp.

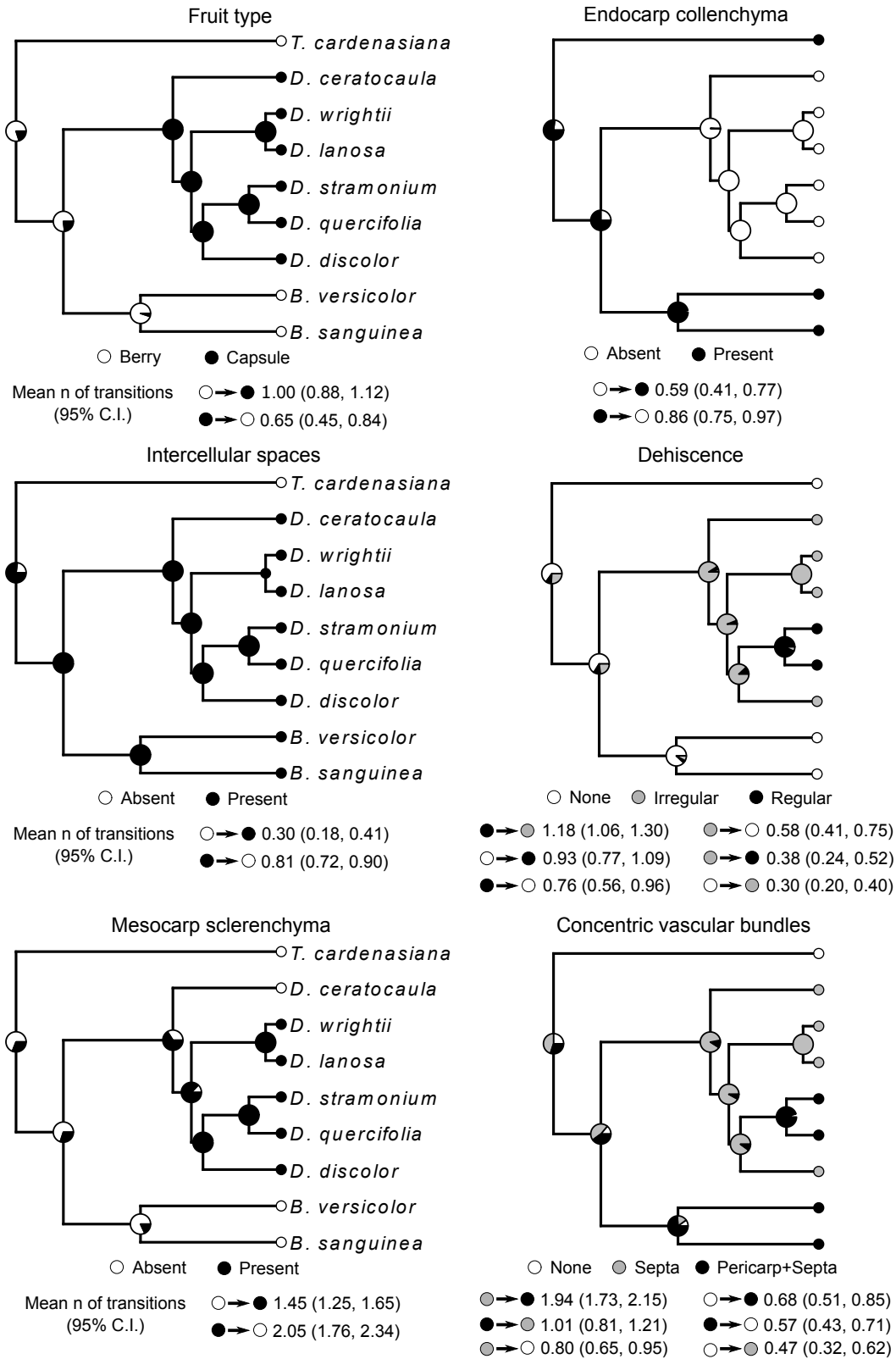


Figure 4.8: Ancestral state reconstruction for six characters: fruit type, dehiscence type, presence of intercellular spaces, presence of sclerenchyma in mesocarp, and placement concentric vascular bundles.

Bibliography

- [1] K. Andreasen, B. G. Baldwin, and B. Bremer. Phylogenetic utility of the nuclear rDNA ITS region in subfamilyIxoroideae (rubiaceae): Comparisons with cpDNArbcL sequence data. Plant Systematics and Evolution, 217(1-2):119–135, 1999.
- [2] A. Antonelli, J. A. A. Nylander, C. Persson, and I. Sanmartin. Tracing the impact of the andean uplift on neotropical plant evolution. Proceedings of the National Academy of Sciences, 106(24):9749–9754, may 2009.
- [3] Christine D. Bacon, Andrés Mora, Warren L. Wagner, and Carlos A. Jaramillo. Testing geological models of evolution of the isthmus of panama in a phylogenetic framework. Botanical Journal of the Linnean Society, 171(1):287–300, aug 2012.
- [4] Christine D. Bacon, Daniele Silvestro, Carlos Jaramillo, Brian Tilston Smith, Prosanta Chakrabarty, and Alexandre Antonelli. Biological evidence supports an early and complex emergence of the isthmus of panama. Proceedings of the National Academy of Sciences, 112(19):6110–6115, apr 2015.
- [5] Arthur Stewart Barclay. Studies in the genus datura (solanaceae). 1959.
- [6] Nigel P. Barker, Peter H. Weston, Frank Rutschmann, and Hervé Sauquet. Molecular dating of the ‘gondwanan’ plant family proteaceae is only partially congruent with the timing of the break-up of gondwana. Journal of Biogeography, 34(12):2012–2027, dec 2007.
- [7] Viviana Barreda and Luis Palazzesi. Patagonian vegetation turnovers during the paleogene-early neogene: origin of arid-adapted floras. The botanical review, 73(1):31–50, 2007.
- [8] David A. Baum, Kenneth J. Sytsma, and Peter C. Hoch. A phylogenetic analysis of epilobium (onagraceae) based on nuclear ribosomal DNA sequences. Systematic Botany, 19(3):363, jul 1994.
- [9] Jeremy M Beaulieu and Michael J Donoghue. Fruit evolution and diversification in campanulid angiosperms. Evolution, 67(11):3132–3144, 2013.
- [10] Jeremy M Beaulieu, David C Tank, and Michael J Donoghue. A southern hemisphere origin for campanulid angiosperms, with traces of the break-up of gondwana. BMC Evolutionary Biology, 13(1):80, 2013.
- [11] David J. Beerling, Brian Huntley, and John P. Bailey. Climate and the distribution ofFallopia japonica: use of an introduced species to test the predictive capacity of response surfaces. Journal of Vegetation Science, 6(2):269–282, apr 1995.

- [12] JJ Bernhardt. Über die arten der gattung datura. Neues Journal der Pharmacie für Aerzte, Apotheker, und Chemiker, 26:118–158, 1833.
- [13] Ed Biffin, Eve J. Lucas, Lyn A. Craven, Itayguara Ribeiro da Costa, Mark G. Harrington, and Michael D. Crisp. Evolution of exceptional species richness among lineages of fleshy-fruited myrtaceae. Annals of Botany, 106(1):79–93, may 2010.
- [14] Lynn Bohs. Phylogeny of the cyphomandra clade of the genus solanum (solanaceae) based on ITS sequence data. Taxon, 56(4):1012, nov 2007.
- [15] Remco Bouckaert, Joseph Heled, Denise Kühnert, Tim Vaughan, Chieh-Hsi Wu, Dong Xie, Marc A. Suchard, Andrew Rambaut, and Alexei J. Drummond. Beast 2: A software platform for bayesian evolutionary analysis. PLoS Computational Biology, 10(4), apr 2014.
- [16] Isabelle Boulangeat, Dominique Gravel, and Wilfried Thuiller. Accounting for dispersal and biotic interactions to disentangle the drivers of species distributions and their abundances. Ecology letters, 15(6):584–593, 2012.
- [17] B Bremer and O Eriksson. Evolution of fruit characters and dispersal modes in the tropical family rubiaceae. Biological Journal of the Linnean Society, 47(1):79–95, 1992.
- [18] Judith L. Bronstein, Travis Huxman, Brianna Horvath, Michael Farabee, and Goggy Davidowitz. Reproductive biology of datura wrightii: the benefits of a herbivorous pollinator. Annals of Botany, 103(9):1435–1443, mar 2009.
- [19] Sven Buerki, Félix Forest, Nadir Alvarez, Johan A. A. Nylander, Nils Arrigo, and Isabel Sanmartín. An evaluation of new parsimony-based versus parametric inference methods in biogeography: a case study using the globally distributed plant family sapindaceae. Journal of Biogeography, 38(3):531–550, dec 2010.
- [20] Georges Louis Leclerc Buffon. Histoire naturelle, générale et particulière. Paris: l’Imprimerie Royale, 1749.
- [21] Georges Louis Leclerc Buffon. Natural history, general and particular, volume 3. London: A. Strahan and T. Cadell, 1791.
- [22] Kenneth P Burnham and David R Anderson. Model selection and multimodel inference: a practical information-theoretic approach. Springer Science & Business Media, 2003.
- [23] Robert Bye and Victoria Sosa. Molecular phylogeny of the jimsonweed genus datura (solanaceae). Systematic Botany, 38(3):818–829, sep 2013.
- [24] Michael L. Cain, Brook G. Milligan, and Allan E. Strand. Long-distance seed dispersal in plant populations. American Journal of Botany, 87(9):1217, sep 2000.
- [25] GL Carson. The crossability of datura quercifolia with seven species of the genus. Doct. dissert. Smith College, Northampton, Mass, 1945.
- [26] Si-Chong Chen, William K. Cornwell, Hong-Xiang Zhang, and Angela T. Moles. Plants show more flesh in the tropics: variation in fruit type along latitudinal and climatic gradients. Ecography, 40(4):531–538, apr 2016.

- [27] Franco Chiarini and Gloria Barboza. Anatomical study of different fruit types in argentine species of solanum subgen. leptostemonum (solanaceae). 64(2):165–175, 2007.
- [28] Maarten J. M. Christenhusz and Mark W. Chase. Biogeographical patterns of plants in the neotropics - dispersal rather than plate tectonics is most explanatory. Botanical Journal of the Linnean Society, 171(1):277–286, oct 2012.
- [29] Gudrun Clausen, Karsten Meyer, and Susanne S Renner. Correlations among fruit traits and evolution of different fruits within melastomataceae. Botanical Journal of the Linnean Society, 133(3):303–326, 2000.
- [30] J. W. Clayton, P. S. Soltis, and D. E. Soltis. Recent long-distance dispersal overshadows ancient biogeographical patterns in a pantropical angiosperm family (simaroubaceae, sapindales). Systematic Biology, 58(4):395–410, aug 2009.
- [31] Michael D Crisp, Mary TK Arroyo, Lyn G Cook, Maria A Gandolfo, Gregory J Jordan, Matt S McGlone, Peter H Weston, Mark Westoby, Peter Wilf, and H Peter Linder. Phylogenetic biome conservatism on a global scale. Nature, 458(7239):754, 2009.
- [32] Sinead M. Crotty and Mark D. Bertness. Positive interactions expand habitat use and the realized niches of sympatric species. Ecology, 96(10):2575–2582, oct 2015.
- [33] G. Cruz-Mazo, M.L. Buide, R. Samuel, and E. Narbona. Molecular phylogeny of scorzoneroideae (asteraceae): Evolution of heterocarpy and annual habit in unpredictable environments. Molecular Phylogenetics and Evolution, 53(3):835–847, dec 2009.
- [34] William G D’Arcy. Solanaceae, Biology and systematics. Columbia University Press, 1986.
- [35] William G D’Arcy. The solanaceae since 1976, with a review of its biogeography. Hawkes, J, G., Lester, R, N., Nee, M., Estrada, N ed (s). Solanaceae III. Taxonomy, chemistry, evolution.. Roy. Bot. Gard.: Kew & Linnean Soc.: London, pages 75–137, 1991.
- [36] Charles Darwin. On the Origin of Species by Means of Natural Selection, or the Preservation of Favoured Races in the Struggle for Life. London: John Murray, 1859.
- [37] YS Dave, ND Patel, and KS Rao. Structural design of the developing fruit of nicotiana tabacum. Phyton, 21:63–71, 1981.
- [38] YS Dave, ND Patel, KS Rao, et al. Morpho-histogenesis in the fruit sculpture of datura innoxia. Phyton, 20:227–234, 1980.
- [39] C. C. Davis, C. D. Bell, S. Mathews, and M. J. Donoghue. Laurasian migration explains gondwanan disjunctions: Evidence from malpighiaceae. Proceedings of the National Academy of Sciences, 99(10):6833–6837, apr 2002.
- [40] Augustin Pyrame de Candolle. Essai élémentaire de géographie botanique. FS Laeraule, 1820.
- [41] Augustin Pyrame de Candolle. Essai élémentaire de géographie botanique. Edinburgh: Blackwood, 1821.

- [42] J. Arturo De-Nova, Rosalinda Medina, Juan Carlos Montero, Andrea Weeks, Julieta A. Rosell, Mark E. Olson, Luis E. Eguiarte, and Susana Magallón. Insights into the historical construction of species-rich mesoamerican seasonally dry tropical forests: the diversification of *Bursera* (burseraceae, sapindales). New Phytologist, 193(1):276–287, sep 2011.
- [43] Carmen Benitez de Rojas and William G. D’Arcy. The genus *Lycianthes* (solanaceae) in venezuela. Annals of the Missouri Botanical Garden, 84(2):167, 1997.
- [44] Donna Lisa De-Silva, Luísa L Mota, Nicolas Chazot, Ricardo Mallarino, Karina L Silva-Brandão, Luz Miryam Gómez Piñerez, André VL Freitas, Gerardo Lamas, Mathieu Joron, James Mallet, et al. North andean origin and diversification of the largest ithomiine butterfly genus. Scientific Reports, 7, 2017.
- [45] Michael O Dillon, Tiejao Tu, Lei Xie, Victor Quipuscoa Silvestre, and Jun Wen. Biogeographic diversification in *Nolana* (solanaceae), a ubiquitous member of the atacama and peruvian deserts along the western coast of south america. Journal of Systematics and Evolution, 47(5):457–476, 2009.
- [46] Philip Dixon. VEGAN, a package of r functions for community ecology. Journal of Vegetation Science, 14(6):927, 2003.
- [47] Michael J Donoghue. A phylogenetic perspective on the distribution of plant diversity. Proceedings of the National Academy of Sciences, 105(Supplement 1):11549–11555, 2008.
- [48] Jeff J Doyle. A rapid dna isolation procedure for small quantities of fresh leaf tissue. Phytochem bull, 19:11–15, 1987.
- [49] Alexei J Drummond, Simon Y. W Ho, Matthew J Phillips, and Andrew Rambaut. Relaxed phylogenetics and dating with confidence. PLoS Biology, 4(5), mar 2006.
- [50] Alexei J. Drummond, Marc A. Suchard, Dong Xie, and Andrew Rambaut. Bayesian phylogenetics with BEAUti and the BEAST 1.7. Molecular Biology and Evolution, 29(8):1969–1973, feb 2012.
- [51] Julia Dupin, Nicholas J. Matzke, Tiina Sarkinen, Sandra Knapp, Richard G. Olmstead, Lynn Bohs, and Stacey D. Smith. Bayesian estimation of the global biogeographical history of the solanaceae. Journal of Biogeography, 44(4):887–899, nov 2016.
- [52] Deren A. R. Eaton, Elizabeth L. Spriggs, Brian Park, and Michael J. Donoghue. Misconceptions on missing data in RAD-seq phylogenetics with a deep-scale example from flowering plants. Systematic Biology, oct 2016.
- [53] R. C. Edgar. MUSCLE: multiple sequence alignment with high accuracy and high throughput. Nucleic Acids Research, 32(5):1792–1797, mar 2004.
- [54] E. J. Edwards and M. J. Donoghue. Is it easy to move and easy to evolve? evolutionary accessibility and adaptation. Journal of Experimental Botany, 64(13):4047–4052, aug 2013.
- [55] H. Ege, E. R. Sobel, E. Scheuber, and V. Jacobshagen. Exhumation history of the southern altiplano plateau (southern bolivia) constrained by apatite fission track thermochronology. Tectonics, 26(1), jan 2007.

- [56] Jane Elith and John R. Leathwick. Species distribution models: Ecological explanation and prediction across space and time. Annual Review of Ecology, Evolution, and Systematics, 40(1):677–697, dec 2009.
- [57] Jane Elith, John R Leathwick, and Trevor Hastie. A working guide to boosted regression trees. Journal of Animal Ecology, 77(4):802–813, 2008.
- [58] Margaret EK Evans, David J Hearn, William J Hahn, Jennifer M Spangle, D Lawrence Venable, and O Pellmyr. Climate and life-history evolution in evening primroses (oenothera, onagraceae): a phylogenetic comparative analysis. Evolution, 59(9):1914–1927, 2005.
- [59] Javier Francisco-Ortega, Janet C. Barber, Arnaldo Santos-Guerra, Rosa Febles-Hernandez, and Robert K. Jansen. Origin and evolution of the endemic genera of gonosperminae (asteraceae: Anthemideae) from the canary islands: Evidence from nucleotide sequences of the internal transcribed spacers of the nuclear ribosomal DNA. American Journal of Botany, 88(1):161, jan 2001.
- [60] J. Friedman and M. J. Rubin. All in good time: Understanding annual and perennial strategies in plants. American Journal of Botany, 102(4):497–499, mar 2015.
- [61] Timothy Gallaher, Martin W. Callmender, Sven Buerki, and Sterling C. Keeley. A long distance dispersal hypothesis for the pandanaceae and the origins of the pandanus tectorius complex. Molecular Phylogenetics and Evolution, 83:20–32, feb 2015.
- [62] Tony Gamble, Aaron M Bauer, Eli Greenbaum, and Todd R Jackman. Out of the blue: a novel, trans-atlantic clade of geckos (gekkota, squamata). Zoologica Scripta, 37(4):355–366, jul 2008.
- [63] Vicente F Garcia and Richard G Olmstead. Phylogenetics of tribe anthocercideae (solanaceae) based on ndhf and trnl/f sequence data. Systematic Botany, 28(3):609–615, 2003.
- [64] Alwyn H. Gentry. Neotropical floristic diversity: Phytogeographical connections between central and south america, pleistocene climatic fluctuations, or an accident of the andean orogeny? Annals of the Missouri Botanical Garden, 69(3):557, 1982.
- [65] Johnnie Lee. Gentry. The generic name Saracha Ruiz & Pavón (Solanaceae) / Johnnie L. Gentry, Jr. Field Museum of Natural History, 1974.
- [66] Thomas C. Giarla and Sharon A. Jansa. The role of physical geography and habitat type in shaping the biogeographical history of a recent radiation of neotropical marsupials (thylamys: Didelphidae). Journal of Biogeography, 41(8):1547–1558, apr 2014.
- [67] Rosemary G. Gillespie, Bruce G. Baldwin, Jonathan M. Waters, Ceridwen I. Fraser, Raisa Nikula, and George K. Roderick. Long-distance dispersal: a framework for hypothesis testing. Trends in Ecology & Evolution, 27(1):47–56, jan 2012.
- [68] Gonzalo Giribet, Prashant P Sharma, Ligia R Benavides, Sarah L Boyer, Ronald M Clouse, Benjamin L De Bivort, Dimitar Dimitrov, Gisele Y Kawauchi, Jerome Muriene, and Peter J Schwendinger. Evolutionary and biogeographical history of an ancient and global group of arachnids (arachnida: Opiliones: Cyphophthalmi) with a new taxonomic arrangement. Biological Journal of the Linnean Society, 105(1):92–130, 2012.

- [69] T. J Givnish, K. C Millam, A. R Mast, T. B Paterson, T. J Theim, A. L Hipp, J. M Henss, J. F Smith, K. R Wood, and K. J Sytsma. Origin, adaptive radiation and diversification of the hawaiian lobeliads (asterales: Campanulaceae). Proceedings of the Royal Society B: Biological Sciences, 276(1656):407–416, feb 2009.
- [70] T. J Givnish, J. C. Pires, S. W Graham, M. A McPherson, L. M Prince, T. B Patterson, H. S Rai, E. H Roalson, T. M Evans, W. J Hahn, K. C Millam, A. W Meerow, M. Molvray, P. J Kores, H. E O’Brien, J. C Hall, W. J. Kress, and K. J Sytsma. Repeated evolution of net venation and fleshy fruits among monocots in shaded habitats confirms a priori predictions: evidence from an *ndhF* phylogeny. Proceedings of the Royal Society B: Biological Sciences, 272(1571):1481–1490, jul 2005.
- [71] Thomas J. Givnish, Kendra C. Millam, Timothy M. Evans, Jocelyn C. Hall, J. Chris Pires, Paul E. Berry, and Kenneth J. Sytsma. Ancient vicariance or recent long-distance dispersal? inferences about phylogeny and south american–african disjunctions in rapateaceae and bromeliaceae based on *ndhF* sequence data. International Journal of Plant Sciences, 165(S4), jul 2004.
- [72] Thomas J. Givnish and Susanne S. Renner. Tropical intercontinental disjunctions: Gondwana breakup, immigration from the boreotropics, and transoceanic dispersal. International Journal of Plant Sciences, 165(S4), jul 2004.
- [73] Alan Graham. The andes: a geological overview from a biological perspective. Annals of the Missouri Botanical Garden, 96(3):371–385, 2009.
- [74] Fred S. Guthery, Kenneth P. Burnham, and David R. Anderson. Model selection and multimodel inference: A practical information-theoretic approach. The Journal of Wildlife Management, 67(3):655, jul 2003.
- [75] L Haegi. Taxonomic account of *datura l.* (solanaceae) in australia with a note on *brugmansia pers.* Australian Journal of Botany, 24(3):415, 1976.
- [76] Jocelyn C. Hall, Tracy E. Tisdale, Kathleen Donohue, and Elena M. Kramer. Developmental basis of an anatomical novelty: Heteroarthrocarpy in *Cakile lanceolata* and *Erucaria erucarioides* (brassicaceae). International Journal of Plant Sciences, 167(4):771–789, jul 2006.
- [77] Chaoying He, Thomas Münster, and Heinz Saedler. On the origin of floral morphological novelties. FEBS Letters, 567(1):147–151, apr 2004.
- [78] Tomislav Hengl, Jorge Mendes de Jesus, Gerard B. M. Heuvelink, Maria Ruiperez Gonzalez, Milan Kilibarda, Aleksandar Blagotić, Wei Shangguan, Marvin N. Wright, Xiaoyuan Geng, Bernhard Bauer-Marschallinger, Mario Antonio Guevara, Rodrigo Vargas, Robert A. MacMillan, Niels H. Batjes, Johan G. B. Leenaars, Eloi Ribeiro, Ichsan Wheeler, Stephan Mantel, and Bas Kempen. SoilGrids250m: Global gridded soil information based on machine learning. PLOS ONE, 12(2), feb 2017.
- [79] Tomislav Hengl, Jorge Mendes de Jesus, Robert A. MacMillan, Niels H. Batjes, Gerard B. M. Heuvelink, Eloi Ribeiro, Alessandro Samuel-Rosa, Bas Kempen, Johan G. B. Leenaars, Markus G. Walsh, and Maria Ruiperez Gonzalez. SoilGrids1km — global soil information based on automated mapping. PLoS ONE, 9(8), aug 2014.

- [80] F. N. Hepper and P. M. L. Jaeger. Name changes for two old world solanum species. Kew Bulletin, 41(2):433, 1986.
- [81] Robert J. Hijmans, Susan E. Cameron, Juan L. Parra, Peter G. Jones, and Andy Jarvis. Very high resolution interpolated climate surfaces for global land areas. International Journal of Climatology, 25(15):1965–1978, 2005.
- [82] D. M. Hillis and J. P. Huelsenbeck. Signal, noise, and reliability in molecular phylogenetic analyses. Journal of Heredity, 83(3):189–195, jun 1992.
- [83] S. Hohna, T. A. Heath, B. Boussau, M. J. Landis, F. Ronquist, and J. P. Huelsenbeck. Probabilistic graphical model representation in phylogenetics. Systematic Biology, 63(5):753–771, jun 2014.
- [84] Sebastian Hohna, Michael J. Landis, Tracy A. Heath, Bastien Boussau, Nicolas Lartillot, Brian R. Moore, John P. Huelsenbeck, and Fredrik Ronquist. RevBayes: Bayesian phylogenetic inference using graphical models and an interactive model-specification language. Systematic Biology, 65(4):726–736, may 2016.
- [85] Carina Hoorn. Marine incursions and the influence of andean tectonics on the miocene depositional history of northwestern amazonia: results of a palynostratigraphic study. Palaeogeography, Palaeoclimatology, Palaeoecology, 105(3-4):267–309, nov 1993.
- [86] Carina Hoorn, Javier Guerrero, Gustavo A. Sarmiento, and Maria A. Lorente. Andean tectonics as a cause for changing drainage patterns in miocene northern south america. Geology, 23(3):237, 1995.
- [87] H F Howe and J Smallwood. Ecology of seed dispersal. Annual Review of Ecology and Systematics, 13(1):201–228, nov 1982.
- [88] Henry F Howe and Maria N Miriti. When seed dispersal matters. BioScience, 54(7):651–660, 2004.
- [89] Jin-Yong Hu and Heinz Saedler. Evolution of the inflated calyx syndrome in solanaceae. Molecular Biology and Evolution, 24(11):2443–2453, sep 2007.
- [90] John P. Huelsenbeck, Rasmus Nielsen, and Jonathan P. Bollback. Stochastic mapping of morphological characters. Systematic Biology, 52(2):131–158, apr 2003.
- [91] C. Hughes and R. Eastwood. Island radiation on a continental scale: Exceptional rates of plant diversification after uplift of the andes. Proceedings of the National Academy of Sciences, 103(27):10334–10339, jun 2006.
- [92] A T Hunziker. Estudios sobre solanaceae viii. part iv. sobre dos nuevas secciones de iochroma y dos novedades a nivel específico. Kurtziana, 10:21–25, 1977.
- [93] AT Hunziker. Genera Solanacearum: the genera of Solanaceae illustrated, arranged according to a new system. ARG Gantner Verlag KG: Ruggell, Liechtenstein, 2001.
- [94] G. E. Hutchinson. Concluding remarks. Cold Spring Harbor Symposia on Quantitative Biology, 22(0):415–427, jan 1957.

- [95] Travis Ingram and D.Luke Mahler. SURFACE: detecting convergent evolution from comparative data by fitting ornstein-uhlenbeck models with stepwise akaike information criterion. Methods in Ecology and Evolution, 4(5):416–425, mar 2013.
- [96] Helen E Ireland, Geoffrey C Kite, Nigel C Veitch, Mark W Chase, Brian Schrire, Matt Lavin, Jose Linares, and R PENNINGTON. Biogeographical, ecological and morphological structure in a phylogenetic analysis of ateleia (swartzieae, fabaceae) derived from combined molecular, morphological and chemical data. Botanical Journal of the Linnean Society, 162(1):39–53, 2010.
- [97] M. Itkin, U. Heinig, O. Tzfadia, A. J. Bhide, B. Shinde, P. D. Cardenas, S. E. Bocobza, T. Unger, S. Malitsky, R. Finkers, Y. Tikunov, A. Bovy, Y. Chikate, P. Singh, I. Rogachev, J. Beekwilder, A. P. Giri, and A. Aharoni. Biosynthesis of antinutritional alkaloids in solanaceous crops is mediated by clustered genes. Science, 341(6142):175–179, jun 2013.
- [98] Michael Friendly J. Oksanen, J. F. Blanchet et al. Stochastic mapping under biogeographical models. Available at <https://CRAN.R-project.org/package=vegan>, 2017.
- [99] Andrew L. Jackson, Richard Inger, Stuart Bearhop, and Andrew Parnell. Erroneous behaviour of MixSIR, a recently published bayesian isotope mixing model: a discussion of moore & semmens (2008). Ecology Letters, 12(3), mar 2009.
- [100] Andrew L. Jackson, Richard Inger, Andrew C. Parnell, and Stuart Bearhop. Comparing isotopic niche widths among and within communities: SIBER - stable isotope bayesian ellipses in r. Journal of Animal Ecology, 80(3):595–602, mar 2011.
- [101] Donald A. Jackson. Stopping rules in principal components analysis: A comparison of heuristic and statistical approaches. Ecology, 74(8):2204–2214, dec 1993.
- [102] Daniel H. Janzen. Herbivores and the number of tree species in tropical forests. The American Naturalist, 104(940):501–528, nov 1970.
- [103] Prakash Chandra Joshi. A Comparative Study of Two Intergeneric Hybrids, Datura Innoxia Mill. X Brugmansia Suaveolens Humb. & Bonpl. and Datura Innoxia Mill. X Brugmansia Rosei Saff., and Their Parents: And Self-sterility in Three Species of Brugmansia Pers. Smith College, 1949.
- [104] Mohammad Khabbazian, Ricardo Kriebel, Karl Rohe, and Cécile Ané. Fast and accurate detection of evolutionary shifts in ornstein-uhlenbeck models. Methods in Ecology and Evolution, 7(7):811–824, feb 2016.
- [105] Sigbert Klinke and Christian Ritter. Graphical aids for statistical data analysis. In XploRe: An Interactive Statistical Computing Environment, pages 63–75. Springer New York, 1995.
- [106] S. Knapp. Tobacco to tomatoes: a phylogenetic perspective on fruit diversity in the solanaceae. Journal of Experimental Botany, 53(377):2001–2022, oct 2002.
- [107] Jette T Knudsen and Lars Tollsten. Trends in floral scent chemistry in pollination syndromes: floral scent composition in moth-pollinated taxa. Botanical Journal of the Linnean Society, 113(3):263–284, 1993.

- [108] Ricardo Kriebel. Phylogenetic placement of the monotypic genus *Schwackaea* (Melastomeae: Melastomataceae) and the evolution of its unique fruit. International Journal of Plant Sciences, 177(5):440–448, 2016.
- [109] L. P. Lagomarsino, A. Antonelli, N. Muchhala, A. Timmermann, S. Mathews, and C. C. Davis. Phylogeny, classification, and fruit evolution of the species-rich neotropical bellflowers (Campanulaceae: Lobelioideae). American Journal of Botany, 101(12):2097–2112, dec 2014.
- [110] M. J. Landis, N. J. Matzke, B. R. Moore, and J. P. Huelsenbeck. Bayesian analysis of biogeography when the number of areas is large. Systematic Biology, 62(6):789–804, jun 2013.
- [111] S Leiva Gonzalez. *Nicandra yacheriana* (Solanaceae) una nueva especie del sur del Perú. Arnaldoa, 17(1):25–31, 2010.
- [112] S Leiva Gonzalez and E Pereyra Villanueva. *Nicandra john-tyleriana* (Solanaceae) una nueva especie del norte del Perú. Arnaldoa, 14(1):45–52, 2007.
- [113] Emily Moriarty Lemmon, Alan R Lemmon, and David C Cannatella. Geological and climatic forces driving speciation in the continentally distributed trilling chorus frogs (*Pseudacris*). Evolution, 61(9):2086–2103, 2007.
- [114] Szabolcs Lengyel, Aaron D. Gove, Andrew M. Latimer, Jonathan D. Majer, and Robert R. Dunn. Ants sow the seeds of global diversification in flowering plants. PLoS ONE, 4(5), may 2009.
- [115] Szabolcs Lengyel, Aaron D. Gove, Andrew M. Latimer, Jonathan D. Majer, and Robert R. Dunn. Convergent evolution of seed dispersal by ants, and phylogeny and biogeography in flowering plants: A global survey. Perspectives in Plant Ecology, Evolution and Systematics, 12(1):43–55, feb 2010.
- [116] Boris Leroy, Christine N. Meynard, Céline Bellard, and Franck Courchamp. *virtualspecies*, an R package to generate virtual species distributions. Ecography, 39(6):599–607, jun 2015.
- [117] R. A. Levin and J. S. Miller. Relationships within tribe Lycieae (Solanaceae): paraphyly of *Lycium* and multiple origins of gender dimorphism. American Journal of Botany, 92(12):2044–2053, dec 2005.
- [118] R. A. Levin, N. R. Myers, and L. Bohs. Phylogenetic relationships among the “spiny solanums” (*Solanum* subgenus *Leptostemonum*, Solanaceae). American Journal of Botany, 93(1):157–169, jan 2006.
- [119] Glenn Litsios, Peter B. Pearman, Déborah Lanterbecq, Nathalie Tolou, and Nicolas Salamin. The radiation of the clownfishes has two geographical replicates. Journal of Biogeography, 41(11):2140–2149, jul 2014.
- [120] Tommie Earl Lockwood. A taxonomic revision of *Brugmansia* (Solanaceae). Harvard University, 1973.
- [121] Claire M Lorts, Trevor Briggeman, and Tao Sang. Evolution of fruit types and seed dispersal: A phylogenetic and ecological snapshot. Journal of Systematics and Evolution, 46(3):396–404, 2008.

- [122] Jonathan B. Losos. Phylogenetic perspectives on community ecology. *Ecology*, 77(5):1344–1354, jul 1996.
- [123] Jonathan B Losos, Manuel Leal, Richard E Glor, Kevin de Queiroz, Paul E Hertz, Lourdes Rodriguez Schettino, Ada Chamizo Lara, Todd R Jackman, and Allan Larson. Niche lability in the evolution of a caribbean lizard community. *Nature*, 424(6948):542–545, 2003.
- [124] Mario Luna-Cavazos, Robert Bye, and Meijun Jiao. The origin of datura metel (solanaceae): genetic and phylogenetic evidence. *Genetic Resources and Crop Evolution*, 56(2):263–275, aug 2008.
- [125] M. Lysy, A. D. Stasko, and H. K. Swanson. nicherover: (niche) (r)egion and niche (over)lap metrics for multidimensional ecological niches. Available at <https://CRAN.R-project.org/package=nicheROVER>, 2014.
- [126] W. P. Maddison and D.R. Maddison. Mesquite: a modular system for evolutionary analysis, version 3.2. Available at <http://mesquiteproject.org>, 2017.
- [127] Susana Magallón, Sandra Gómez-Acevedo, Luna L. Sánchez-Reyes, and Tania Hernández-Hernández. A metacalibrated time-tree documents the early rise of flowering plant phylogenetic diversity. *New Phytologist*, 207(2):437–453, jan 2015.
- [128] K. Mao, R. I. Milne, L. Zhang, Y. Peng, J. Liu, P. Thomas, R. R. Mill, and S. S. Renner. Distribution of living cupressaceae reflects the breakup of pangea. *Proceedings of the National Academy of Sciences*, 109(20):7793–7798, may 2012.
- [129] E. Martínez-Meyer and A. T. Peterson. Conservatism of ecological niche characteristics in north american plant species over the pleistocene-to-recent transition. *Journal of Biogeography*, 33(10):1779–1789, sep 2006.
- [130] W. A. Marussich. Testing myrmecochory from the ant’s perspective: The effects of datura wrightii and d. discolor on queen survival and brood production in pogonomyrmex californicus. *Insectes Sociaux*, 53(4):403–411, nov 2006.
- [131] R. J. Mason-Gamer and E. A. Kellogg. Testing for phylogenetic conflict among molecular data sets in the tribe triticeae (gramineae). *Systematic Biology*, 45(4):524–545, dec 1996.
- [132] Roberta J Mason-Gamer, Elizabeth A Kellogg, and Richard Olmstead. Testing for phylogenetic conflict among molecular data sets in the tribe triticeae (gramineae). *Systematic biology*, 45(4):524–545, 1996.
- [133] Pável Matos-Maraví, Rayner Núñez Águila, Carlos Peña, Jacqueline Y Miller, Andrei Sourakov, and Niklas Wahlberg. Causes of endemic radiation in the caribbean: evidence from the historical biogeography and diversification of the butterfly genus calisto(nymphalidae: Satyrinae: Satyrini). *BMC Evolutionary Biology*, 14(1), sep 2014.
- [134] N. J. Matzke. Model selection in historical biogeography reveals that founder-event speciation is a crucial process in island clades. *Systematic Biology*, 63(6):951–970, aug 2014.
- [135] N. J. Matzke. Stochastic mapping under biogeographical models. Available at http://phylo.wikidot.com/biogeobears#stochastic_mapping, accessed on June 1 2015, 2015.

- [136] N.J. Matzke. Biogeobears: Biogeography with bayesian (and likelihood) evolutionary analysis in r scripts. R package, version 0.2.1, published July 27, 2013 at: <http://CRAN.R-project.org/package=BioGeoBEARS>, 2013.
- [137] Ernst Mayr. *Systematics and the origin of species, from the viewpoint of a zoologist*. Harvard University Press, 1942.
- [138] Stephen McLoughlin. The breakup history of gondwana and its impact on pre-cenozoic floristic provincialism. *Australian Journal of Botany*, 49(3):271, 2001.
- [139] John McNeill, FR Barrie, WR Buck, V Demoulin, Werner Greuter, DL Hawksworth, PS Herendeen, S Knapp, K Marhold, J Prado, et al. International code of nomenclature for algae, fungi and plants. *Regnum vegetabile*, 154, 2012.
- [140] Eliane S Meier, Felix Kienast, Peter B Pearman, Jens-Christian Svenning, Wilfried Thuiller, Miguel B Araújo, Antoine Guisan, and Niklaus E Zimmermann. Biotic and abiotic variables show little redundancy in explaining tree species distributions. *Ecography*, 33(6):1038–1048, 2010.
- [141] Thomas Mione, Richard C. Olmstead, Robert K. Jansen, and Gregory J. Anderson. Systematic implications of chloroplast DNA variation in jaltomata and selected physaloid genera (solanaceae). *American Journal of Botany*, 81(7):912, jul 1994.
- [142] C. Montes, A. Cardona, R. McFadden, S. E. Moron, C. A. Silva, S. Restrepo-Moreno, D. A. Ramirez, N. Hoyos, J. Wilson, D. Farris, G. A. Bayona, C. A. Jaramillo, V. Valencia, J. Bryan, and J. A. Flores. Evidence for middle eocene and younger land emergence in central panama: Implications for isthmus closure. *Geological Society of America Bulletin*, 124(5-6):780–799, jan 2012.
- [143] Andres Mora, Patrice Baby, Martin Roddaz, Mauricio Parra, Stéphane Brusset, Wilber Hermoza, and Nicolas Espurt. Tectonic history of the andes and sub-andean zones: Implications for the development of the amazon drainage basin. In *Amazonia: Landscape and Species Evolution*, pages 38–60. Wiley-Blackwell Publishing Ltd., jul 2011.
- [144] P. L. Morrell, J. M. Porter, and E. A. Friar. Intercontinental dispersal: The origin of the widespread south american plant species *Gilia laciniata* (polemoniaceae) from a rare california and oregon coastal endemic. *Plant Systematics and Evolution*, 224(1-2):13–32, 2000.
- [145] Thomas W Mulroy and Philip W Rundel. Annual plants: adaptations to desert environments. *Bioscience*, 27(2):109–114, 1977.
- [146] Klaus Mummenhoff, Alexander Polster, Andreas Mühlhausen, and Günter Theißen. *Lepidium* as a model system for studying the evolution of fruit development in brassicaceae. *Journal of Experimental Botany*, 60(5):1503–1513, dec 2008.
- [147] J. Munoz. Wind as a long-distance dispersal vehicle in the southern hemisphere. *Science*, 304(5674):1144–1147, may 2004.
- [148] Mary Aileen Murray. Carpellary and placental structure in the solanaceae. *Botanical Gazette*, 107(2):243–260, 1945.
- [149] R. Nathan. Long-distance dispersal of plants. *Science*, 313(5788):786–788, aug 2006.

- [150] Lars Nauheimer, Dirk Metzler, and Susanne S. Renner. Global history of the ancient monocot family araceae inferred with models accounting for past continental positions and previous ranges based on fossils. New Phytologist, 195(4):938–950, jul 2012.
- [151] Julienne Ng and Stacey D. Smith. Widespread flower color convergence in solanaceae via alternate biochemical pathways. New Phytologist, 209(1):407–417, jul 2015.
- [152] Rasmus Nielsen. Mapping mutations on phylogenies. Systematic Biology, 51(5):729–739, sep 2002.
- [153] Matthew L Niemiller, James R McCandless, R Graham Reynolds, James Caddle, Thomas J Near, Christopher R Tillquist, William D Pearson, and Benjamin M Fitzpatrick. Effects of climatic and geological processes during the pleistocene on the evolutionary history of the northern cavefish, *amblyopsis spelaea* (teleostei: Amblyopsidae). Evolution, 67(4):1011–1025, 2013.
- [154] Manuel Nogales, Ruben Heleno, Anna Traveset, and Pablo Vargas. Evidence for overlooked mechanisms of long-distance seed dispersal to and between oceanic islands. New Phytologist, 194(2):313–317, jan 2012.
- [155] Clive Patrick Nuttall. A review of the Tertiary non-marine molluscan faunas of the Pebasian and other inland basins of north-western South America. British museum (Natural history), 1990.
- [156] A. ODea, H. A. Lessios, A. G. Coates, R. I. Eytan, S. A. Restrepo-Moreno, A. L. Cione, L. S. Collins, A. de Queiroz, D. W. Farris, R. D. Norris, R. F. Stallard, M. O. Woodburne, O. Aguilera, M.-P. Aubry, W. A. Berggren, A. F. Budd, M. A. Cozzuol, S. E. Coppard, H. Duque-Caro, S. Finnegan, G. M. Gasparini, E. L. Grossman, K. G. Johnson, L. D. Keigwin, N. Knowlton, E. G. Leigh, J. S. Leonard-Pingel, P. B. Marko, N. D. Pyenson, P. G. Rachello-Dolmen, E. Soibelzon, L. Soibelzon, J. A. Todd, G. J. Vermeij, and J. B. C. Jackson. Formation of the isthmus of panama. Science Advances, 2(8), aug 2016.
- [157] Dennis J. O’Dowd and Mark E. Hay. Mutualism between harvester ants and a desert ephemeral: Seed escape from rodents. Ecology, 61(3):531–540, jun 1980.
- [158] Huw A Ogilvie and Alexei J Drummond. Starbeast2 brings faster species tree inference and accurate estimates of substitution rates. bioRxiv, page 070169, 2016.
- [159] R. G. Olmstead and J. A. Sweere. Combining data in phylogenetic systematics: An empirical approach using three molecular data sets in the solanaceae. Systematic Biology, 43(4):467–481, dec 1994.
- [160] Richard G. Olmstead. Phylogeny and biogeography in solanaceae, verbenaceae and bignoniaceae: a comparison of continental and intercontinental diversification patterns. Botanical Journal of the Linnean Society, 171(1):80–102, oct 2012.
- [161] Richard G Olmstead, Lynn Bohs, Hala Abdel Migid, Eugenio Santiago-Valentin, Vicente F Garcia, and Sarah M Collier. A molecular phylogeny of the solanaceae. Taxon, 57(4):1159–1181, 2008.

- [162] Richard G. Olmstead and Jeffrey D. Palmer. A chloroplast DNA phylogeny of the solanaceae: Subfamilial relationships and character evolution. Annals of the Missouri Botanical Garden, 79(2):346, 1992.
- [163] Richard G Olmstead, Jennifer A Sweere, Russell E Spangler, Lynn Bohs, and Jeffrey D Palmer. Phylogeny and provisional classification of the solanaceae based on chloroplast dna. Solanaceae IV, 1(1):1–137, 1999.
- [164] N. Pabon-Mora and A. Litt. Comparative anatomical and developmental analysis of dry and fleshy fruits of solanaceae. American Journal of Botany, 98(9):1415–1436, aug 2011.
- [165] Mark Pagel. The maximum likelihood approach to reconstructing ancestral character states of discrete characters on phylogenies. Systematic Biology, 48(3):612–622, jul 1999.
- [166] Mark Pagel, Andrew Meade, and Daniel Barker. Bayesian estimation of ancestral character states on phylogenies. Systematic biology, 53(5):673–684, 2004.
- [167] E. Paradis, J. Claude, and K. Strimmer. APE: Analyses of phylogenetics and evolution in r language. Bioinformatics, 20(2):289–290, jan 2004.
- [168] Mauricio Parra, Andrés Mora, Carlos Jaramillo, Manfred R Strecker, and Gabriel Veloza. New stratigraphic data on the initiation of mountain building at the eastern front of the colombian eastern cordillera. In International Symposium on Andean Geodynamics, Extended Abstracts, pages 567–571, 2005.
- [169] Mauricio Parra, Andres Mora, Edward R. Sobel, Manfred R. Strecker, and Román González. Episodic orogenic front migration in the northern andes: Constraints from low-temperature thermochronology in the eastern cordillera, colombia. Tectonics, 28(4), jul 2009.
- [170] Peter B Pearman, Antoine Guisan, Olivier Broennimann, and Christophe F Randin. Niche dynamics in space and time. Trends in Ecology & Evolution, 23(3):149–158, 2008.
- [171] Richard G. Pearson and Terence P. Dawson. Predicting the impacts of climate change on the distribution of species: are bioclimate envelope models useful? Global Ecology and Biogeography, 12(5):361–371, sep 2003.
- [172] R. T. Pennington, M. Lavin, D. E. Prado, C. A. Pendry, S. K. Pell, and C. A. Butterworth. Historical climate change and speciation: neotropical seasonally dry forest plants show patterns of both tertiary and quaternary diversification. Philosophical Transactions of the Royal Society B: Biological Sciences, 359(1443):515–538, mar 2004.
- [173] R. T. Pennington, M. Lavin, T. Sarkinen, G. P. Lewis, B. B. Klitgaard, and C. E. Hughes. Contrasting plant diversification histories within the andean biodiversity hotspot. Proceedings of the National Academy of Sciences, 107(31):13783–13787, jul 2010.
- [174] Iris E. Peralta and David M. Spooner. Granule-bound starch synthase (GBSSI) gene phylogeny of wild tomatoes (solanum l. section lycopersicon [mill.] wettst. subsection lycopersicon). American Journal of Botany, 88(10):1888, oct 2001.
- [175] Mathieu Perret, Alain Chautems, Andréa Onofre De Araujo, and Nicolas Salamin. Temporal and spatial origin of gesneriaceae in the new world inferred from plastid DNA sequences. Botanical Journal of the Linnean Society, 171(1):61–79, nov 2012.

- [176] C. H. Persoon. Synopsis plantarum, seu Enchiridium botanicum, complectens enumerationem systematicam specierum hucusque cognitarum. C.F. Cramerum,, 1805.
- [177] A Townsend Peterson. Ecological niches and geographic distributions (MPB-49). Number 49. Princeton University Press, 2011.
- [178] B. Petitpierre, C. Kueffer, O. Broennimann, C. Randin, C. Daehler, and A. Guisan. Climatic niche shifts are rare among terrestrial plant invaders. Science, 335(6074):1344–1348, mar 2012.
- [179] Steven J Phillips, Robert P Anderson, and Robert E Schapire. Maximum entropy modeling of species geographic distributions. Ecological modelling, 190(3):231–259, 2006.
- [180] Alex L. Pigot and Joseph A. Tobias. Species interactions constrain geographic range expansion over evolutionary time. Ecology Letters, 16(3):330–338, dec 2012.
- [181] I. Colin Prentice, Wolfgang Cramer, Sandy P. Harrison, Rik Leemans, Robert A. Monserud, and Allen M. Solomon. Special paper: A global biome model based on plant physiology and dominance, soil properties and climate. Journal of Biogeography, 19(2):117, mar 1992.
- [182] Jonathan P Price and Warren L Wagner. Speciation in hawaiian angiosperm lineages: cause, consequence, and mode. Evolution, 58(10):2185–2200, 2004.
- [183] D. Prothero. The late eocene-oligocene extinctions. Annual Review of Earth and Planetary Sciences, 22(1):145–165, jan 1994.
- [184] R Core Team. R: a language and environment for statistical computing. R Foundation for statistical computing, Vienna, Austria. Available at: <http://www.R-project.org/>, 2015.
- [185] Charles-Elie Rabier. On stochastic processes for quantitative trait locus mapping under selective genotyping. Statistics, 49(1):19–34, nov 2013.
- [186] Robert A. Raguso, Cynthia Henzel, Stephen L. Buchmann, and Gary P. Nabhan. Trumpet flowers of the sonoran desert: Floral biology of *Peniocereus* Cacti and *Sacred Datura*. International Journal of Plant Sciences, 164(6):877–892, nov 2003.
- [187] A Rambaut, MA Suchard, D Xie, and AJ Drummond. Tracer v1.6. Available at <http://beast.bio.ed.ac.uk/Tracer>, 2014.
- [188] Claus Rasmussen and Sydney A Cameron. Global stingless bee phylogeny supports ancient divergence, vicariance, and long distance dispersal. Biological Journal of the Linnean Society, 99(1):206–232, 2010.
- [189] Peter H. Raven and Harlan Lewis. The relationship of clarkias from two continents. Brittonia, 11(4):193, oct 1959.
- [190] R. H. Ree and S. A. Smith. Maximum likelihood inference of geographic range evolution by dispersal, local extinction, and cladogenesis. Systematic Biology, 57(1):4–14, feb 2008.
- [191] Susanne Renner. Plant dispersal across the tropical atlantic by wind and sea currents. International Journal of Plant Sciences, 165(S4), jul 2004.

- [192] Liam J Revell. Size-correction and principal components for interspecific comparative studies. Evolution, 63(12):3258–3268, 2009.
- [193] Liam J. Revell. phytools: an r package for phylogenetic comparative biology (and other things). Methods in Ecology and Evolution, 3(2):217–223, dec 2011.
- [194] F. Ronquist. Dispersal-vicariance analysis: A new approach to the quantification of historical biogeography. Systematic Biology, 46(1):195–203, mar 1997.
- [195] Ingrid Roth. Fruits of angiosperms. Schweizerbart’sche Verlagsbuchhandlung, 1977.
- [196] William E Safford. Synopsis of the genus datura. Journal of the Washington Academy of Sciences, 11(8):173–189, 1921.
- [197] Isabel Sanmartín, Henrik Enghoff, and Fredrik Ronquist. Patterns of animal dispersal, vicariance and diversification in the holarctic. Biological Journal of the Linnean Society, 73(4):345–390, 2001.
- [198] Isabel Sanmartín and Fredrik Ronquist. Southern hemisphere biogeography inferred by event-based models: Plant versus animal patterns. Systematic Biology, 53(2):216–243, apr 2004.
- [199] Isabel Sanmartín, Livia Wanntorp, and Richard C. Winkworth. West wind drift revisited: testing for directional dispersal in the southern hemisphere using event-based tree fitting. Journal of Biogeography, 34(3):398–416, mar 2007.
- [200] Tiina Särkinen, Lynn Bohs, Richard G Olmstead, and Sandra Knapp. A phylogenetic framework for evolutionary study of the nightshades (solanaceae): a dated 1000-tip tree. BMC Evolutionary Biology, 13(1):214, 2013.
- [201] Tiina Särkinen, R. Toby Pennington, Matt Lavin, Marcelo F. Simon, and Colin E. Hughes. Evolutionary islands in the andes: persistence and isolation explain high endemism in andean dry tropical forests. Journal of Biogeography, 39(5):884–900, dec 2011.
- [202] S Sato, S Tabata, H Hirakawa, RM Klein Lankhorst, H de Jong, RCHJ van Ham, E Datema, S Smit, EGWM Schijlen, JC van Haarst, et al. The tomato genome sequence provides insights into fleshy fruit evolution. Nature, 485:635–641, 2012.
- [203] Dolph Schluter, Trevor Price, Arne Ø Mooers, and Donald Ludwig. Likelihood of ancestor states in adaptive radiation. Evolution, pages 1699–1711, 1997.
- [204] Rudolf Schmid and Armando T. Hunziker. Genera solanacearum: The genera of solanaceae illustrated, arranged according to a new system. Taxon, 50(4):1294, nov 2001.
- [205] Richard Evans Schultes and Albert Hofmann. The botany and chemistry of hallucinogens. Springfield, Illinois.: Charles C. Thomas 267pp.. Hallucinogens: Fungi, 1973.
- [206] Elizabeth A. Schultz and George W. Haughn. LEAFY, a homeotic gene that regulates inflorescence development in arabidopsis. The Plant Cell, 3(8):771, aug 1991.
- [207] M Sébrier, Alain Lavenu, Michel Fornari, and JP Soulas. Tectonics and uplift in central andes (peru, bolivia and northern chile) from eocene to present. Géodynamique, 3(1-2):85–106, 1988.

- [208] E. B. Sessa, E. A. Zimmer, and T. J. Givnish. Phylogeny, divergence times, and historical biogeography of new world dryopteris (dryopteridaceae). American Journal of Botany, 99(4):730–750, mar 2012.
- [209] B. C. Shabman. Tannic acid and iron alum with safranin and orange g in studies of the shoot apex. Stain Technology, 18(3):105–111, jan 1943.
- [210] Smith. High species diversity in fleshy-fruited tropical understory plants. The American Naturalist, 157(6):646, 2001.
- [211] Stacey DeWitt Smith and David A Baum. Phylogenetics of the florally diverse andean clade iochrominae (solanaceae). American Journal of Botany, 93(8):1140–1153, 2006.
- [212] Douglas E. Soltis and Robert K. Kuzoff. Discordance between nuclear and chloroplast phylogenies in the heuchera group (saxifragaceae). Evolution, 49(4):727, aug 1995.
- [213] H. N. Southern and N. P. Naumov. The ecology of animals. The Journal of Animal Ecology, 43(2):602, jun 1974.
- [214] Caroline A.E. Stromberg. Evolution of grasses and grassland ecosystems. Annual Review of Earth and Planetary Sciences, 39(1):517–544, may 2011.
- [215] Heidi K. Swanson, Martin Lysy, Michael Power, Ashley D. Stasko, Jim D. Johnson, and James D. Reist. A new probabilistic method for quantifyingn-dimensional ecological niches and niche overlap. Ecology, 96(2):318–324, feb 2015.
- [216] David L Swofford. PAUP* Phylogenetic analysis using parsimony (* and other methods), Version 4. Sinauer Associates Sunderland, MA, 2003.
- [217] David Symon and L Haegi. *Datura* (solanaceae) is a new world genus. Publication of the Royal Botanic Gardens, Kew, UK for the Linnaean Soc. of London, pages 197–210, 1991.
- [218] P Szövényi, S Terracciano, M Ricca, S Giordano, and AJ Shaw. Recent divergence, intercontinental dispersal and shared polymorphism are shaping the genetic structure of amphi-atlantic peatmoss populations. Molecular ecology, 17(24):5364–5377, 2008.
- [219] Christine E. Thacker. Biogeography of goby lineages (gobiiformes: Gobioidei): origin, invasions and extinction throughout the cenozoic. Journal of Biogeography, 42(9):1615–1625, jun 2015.
- [220] Wilfried Thuiller, Bruno Lafourcade, Robin Engler, and Miguel B Araújo. Biomod – a platform for ensemble forecasting of species distributions. Ecography, 32(3):369–373, 2009.
- [221] Richard M. Tosdal. The amazon-laurentian connection as viewed from the middle proterozoic rocks in the central andes, western bolivia and northern chile. Tectonics, 15(4):827–842, aug 1996.
- [222] E T Tozer. Uppermost cretaceous and paleocene non-marine molluscan faunas of western alberta. Technical report, 1956.
- [223] E. A. Tripp and L. A. McDade. A rich fossil record yields calibrated phylogeny for acanthaceae (lamiales) and evidence for marked biases in timing and directionality of intercontinental disjunctions. Systematic Biology, 63(5):660–684, apr 2014.

- [224] Tieyao Tu, Michael O. Dillon, Hang Sun, and Jun Wen. Phylogeny of *nolana* (solanaceae) of the atacama and peruvian deserts inferred from sequences of four plastid markers and the nuclear LEAFY second intron. Molecular Phylogenetics and Evolution, 49(2):561–573, nov 2008.
- [225] Felix Velichkevich and Ewa Zastawniak. The pliocene flora of kholmech, south-eastern belarus and its correlation with other pliocene floras of europe. Acta palaeobot, 43:137–259, 2003.
- [226] K. Vijverberg, P. Kuperus, J. A. J. Breeuwer, and K. Bachmann. Incipient adaptive radiation of new zealand and australian microseris (asteraceae): an amplified fragment length polymorphism (AFLP) study. Journal of Evolutionary Biology, 13(6):997–1008, nov 2000.
- [227] Gary Voelker, Joshua V. Peñalba, Jerry W. Huntley, and Rauri C.K. Bowie. Diversification in an afro-asian songbird clade (erythropygia–copsychus) reveals founder-event speciation via trans-oceanic dispersals and a southern to northern colonization pattern in africa. Molecular Phylogenetics and Evolution, 73:97–105, apr 2014.
- [228] Alexander von Humboldt and Aimé Bonpland. Essai sur la géographie des plantes. Paris: Levrault, Schoell et Cie, 1805.
- [229] Maria. S. Vorontsova, Stephen Stern, Lynn Bohs, and Sandra Knapp. African spiny solanum (subgenus leptostemonum, solanaceae): a thorny phylogenetic tangle. Botanical Journal of the Linnean Society, 173(2):176–193, jun 2013.
- [230] Alfred Russel Wallace. The Geographical Distribution of Animals. London: John Murray, 1876.
- [231] Alfred Wegener. The origin of continents and oceans. London: Methuen, 4th edition, 1924.
- [232] Maximilian Weigend. Observations on the biogeography of the amotape-huancabamba zone in northern peru. The Botanical Review, 68(1):38–54, jan 2002.
- [233] Martha R. Weiss. Floral color change: A widespread functional convergence. American Journal of Botany, 82(2):167, feb 1995.
- [234] Jonathan F. Wendel and Jeff J. Doyle. Phylogenetic incongruence: Window into genome history and molecular evolution. In Molecular Systematics of Plants II, pages 265–296. Springer US, 1998.
- [235] R Wettstein. Die Natürlichen Pflanzenfamilien 4(3b), chapter Nicandreae. 10. Leipzig, Germany: Wilhelm Engelmann, 1895.
- [236] Alexander E. White. Geographical barriers and dispersal propensity interact to limit range expansions of himalayan birds. The American Naturalist, 188(1):99–112, jul 2016.
- [237] Thomas J White, Thomas Bruns, SJWT Lee, JW Taylor, et al. Amplification and direct sequencing of fungal ribosomal rna genes for phylogenetics. volume 18, pages 315–322. Academic Press, San Diego, CA, 1990.
- [238] Maggie Whitson, Paul S Manos, and Gregory M Plunkett. Untangling physalis (solanaceae) from the physaloids: a two-gene phylogeny of the physalinae. Systematic Botany, 30(1):216–230, 2005.

- [239] John J. Wiens and Michael J. Donoghue. Historical biogeography, ecology and species richness. Trends in Ecology & Evolution, 19(12):639–644, dec 2004.
- [240] Peter Wilf, Mónica R. Carvalho, María A. Gandolfo, and N. Rubén Cúneo. Eocene lantern fruits from gondwanan patagonia and the early origins of solanaceae. Science, 355(6320):71–75, jan 2017.
- [241] E. Wilson and R. H. McArthur. The theory of island biogeography, volume 1. Princeton, NJ, 1967.
- [242] Mary Susanne Wisz, Julien Pottier, W Daniel Kissling, Loïc Pellissier, Jonathan Lenoir, Christian F Damgaard, Carsten F Dormann, Mads C Forchhammer, John-Arvid Grytnes, Antoine Guisan, et al. The role of biotic interactions in shaping distributions and realised assemblages of species: implications for species distribution modelling. Biological Reviews, 88(1):15–30, 2013.
- [243] Alan C. Yen and Richard G. Olmstead. Molecular systematics of cyperaceae tribe cariceae based on two chloroplast DNA regions: ndhF and trnL intron-intergenic spacer. Systematic Botany, 25(3):479, jul 2000.
- [244] Anne D. Yoder and Michael D. Nowak. Has vicariance or dispersal been the predominant biogeographic force in madagascar? only time will tell. Annual Review of Ecology, Evolution, and Systematics, 37(1):405–431, dec 2006.
- [245] Yan Yu, A.J. Harris, Christopher Blair, and Xingjin He. RASP (reconstruct ancestral state in phylogenies): A tool for historical biogeography. Molecular Phylogenetics and Evolution, 87:46–49, jun 2015.
- [246] J. Zachos. Trends, rhythms, and aberrations in global climate 65 ma to present. Science, 292(5517):686–693, apr 2001.
- [247] James C. Zachos, Gerald R. Dickens, and Richard E. Zeebe. An early cenozoic perspective on greenhouse warming and carbon-cycle dynamics. Nature, 451(7176):279–283, jan 2008.

Appendix A

Supporting information to Chapter 1

This appendix contains supporting information for Chapter 1.

A.1 Supplementary tables and algorithm validation

SUPPORTING INFORMATION

Bayesian estimation of the global biogeographical history of the Solanaceae.

Julia Dupin, Nicholas J. Matzke, Tiina Särkinen, Sandra Knapp, Richard G. Olmstead, Lynn Bohs and Stacey D. Smith

Appendix S1. Supplementary tables, Dispersal multiplier matrices and Algorithm validation for Biogeographical Stochastic Mapping in ‘BioGeoBEARS’

Supplementary tables

Table S1.1. Species list from Solanaceae phylogeny (Särkinen *et al.*, 2013) that were pruned due to cultivation or duplicates, and that had their names corrected according to more recent literature.

Cultivated taxa pruned	<i>Capsicum annuum</i> <i>Nicotiana rustica</i> <i>Nicotiana tabacum</i> <i>Solanum lycopersicum</i> <i>Solanum mammosum</i> <i>Solanum melongena</i> <i>Solanum pseudocapsicum</i> <i>Solanum tuberosum</i>
Synonyms (pruned = kept)	<i>Datura bernhardii</i> = <i>Datura stramonium</i> <i>Datura ferox</i> = <i>Datura quercifolia</i> <i>Datura laevis</i> = <i>Datura stramonium</i> <i>Datura rosei</i> = <i>Brugmansia sanguinea</i> <i>Metternichia sp</i> = <i>Metternichia princeps</i> <i>Nicotiana digluta</i> = artificial polyploid <i>Nicotiana eastii</i> = artificial polyploid <i>Nicotiana palmeri</i> = <i>Nicotiana obtusifolia</i> <i>Nicotiana picilla</i> = <i>Nicotiana plumbaginifolia</i> <i>Nicotiana trigonophylla</i> = <i>Nicotiana obtusifolia</i> <i>Lycium duplicatum</i> = unresolved species <i>Solanum aggregatum</i> = <i>Solanum guineense</i> <i>Solanum bukasovii</i> = <i>Solanum candolleanum</i> <i>Solanum capsicastrum</i> = <i>Solanum pseudocapsicum</i> <i>Solanum kurzii</i> = <i>Solanum violaceum</i> <i>Solanum marginatum</i> = <i>Solanum candolleanum</i> <i>Solanum nakurense</i> = <i>Solanum terminale</i> <i>Solanum ovigerum</i> = <i>Solanum melongena</i> <i>Solanum panduriforme</i> = <i>Solanum campylacanthum</i> <i>Solanum rigescentoides</i> = <i>Solanum humile</i> <i>Solanum sessilistellatum</i> = <i>Solanum nigriviolaceum</i> <i>Solanum tundalomense</i> = <i>Solanum colombianum</i> <i>Vestia lycioides</i> = <i>Vestia foetida</i>
Taxa renamed	<i>Cestrum megalophyllum</i> -> <i>Cestrum schlechtendalii</i> <i>Datura leichhardtii</i> -> <i>Datura pruinosa</i> <i>Leucophysalis viscosa</i> -> <i>Schraderanthus sp</i> <i>Mandragora autumnalis</i> -> <i>Mandragora officinalis</i> <i>Solanum adhaerens</i> -> <i>Solanum volubile</i> <i>Solanum circaeifolium</i> -> <i>Solanum stipuloideum</i>

	<i>Solanum cumingii</i> -> <i>Solanum insanum</i> <i>Solanum drymophilum</i> -> <i>Solanum ensifolium</i> <i>Solanum kwebense</i> -> <i>Solanum tettense</i> <i>Solanum megistacrolobum</i> -> <i>Solanum boliviense</i> <i>Solanum quadrangulare</i> -> <i>Solanum africanum</i> <i>Solanum thruppii</i> -> <i>Solanum coagulans</i> <i>Solanum tredecimgranum</i> -> <i>Solanum furcatum</i> <i>Solanum tridynamum</i> -> <i>Solanum houstonii</i>
--	---

Table S1.2. Solanaceae species distribution today according to a seven-area coding. Distribution scoring: South America (SAm), Central America (CAm), the Caribbean (Car), North America (NAm), Africa (AF), Eurasia (EU), and Australia (OZ). The x=12 clade (marked with an asterisk on Fig. 2) includes the clades Solaneae, Capsiceae, Physaleae, “Salpichroina”, Datureae, *Mandragora*, Juanulloae, *Nicandra*, *Exodeconus*, “Atropina” and Nicotianoideae

Taxon	Clade	Distribution
<i>Acnistus arborescens</i>	Physaleae	SAm&CAm&Car
<i>Anisodus acutangulus</i>	Atropina	EU
<i>Anisodus carniolicoides</i>	Atropina	EU
<i>Anisodus luridus</i>	Atropina	EU
<i>Anisodus tanguticus</i>	Atropina	EU
<i>Anthocercis angustifolia</i>	Nicotianoideae	OZ
<i>Anthocercis gracilis</i>	Nicotianoideae	OZ
<i>Anthocercis ilicifolia</i>	Nicotianoideae	OZ
<i>Anthocercis intricata</i>	Nicotianoideae	OZ
<i>Anthocercis littorea</i>	Nicotianoideae	OZ
<i>Anthocercis myosotidea</i>	Nicotianoideae	OZ
<i>Anthocercis racemosa</i>	Nicotianoideae	OZ
<i>Anthocercis sylvicola</i>	Nicotianoideae	OZ
<i>Anthocercis viscosa</i>	Nicotianoideae	OZ
<i>Anthotroche blackii</i>	Nicotianoideae	OZ
<i>Anthotroche myoporoides</i>	Nicotianoideae	OZ
<i>Anthotroche pannosa</i>	Nicotianoideae	OZ
<i>Anthotroche walcottii</i>	Nicotianoideae	OZ
<i>Athenaea pogogena</i>	Physaleae	SAm
<i>Athenaea sp</i>	Physaleae	SAm
<i>Atropa belladonna</i>	Atropina	EU
<i>Atropa komarovii</i>	Atropina	EU
<i>Atropanthe sinensis</i>	Atropina	EU
<i>Aureliana fasciculata</i>	Physaleae	SAm
<i>Benthamiella patagonica</i>	Benthamielleae	SAm
<i>Benthamiella skottsbergii</i>	Benthamielleae	SAm
<i>Bouchetia anomala</i>	Petunieae	SAm
<i>Bouchetia erecta</i>	Petunieae	NAm&CAm
<i>Brachistus stramonifolius</i>	Physaleae	NAm&CAm
<i>Browallia eludens</i>	Cestroideae	NAm&CAm
<i>Browallia speciosa</i>	Cestroideae	SAm&CAm
<i>Brugmansia arborea</i>	Datureae	SAm
<i>Brugmansia aurea</i>	Datureae	SAm
<i>Brugmansia sanguinea</i>	Datureae	SAm
<i>Brunfelsia americana</i>	Petunieae	Car
<i>Brunfelsia uniflora</i>	Petunieae	SAm

<i>Calibrachoa parviflora</i>	Petunieae	SAm&NAm
<i>Calibrachoa pygmaea</i>	Petunieae	SAm
<i>Calibrachoa sellowiana</i>	Petunieae	SAm
<i>Capsicum baccatum</i>	Capsiceae	SAm
<i>Capsicum campylopodium</i>	Capsiceae	SAm
<i>Capsicum cardenasii</i>	Capsiceae	SAm
<i>Capsicum ceratocalyx</i>	Capsiceae	SAm
<i>Capsicum chacoense</i>	Capsiceae	SAm
<i>Capsicum chinense</i>	Capsiceae	SAm&CAm
<i>Capsicum ciliatum</i>	Capsiceae	NAm&SAm&CAm
<i>Capsicum coccineum</i>	Capsiceae	SAm
<i>Capsicum eximium</i>	Capsiceae	SAm
<i>Capsicum flexuosum</i>	Capsiceae	SAm
<i>Capsicum frutescens</i>	Capsiceae	NAm&SAm&CAm
<i>Capsicum galapagoense</i>	Capsiceae	SAm
<i>Capsicum geminifolium</i>	Capsiceae	SAm
<i>Capsicum hunzikerianum</i>	Capsiceae	SAm
<i>Capsicum lanceolatum</i>	Capsiceae	NAm&CAm
<i>Capsicum lycianthoides</i>	Capsiceae	SAm
<i>Capsicum minutiflorum</i>	Capsiceae	SAm
<i>Capsicum pereirae</i>	Capsiceae	SAm
<i>Capsicum pubescens</i>	Capsiceae	SAm
<i>Capsicum recurvatum</i>	Capsiceae	SAm
<i>Capsicum rhomboideum</i>	Capsiceae	SAm
<i>Capsicum schottianum</i>	Capsiceae	SAm
<i>Capsicum tovarii</i>	Capsiceae	SAm
<i>Capsicum villosum</i>	Capsiceae	SAm
<i>Cestrum acutifolium</i>	Cestroideae	Car
<i>Cestrum aurantiacum</i>	Cestroideae	NAm&CAm
<i>Cestrum chiriquianum</i>	Cestroideae	CAm
<i>Cestrum dasyanthum</i>	Cestroideae	CAm
<i>Cestrum diurnum</i>	Cestroideae	NAm&CAm&Car
<i>Cestrum elegans</i>	Cestroideae	NAm
<i>Cestrum endlicheri</i>	Cestroideae	NAm
<i>Cestrum fasciculatum</i>	Cestroideae	NAm
<i>Cestrum fragile</i>	Cestroideae	CAm
<i>Cestrum fulvescens</i>	Cestroideae	NAm

<i>Cestrum glanduliferum</i>	Cestroideae	NAm&CAm
<i>Cestrum guatemalense</i>	Cestroideae	NAm&CAm
<i>Cestrum inclusum</i>	Cestroideae	Car
<i>Cestrum irazuense</i>	Cestroideae	CAm
<i>Cestrum laxum</i>	Cestroideae	NAm
<i>Cestrum luteovirescens</i>	Cestroideae	NAm&CAm
<i>Cestrum macrophyllum</i>	Cestroideae	SAm&CAm&Car
<i>Cestrum schlechtendalii</i>	Cestroideae	NAm&SAm&CAm&Car
<i>Cestrum milciomejiae</i>	Cestroideae	Car
<i>Cestrum miradoreense</i>	Cestroideae	NAm
<i>Cestrum mortonianum</i>	Cestroideae	CAm
<i>Cestrum nocturnum</i>	Cestroideae	NAm&SAm&CAm&Car
<i>Cestrum oblongifolium</i>	Cestroideae	NAm
<i>Cestrum pacayense</i>	Cestroideae	CAm
<i>Cestrum pittieri</i>	Cestroideae	CAm
<i>Cestrum poasanum</i>	Cestroideae	CAm
<i>Cestrum regelii</i>	Cestroideae	NAm&CAm
<i>Cestrum rigidum</i>	Cestroideae	SAm
<i>Cestrum roseum</i>	Cestroideae	NAm
<i>Cestrum sphaerocarpum</i>	Cestroideae	Car
<i>Cestrum strigilatum</i>	Cestroideae	CAm&SAm
<i>Cestrum thyrsoideum</i>	Cestroideae	NAm
<i>Cestrum tomentosum</i>	Cestroideae	SAm&CAm
<i>Cestrum tuerckheimii</i>	Cestroideae	Car
<i>Cestrum violaceum</i>	Cestroideae	Car
<i>Cestrum virgaurea</i>	Cestroideae	Car
<i>Chamaesaracha coronopus</i>	Physaleae	NAm
<i>Chamaesaracha sordida</i>	Physaleae	NAm
<i>Coeloneurum ferrugineum</i>	Goetzeoideae	Car
<i>Combera paradoxa</i>	Benthamielleae	SAm
<i>Crenidium spinescens</i>	Nicotianoideae	OZ
<i>Cuatresia exiguiflora</i>	Physaleae	SAm&CAm
<i>Cuatresia riparia</i>	Physaleae	SAm&CAm
<i>Cyphanthera albicans</i>	Nicotianoideae	OZ
<i>Cyphanthera anthocercidea</i>	Nicotianoideae	OZ
<i>Cyphanthera microphylla</i>	Nicotianoideae	OZ
<i>Cyphanthera odgersii</i>	Nicotianoideae	OZ
<i>Datura ceratocaula</i>	Datureae	NAm
<i>Datura discolor</i>	Datureae	NAm
<i>Datura inoxia</i>	Datureae	NAm&CAm
<i>Datura pruinosa</i>	Datureae	NAm
<i>Datura metel</i>	Datureae	NAm&CAm
<i>Datura quercifolia</i>	Datureae	NAm

<i>Datura stramonium</i>	Datureae	NAm&CAm
<i>Deprea bitteriana</i>	Physaleae	SAm
<i>Deprea orinocensis</i>	Physaleae	SAm&CAm
<i>Deprea paneroi</i>	Physaleae	SAm
<i>Deprea sylvaticum</i>	Physaleae	SAm&CAm
<i>Discopodium penninervium</i>	Physaleae	AF
<i>Duboisia hopwoodii</i>	Nicotianoideae	OZ
<i>Duboisia leichhardtii</i>	Nicotianoideae	OZ
<i>Duboisia myoporoides</i>	Nicotianoideae	OZ
<i>Duckeodendron cestroides</i>	Duckeodendron	SAm
<i>Dunalia brachyacantha</i>	Physaleae	SAm
<i>Dunalia obovata</i>	Physaleae	SAm
<i>Dunalia solanacea</i>	Physaleae	SAm
<i>Dunalia spathulata</i>	Physaleae	SAm
<i>Dunalia spinosa</i>	Physaleae	SAm
<i>Dyssochroma viridiflora</i>	Juanulloae	SAm
<i>Eriolarynx fasciculata</i>	Physaleae	SAm
<i>Eriolarynx lorentzii</i>	Physaleae	SAm
<i>Espadaea amoena</i>	Goetzeoideae	Car
<i>Exodeconus miersii</i>	Exodeconus	SAm
<i>Fabiana imbricata</i>	Petunieae	SAm
<i>Goetzea ekmanii</i>	Goetzeoideae	Car
<i>Goetzea elegans</i>	Goetzeoideae	Car
<i>Grammosolen dixonii</i>	Nicotianoideae	OZ
<i>Grammosolen truncatus</i>	Nicotianoideae	OZ
<i>Henoonia myrtifolia</i>	Goetzeoideae	Car
<i>Heteranthia decipiens</i>	Schwenckieae	SAm
<i>Hunzikeria texana</i>	Petunieae	NAm
<i>Hyoscyamus albus</i>	Atropina	EU&AF
<i>Hyoscyamus aureus</i>	Atropina	EU&AF
<i>Hyoscyamus desertorum</i>	Atropina	EU
<i>Hyoscyamus leptocalyx</i>	Atropina	EU
<i>Hyoscyamus muticus</i>	Atropina	EU&AF
<i>Hyoscyamus niger</i>	Atropina	EU
<i>Hyoscyamus pusillus</i>	Atropina	EU
<i>Hyoscyamus turcomanicus</i>	Atropina	EU
<i>Iochroma australe</i>	Physaleae	SAm
<i>Iochroma calycinum</i>	Physaleae	SAm
<i>Iochroma cardenasiatum</i>	Datureae	SAm
<i>Iochroma confertiflorum</i>	Physaleae	SAm
<i>Iochroma cornifolium</i>	Physaleae	SAm
<i>Iochroma cyaneum</i>	Physaleae	SAm
<i>Iochroma edule</i>	Physaleae	SAm

<i>Iochroma ellipticum</i>	Physaleae	SAm
<i>Iochroma fuchsoides</i>	Physaleae	SAm
<i>Iochroma gesnerioides</i>	Physaleae	SAm
<i>Iochroma grandiflorum</i>	Physaleae	SAm
<i>Iochroma lehmannii</i>	Physaleae	SAm
<i>Iochroma loxense</i>	Physaleae	SAm
<i>Iochroma nitidum</i>	Physaleae	SAm
<i>Iochroma parvifolium</i>	Physaleae	SAm
<i>Iochroma salpoanum</i>	Physaleae	SAm
<i>Iochroma squamosum</i>	Physaleae	SAm
<i>Iochroma stenanthum</i>	Physaleae	SAm
<i>Iochroma umbellatum</i>	Physaleae	SAm
<i>Ipomoea</i>	Outgroup	NAm&SAm&CAm&Car&EU&OZ&AF
<i>Jaborosa integrifolia</i>	Atropina	SAm
<i>Jaborosa sativa</i>	Atropina	SAm
<i>Jaborosa squarrosa</i>	Atropina	SAm
<i>Jaltomata andersonii</i>	Solaneae	SAm
<i>Jaltomata antillana</i>	Solaneae	Car
<i>Jaltomata aspera</i>	Solaneae	SAm
<i>Jaltomata auriculata</i>	Solaneae	SAm
<i>Jaltomata bernardelloana</i>	Solaneae	SAm
<i>Jaltomata bicolor</i>	Solaneae	SAm
<i>Jaltomata biflora</i>	Solaneae	SAm
<i>Jaltomata bohsiana</i>	Solaneae	NAm
<i>Jaltomata cajacayensis</i>	Solaneae	SAm
<i>Jaltomata chihuahuensis</i>	Solaneae	NAm
<i>Jaltomata chotanae</i>	Solaneae	SAm
<i>Jaltomata contumacensis</i>	Solaneae	SAm
<i>Jaltomata darciana</i>	Solaneae	CAm
<i>Jaltomata dendroidea</i>	Solaneae	SAm
<i>Jaltomata dentata</i>	Solaneae	SAm
<i>Jaltomata grandiflora</i>	Solaneae	NAm
<i>Jaltomata guillermoguerrae</i>	Solaneae	SAm
<i>Jaltomata herrerae</i>	Solaneae	SAm
<i>Jaltomata lanata</i>	Solaneae	SAm
<i>Jaltomata leivae</i>	Solaneae	SAm
<i>Jaltomata lezamae</i>	Solaneae	SAm
<i>Jaltomata lojiae</i>	Solaneae	SAm
<i>Jaltomata lomana</i>	Solaneae	SAm
<i>Jaltomata mionei</i>	Solaneae	SAm
<i>Jaltomata nigricolor</i>	Solaneae	SAm
<i>Jaltomata oppositifolia</i>	Solaneae	SAm
<i>Jaltomata paneroi</i>	Solaneae	SAm

<i>Jaltomata procumbens</i>	Solaneae	NAm&SAm&CAm
<i>Jaltomata repandidentata</i>	Solaneae	NAm&SAm&CAm
<i>Jaltomata sagastegui</i>	Solaneae	SAm
<i>Jaltomata salpoensis</i>	Solaneae	SAm
<i>Jaltomata sanchezvegae</i>	Solaneae	SAm
<i>Jaltomata sinuosa</i>	Solaneae	SAm
<i>Jaltomata tayabambae</i>	Solaneae	SAm
<i>Jaltomata truxillana</i>	Solaneae	SAm
<i>Jaltomata umbellata</i>	Solaneae	SAm
<i>Jaltomata ventricosa</i>	Solaneae	SAm
<i>Jaltomata viridiflora</i>	Solaneae	SAm
<i>Jaltomata weberbaueri</i>	Solaneae	SAm
<i>Jaltomata yacheri</i>	Solaneae	SAm
<i>Jaltomata yungayensis</i>	Solaneae	SAm
<i>Juanulloa mexicana</i>	Juanulloae	NAm&SAm&CAm
<i>Larnax dilloniana</i>	Physaleae	SAm
<i>Larnax hawkesii</i>	Physaleae	SAm
<i>Larnax nieva</i>	Physaleae	SAm
<i>Larnax parviflora</i>	Physaleae	SAm
<i>Larnax peruviana</i>	Physaleae	SAm
<i>Larnax psilophyta</i>	Physaleae	SAm
<i>Larnax purpurea</i>	Physaleae	SAm
<i>Larnax sachapapa</i>	Physaleae	SAm
<i>Larnax subtriflora</i>	Physaleae	SAm
<i>Larnax suffruticosa</i>	Physaleae	SAm
<i>Larnax sylvarum</i>	Physaleae	SAm&CAm
<i>Latua pubiflora</i>	Atropina	SAm
<i>Leptoglossis darciana</i>	Petunieae	SAm
<i>Leucophysalis grandiflora</i>	Physaleae	NAm
<i>Leucophysalis nana</i>	Physaleae	NAm
<i>Schraderanthus sp</i>	Physaleae	CAm
<i>Lycianthes acapulcensis</i>	Capsiceae	NAm
<i>Lycianthes acutifolia</i>	Capsiceae	SAm
<i>Lycianthes amatitlanensis</i>	Capsiceae	NAm&SAm&CAm
<i>Lycianthes asarifolia</i>	Capsiceae	SAm
<i>Lycianthes beckneriana</i>	Capsiceae	CAm
<i>Lycianthes biflora</i>	Capsiceae	EU
<i>Lycianthes ciliolata</i>	Capsiceae	NAm&CAm
<i>Lycianthes dejecta</i>	Capsiceae	NAm
<i>Lycianthes denticulata</i>	Capsiceae	EU
<i>Lycianthes fasciculata</i>	Capsiceae	SAm
<i>Lycianthes furcatistellata</i>	Capsiceae	CAm
<i>Lycianthes geminiflora</i>	Capsiceae	NAm&CAm

<i>Lycianthes glandulosa</i>	Capsiceae	SAm
<i>Lycianthes heteroclita</i>	Capsiceae	NAm&CAm
<i>Lycianthes inaequilatera</i>	Capsiceae	SAm
<i>Lycianthes jalicensis</i>	Capsiceae	NAm
<i>Lycianthes jelskii</i>	Capsiceae	SAm
<i>Lycianthes lenta</i>	Capsiceae	NAm&CAm&Car
<i>Lycianthes lycioides</i>	Capsiceae	SAm
<i>Lycianthes lysimachioides</i>	Capsiceae	EU
<i>Lycianthes moziniana</i>	Capsiceae	NAm
<i>Lycianthes multiflora</i>	Capsiceae	CAm&NAm
<i>Lycianthes nitida</i>	Capsiceae	NAm&SAm&CAm
<i>Lycianthes peduncularis</i>	Capsiceae	NAm
<i>Lycianthes pringlei</i>	Capsiceae	NAm
<i>Lycianthes pseudolycioides</i>	Capsiceae	SAm
<i>Lycianthes radiata</i>	Capsiceae	SAm
<i>Lycianthes rantonnei</i>	Capsiceae	SAm
<i>Lycianthes rzedowskii</i>	Capsiceae	NAm
<i>Lycianthes saltensis</i>	Capsiceae	SAm
<i>Lycianthes sanctaeclarae</i>	Capsiceae	CAm
<i>Lycianthes shanesii</i>	Capsiceae	OZ
<i>Lycianthes stephanocalyx</i>	Capsiceae	NAm&CAm
<i>Lycianthes surotatensis</i>	Capsiceae	NAm
<i>Lycianthes synanthera</i>	Capsiceae	NAm&SAm&CAm
<i>Lycianthes tricolor</i>	Capsiceae	NAm&CAm
<i>Lycium acutifolium</i>	Atropina	AF
<i>Lycium afrum</i>	Atropina	AF
<i>Lycium ameghinoi</i>	Atropina	SAm
<i>Lycium americanum</i>	Atropina	SAm&Car
<i>Lycium amoenum</i>	Atropina	AF
<i>Lycium andersonii</i>	Atropina	NAm
<i>Lycium arenicola</i>	Atropina	AF
<i>Lycium athium</i>	Atropina	SAm
<i>Lycium australe</i>	Atropina	OZ
<i>Lycium barbarum</i>	Atropina	EU
<i>Lycium berlandieri</i>	Atropina	NAm
<i>Lycium boerhaviifolium</i>	Atropina	NAm&SAm
<i>Lycium bosciifolium</i>	Atropina	AF
<i>Lycium brevipes</i>	Atropina	NAm
<i>Lycium californicum</i>	Atropina	NAm
<i>Lycium carolinianum</i>	Atropina	NAm
<i>Lycium cestroides</i>	Atropina	SAm
<i>Lycium chanar</i>	Atropina	SAm
<i>Lycium chilense</i>	Atropina	SAm

<i>Lycium chinense</i>	Atropina	EU
<i>Lycium ciliatum</i>	Atropina	SAm
<i>Lycium cinereum</i>	Atropina	AF
<i>Lycium cooperi</i>	Atropina	NAm
<i>Lycium cuneatum</i>	Atropina	SAm
<i>Lycium dasystemum</i>	Atropina	EU
<i>Lycium decumbens</i>	Atropina	AF
<i>Lycium depressum</i>	Atropina	EU
<i>Lycium deserti</i>	Atropina	SAm
<i>Lycium eenii</i>	Atropina	AF
<i>Lycium elongatum</i>	Atropina	SAm
<i>Lycium europaeum</i>	Atropina	EU
<i>Lycium exsertum</i>	Atropina	NAm
<i>Lycium ferocissimum</i>	Atropina	AF
<i>Lycium fremontii</i>	Atropina	NAm
<i>Lycium fuscum</i>	Atropina	SAm
<i>Lycium gariepense</i>	Atropina	AF
<i>Lycium gilliesianum</i>	Atropina	SAm
<i>Lycium grandicalyx</i>	Atropina	AF
<i>Lycium hirsutum</i>	Atropina	AF
<i>Lycium horridum</i>	Atropina	AF
<i>Lycium infaustum</i>	Atropina	SAm
<i>Lycium macrodon</i>	Atropina	NAm
<i>Lycium microphyllum</i>	Atropina	SAm
<i>Lycium minimum</i>	Atropina	SAm
<i>Lycium minutifolium</i>	Atropina	SAm
<i>Lycium morongii</i>	Atropina	SAm
<i>Lycium nodosum</i>	Atropina	SAm
<i>Lycium oxycarpum</i>	Atropina	AF
<i>Lycium pallidum</i>	Atropina	NAm
<i>Lycium parishii</i>	Atropina	NAm
<i>Lycium pilifolium</i>	Atropina	AF
<i>Lycium puberulum</i>	Atropina	NAm
<i>Lycium pumilum</i>	Atropina	AF
<i>Lycium rachidocladum</i>	Atropina	SAm
<i>Lycium ruthenicum</i>	Atropina	EU
<i>Lycium sandwicense</i>	Atropina	OZ
<i>Lycium schizocalyx</i>	Atropina	AF
<i>Lycium schweinfurthii</i>	Atropina	AF
<i>Lycium shawii</i>	Atropina	AF
<i>Lycium shockleyi</i>	Atropina	NAm
<i>Lycium stenophyllum</i>	Atropina	SAm
<i>Lycium strandveldense</i>	Atropina	AF

<i>Lycium tenue</i>	Atropina	AF
<i>Lycium tenuispinosum</i>	Atropina	SAm
<i>Lycium tetrandrum</i>	Atropina	AF
<i>Lycium texanum</i>	Atropina	NAm
<i>Lycium torreyi</i>	Atropina	NAm
<i>Lycium truncatum</i>	Atropina	EU
<i>Lycium villosum</i>	Atropina	AF
<i>Lycium vimineum</i>	Atropina	SAm
<i>Lycium yunnanense</i>	Atropina	EU
<i>Mandragora officinalis</i>	Mandragora	EU&AF
<i>Mandragora caulescens</i>	Mandragora	EU
<i>Mandragora chinghaiensis</i>	Mandragora	EU
<i>Mandragora officinarum</i>	Mandragora	EU&AF
<i>Mandragora turcomanica</i>	Mandragora	EU
<i>Markea panamensis</i>	Juanulloaeae	CAm
<i>Markea ulei</i>	Juanulloaeae	SAm
<i>Melananthus guatemalensis</i>	Schwenckieae	SAm&CAm
<i>Mellissia begoniifolia</i>	Physaleae	AF
<i>Merinthopodium neuranthum</i>	Juanulloaeae	CAm
<i>Metternichia princeps</i>	Goetzeoideae	SAm
<i>Nectouxia formosa</i>	Salpichroina	NAm
<i>Nicandra physalodes</i>	Nicandra	SAm
<i>Nicotiana acaulis</i>	Nicotianoideae	SAm
<i>Nicotiana acuminata</i>	Nicotianoideae	SAm
<i>Nicotiana africana</i>	Nicotianoideae	AF
<i>Nicotiana alata</i>	Nicotianoideae	SAm
<i>Nicotiana amplexicaulis</i>	Nicotianoideae	OZ
<i>Nicotiana arentsii</i>	Nicotianoideae	SAm
<i>Nicotiana benavidesii</i>	Nicotianoideae	SAm
<i>Nicotiana bonariensis</i>	Nicotianoideae	SAm
<i>Nicotiana cavicola</i>	Nicotianoideae	OZ
<i>Nicotiana clevelandii</i>	Nicotianoideae	NAm
<i>Nicotiana cordifolia</i>	Nicotianoideae	SAm
<i>Nicotiana corymbosa</i>	Nicotianoideae	SAm
<i>Nicotiana excelsior</i>	Nicotianoideae	OZ
<i>Nicotiana exigua</i>	Nicotianoideae	OZ
<i>Nicotiana forgetiana</i>	Nicotianoideae	SAm
<i>Nicotiana forsteri</i>	Nicotianoideae	OZ
<i>Nicotiana glauca</i>	Nicotianoideae	SAm
<i>Nicotiana glutinosa</i>	Nicotianoideae	SAm
<i>Nicotiana goodspeedii</i>	Nicotianoideae	OZ
<i>Nicotiana gossei</i>	Nicotianoideae	OZ
<i>Nicotiana kawakamii</i>	Nicotianoideae	SAm

<i>Nicotiana knightiana</i>	Nicotianoideae	SAm
<i>Nicotiana langsdorffii</i>	Nicotianoideae	SAm
<i>Nicotiana linearis</i>	Nicotianoideae	SAm
<i>Nicotiana longiflora</i>	Nicotianoideae	SAm
<i>Nicotiana maritima</i>	Nicotianoideae	OZ
<i>Nicotiana megalosiphon</i>	Nicotianoideae	OZ
<i>Nicotiana miersii</i>	Nicotianoideae	SAm
<i>Nicotiana nesophila</i>	Nicotianoideae	NAm
<i>Nicotiana noctiflora</i>	Nicotianoideae	SAm
<i>Nicotiana nudicaulis</i>	Nicotianoideae	NAm
<i>Nicotiana obtusifolia</i>	Nicotianoideae	NAm
<i>Nicotiana occidentalis</i>	Nicotianoideae	OZ
<i>Nicotiana otophora</i>	Nicotianoideae	SAm
<i>Nicotiana paniculata</i>	Nicotianoideae	SAm
<i>Nicotiana pauciflora</i>	Nicotianoideae	SAm
<i>Nicotiana petunioides</i>	Nicotianoideae	SAm
<i>Nicotiana plumbaginifolia</i>	Nicotianoideae	NAm&SAm&CAm
<i>Nicotiana quadrivalvis</i>	Nicotianoideae	NAm
<i>Nicotiana raimondii</i>	Nicotianoideae	SAm
<i>Nicotiana repanda</i>	Nicotianoideae	NAm&CAm&Car
<i>Nicotiana rosulata</i>	Nicotianoideae	OZ
<i>Nicotiana rotundifolia</i>	Nicotianoideae	OZ
<i>Nicotiana simulans</i>	Nicotianoideae	OZ
<i>Nicotiana solanifolia</i>	Nicotianoideae	SAm
<i>Nicotiana spagazzinii</i>	Nicotianoideae	SAm
<i>Nicotiana stocktonii</i>	Nicotianoideae	NAm
<i>Nicotiana suaveolens</i>	Nicotianoideae	OZ
<i>Nicotiana sylvestris</i>	Nicotianoideae	SAm
<i>Nicotiana thyrsoiflora</i>	Nicotianoideae	SAm
<i>Nicotiana tomentosa</i>	Nicotianoideae	SAm
<i>Nicotiana tomentosiformis</i>	Nicotianoideae	SAm
<i>Nicotiana umbratica</i>	Nicotianoideae	OZ
<i>Nicotiana undulata</i>	Nicotianoideae	SAm
<i>Nicotiana velutina</i>	Nicotianoideae	OZ
<i>Nicotiana wigandioides</i>	Nicotianoideae	SAm
<i>Nierembergia andina</i>	Petunieae	SAm
<i>Nierembergia angustifolia</i>	Petunieae	SAm
<i>Nierembergia aristata</i>	Petunieae	SAm
<i>Nierembergia boliviana</i>	Petunieae	SAm
<i>Nierembergia browalliioides</i>	Petunieae	SAm
<i>Nierembergia calycina</i>	Petunieae	SAm
<i>Nierembergia ericoides</i>	Petunieae	SAm
<i>Nierembergia graveolens</i>	Petunieae	SAm

<i>Nierembergia hatschbachii</i>	Petunieae	SAm
<i>Nierembergia hippomanica</i>	Petunieae	SAm
<i>Nierembergia linariifolia</i>	Petunieae	SAm
<i>Nierembergia micrantha</i>	Petunieae	SAm
<i>Nierembergia pinifolia</i>	Petunieae	SAm
<i>Nierembergia pulchella</i>	Petunieae	SAm
<i>Nierembergia repens</i>	Petunieae	SAm
<i>Nierembergia rigida</i>	Petunieae	SAm
<i>Nierembergia rivularis</i>	Petunieae	SAm
<i>Nierembergia scoparia</i>	Petunieae	SAm
<i>Nierembergia spathulata</i>	Petunieae	SAm
<i>Nierembergia tucumanensis</i>	Petunieae	SAm
<i>Nierembergia veitchii</i>	Petunieae	SAm
<i>Nolana acuminata</i>	Atropina	SAm
<i>Nolana adansonii</i>	Atropina	SAm
<i>Nolana albescens</i>	Atropina	SAm
<i>Nolana aplocaryoides</i>	Atropina	SAm
<i>Nolana arequipensis</i>	Atropina	SAm
<i>Nolana aticoana</i>	Atropina	SAm
<i>Nolana baccata</i>	Atropina	SAm
<i>Nolana balsamiflua</i>	Atropina	SAm
<i>Nolana carnosa</i>	Atropina	SAm
<i>Nolana cerrateana</i>	Atropina	SAm
<i>Nolana chancoana</i>	Atropina	SAm
<i>Nolana chapiensis</i>	Atropina	SAm
<i>Nolana clivicola</i>	Atropina	SAm
<i>Nolana coelestis</i>	Atropina	SAm
<i>Nolana confinis</i>	Atropina	SAm
<i>Nolana coronata</i>	Atropina	SAm
<i>Nolana crassulifolia</i>	Atropina	SAm
<i>Nolana diffusa</i>	Atropina	SAm
<i>Nolana divaricata</i>	Atropina	SAm
<i>Nolana elegans</i>	Atropina	SAm
<i>Nolana filifolia</i>	Atropina	SAm
<i>Nolana flaccida</i>	Atropina	SAm
<i>Nolana galapagensis</i>	Atropina	SAm
<i>Nolana gayana</i>	Atropina	SAm
<i>Nolana humifusa</i>	Atropina	SAm
<i>Nolana incana</i>	Atropina	SAm
<i>Nolana inflata</i>	Atropina	SAm
<i>Nolana intonsa</i>	Atropina	SAm
<i>Nolana johnstonii</i>	Atropina	SAm
<i>Nolana laxa</i>	Atropina	SAm

<i>Nolana leptophylla</i>	Atropina	SAm
<i>Nolana lezamae</i>	Atropina	SAm
<i>Nolana linearifolia</i>	Atropina	SAm
<i>Nolana lycioides</i>	Atropina	SAm
<i>Nolana mollis</i>	Atropina	SAm
<i>Nolana onoana</i>	Atropina	SAm
<i>Nolana pallida</i>	Atropina	SAm
<i>Nolana paradoxa</i>	Atropina	SAm
<i>Nolana parviflora</i>	Atropina	SAm
<i>Nolana peruviana</i>	Atropina	SAm
<i>Nolana pilosa</i>	Atropina	SAm
<i>Nolana plicata</i>	Atropina	SAm
<i>Nolana pterocarpa</i>	Atropina	SAm
<i>Nolana ramosissima</i>	Atropina	SAm
<i>Nolana rostrata</i>	Atropina	SAm
<i>Nolana rupicola</i>	Atropina	SAm
<i>Nolana salsoloides</i>	Atropina	SAm
<i>Nolana scaposa</i>	Atropina	SAm
<i>Nolana sedifolia</i>	Atropina	SAm
<i>Nolana sessiliflora</i>	Atropina	SAm
<i>Nolana spathulata</i>	Atropina	SAm
<i>Nolana sphaerophylla</i>	Atropina	SAm
<i>Nolana stenophylla</i>	Atropina	SAm
<i>Nolana tarapacana</i>	Atropina	SAm
<i>Nolana thinophila</i>	Atropina	SAm
<i>Nolana tocopillensis</i>	Atropina	SAm
<i>Nolana tomentella</i>	Atropina	SAm
<i>Nolana urubambae</i>	Atropina	SAm
<i>Nolana villosa</i>	Atropina	SAm
<i>Nolana volcanica</i>	Atropina	SAm
<i>Nolana weissiana</i>	Atropina	SAm
<i>Nolana werdermannii</i>	Atropina	SAm
<i>Nolana willeana</i>	Atropina	SAm
<i>Nothoestrum latifolium</i>	Physaleae	OZ
<i>Nothoestrum longifolium</i>	Physaleae	OZ
<i>Oryctes nevadensis</i>	Physaleae	NAm
<i>Pantacantha ameghinoi</i>	Benthamielleae	SAm
<i>Petunia altiplana</i>	Petunieae	SAm
<i>Petunia axillaris</i>	Petunieae	SAm
<i>Petunia bonjardinensis</i>	Petunieae	SAm
<i>Petunia exserta</i>	Petunieae	SAm
<i>Petunia integrifolia</i>	Petunieae	SAm
<i>Petunia littoralis</i>	Petunieae	SAm

<i>Petunia mantiqueirensis</i>	Petunieae	SAm
<i>Petunia reitzii</i>	Petunieae	SAm
<i>Petunia saxicola</i>	Petunieae	SAm
<i>Petunia scheideana</i>	Petunieae	SAm
<i>Petunia secreta</i>	Petunieae	SAm
<i>Physalis acutifolia</i>	Physaleae	NAm
<i>Physalis alkekengi</i>	Physaleae	EU
<i>Physalis angulata</i>	Physaleae	NAm&SAm&CAm&Car
<i>Physalis angustifolia</i>	Physaleae	NAm
<i>Physalis angustiphysa</i>	Physaleae	NAm&CAm
<i>Physalis arborescens</i>	Physaleae	NAm
<i>Physalis arenicola</i>	Physaleae	NAm
<i>Physalis campanulata</i>	Physaleae	NAm
<i>Physalis carpenteri</i>	Physaleae	NAm
<i>Physalis caudella</i>	Physaleae	NAm
<i>Physalis cinerascens</i>	Physaleae	NAm
<i>Physalis cordata</i>	Physaleae	NAm&CAm&Car
<i>Physalis coztomatl</i>	Physaleae	NAm
<i>Physalis crassifolia</i>	Physaleae	NAm
<i>Physalis glutinosa</i>	Physaleae	NAm
<i>Physalis greenmanii</i>	Physaleae	NAm
<i>Physalis hederifolia</i>	Physaleae	NAm
<i>Physalis heterophylla</i>	Physaleae	NAm
<i>Physalis ignota</i>	Physaleae	CAm&Car
<i>Physalis lagascae</i>	Physaleae	NAm&SAm&CAm&Car
<i>Physalis lanceolata</i>	Physaleae	NAm
<i>Physalis lassa</i>	Physaleae	NAm&CAm
<i>Physalis longifolia</i>	Physaleae	NAm
<i>Physalis melanocystis</i>	Physaleae	NAm&CAm
<i>Physalis microcarpa</i>	Physaleae	NAm&CAm&Car
<i>Physalis microphysa</i>	Physaleae	NAm
<i>Physalis minima</i>	Physaleae	AF&EU
<i>Physalis minimaculata</i>	Physaleae	NAm
<i>Physalis mollis</i>	Physaleae	NAm
<i>Physalis nicandroides</i>	Physaleae	NAm&CAm
<i>Physalis patula</i>	Physaleae	NAm
<i>Physalis peruviana</i>	Physaleae	SAm
<i>Physalis philadelphica</i>	Physaleae	NAm
<i>Physalis pruinosa</i>	Physaleae	NAm&SAm&CAm
<i>Physalis pubescens</i>	Physaleae	NAm&SAm&CAm
<i>Physalis pumila</i>	Physaleae	NAm
<i>Physalis sordida</i>	Physaleae	NAm
<i>Physalis virginiana</i>	Physaleae	NAm

<i>Physalis viscosa</i>	Physaleae	NAm&SAm
<i>Physalis walteri</i>	Physaleae	NAm
<i>Physochlaina infundibularis</i>	Atropina	EU
<i>Physochlaina orientalis</i>	Atropina	EU
<i>Physochlaina physaloides</i>	Atropina	EU
<i>Physochlaina praealta</i>	Atropina	EU
<i>Plowmania nyctaginoides</i>	Petunieae	CAm
<i>Protoschwenkia mandonii</i>	Cestroidaeae	SAm
<i>Przewalskia tangutica</i>	Atropina	EU
<i>Quincula lobata</i>	Physaleae	NAm
<i>Reyesia sp</i>	Reyesia	SAm
<i>Salpichroa organifolia</i>	Salpichroina	SAm
<i>Salpiglossis sinuata</i>	Cestroidaeae	SAm
<i>Saracha punctata</i>	Physaleae	SAm
<i>Saracha quitensis</i>	Physaleae	SAm
<i>Schizanthus alpestris</i>	Schizanthus	SAm
<i>Schizanthus candidus</i>	Schizanthus	SAm
<i>Schizanthus grahamii</i>	Schizanthus	SAm
<i>Schizanthus hookeri</i>	Schizanthus	SAm
<i>Schizanthus integrifolius</i>	Schizanthus	SAm
<i>Schizanthus lacteus</i>	Schizanthus	SAm
<i>Schizanthus laetus</i>	Schizanthus	SAm
<i>Schizanthus litoralis</i>	Schizanthus	SAm
<i>Schizanthus parvulus</i>	Schizanthus	SAm
<i>Schizanthus pinnatus</i>	Schizanthus	SAm
<i>Schizanthus porrigens</i>	Schizanthus	SAm
<i>Schizanthus tricolor</i>	Schizanthus	SAm
<i>Schultesianthus leucanthus</i>	Juanulloaeae	CAm&SAm
<i>Schultesianthus megalandrus</i>	Juanulloaeae	SAm
<i>Schwenckia glabrata</i>	Schwenckieae	SAm
<i>Schwenckia lateriflora</i>	Schwenckieae	SAm&CAm
<i>Sclerophylax adnatifolia</i>	Atropina	SAm
<i>Sclerophylax gilliesii</i>	Atropina	SAm
<i>Sclerophylax sp</i>	Atropina	SAm
<i>Sclerophylax spinescens</i>	Atropina	SAm
<i>Scopolia carniolica</i>	Atropina	EU
<i>Scopolia japonica</i>	Atropina	EU
<i>Scopolia lutescens</i>	Atropina	EU
<i>Scopolia parviflora</i>	Atropina	EU
<i>Sessea corymbiflora</i>	Cestroidaeae	SAm
<i>Sessea stipulata</i>	Cestroidaeae	SAm
<i>Sessea vestita</i>	Cestroidaeae	SAm
<i>Solandra brachycalyx</i>	Juanulloaeae	CAm

<i>Solanandra grandiflora</i>	Juanulloaeae	CAm&Car
<i>Solanum absconditum</i>	Solaneae	SAm
<i>Solanum abutiloides</i>	Solaneae	SAm
<i>Solanum acanthodapis</i>	Solaneae	OZ
<i>Solanum acaule</i>	Solaneae	SAm
<i>Solanum accrescens</i>	Solaneae	CAm&SAm
<i>Solanum acerifolium</i>	Solaneae	NAm&SAm&CAm
<i>Solanum achacachense</i>	Solaneae	SAm
<i>Solanum acroscopicum</i>	Solaneae	SAm
<i>Solanum aculeastrum</i>	Solaneae	AF
<i>Solanum aculeatissimum</i>	Solaneae	SAm
<i>Solanum acutilobum</i>	Solaneae	SAm
<i>Solanum volubile</i>	Solaneae	NAm&SAm&CAm&Car
<i>Solanum adscendens</i>	Solaneae	SAm
<i>Solanum aethiopicum</i>	Solaneae	AF
<i>Solanum agrarium</i>	Solaneae	SAm&Car
<i>Solanum agrimonifolium</i>	Solaneae	NAm&CAm
<i>Solanum alandiae</i>	Solaneae	SAm
<i>Solanum albicans</i>	Solaneae	SAm
<i>Solanum albidum</i>	Solaneae	SAm
<i>Solanum aligerum</i>	Solaneae	NAm&SAm&CAm
<i>Solanum allophyllum</i>	Solaneae	SAm&CAm
<i>Solanum amblymerum</i>	Solaneae	OZ
<i>Solanum americanum</i>	Solaneae	NAm&Car&SAm&CAm
<i>Solanum amygdalifolium</i>	Solaneae	SAm
<i>Solanum anceps</i>	Solaneae	SAm
<i>Solanum andreanum</i>	Solaneae	SAm
<i>Solanum anguivi</i>	Solaneae	AF
<i>Solanum angustialatum</i>	Solaneae	SAm
<i>Solanum angustifolium</i>	Solaneae	NAm
<i>Solanum annuum</i>	Solaneae	SAm
<i>Solanum aphyodendron</i>	Solaneae	SAm&CAm&NAm
<i>Solanum appendiculatum</i>	Solaneae	NAm&CAm
<i>Solanum arachnidanthum</i>	Solaneae	SAm
<i>Solanum arboreum</i>	Solaneae	SAm&CAm
<i>Solanum argentinum</i>	Solaneae	SAm
<i>Solanum argopetalum</i>	Solaneae	OZ
<i>Solanum arnezii</i>	Solaneae	SAm
<i>Solanum arundo</i>	Solaneae	AF
<i>Solanum asperolanatum</i>	Solaneae	SAm
<i>Solanum asperum</i>	Solaneae	SAm&CAm
<i>Solanum asterophorum</i>	Solaneae	SAm
<i>Solanum asteropilodes</i>	Solaneae	SAm

<i>Solanum asymmetriphyllum</i>	Solaneae	OZ
<i>Solanum atropurpureum</i>	Solaneae	SAm
<i>Solanum aturense</i>	Solaneae	SAm
<i>Solanum aviculare</i>	Solaneae	OZ
<i>Solanum avilesii</i>	Solaneae	SAm
<i>Solanum bahamense</i>	Solaneae	NAm&Car
<i>Solanum batoides</i>	Solaneae	AF
<i>Solanum beaugleholei</i>	Solaneae	OZ
<i>Solanum berthaultii</i>	Solaneae	SAm
<i>Solanum betaceum</i>	Solaneae	SAm
<i>Solanum bicornis</i>	Solaneae	NAm
<i>Solanum bolivianum</i>	Solaneae	SAm
<i>Solanum bonariense</i>	Solaneae	SAm
<i>Solanum brevicaule</i>	Solaneae	SAm
<i>Solanum brevifolium</i>	Solaneae	SAm
<i>Solanum brownii</i>	Solaneae	OZ
<i>Solanum buddleifolium</i>	Solaneae	SAm
<i>Solanum bulbocastanum</i>	Solaneae	NAm
<i>Solanum bumeliifolium</i>	Solaneae	AF
<i>Solanum cacosmum</i>	Solaneae	SAm
<i>Solanum caesium</i>	Solaneae	SAm
<i>Solanum cajanumense</i>	Solaneae	SAm
<i>Solanum calileguae</i>	Solaneae	SAm
<i>Solanum CAMpanulatum</i>	Solaneae	OZ
<i>Solanum CAMpylacanthum</i>	Solaneae	AF
<i>Solanum candidum</i>	Solaneae	SAm&CAm
<i>Solanum candolleianum</i>	Solaneae	SAm
<i>Solanum capense</i>	Solaneae	AF
<i>Solanum capsiciforme</i>	Solaneae	OZ
<i>Solanum capsicoides</i>	Solaneae	SAm
<i>Solanum cardiophyllum</i>	Solaneae	NAm
<i>Solanum carduiforme</i>	Solaneae	OZ
<i>Solanum caricifolium</i>	Solaneae	SAm
<i>Solanum caripense</i>	Solaneae	SAm&CAm
<i>Solanum carolinense</i>	Solaneae	NAm
<i>Solanum cataphractum</i>	Solaneae	OZ
<i>Solanum centrale</i>	Solaneae	OZ
<i>Solanum cerasiferum</i>	Solaneae	AF
<i>Solanum chacoense</i>	Solaneae	SAm
<i>Solanum chamaepolybotryon</i>	Solaneae	SAm
<i>Solanum cheesmaniae</i>	Solaneae	SAm
<i>Solanum chenopodium</i>	Solaneae	OZ
<i>Solanum chenopodium</i>	Solaneae	OZ

<i>Solanum chilense</i>	Solaneae	SAm
<i>Solanum chippendalei</i>	Solaneae	OZ
<i>Solanum chmielewskii</i>	Solaneae	SAm
<i>Solanum chomatophilum</i>	Solaneae	SAm
<i>Solanum chrysotrichum</i>	Solaneae	NAm&CAm&SAm
<i>Solanum cinereum</i>	Solaneae	OZ
<i>Solanum stipuloideum</i>	Solaneae	SAm
<i>Solanum circinatum</i>	Solaneae	SAm&CAm
<i>Solanum citrullifolium</i>	Solaneae	NAm
<i>Solanum clandestinum</i>	Solaneae	SAm
<i>Solanum clarkiae</i>	Solaneae	OZ
<i>Solanum clarum</i>	Solaneae	NAm&CAm
<i>Solanum cleistogamum</i>	Solaneae	OZ
<i>Solanum coactiliferum</i>	Solaneae	OZ
<i>Solanum colombianum</i>	Solaneae	SAm
<i>Solanum comarapanum</i>	Solaneae	SAm
<i>Solanum comptum</i>	Solaneae	SAm
<i>Solanum conditum</i>	Solaneae	SAm
<i>Solanum confusum</i>	Solaneae	SAm
<i>Solanum conicum</i>	Solaneae	SAm
<i>Solanum cookii</i>	Solaneae	OZ
<i>Solanum cordovense</i>	Solaneae	NAm&CAm&SAm
<i>Solanum coriaceum</i>	Solaneae	SAm
<i>Solanum corifolium</i>	Solaneae	OZ
<i>Solanum crinitipes</i>	Solaneae	SAm
<i>Solanum crinitum</i>	Solaneae	SAm
<i>Solanum crispum</i>	Solaneae	SAm
<i>Solanum crotonoides</i>	Solaneae	Car
<i>Solanum insanum</i>	Solaneae	EU
<i>Solanum cunninghamii</i>	Solaneae	OZ
<i>Solanum curvicaepe</i>	Solaneae	OZ
<i>Solanum cyaneopurpureum</i>	Solaneae	AF
<i>Solanum cylindricum</i>	Solaneae	SAm
<i>Solanum dasyphyllum</i>	Solaneae	AF
<i>Solanum davisense</i>	Solaneae	NAm
<i>Solanum decompositiflorum</i>	Solaneae	SAm
<i>Solanum delitescens</i>	Solaneae	SAm
<i>Solanum demissum</i>	Solaneae	NAm&CAm
<i>Solanum densevestitum</i>	Solaneae	OZ
<i>Solanum dianthophorum</i>	Solaneae	OZ
<i>Solanum dimorphispinum</i>	Solaneae	OZ
<i>Solanum dioicum</i>	Solaneae	OZ
<i>Solanum diphyllum</i>	Solaneae	NAm&CAm

<i>Solanum diploconos</i>	Solaneae	SAm
<i>Solanum discolor</i>	Solaneae	OZ
<i>Solanum dissectum</i>	Solaneae	OZ
<i>Solanum ditrichum</i>	Solaneae	OZ
<i>Solanum diversiflorum</i>	Solaneae	OZ
<i>Solanum doddsii</i>	Solaneae	SAm
<i>Solanum donianum</i>	Solaneae	NAm&CAm&Car
<i>Solanum ensifolium</i>	Solaneae	Car
<i>Solanum dulCAMara</i>	Solaneae	EU&AF
<i>Solanum echinatum</i>	Solaneae	OZ
<i>Solanum ehrenbergii</i>	Solaneae	NAm
<i>Solanum elachophyllum</i>	Solaneae	OZ
<i>Solanum elaeagnifolium</i>	Solaneae	NAm&SAm
<i>Solanum ellipticum</i>	Solaneae	OZ
<i>Solanum enantiophyllum</i>	Solaneae	SAm
<i>Solanum endopogon</i>	Solaneae	SAm
<i>Solanum esuriale</i>	Solaneae	OZ
<i>Solanum etuberosum</i>	Solaneae	SAm
<i>Solanum evolulifolium</i>	Solaneae	SAm&CAm
<i>Solanum exiguum</i>	Solaneae	SAm
<i>Solanum fallax</i>	Solaneae	SAm
<i>Solanum felinum</i>	Solaneae	SAm
<i>Solanum ferocissimum</i>	Solaneae	OZ
<i>Solanum fiebrigii</i>	Solaneae	SAm
<i>Solanum fraxinifolium</i>	Solaneae	SAm&CAm
<i>Solanum fructotecto</i>	Solaneae	NAm
<i>Solanum furfuraceum</i>	Solaneae	OZ
<i>Solanum fusiforme</i>	Solaneae	SAm
<i>Solanum gabriellae</i>	Solaneae	OZ
<i>Solanum galapagense</i>	Solaneae	SAm
<i>Solanum gardneri</i>	Solaneae	SAm
<i>Solanum giganteum</i>	Solaneae	AF&EU
<i>Solanum glabratum</i>	Solaneae	AF&EU
<i>Solanum glaucophyllum</i>	Solaneae	SAm
<i>Solanum glutinosum</i>	Solaneae	SAm
<i>Solanum goetzei</i>	Solaneae	AF
<i>Solanum grayi</i>	Solaneae	NAm
<i>Solanum guerreroense</i>	Solaneae	NAm
<i>Solanum guineense</i>	Solaneae	AF
<i>Solanum gympiense</i>	Solaneae	OZ
<i>Solanum habrochaites</i>	Solaneae	SAm
<i>Solanum hapalum</i>	Solaneae	OZ
<i>Solanum hasslerianum</i>	Solaneae	SAm

<i>Solanum havanense</i>	Solaneae	Car
<i>Solanum hayesii</i>	Solaneae	SAm&CAm
<i>Solanum heinianum</i>	Solaneae	AF
<i>Solanum herculeum</i>	Solaneae	EU&AF
<i>Solanum heterodoxum</i>	Solaneae	NAm
<i>Solanum heteropodium</i>	Solaneae	OZ
<i>Solanum hexandrum</i>	Solaneae	SAm
<i>Solanum hibernum</i>	Solaneae	SAm
<i>Solanum hieronymi</i>	Solaneae	SAm
<i>Solanum hindsianum</i>	Solaneae	NAm
<i>Solanum hirtum</i>	Solaneae	SAm&CAm
<i>Solanum hjertingii</i>	Solaneae	NAm
<i>Solanum hoehnei</i>	Solaneae	SAm
<i>Solanum hoplopetalum</i>	Solaneae	OZ
<i>Solanum horridum</i>	Solaneae	OZ
<i>Solanum hougasii</i>	Solaneae	NAm
<i>Solanum humile</i>	Solaneae	AF
<i>Solanum hyporhodium</i>	Solaneae	SAm
<i>Solanum hystrix</i>	Solaneae	OZ
<i>Solanum immite</i>	Solaneae	SAm
<i>Solanum inaequilaterum</i>	Solaneae	OZ
<i>Solanum inCAMayoense</i>	Solaneae	SAm
<i>Solanum incanum</i>	Solaneae	AF&EU
<i>Solanum incarceratum</i>	Solaneae	SAm
<i>Solanum incompletum</i>	Solaneae	OZ
<i>Solanum incurvum</i>	Solaneae	SAm
<i>Solanum inelegans</i>	Solaneae	SAm
<i>Solanum infundibuliforme</i>	Solaneae	SAm
<i>Solanum innoxium</i>	Solaneae	OZ
<i>Solanum iopetalum</i>	Solaneae	NAm
<i>Solanum jabrense</i>	Solaneae	SAm
<i>Solanum jamaicense</i>	Solaneae	NAm&Car&SAm&CAm
<i>Solanum jamesii</i>	Solaneae	NAm
<i>Solanum johnsonianum</i>	Solaneae	OZ
<i>Solanum johnstonii</i>	Solaneae	NAm
<i>Solanum jucundum</i>	Solaneae	OZ
<i>Solanum juglandifolium</i>	Solaneae	SAm
<i>Solanum juvenale</i>	Solaneae	SAm
<i>Solanum kurtzianum</i>	Solaneae	SAm
<i>Solanum tettense</i>	Solaneae	AF
<i>Solanum laciniatum</i>	Solaneae	OZ
<i>Solanum lamprocarpum</i>	Solaneae	AF
<i>Solanum lanceifolium</i>	Solaneae	NAm&SAm&CAm&Car

<i>Solanum lanceolatum</i>	Solaneae	NAm&CAm
<i>Solanum lasiocarpum</i>	Solaneae	EU
<i>Solanum lasiophyllum</i>	Solaneae	OZ
<i>Solanum latens</i>	Solaneae	OZ
<i>Solanum latiflorum</i>	Solaneae	SAm
<i>Solanum laxissimum</i>	Solaneae	SAm
<i>Solanum laxum</i>	Solaneae	SAm
<i>Solanum leopoldense</i>	Solaneae	OZ
<i>Solanum lepidotum</i>	Solaneae	SAm&CAm
<i>Solanum leptophyes</i>	Solaneae	SAm
<i>Solanum lichtensteinii</i>	Solaneae	AF
<i>Solanum lidii</i>	Solaneae	AF
<i>Solanum lignicaule</i>	Solaneae	SAm
<i>Solanum limitare</i>	Solaneae	OZ
<i>Solanum linearifolium</i>	Solaneae	OZ
<i>Solanum linnaeanum</i>	Solaneae	AF
<i>Solanum longiconicum</i>	Solaneae	CAm
<i>Solanum lucani</i>	Solaneae	OZ
<i>Solanum lumholtzianum</i>	Solaneae	NAm
<i>Solanum luteoalbum</i>	Solaneae	SAm
<i>Solanum lycocarpum</i>	Solaneae	SAm
<i>Solanum lycopersicoides</i>	Solaneae	SAm
<i>Solanum lyratum</i>	Solaneae	EU
<i>Solanum lythrocarpum</i>	Solaneae	OZ
<i>Solanum macoorai</i>	Solaneae	OZ
<i>Solanum macrocarpon</i>	Solaneae	AF
<i>Solanum maglia</i>	Solaneae	SAm
<i>Solanum mahoriense</i>	Solaneae	AF
<i>Solanum mapiriense</i>	Solaneae	SAm
<i>Solanum marginatum</i>	Solaneae	AF
<i>Solanum maternum</i>	Solaneae	SAm
<i>Solanum mauritanum</i>	Solaneae	SAm
<i>Solanum megalonyx</i>	Solaneae	SAm
<i>Solanum boliviense</i>	Solaneae	SAm
<i>Solanum melanospermum</i>	Solaneae	OZ
<i>Solanum melissarum</i>	Solaneae	SAm
<i>Solanum microdontum</i>	Solaneae	SAm
<i>Solanum microphyllum</i>	Solaneae	Car
<i>Solanum mitchellianum</i>	Solaneae	OZ
<i>Solanum mite</i>	Solaneae	SAm
<i>Solanum mitlense</i>	Solaneae	NAm
<i>Solanum monachophyllum</i>	Solaneae	SAm
<i>Solanum monarchostemon</i>	Solaneae	SAm

<i>Solanum montanum</i>	Solaneae	SAm
<i>Solanum morelliforme</i>	Solaneae	NAm&CAm&SAm
<i>Solanum mortonii</i>	Solaneae	SAm
<i>Solanum moscopanum</i>	Solaneae	SAm
<i>Solanum moxosense</i>	Solaneae	SAm
<i>Solanum multifidum</i>	Solaneae	SAm
<i>Solanum multiinterruptum</i>	Solaneae	SAm
<i>Solanum multispinum</i>	Solaneae	SAm
<i>Solanum multivenosum</i>	Solaneae	OZ
<i>Solanum muricatum</i>	Solaneae	SAm
<i>Solanum myoxotrichum</i>	Solaneae	AF
<i>Solanum myriacanthum</i>	Solaneae	NAm&CAm
<i>Solanum nemophilum</i>	Solaneae	OZ
<i>Solanum nemorense</i>	Solaneae	SAm
<i>Solanum neoanglicum</i>	Solaneae	OZ
<i>Solanum neorickii</i>	Solaneae	SAm
<i>Solanum nigriviolaecum</i>	Solaneae	AF
<i>Solanum nigrum</i>	Solaneae	EU&AF
<i>Solanum nitidum</i>	Solaneae	SAm
<i>Solanum nobile</i>	Solaneae	OZ
<i>Solanum nummularium</i>	Solaneae	OZ
<i>Solanum obliquum</i>	Solaneae	SAm
<i>Solanum occultum</i>	Solaneae	SAm
<i>Solanum ochranthum</i>	Solaneae	SAm
<i>Solanum ochrophyllum</i>	Solaneae	SAm
<i>Solanum oedipus</i>	Solaneae	OZ
<i>Solanum okadae</i>	Solaneae	SAm
<i>Solanum oldfieldii</i>	Solaneae	OZ
<i>Solanum oligacanthum</i>	Solaneae	OZ
<i>Solanum opacum</i>	Solaneae	OZ
<i>Solanum oplocense</i>	Solaneae	SAm
<i>Solanum orbiculatum</i>	Solaneae	OZ
<i>Solanum oxycarpum</i>	Solaneae	NAm
<i>Solanum oxyphyllum</i>	Solaneae	SAm
<i>Solanum palinacanthum</i>	Solaneae	SAm
<i>Solanum palitans</i>	Solaneae	SAm
<i>Solanum pallidum</i>	Solaneae	SAm
<i>Solanum paludosum</i>	Solaneae	SAm
<i>Solanum palustre</i>	Solaneae	SAm
<i>Solanum pampasense</i>	Solaneae	SAm
<i>Solanum pancheri</i>	Solaneae	OZ
<i>Solanum paniculatum</i>	Solaneae	SAm
<i>Solanum papaverifolium</i>	Solaneae	OZ

<i>Solanum paposanum</i>	Solaneae	SAm
<i>Solanum paraibanum</i>	Solaneae	SAm
<i>Solanum pascoense</i>	Solaneae	SAm
<i>Solanum pectinatum</i>	Solaneae	SAm&CAm
<i>Solanum pedemontanum</i>	Solaneae	SAm
<i>Solanum pendulum</i>	Solaneae	SAm
<i>Solanum pennellii</i>	Solaneae	SAm
<i>Solanum peruvianum</i>	Solaneae	SAm
<i>Solanum petraeum</i>	Solaneae	OZ
<i>Solanum petrophilum</i>	Solaneae	OZ
<i>Solanum phaseoloides</i>	Solaneae	CAm&SAm
<i>Solanum phlomoides</i>	Solaneae	OZ
<i>Solanum physalifolium</i>	Solaneae	SAm
<i>Solanum pimpinellifolium</i>	Solaneae	SAm
<i>Solanum pinetorum</i>	Solaneae	SAm
<i>Solanum pinnatisectum</i>	Solaneae	NAm
<i>Solanum piurae</i>	Solaneae	SAm
<i>Solanum platense</i>	Solaneae	SAm
<i>Solanum pluviale</i>	Solaneae	CAm
<i>Solanum poinsettifolium</i>	Solaneae	SAm
<i>Solanum polyadenium</i>	Solaneae	NAm
<i>Solanum polytrichum</i>	Solaneae	SAm
<i>Solanum prinophyllum</i>	Solaneae	OZ
<i>Solanum proteanthum</i>	Solaneae	SAm
<i>Solanum pseudolulo</i>	Solaneae	SAm
<i>Solanum ptychanthum</i>	Solaneae	NAm
<i>Solanum pubigerum</i>	Solaneae	NAm&CAm
<i>Solanum pungetium</i>	Solaneae	OZ
<i>Solanum pyracanthos</i>	Solaneae	AF
<i>Solanum africanum</i>	Solaneae	AF
<i>Solanum quadriloculatum</i>	Solaneae	OZ
<i>Solanum quitoense</i>	Solaneae	SAm
<i>Solanum raphanifolium</i>	Solaneae	SAm
<i>Solanum reductum</i>	Solaneae	SAm
<i>Solanum reflexiflorum</i>	Solaneae	SAm
<i>Solanum refractum</i>	Solaneae	NAm
<i>Solanum repandum</i>	Solaneae	OZ
<i>Solanum reptans</i>	Solaneae	SAm
<i>Solanum retroflexum</i>	Solaneae	AF
<i>Solanum rhytidoandrum</i>	Solaneae	SAm
<i>Solanum riojense</i>	Solaneae	SAm
<i>Solanum rioxosum</i>	Solaneae	OZ
<i>Solanum robustum</i>	Solaneae	SAm

<i>Solanum roseum</i>	Solaneae	SAm
<i>Solanum rostratum</i>	Solaneae	NAm
<i>Solanum rovirosanum</i>	Solaneae	CAM&NAm
<i>Solanum rudepannum</i>	Solaneae	NAm&CAm
<i>Solanum rugosum</i>	Solaneae	SAm&CAm
<i>Solanum rupincola</i>	Solaneae	SAm
<i>Solanum sandwicense</i>	Solaneae	OZ
<i>Solanum santolallae</i>	Solaneae	SAm
<i>Solanum savanillense</i>	Solaneae	SAm
<i>Solanum scabrifolium</i>	Solaneae	SAm
<i>Solanum scabrum</i>	Solaneae	AF
<i>Solanum schenckii</i>	Solaneae	NAm
<i>Solanum schimperianum</i>	Solaneae	AF
<i>Solanum schlechtendalianum</i>	Solaneae	SAm&CAm
<i>Solanum schomburgkii</i>	Solaneae	SAm
<i>Solanum sciadostylis</i>	Solaneae	SAm
<i>Solanum sejunctum</i>	Solaneae	OZ
<i>Solanum semiarmatum</i>	Solaneae	OZ
<i>Solanum sendtnerianum</i>	Solaneae	SAm
<i>Solanum serpens</i>	Solaneae	OZ
<i>Solanum sessiliflorum</i>	Solaneae	SAm
<i>Solanum shirleyanum</i>	Solaneae	OZ
<i>Solanum sibundoyense</i>	Solaneae	SAm
<i>Solanum simile</i>	Solaneae	OZ
<i>Solanum sisymbriifolium</i>	Solaneae	SAm
<i>Solanum sitiens</i>	Solaneae	SAm
<i>Solanum sparsipilum</i>	Solaneae	SAm
<i>Solanum spegazzinii</i>	Solaneae	SAm
<i>Solanum stagnale</i>	Solaneae	SAm
<i>Solanum stellatovelutinum</i>	Solaneae	SAm
<i>Solanum stelligerum</i>	Solaneae	OZ
<i>Solanum stenandrum</i>	Solaneae	SAm
<i>Solanum stenophyllidium</i>	Solaneae	NAm
<i>Solanum stenopterum</i>	Solaneae	OZ
<i>Solanum stoloniferum</i>	Solaneae	NAm
<i>Solanum stramonifolium</i>	Solaneae	SAm&CAm&Car
<i>Solanum stuckertii</i>	Solaneae	SAm
<i>Solanum stupefactum</i>	Solaneae	OZ
<i>Solanum sturtianum</i>	Solaneae	OZ
<i>Solanum subinerme</i>	Solaneae	SAm
<i>Solanum subpanduratum</i>	Solaneae	SAm
<i>Solanum sucrense</i>	Solaneae	SAm
<i>Solanum supinum</i>	Solaneae	AF

<i>Solanum symonii</i>	Solaneae	OZ
<i>Solanum taeniotrichum</i>	Solaneae	CAM
<i>Solanum talarense</i>	Solaneae	SAm
<i>Solanum tampicense</i>	Solaneae	NAm&CAm&SAm&Car
<i>Solanum tarijense</i>	Solaneae	SAm
<i>Solanum tegore</i>	Solaneae	SAm
<i>Solanum tenuipes</i>	Solaneae	NAm
<i>Solanum tenuisetosum</i>	Solaneae	SAm
<i>Solanum tenuispinum</i>	Solaneae	SAm
<i>Solanum terminale</i>	Solaneae	AF
<i>Solanum ternatum</i>	Solaneae	SAm
<i>Solanum tetramerum</i>	Solaneae	Car
<i>Solanum tetrahectum</i>	Solaneae	OZ
<i>Solanum thelopodium</i>	Solaneae	SAm
<i>Solanum thomasiifolium</i>	Solaneae	SAm
<i>Solanum coagulans</i>	Solaneae	AF
<i>Solanum tobagense</i>	Solaneae	SAm
<i>Solanum toliaraea</i>	Solaneae	AF
<i>Solanum tomentosum</i>	Solaneae	AF
<i>Solanum torvum</i>	Solaneae	SAm&CAm&Car
<i>Solanum furcatum</i>	Solaneae	SAm
<i>Solanum tribulosum</i>	Solaneae	NAm
<i>Solanum houstonii</i>	Solaneae	NAm
<i>Solanum triflorum</i>	Solaneae	NAm&SAm
<i>Solanum tripartitum</i>	Solaneae	SAm
<i>Solanum trisectum</i>	Solaneae	AF
<i>Solanum tudununggae</i>	Solaneae	OZ
<i>Solanum turneroides</i>	Solaneae	SAm
<i>Solanum ugentii</i>	Solaneae	SAm
<i>Solanum uncinellum</i>	Solaneae	SAm
<i>Solanum unilobum</i>	Solaneae	SAm
<i>Solanum ursinum</i>	Solaneae	SAm
<i>Solanum urticans</i>	Solaneae	SAm
<i>Solanum vaccinioides</i>	Solaneae	OZ
<i>Solanum valdiviense</i>	Solaneae	SAm
<i>Solanum vansittartense</i>	Solaneae	OZ
<i>Solanum vernei</i>	Solaneae	SAm
<i>Solanum verrucosum</i>	Solaneae	NAm
<i>Solanum vescum</i>	Solaneae	OZ
<i>Solanum vespertilio</i>	Solaneae	AF
<i>Solanum vestissimum</i>	Solaneae	SAm
<i>Solanum viarum</i>	Solaneae	SAm
<i>Solanum vicinum</i>	Solaneae	OZ

<i>Solanum villosum</i>	Solaneae	AF&EU
<i>Solanum</i>	Solaneae	SAm
<i>Solanum violaceum</i>	Solaneae	EU
<i>Solanum viridifolium</i>	Solaneae	OZ
<i>Solanum wallacei</i>	Solaneae	NAm
<i>Solanum wendlandii</i>	Solaneae	CAm&NAm
<i>Solanum whalenii</i>	Solaneae	SAm
<i>Solanum wrightii</i>	Solaneae	SAm
<i>Solanum yungasense</i>	Solaneae	SAm
<i>Streptosolen jamesonii</i>	Cestroideae	SAm
<i>Symonanthus aromaticus</i>	Nicotianoideae	OZ
<i>Symonanthus bancroftii</i>	Nicotianoideae	OZ
<i>Trianaea sp</i>	Juanulloeae	SAm
<i>Trianaea speciosa</i>	Juanulloeae	SAm
<i>Tsoala tubiflora</i>	Goetzeoideae	AF
<i>Tzeltalia amphitricha</i>	Physaleae	NAm&CAm
<i>Tzeltalia calidaria</i>	Physaleae	CAm
<i>Vassobia breviflora</i>	Physaleae	SAm
<i>Vassobia dichotoma</i>	Physaleae	SAm
<i>Vestia foetida</i>	Cestroideae	SAm
<i>Withania coagulans</i>	Physaleae	EU
<i>Withania somnifera</i>	Physaleae	AF&EU
<i>Witheringia cuneata</i>	Physaleae	CAm
<i>Witheringia macrantha</i>	Physaleae	CAm
<i>Witheringia meiantha</i>	Physaleae	CAm
<i>Witheringia solanacea</i>	Physaleae	CAm&Car&SAm

Table S1.3. Biogeographical models tested in this study, along with estimated parameters, log-likelihoods and AIC values. Models were classified according to the number of free parameters and whether the input dispersal multiplier matrices included time-stratified (TS) probabilities of dispersal between areas. Model suitability was examined using AIC comparisons. Model 16 (in bold italics) is the best model and the estimated parameters under that model were used for the Biogeographical Stochastic Mappings. Default values for j and w when they were not free are 0 and 1, respectively. $j = 0$ means founder-events were not allowed, while $w = 1$ means the dispersal multiplier matrices have an exponent of 1.

#	Models	Dispersal multipliers	Free parameters					Log-Likelihood	AIC	Δ AIC	AIC weights
			Number	$d^{(1)}$	$e^{(2)}$	$j^{(3)}$	$w^{(4)}$				
Basic Models											
1	DEC_NonTS	Non-TS	2	0.011	0.000	0.000	1.000	-1341.413	2686.826	317.604	0.000
2	DIVALIKE_NonTS	Non-TS	2	0.013	0.000	0.000	1.000	-1401.936	2807.871	438.648	0.000
3	BayAreaLIKE_NonTS	Non-TS	2	0.009	0.049	0.000	1.000	-1528.828	3061.656	692.433	0.000
Time-Stratified Models											
4	DEC_TS	TS	2	0.025	0.000	0.000	1.000	-1210.832	2425.663	56.441	0.000
5	DIVALIKE_TS	TS	2	0.029	0.000	0.000	1.000	-1252.831	2509.661	140.438	0.000
6	BayAreaLIKE_TS	TS	2	0.023	0.044	0.000	1.000	-1430.614	2865.227	496.004	0.000
+j Models											
7	DEC_NonTS_ j	Non-TS	3	0.010	0.000	0.003	1.000	-1324.525	2655.050	285.828	0.000
8	DIVALIKE_NonTS_ j	Non-TS	3	0.011	0.000	0.003	1.000	-1387.768	2781.536	412.313	0.000
9	BayAreaLIKE_NonTS_ j	Non-TS	3	0.007	0.004	0.009	1.000	-1335.728	2677.457	308.234	0.000
10	DEC_TS_ j	TS	3	0.022	0.000	0.008	1.000	-1191.907	2389.813	20.590	0.000
11	DIVALIKE_TS_ j	TS	3	0.025	0.000	0.007	1.000	-1239.123	2484.246	115.024	0.000
12	BayAreaLIKE_TS_ j	TS	3	0.015	0.001	0.020	1.000	-1213.992	2433.984	64.762	0.000
+w Models											
13	DEC_TS_ w	TS	3	0.026	0.000	0.000	1.114	-1204.980	2415.960	46.738	0.000
14	DIVALIKE_TS_ w	TS	3	0.032	0.000	0.000	1.201	-1250.615	2507.231	138.008	0.000
15	BayAreaLIKE_TS_ w	TS	3	0.026	0.045	0.000	1.307	-1425.518	2857.036	487.813	0.000
+j +w Models											
16	<i>DEC_TS_j_w</i>	<i>TS</i>	<i>4</i>	<i>0.029</i>	<i>0.000</i>	<i>0.009</i>	<i>1.887</i>	<i>-1180.611</i>	<i>2369.223</i>	<i>0.000</i>	<i>0.999</i>
17	DIVALIKE_TS_ j_w	TS	4	0.027	0.000	0.007	1.344	-1221.864	2451.729	82.506	0.000
18	BayAreaLIKE_TS_ j_w	TS	4	0.016	0.001	0.021	1.117	-1210.247	2428.494	59.271	0.000

- (1) rate of range expansion
- (2) rate of range contraction
- (3) relative per-event weight of jump dispersal
- (4) exponent on manual dispersal multipliers (modifies d and j)

Table S1.4. Species richness, within-area speciation events, and dispersal events estimated for each of the seven delimited areas. The mean numbers of events were calculated from the 100 stochastic maps. Areas are ranked from highest to lowest numbers of species per area in the phylogeny. The number of species within each area in the phylogeny and in the entire family are given for comparison. *The number of species in each area is a rough approximation based on expert opinion, existing floristic treatments, and monographs. The raw species counts underlying this estimate is available from the authors upon request.

Area	Overall number of species per area in the family; proportion of total*	Number of species per area in the phylogeny; proportion of total in the phylogeny	Mean within-area speciation events / Events per species in the phylogeny / Proportion of total within-area events estimated	Mean dispersal events from the area / Events per species in the phylogeny / Proportion of total dispersal events estimated
South America	1624; 63.5%	584; 55.9 %	529.3 / 0.90 / 60.2%	119.7 / 0.20 / 47%
North America	208; 8.1%	186; 17.8 %	98.2 / 0.53 / 11.1%	53.21 / 0.29 / 20%
Australia	240; 9.4%	145; 13.9 %	133.1 / 0.92 / 15.1%	2.53 / 0.02 / 1%
Central America	315; 12.3%	126; 12.1 %	17.6 / 0.14 / 2.0%	45.62 / 0.32 / 18%
Africa	143; 5.6%	79; 7.6 %	59.5 / 0.75 / 6.8%	14.31 / 0.18 / 6%
Eurasia	119; 4.7%	56; 5.4 %	33.8 / 0.60 / 3.8%	11.51 / 0.34 / 4%
Caribbean	99; 3.9%	45; 4.3 %	8.8 / 0.20 / 0.9%	8.97 / 0.20 / 4%

Table S1.5. Vicariant events estimated from BSM. In ‘BioGeoBEARS’, vicariance events involve the split of an ancestral range comprising two or more regions into descendant ranges that are subsets of the ancestral range (Appendix S2). The mean number of each type of event (row in the table) and standard deviation was computed from the 100 stochastic maps.

Ancestral range	Daughter species ranges	Mean number of events (StDev)
South America+North America	South America; North America	10.94 (2.81)
South America+Central America+North America	South America; Central America+North America	4.62 (1.28)
South America+Central America	South America; Central America	4.45(1.04)
South America+Caribbean	South America; Caribbean	2.89 (0.57)
South America+Africa	South America; Africa	2.01(1.32)
South America+Australia	South America; Australia	1.69 (0.46)
Central America+North America	Central America; North America	1.64 (1.02)
Africa+Eurasia	Africa; Eurasia	1.56 (1.44)
North America+Eurasia	North America; Eurasia	1.41 (1.94)
South America+Africa+Australia	South America +Australia; Africa	1.2 (2.88)
South America+Eurasia	South America; Eurasia	1.17 (2.56)
Africa+Australia	Africa; Australia	1 (4.22)

Table S1.6. Transoceanic dispersals in Solanaceae from New World to Old World inferred from BSM. These events happened either within the clade or along its ancestral branch. See Fig. 3 (orange branches and nodes) and Appendix S2 for full ancestral state reconstruction.

Clade	Number of transoceanic dispersals
Anthocercidae	1
Hyoscyameae	1
<i>Lycianthes</i>	1
<i>Lycium</i>	2
<i>Mandragora</i>	1
<i>Physalis</i>	2
<i>Solanum</i>	8
<i>Tsoala</i>	1
Withaninae	1
Others	2
TOTAL	20

Table S1.7. Solanaceae species that presented range expansions, description of the major terrestrial ecoregions of the areas they occupy today, and their fruit type (dry or fleshy according to Knapp, 2002). Ecoregions retrieved from the World Wildlife Foundation database, <http://www.worldwildlife.org/>. Solanaceae are found in three of the six ecoregions: tropical dry (deserts, shrublands, grasslands), tropical wet, and temperate (including Mediterranean); they are not found in boreal forests, tundra, or mangroves. The species listed below represent 5% (14 of 263) of the total of species with dry fruits in the tree and 14% (109 of 803) of the species with fleshy fruits (i.e., berries, drupes, or pyrenes) in the tree.

Species	Distribution	Ecoregion	Fruit type
<i>Acnistus arborescens</i>	SAm&CAm&Car	Tropical Dry	Fleshy
<i>Bouchetia erecta</i>	NAm&CAm	Tropical Dry	Dry
<i>Brachistus stramonifolius</i>	NAm&CAm	Tropical Wet	Fleshy
<i>Browallia eludens</i>	NAm&CAm	Tropical Dry	Dry
<i>Browallia speciosa</i>	SAm&CAm	Tropical Wet	Dry
<i>Calibrachoa parviflora</i>	SAm&NAm	Tropical Dry	Dry
<i>Capsicum chinense</i>	SAm&CAm	Tropical Wet	Fleshy
<i>Capsicum ciliatum</i>	NAm&SAm&CAm	Tropical Wet	Fleshy
<i>Capsicum frutescens</i>	NAm&SAm&CAm	Tropical Wet	Fleshy
<i>Capsicum lanceolatum</i>	NAm&CAm	Tropical Wet	Fleshy
<i>Cestrum aurantiacum</i>	NAm&CAm	Tropical Wet	Fleshy
<i>Cestrum diurnum</i>	NAm&CAm&Car	Tropical Wet	Fleshy
<i>Cestrum glanduliferum</i>	NAm&CAm	Tropical Wet	Fleshy
<i>Cestrum guatemalense</i>	NAm&CAm	Tropical Wet	Fleshy
<i>Cestrum luteovirescens</i>	NAm&CAm	Tropical Wet	Fleshy
<i>Cestrum macrophyllum</i>	SAm&CAm&Car	Tropical Wet	Fleshy
<i>Cestrum nocturnum</i>	NAm&SAm&CAm&Car	Tropical Wet	Fleshy
<i>Cestrum regelii</i>	NAm&CAm	Tropical Wet	Fleshy
<i>Cestrum schlechtendalii</i>	NAm&SAm&CAm&Car	Tropical Wet	Fleshy
<i>Cestrum strigilatum</i>	CAm&SAm	Tropical Wet	Fleshy
<i>Cestrum tomentosum</i>	SAm&CAm	Tropical Wet	Fleshy
<i>Cuatresia exiguiflora</i>	SAm&CAm	Tropical Wet	Fleshy
<i>Cuatresia riparia</i>	SAm&CAm	Tropical Wet	Fleshy
<i>Datura inoxia</i>	NAm&CAm	Tropical Dry	Dry
<i>Datura metel</i>	NAm&CAm	Tropical Dry	Dry
<i>Datura stramonium</i>	NAm&CAm	Tropical Dry	Dry
<i>Deprea orinocensis</i>	SAm&CAm	Tropical Wet	Fleshy
<i>Deprea sylvaticum</i>	SAm&CAm	Tropical Wet	Fleshy
<i>Hyoscyamus albus</i>	EU&AF	Tropical Dry	Dry
<i>Hyoscyamus aureus</i>	EU&AF	Tropical Dry	Dry
<i>Hyoscyamus muticus</i>	EU&AF	Tropical Dry	Dry
<i>Jaltomata procumbens</i>	NAm&SAm&CAm	Tropical Wet	Fleshy
<i>Jaltomata repandidentata</i>	NAm&SAm&CAm	Tropical Wet	Fleshy
<i>Juanulloa mexicana</i>	NAm&SAm&CAm	Tropical Wet	Fleshy
<i>Larnax sylvarum</i>	SAm&CAm	Tropical Wet	Fleshy
<i>Lycianthes amatitlanensis</i>	NAm&SAm&CAm	Tropical Wet	Fleshy
<i>Lycianthes ciliolata</i>	NAm&CAm	Tropical Wet	Fleshy
<i>Lycianthes geminiflora</i>	NAm&CAm	Tropical Wet	Fleshy

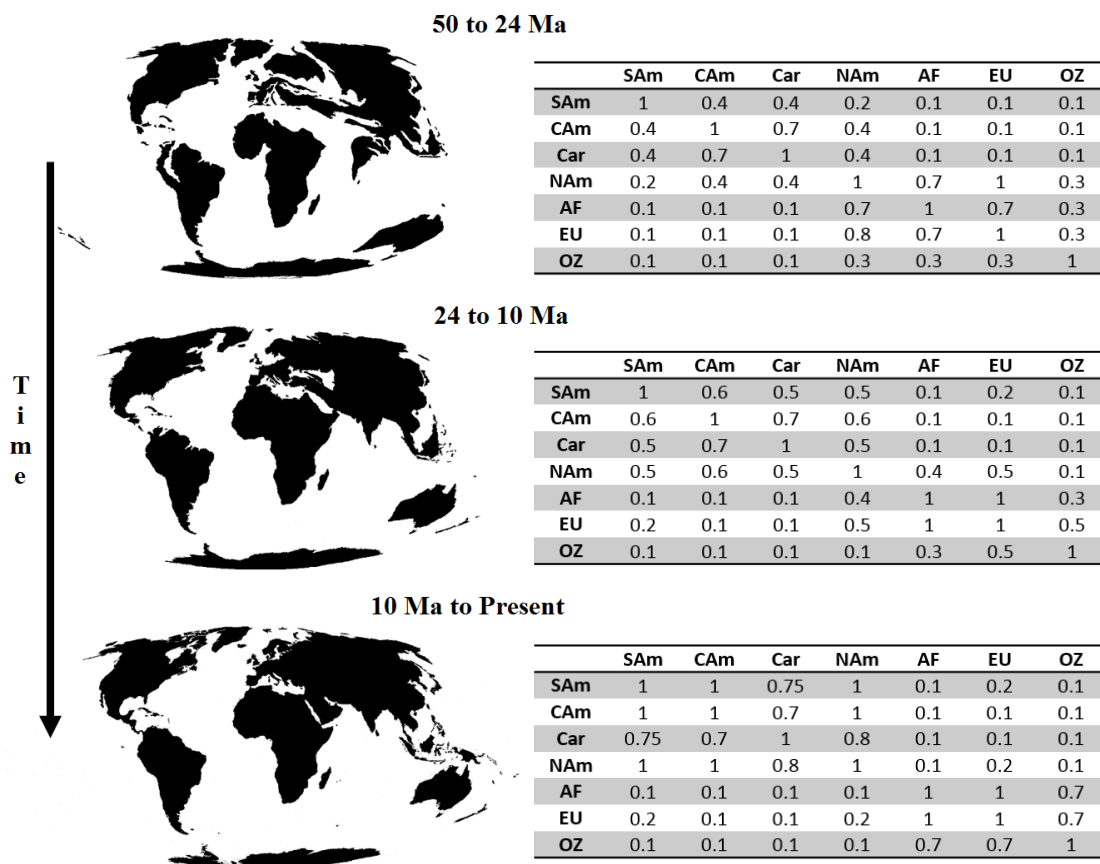
<i>Lycianthes heteroclita</i>	NAm&CAm	Tropical Wet	Fleshy
<i>Lycianthes lenta</i>	NAm&CAm&Car	Tropical Wet	Fleshy
<i>Lycianthes multiflora</i>	CAm&NAm	Tropical Wet	Fleshy
<i>Lycianthes nitida</i>	NAm&SAm&CAm	Tropical Wet	Fleshy
<i>Lycianthes stephanocalyx</i>	NAm&CAm	Tropical Wet	Fleshy
<i>Lycianthes synanthera</i>	NAm&SAm&CAm	Tropical Wet	Fleshy
<i>Lycianthes tricolor</i>	NAm&CAm	Tropical Wet	Fleshy
<i>Lycium americanum</i>	SAm&Car	Tropical Wet	Fleshy
<i>Lycium boerhaviifolium</i>	NAm&SAm	Tropical Dry	Fleshy
<i>Mandragora officinalis</i>	EU&AF	Tropical Dry	Fleshy
<i>Mandragora officinarum</i>	EU&AF	Tropical Dry	Fleshy
<i>Melananthus guatemalensis</i>	SAm&CAm	Tropical Wet	Dry
<i>Nicotiana plumbaginifolia</i>	NAm&SAm&CAm	Tropical Wet	Dry
<i>Nicotiana repanda</i>	NAm&CAm&Car	Tropical Dry	Dry
<i>Physalis angulata</i>	NAm&SAm&CAm&Car	Tropical Wet	Fleshy
<i>Physalis angustiphysa</i>	NAm&CAm	Tropical Wet	Fleshy
<i>Physalis cordata</i>	NAm&CAm&Car	Tropical Wet	Fleshy
<i>Physalis ignota</i>	CAm&Car	Tropical Wet	Fleshy
<i>Physalis lagascae</i>	NAm&SAm&CAm&Car	Tropical Wet	Fleshy
<i>Physalis lassa</i>	NAm&CAm	Tropical Wet	Fleshy
<i>Physalis melanocystis</i>	NAm&CAm	Tropical Wet	Fleshy
<i>Physalis microcarpa</i>	NAm&CAm&Car	Tropical Wet	Fleshy
<i>Physalis minima</i>	AF&EU	Tropical Dry	Fleshy
<i>Physalis nicandroides</i>	NAm&CAm	Tropical Wet	Fleshy
<i>Physalis pruinosa</i>	NAm&SAm&CAm	Tropical Wet	Fleshy
<i>Physalis pubescens</i>	NAm&SAm&CAm	Tropical Wet	Fleshy
<i>Physalis viscosa</i>	NAm&SAm	Tropical Wet	Fleshy
<i>Schultesianthus leucanthus</i>	CAm&SAm	Tropical Wet	Fleshy
<i>Schwenckia lateriflora</i>	SAm&CAm	Tropical Wet	Dry
<i>Solandra grandiflora</i>	CAm&Car	Tropical Wet	Fleshy
<i>Solanum accrescens</i>	CAm&SAm	Tropical Wet	Fleshy
<i>Solanum acerifolium</i>	NAm&SAm&CAm	Tropical Wet	Fleshy
<i>Solanum agrarium</i>	SAm&Car	Tropical Wet	Fleshy
<i>Solanum agrimonifolium</i>	NAm&CAm	Tropical Wet	Fleshy
<i>Solanum aligerum</i>	NAm&SAm&CAm	Tropical Wet	Fleshy
<i>Solanum allophyllum</i>	SAm&CAm	Tropical Wet	Fleshy
<i>Solanum americanum</i>	NAm&Car&SAm&CAm	Tropical Wet	Fleshy
<i>Solanum aphyodendron</i>	SAm&CAm&NAm	Tropical Wet	Fleshy
<i>Solanum appendiculatum</i>	NAm&CAm	Tropical Wet	Fleshy
<i>Solanum arboreum</i>	SAm&CAm	Tropical Wet	Fleshy
<i>Solanum asperum</i>	SAm&CAm	Tropical Wet	Fleshy
<i>Solanum bahamense</i>	NAm&Car	Tropical Wet	Fleshy
<i>Solanum candidum</i>	SAm&CAm	Tropical Wet	Fleshy
<i>Solanum caripense</i>	SAm&CAm	Tropical Wet	Fleshy
<i>Solanum chrysotrichum</i>	NAm&CAm&SAm	Tropical Wet	Fleshy
<i>Solanum circinatum</i>	SAm&CAm	Tropical Wet	Fleshy
<i>Solanum clarum</i>	NAm&CAm	Tropical Wet	Fleshy

<i>Solanum cordovense</i>	NAm&CAm&SAm	Tropical Wet	Fleshy
<i>Solanum demissum</i>	NAm&CAm	Tropical Dry	Fleshy
<i>Solanum diphyllum</i>	NAm&CAm	Tropical Wet	Fleshy
<i>Solanum donianum</i>	NAm&CAm&Car	Tropical Wet	Fleshy
<i>Solanum dulcamara</i>	EU&AF	Temperate	Fleshy
<i>Solanum elaeagnifolium</i>	NAm&SAm	Tropical Dry	Fleshy
<i>Solanum evolvulifolium</i>	SAm&CAm	Tropical Wet	Fleshy
<i>Solanum fraxinifolium</i>	SAm&CAm	Tropical Wet	Fleshy
<i>Solanum giganteum</i>	AF&EU	Temperate	Fleshy
<i>Solanum glabratum</i>	AF&EU	Tropical Dry	Fleshy
<i>Solanum hayesii</i>	SAm&CAm	Tropical Wet	Fleshy
<i>Solanum herculeum</i>	EU&AF	Tropical Dry	Fleshy
<i>Solanum hirtum</i>	SAm&CAm	Tropical Wet	Fleshy
<i>Solanum incanum</i>	AF&EU	Tropical Wet	Fleshy
<i>Solanum jamaicense</i>	NAm&Car&SAm&CAm	Tropical Wet	Fleshy
<i>Solanum lanceifolium</i>	NAm&SAm&CAm&Car	Tropical Wet	Fleshy
<i>Solanum lanceolatum</i>	NAm&CAm	Tropical Wet	Fleshy
<i>Solanum lepidotum</i>	SAm&CAm	Tropical Wet	Fleshy
<i>Solanum morelliforme</i>	NAm&CAm&SAm	Tropical Wet	Fleshy
<i>Solanum myriacanthum</i>	NAm&CAm	Tropical Wet	Fleshy
<i>Solanum nigrum</i>	EU&AF	Temperate	Fleshy
<i>Solanum pectinatum</i>	SAm&CAm	Tropical Wet	Fleshy
<i>Solanum phaseoloides</i>	CAm&SAm	Tropical Wet	Fleshy
<i>Solanum pubigerum</i>	NAm&CAm	Tropical Wet	Fleshy
<i>Solanum rovirosanum</i>	CAm&NAm	Tropical Wet	Fleshy
<i>Solanum rudepannum</i>	NAm&CAm	Tropical Wet	Fleshy
<i>Solanum rugosum</i>	SAm&CAm	Tropical Wet	Fleshy
<i>Solanum schlechtendalianum</i>	SAm&CAm	Tropical Wet	Fleshy
<i>Solanum stramonifolium</i>	SAm&CAm&Car	Tropical Wet	Fleshy
<i>Solanum tampicense</i>	NAm&CAm&SAm&Car	Tropical Wet	Fleshy
<i>Solanum torvum</i>	SAm&CAm&Car	Tropical Wet	Fleshy
<i>Solanum triflorum</i>	NAm&SAm	Temperate	Fleshy
<i>Solanum villosum</i>	AF&EU	Tropical Dry	Fleshy
<i>Solanum volubile</i>	NAm&SAm&CAm&Car	Tropical Wet	Fleshy
<i>Solanum wendlandii</i>	CAm&NAm	Tropical Wet	Fleshy
<i>Tzeltalia amphitricha</i>	NAm&CAm	Tropical Wet	Fleshy
<i>Withania somnifera</i>	AF&EU	Temperate	Fleshy
<i>Witheringia solanacea</i>	CAm&Car&SAm	Tropical Wet	Fleshy

Dispersal Multiplier Matrices

Dispersal probability multiplier matrices were first introduced in the program Lagrange (Ree & Smith, 2008), and they are commonly used as a way to represent relative connectivity between regions in particular time periods. Despite their popularity, one criticism is that dispersal probability multipliers are typically determined subjectively. If it is certain that dispersal was either possible or impossible, the multipliers are clear (1 or 0), but usually there is some nonzero probability of long-distance dispersal between disconnected regions. One might therefore put a dispersal multiplier of 0.1 between regions that are disconnected but nearby (for example, North America and Asia), and a dispersal multiplier of 0.01 between regions that are very far apart (North America and Australia). However, the actual values of the multipliers are subjective and somewhat arbitrary, such that multipliers of 0.5 and 0.001, for instance, might be equally plausible. Thus, we can include, in our model fitting, parameters that modify the values of the matrix, e.g., multiplying or dividing all of the dispersal probabilities or raising them to a power. Here we introduce “ w ” parameter, which is incorporated into ‘BioGeoBEARS’. In $+w$ models, each dispersal probability multiplier is raised to the power w . The parameter w can be fixed to its default, 1, which replicates the traditional Lagrange approach, keeping the dispersal probability multipliers unchanged. If w is 0, all dispersal probability multipliers are converted to 1, and thus the model converts to a “unconstrained” model with equal rates of dispersal between regions. Alternatively, w can be made a free parameter and estimated via ML, along with all other free parameters (Matzke, 2014). Estimates of $w < 1$ indicate that a better fit to the data is obtained if the differences between user-specified dispersal probability multipliers are reduced; estimates of $w > 1$ indicate that the differences between multipliers should be increased. While there is still subjectivity in determining the base dispersal probability multiplier matrix, its influence on results is much reduced in $+w$ models, and all of the standard tools of statistical model choice (e.g., Likelihood Ratio Test, Akaike Information Criterion (AIC); Burnham & Anderson, 2002) may be applied.

Among our set of 18 biogeographical models for Solanaceae, we tested those with and without dispersal multiplier matrices (“_TS” in Table S1.3). For those models with dispersal multiplier matrices, we then estimated models with and without w . The base dispersal multiplier matrices used in this study (shown below) represent three time strata: 50 to 24 Ma, 24 to 10 Ma and 10 Ma to present. Rows represent areas from where the taxon is moving and columns to where they are dispersing. Movements between the Americas, for instance, become more probable towards the present with the formation of the Panama Isthmus. We set the probability of moving between the Old World and New World lower toward the present as the areas become more widely separated over time. The best model included dispersal multiplier matrices with a w of 1.88, suggesting that the best-fit dispersal multipliers between areas are unequal, and the differences are somewhat more extreme than those selected in the base matrices (below).



Algorithm Validation for Biogeographical Stochastic Mapping in 'BioGeoBEARS'

Biogeographical Stochastic Mapping: Algorithm and Validation

As with traditional stochastic mapping (Nielsen, 2002; Huelsenbeck et al., 2003), biogeographical stochastic mapping (BSM) is a straightforward application of the Markov models used to calculate the likelihood of the data on the tree and the ancestral state probabilities. Here, the term “states” and “geographical ranges” are used interchangeably, because in Lagrange/BioGeoBEARS-type models, every geographical range is a just a state in a very large state space.

The BSM algorithm is as follows:

(1) The conditional probabilities calculated during the downpass likelihood calculation are saved.

(2) The ancestral state at the root is randomly sampled from the ancestral state probabilities.

(3) A cladogenetic range inheritance scenario is sampled conditional on the ancestral state, the downpass likelihoods at the bottom of each branch just after speciation, and the probability of each cladogenesis scenario according to the model parameters; the range inheritance scenario automatically specifies the states just after cladogenesis. This step is the only one that differs from traditional stochastic mapping.

(4) The states at the top of each of the two descendant branches are drawn, conditional on the downpass likelihoods and the probabilities passed up conditional on the states at the bottom of each branch.

(5) With the states now “known” at the bottom and top of each branch (for this particular stochastic mapping realisation), the history of range expansion and contraction events along the branch is simulated, starting from the branch bottom. Simulations that fail to

produce the known state at the top of the branch are discarded. The process is repeated until a successful simulation occurs.

(6) Steps 2-5 are repeated for each node in the tree, moving from the root up to the tips.

The result of this procedure is a sample from the Bayesian posterior distribution of possible histories, conditional on the data, the tree, and the model. It constitutes one of many possible exact histories. By sampling many BSM realisations (at least 50), and counting the number of events of each type in each BSM, estimates of the frequency of each event are easily produced, along with the uncertainty in these estimates. The BSM can be run across a posterior sample of trees (e.g., from a Bayesian phylogenetic analysis) in order to incorporate phylogenetic uncertainty. This procedure is thus superior to counts of events produced by “eyeballing” a plot of ancestral states under the ML model; while the latter procedure will bear some resemblance to the actual event counts, it will tend to underestimate the actual number of events, and it tends to ignore the fact that some nodes may have ancestral states that are highly uncertain.

The ‘BioGeoBEARS’ BSM procedure was validated in several ways. First, for any given biogeographical model, averaging many BSMs should reproduce the ancestral state probabilities calculated analytically under ML, within the stochastic uncertainty determined by the number of BSMs. As the number of BSMs increases, the ancestral state probabilities should become increasingly close to the analytic estimates. Second, the same should apply in time-stratified analyses, which are programmed separately in ‘BioGeoBEARS’. Time-stratified and non-stratified analyses should also produce identical results when “dummy” dispersal multiplier matrices (all 1s) are used in the time stratification. Third, a special case of the ‘BioGeoBEARS’ supermodel, “BAYAREALIKE+ a ”, is identical to traditional morphological models, and thus can be compared to the ancestral state probabilities and

stochastic maps produced by another R package, phytools (Revell, 2012). For all of these tests, 1:1 correlation plots indicate a successful result. ‘BioGeoBEARS’ passed all of the above-described tests; the results are available in the online ‘BioGeoBEARS’ documentation at: <http://phylo.wikidot.com/biogeobears-validation>. The comparison of ML and BSM state probabilities was also repeated on the ML model for the Solanaceae dataset.

Validation of BSM for DEC+j+w model

Linear regression of the ML ancestral range probabilities with the mean of BSMs for the Solanaceae dataset under the DEC+j+w model (Figure S2.1) gave strong verification that the two are equivalent (slope=1, 95% CI=0.000203; $p=0$; $R^2=0.999$).

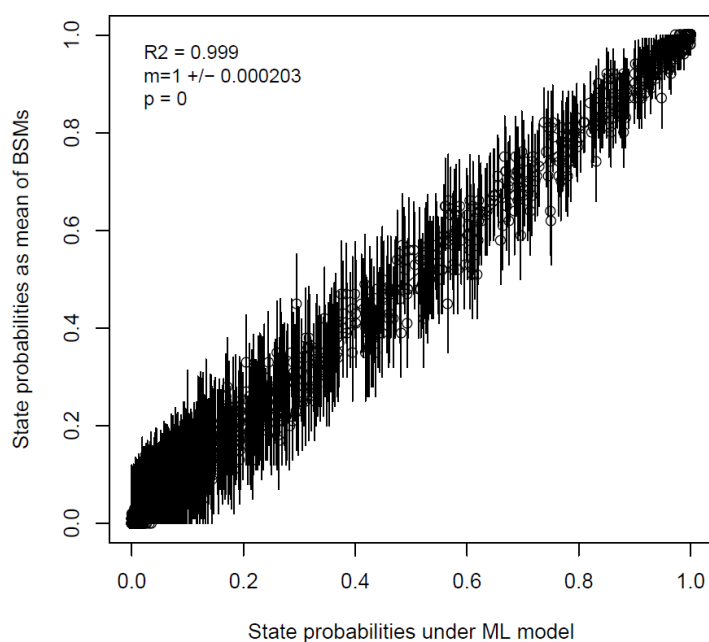


Figure S2.1. Validation of the ‘BioGeoBEARS’ stochastic mapping algorithm when comparing the estimated state probabilities under ML model versus estimated state probabilities as mean of BSMs. Vertical lines are the 95% confidence intervals on the mean BSM probabilities, as calculated using the R package MultinomialCI.

Revell, L.J. (2012) phytools: An R package for phylogenetic comparative biology (and other things). *Methods in Ecology and Evolution*, **3**, 217–223.

A.2 Maximum likelihood ancestral range estimates

This material cannot be displayed in this document, please see files on the online version of the journal paper at <http://onlinelibrary.wiley.com/doi/10.1111/jbi.12898/full>

A.3 Example of a BSM realization

This material cannot be displayed in this document, please see files on the online version of the journal paper at <http://onlinelibrary.wiley.com/doi/10.1111/jbi.12898/full>

Appendix B

Supporting information to Chapter 2

This appendix contains supporting information for Chapter 2

B.1 Voucher information

B.1 Voucher information

genus	species epithet	authority	country	largest political subdi- vision	collector(s) and collector number	herbarium
<i>Brugmansia</i>	<i>arborea</i>	(L.) Lagerh.	-	Cultivated in Botanic Garden Munich, Germany	2012/2883w7	(MSB)
<i>Brugmansia</i>	<i>arborea</i>	(L.) Lagerh.	Peru	Pasco	Smith 545	-
<i>Brugmansia</i>	<i>aurea</i>	Lagerh.	Ecuador	Pichincha	Dupin 42	(QCA)
<i>Brugmansia</i>	<i>aurea</i>	Lagerh.	-	Cultivated in Botanic Garden Munich, Germany	2012/2880w	(MSB)
<i>Brugmansia</i>	<i>sanguinea</i>	(Ruiz & Pav.) D. Don	Ecuador	Pichincha	Dupin 43	(QCA)
<i>Brugmansia</i>	<i>sanguinea</i>	(Ruiz & Pav.) D. Don	-	Cultivated in Botanic Garden Munich, Germany	2012/2888	(MSB)
<i>Brugmansia</i>	<i>suaveolens</i>	(Humb. & Bonpl. ex Willd.) Sweet	Costa Rica	San Jose	Dupin 2	(COLO)
<i>Brugmansia</i>	<i>suaveolens</i>	(Humb. & Bonpl. ex Willd.) Sweet	-	Cultivated in Botanic Garden Munich, Germany	2012/2889	(MSB)

<i>Brugmansia</i>	<i>versicolor</i>	Lagerh.	Ecuador	Cultivated in Huntington Botanical Gardens, CA	43862	(HNT)
<i>Brugmansia</i>	<i>versicolor</i>	Lagerh.	-	Cultivated in Botanic Garden Munich, Germany	2012/2890	(MSB)
<i>Datura</i>	<i>arenicola</i>	Gentry ex Bye & Luna-Cavazos	Mexico	Baja California Sur	<i>H.S. Gentry 7881</i>	(RSA)
<i>Datura</i>	<i>ceratocaula</i>	Ortega	Mexico	Jalisco	<i>Dupin 50</i>	(COLO)
<i>Datura</i>	<i>ceratocaula</i>	Ortega	Mexico	Jalisco	<i>Dupin 51</i>	(COLO)
<i>Datura</i>	<i>ceratocaula</i>	Ortega	Mexico	Hidalgo	<i>A. Ventura A. 91</i>	(WIS)
<i>Datura</i>	<i>ceratocaula</i>	Ortega	Mexico	Durango	<i>Wieder, Bennett, Dunn & Torke 208</i>	(WIS)
<i>Datura</i>	<i>discolor</i>	Bernh.	USA	California	<i>S.D. White 11262</i>	(RSA)
<i>Datura</i>	<i>inoxia</i>	Mill.	USA	California	<i>M. DeDecker 2669</i>	(RSA)
<i>Datura</i>	<i>inoxia</i>	Mill.	Mexico	Jalisco	<i>Dupin 52</i>	(COLO)
<i>Datura</i>	<i>kymatocarpa</i>	A.S. Barclay	Mexico	Michoacan	<i>J.M. Porter & V.W. Steinmann 14726</i>	(RSA)
<i>Datura</i>	<i>kymatocarpa</i>	A.S. Barclay	Mexico	Guerrero	<i>J. C. Soto 14914</i>	(MEXU)

<i>Datura</i>	<i>lanosa</i>	Barclay ex Bye	Mexico	Sonora	<i>A.L. Reina G 96-542</i>	(RSA)
<i>Datura</i>	<i>lanosa</i>	Barclay ex Bye	Mexico	Chihuahua	<i>R. Bye & E. Linares 14252</i>	(MEXU)
<i>Datura</i>	<i>lanosa</i>	Barclay ex Bye	Mexico	Sonora	<i>R. Bye 28391</i>	(MEXU)
<i>Datura</i>	<i>leichhardtii</i> ssp. <i>pruinosa</i>	(Greenm.) A.S. Barclay ex K. Hammer	Mexico	Puebla	<i>J. Dupin 38</i>	(COLO)
<i>Datura</i>	<i>leichhardtii</i> ssp. <i>pruinosa</i>	(Greenm.) A.S. Barclay ex K. Hammer	Mexico	Oaxaca	<i>R. Bye & L. Cervantes</i>	(MEXU)
<i>Datura</i>	<i>leichhardtii</i> ssp. <i>pruinosa</i>	(Greenm.) A.S. Barclay ex K. Hammer	Mexico	Oaxaca	<i>A. Mendoza</i>	(WIS)
<i>Datura</i>	<i>metel</i>	L.	Mexico	Michoacan	<i>J. Soto Nunez, A. R. Soto & F. Soto 7080</i>	(MEXU)
<i>Datura</i>	<i>metel</i>	L.	Mexico	Mexico	<i>R. Bye 26964</i>	(MEXU)
<i>Datura</i>	<i>quercifolia</i>	Kunth	USA	California	<i>A.C. Sanders 5337</i>	(RSA)

<i>Datura</i>	<i>quercifolia</i>	Kunth	Mexico	Aguascalientes	<i>G. Garcia</i> 5004	(MEXU)
<i>Datura</i>	<i>quercifolia</i>	Kunth	Mexico	Guanajuato	<i>E. Martinez</i> 39665	(MEXU)
<i>Datura</i>	<i>quercifolia</i>	Kunth	-	-	<i>J. Dupin</i> 53	(COLO)
<i>Datura</i>	<i>reburra</i>	A.S. Barclay	Mexico	Sonora	<i>Gentry, Barclay</i> & <i>Arguelles</i> 19249	(COLO)
<i>Datura</i>	<i>reburra</i>	A.S. Barclay	Mexico	Sinaloa	<i>Gentry, Barclay</i> & <i>Arguelles</i> 19442	(COLO)
<i>Datura</i>	<i>reburra</i>	A.S. Barclay	Mexico	Sinaloa	<i>B. Templeton</i> 7079	(RSA)
<i>Datura</i>	<i>stramonium</i>	L.	USA	California	<i>B. Ertter</i> 8885	(RSA)
<i>Datura</i>	<i>stramonium</i>	L.	USA	Kansas	<i>J. Dupin</i> 54	(COLO)
<i>Datura</i>	<i>wrightii</i>	Regel	USA	Nebraska	<i>J. Dupin</i> 35	(COLO)
<i>Datura</i>	<i>wrightii</i>	Regel	USA	Arizona	<i>J. Dupin</i> 48	(COLO)
<i>Datura</i>	<i>wrightii</i>	Regel	USA	Utah	<i>J. Dupin</i> 49	(COLO)
<i>Trompettia</i>	<i>cardenasiana</i>	(Hunz.) J. Dupin	Bolivia	Potosi	<i>S. Smith</i> 383	(WIS)
<i>Trompettia</i>	<i>cardenasiana</i>	(Hunz.) J. Dupin	Bolivia	Potosi	<i>S. Smith</i> 385	(WIS)
<i>Capsicum</i>	<i>lycianthoides</i>	Bitter	Ecuador	Pichincha	<i>S. Smith</i> 203	(WIS)
<i>Juanulloa</i>	<i>speciosa</i>	(Miers) Dunal	Colombia	Tolima	<i>J. Ng</i> 023	(COLO)

<i>Lycium</i>	<i>tenue</i>	Willd.	South Africa	Western Cape	<i>R. Olmstead 99-13</i>	(WTU)
<i>Mandragora</i>	<i>chinghaiensis</i>	Kuang & A.M. Lu	China	Qinghai	<i>Z.Y. Zhang 089</i>	(HNWP)
<i>Mandragora</i>	<i>chinghaiensis</i>	Kuang & A.M. Lu	China	Qinghai	<i>T. Tu Tu521-1</i>	-
<i>Nicandra</i>	<i>physalodes</i>	(L.) Gaertn.	Peru	Cultivated in Beal Botanical Garden, Michigan State University	<i>R. Olmstead S-38</i>	(WTU)
<i>Physalis</i>	<i>peruviana</i>	L.	Ecuador	Pichincha	<i>S. Smith 217</i>	(WIS)
<i>Solanum</i>	<i>demissum</i>	Lindl.	-	-	-	(PI-545757)
<i>Nicotiana</i>	<i>tabacum</i>	L.	-	-	-	(AYMY0000000.1)

B.2 *lfy* primers designed for this study

All primers with an F (forward) in the name are placed on the exon 2 of *lfy*, the ones with an R (reverse) are found on the exon 3; and the one with Ri (reverse, internal) is placed on the intro II.

B.2 *lfy* primers designed for this study

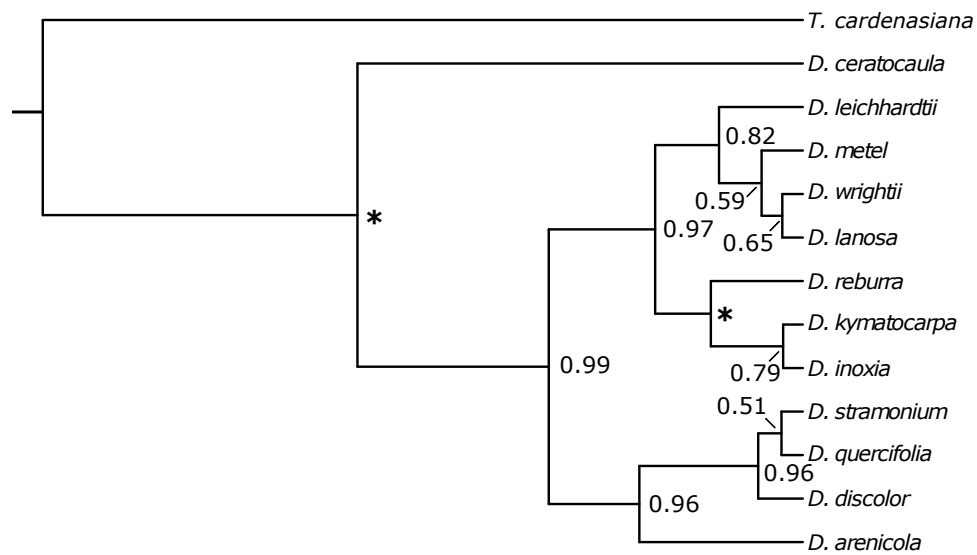
Primer name	Sequence 5' - 3'
LFYDatF1	GATTACTTGTTCCATCTCTATGAGCAATGC
LFYDatF2	AGGGAGCATCCGTTTATCGTGACG
LFYDatF3	TATCAACGAGGGCGGAGGAGGAGGAGTAAGC
LFYDatF4	AGGAGGACGATGAAACGGAGGAATTAGG
LFYDatF5	GGAAATAATGGTGAGAGGAAGAAGGC
LFYDatR1	GTTTATGTAGCTTGCCCCTGCCTTCTTCGCG
LFYDatR2	GGAGCCATCCTCGTCAAGACAATGAAGTGCG
LFYDatR3	CCTTGTCGAGCAGCTATGGCTACCAGGGGC
LFYDatR4	ACTGCAAACTGAACCTGAGTCG
LFYDatR5	AACACAATCAGACTAACCATCCAACGC
LFYDatRi6	TTGAGTGGAAGTACAAATGGAGTAATGGGC

B.3 starBEAST2 analysis of *Datura*

Analysis from starBEAST2 of *Datura* (showing only results for the ingroup). Nodes with an asterisk have a *pp* of 1.00.

B.4 Divergence times with confidence intervals for *Datureae* and outgroups

Divergence times with confidence intervals for *Datureae* and outgroups. (MRCA = most recent common ancestor)



B.3 starBEAST2 analysis of *Datura*

B.4 Divergence times with confidence intervals for Datureae and outgroups. (1) MRCA = most recent common ancestor.

MRCA (1)	Median age (Ma)	95% CI (Ma)
<i>Brugmansia</i>	18.4	27.5, 10.8
<i>Brugmansia arborea</i> + <i>B. sanguinea</i>	12	20.2, 5.1
<i>Brugmansia aurea</i> + <i>B. suaveolens</i>	9.3	15.7, 4.4
<i>Datura</i>	14.2	20.6, 8.8
<i>Datura arenicola</i> + <i>D. stramonium</i>	11.4	16.1, 6.4
<i>Datura kymatocarpa</i> + <i>D. leichhardtii</i>	10.7	16.6, 7.1
<i>Datura</i> + <i>Brugmansia</i>	28.5	39.2, 18.7
Datureae	34.7	46.9, 23.8
Datureae + <i>Nicandra</i>	42.7	55.5, 30.6
Solanoideae	54.1	67.4, 52.2

Appendix C

Supporting information to Chapter 3

This appendix contains supporting information for Chapter 3.

C.1 Biogeographical models tested in this study

Biogeographical models tested in this study, along with estimated free parameters, log-likelihoods, AIC values and Akaike weights. Models were classified according to the time periods chosen depending on the reported date of the closure of the Panama isthmus: 3.5 Ma, 12 Ma or 20 Ma. Model suitability was examined using AIC comparisons. Models that included the j parameter presented better AIC values and, consequently, higher Akaike weights, but there was no significant difference between the six values that do included J as a free parameter. $j = 0$ means founder-events were not allowed. (1) rate of range expansion. (2) rate of range contraction. (3) exponent on manual dispersal multipliers (modifies d and j). (4) relative per-event weight of jump dispersal.

C.1 Biogeographical models tested in this study

Model name	Log-Likelihood	Free parameters				AIC	Akaike weights
		$d(1)$	$e(2)$	$w(3)$	$j(4)$		
DEC_3.5	-10.81	2.60E-03	0.00	1.32	0.00	27.62	0.032
DEC+ j _3.5	-07.89	1.00E-07	0.00	2.39	0.14	23.78	0.221
DIVALIKE_3.5	-10.48	7.20E-03	0.00	1.36	0.00	26.96	0.045
DIVALIKE+ j _3.5	-08.30	1.00E-07	0.00	1.60	0.09	24.60	0.147
DEC_12	-10.95	1.10E-03	0.00	0.38	0.00	27.90	0.028
DEC+ j _12	-08.12	1.00E-07	0.00	10.0	0.43	24.24	0.176
DIVALIKE_12	-10.71	4.60E-03	0.00	0.66	0.00	27.42	0.036
DIVALIKE+ j _12	-08.90	1.00E-07	0.00	0.94	0.05	25.80	0.080
DEC_20	-10.94	1.20E-03	0.00	0.59	0.00	27.88	0.028
DEC+ j _20	-08.71	1.00E-07	0.00	0.77	0.04	25.42	0.097
DIVALIKE_20	-10.72	4.70E-03	0.00	0.80	0.00	27.44	0.035
DIVALIKE+ j _20	-08.99	1.00E-07	0.00	0.94	0.05	25.98	0.073

C.2 List of environmental variables considered for this study

Initial list of environmental variables considered for this study, their sources and final 12 selected (marked with asterisk) to be used in subsequent pPCA after collinearity test. Numbers by soil variables represent the depth of the measurement. 'Worldclim' is from [81], 'SoilGrids 1km' is from [79].

C.2 List of environmental variables considered for this study

Variable	Source
<i>*Annual Mean Temperature</i>	Worldclim
<i>*Mean Temperature Warmest Quarter</i>	Worldclim
Mean Temperature Coldest Quarter	Worldclim
<i>*Annual Precipitation</i>	Worldclim
Precipitation Wettest Month	Worldclim
Precipitation Driest Month	Worldclim
<i>*Precipitation Seasonality</i>	Worldclim
Precipitation Wettest Quarter	Worldclim
<i>*Precipitation Driest Quarter</i>	Worldclim
<i>*Precipitation Warmest Quarter</i>	Worldclim
Precipitation Coldest Quarter	Worldclim
<i>*Mean Diurnal Range</i>	Worldclim
Isothermality	Worldclim
Temperature Seasonality	Worldclim
Max Temperature Warmest Month	Worldclim
Min Temperature Coldest Month	Worldclim
Temperature Annual Range	Worldclim
Mean Temperature Wettest Quarter	Worldclim
Mean Temperature Driest Quarter	Worldclim
<i>*Soil bulk 0.3m</i>	SoilGrids 1km
Soil bulk 0m	SoilGrids 1km
Soil bulk 1m	SoilGrids 1km
<i>*Soil clay 0.3m</i>	SoilGrids 1km
Soil clay 0m	SoilGrids 1km
Soil clay 1m	SoilGrids 1km
<i>*Soil fragment 0.3m</i>	SoilGrids 1km
Soil fragment 0m	SoilGrids 1km
Soil fragment 1m	SoilGrids 1km
<i>*Soil sand 0.3m</i>	SoilGrids 1km
Soil sand 0m	SoilGrids 1km
Soil sand 1m	SoilGrids 1km
<i>*Soil silt 0.3m</i>	SoilGrids 1km
Soil silt 0m	SoilGrids 1km
Soil silt 1m	SoilGrids 1km